SSRP 2017

20. Steirisches Seminar über Regelungstechnik und Prozessautomatisierung

20th Styrian Workshop on Automatic Control

Proceedings

M. Steinberger, M. Horn (Eds.)

11.09. - 13.09.2017
Schloss Retzhof, Leitring/Wagna, Austria

ISBN: 978-3-901439-12-4

IRT

http://www.irt.tugraz.at

TU Graz

Graz University of Technology

Contents

Part I.

Tuesday

Robustness of Distributed Frequency Control in Modern Power Systems: Time Delays & Dynamic Communication Topology

Johannes Schiffer[a] **Florian Dörfler**[b] **Emilia Fridman**[c]

One of the most relevant control applications in power systems is frequency control. This control task is typically divided into three hierarchical layers: primary, secondary and tertiary control [6]. In the present talk, we focus on secondary control which is responsible for the regulation of the frequency to a nominal value in an economically efficient way and subject to maintaining the net area power balance. Traditionally, secondary frequency control has been carried out on the high-voltage transmission system by using large fossil-fueled power plants as actuators [6]. Yet, the increasing penetration of distributed renewable generation interfaced to the network via power inverters renders these conventional schemes inaproppriate, creating a clear need for robust and distributed solutions with plug-and-play capabilities [10].

Multi-agent systems (MAS) represent a promising framework to enable such solutions. A popular distributed control strategy for MAS is the distributed averaging-based integral (DAI) algorithm, also known as consensus filter [7], that relies on averaging of integral actions through a communication network. The distributed character of this type of protocol has the advantage that no central computation unit is needed and the individual agents, i.e., generation units, only have to exchange information with their neighbors [1]. DAI algorithms have been proposed previously to address the objectives of secondary frequency control in bulk power systems [11, 8] and also in microgrids (i.e., small-footprint power systems on the low and medium voltage level) [9, 1, 2].

The closed-loop DAI-controlled power system is a cyber-physical system whose stability and performance crucially relies on nearest-neighbor communication. Despite all recent advances, communication-based controllers (in power systems) are subject to considerable uncertainties such as message delays, message losses, and link failures [10] that can severely reduce the performance – or even affect the stability – of the overall cyber-physical system. Such cyber-physical phenomena and uncertainties have not been considered thus far in DAI-controlled power system analysis.

Motivated by this, we present conditions for robust stability of nonlinear DAI-controlled power systems under communication uncertainties. With regards to delays, we consider constant as well as fast-varying delays. The latter are a common phenomenon in sampled data networked control systems, due to digital control [4, 3] and as the network access and transmission delays depend on the actual network conditions, e.g., in terms of congestion and channel quality [5]. In addition to delays, in practical applications the topology of the communication network can be time-varying due to message losses and link failures [7]. This

[a]School of Electronic & Electrical Engineering, University of Leeds, United Kingdom, LS2 9JT, E-mail: `j.schiffer@leeds.ac.uk`

[b]Automatic Control Laboratory, Swiss Federal Institute of Technology (ETH) Zürich, Switzerland, 8092, E-Mail: `dorfler@control.ee.ethz.ch`

[c]Tel Aviv University, Tel Aviv 69978, Israel, E-Mail: `emilia@eng.tau.ac.il`

can be modeled by a switching communication network [7]. Thus, the explicit consideration of communication uncertainties leads to a switched nonlinear power system model with (time-varying) heterogeneous delays. For such systems, we provide sufficient delay-dependent conditions for robust stability by constructing a common Lyapunov-Krasovskii functional. Our stability conditions can be verified without exact knowledge of the operating state and reflect a fundamental trade-off between robustness and performance of DAI control. The effectiveness of the derived approach is illustrated on a numerical benchmark example, namely Kundur's four-machine-two-area test system [6, Example 12.6].

[1] A. Bidram, F. Lewis, and A. Davoudi. Distributed control systems for small-scale power networks: Using multiagent cooperative control theory. *IEEE Control Systems*, 34(6):56–77, 2014.

[2] F. Dörfler, J. W. Simpson-Porco, and F. Bullo. Breaking the hierarchy: Distributed control and economic optimality in microgrids. *IEEE Transactions on Control of Network Systems*, 3(3):241–253, 2016.

[3] E. Fridman. *Introduction to time-delay systems: analysis and control*. Birkhäuser, 2014.

[4] E. Fridman. Tutorial on Lyapunov-based methods for time-delay systems. *European Journal of Control*, 20(6):271–283, 2014.

[5] J. P. Hespanha, P. Naghshtabrizi, and Y. Xu. A survey of recent results in networked control systems. *Proceedings of the IEEE*, 95(1):138, 2007.

[6] P. Kundur. *Power System Stability and Control*. McGraw-Hill, 1994.

[7] R. Olfati-Saber, A. Fax, and R. M. Murray. Consensus and cooperation in networked multi-agent systems. *Proceedings of the IEEE*, 95(1):215–233, 2007.

[8] J. Schiffer and F. Dörfler. On stability of a distributed averaging PI frequency and active power controlled differential-algebraic power system model. In *European Control Conference*, pages 1487–1492, 2016.

[9] J. W. Simpson-Porco, F. Dörfler, and F. Bullo. Synchronization and power sharing for droop-controlled inverters in islanded microgrids. *Automatica*, 49(9):2603–2611, 2013.

[10] G. Strbac, N. Hatziargyriou, J. P. Lopes, C. Moreira, A. Dimeas, and D. Papadaskalopoulos. Microgrids: Enhancing the resilience of the European megagrid. *Power and Energy Magazine, IEEE*, 13(3):35–43, 2015.

[11] S. Trip, M. Bürger, and C. De Persis. An internal model approach to (optimal) frequency regulation in power grids with time-varying voltages. *Automatica*, 64:240–253, 2016.

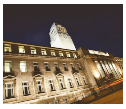

UNIVERSITY OF LEEDS

Robustness of distributed frequency control in modern power systems: Time delays & dynamic communication topology

Joint work with E. Fridman and F. Dörfler

Johannes Schiffer
School of Electronic & Electrical Engineering
University of Leeds

Renewables change power system structure

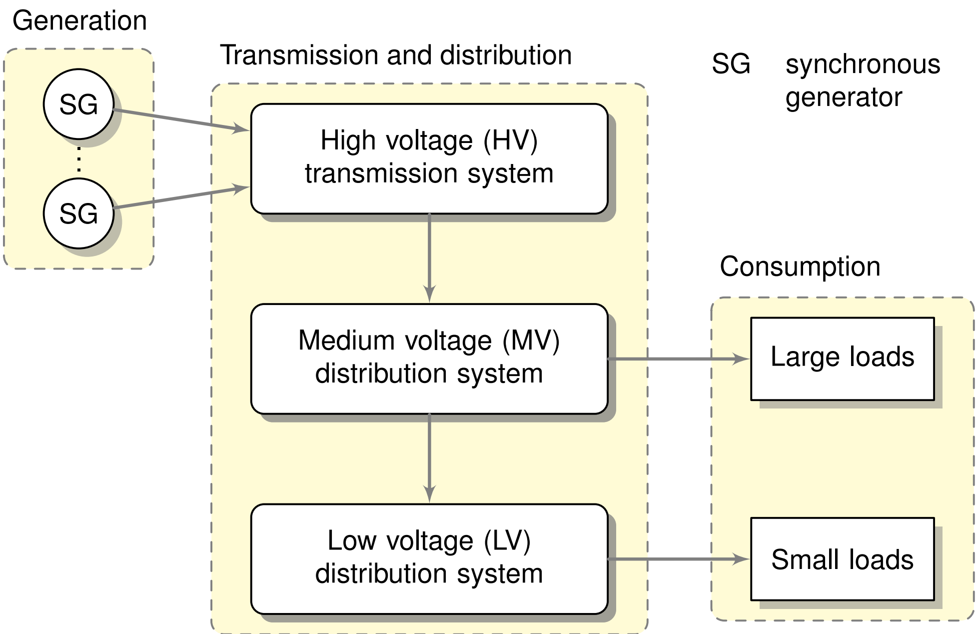

Renewables change power system structure

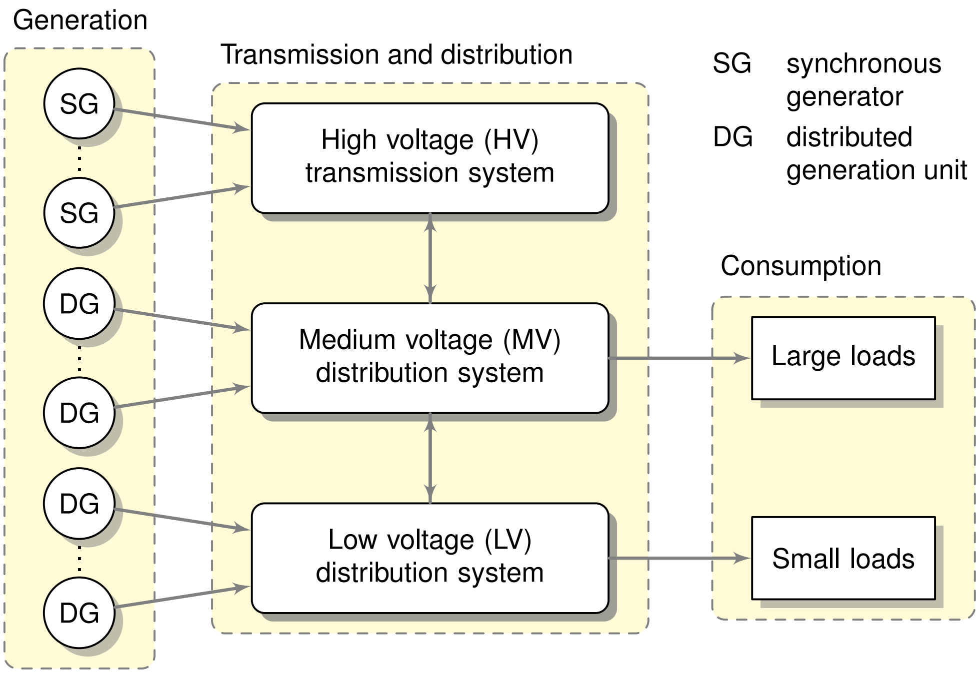

2 / 31

Frequency control

Automatic frequency control

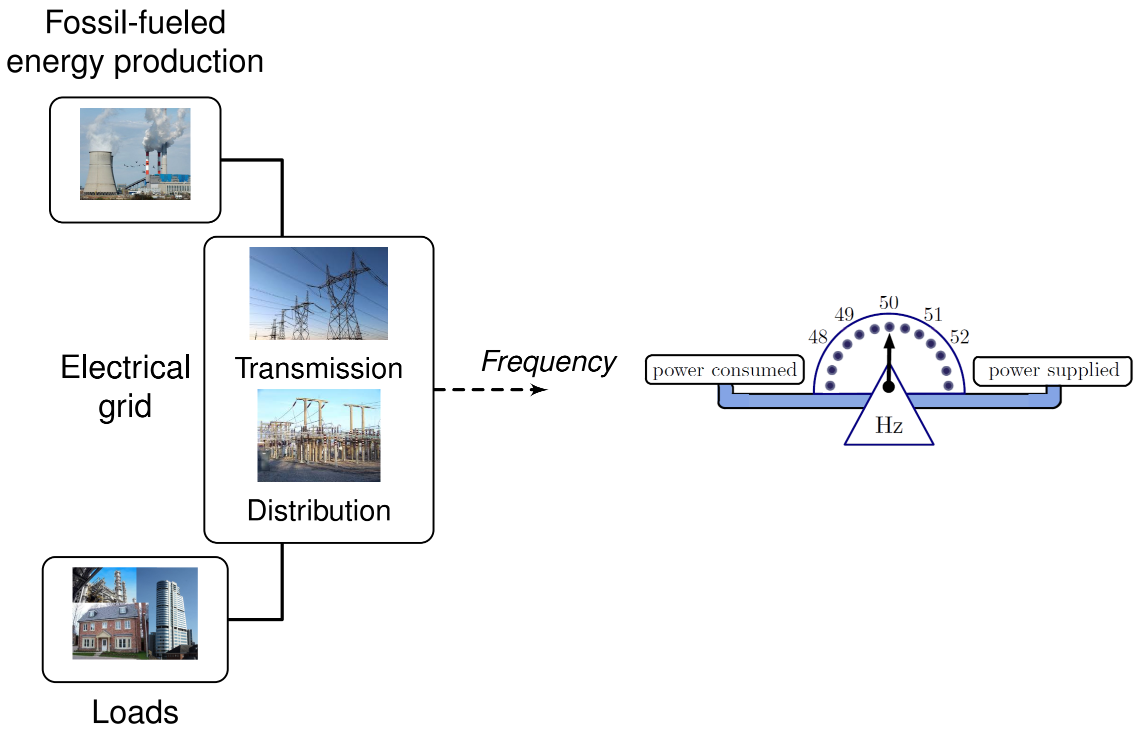

4 / 31

Primary frequency control

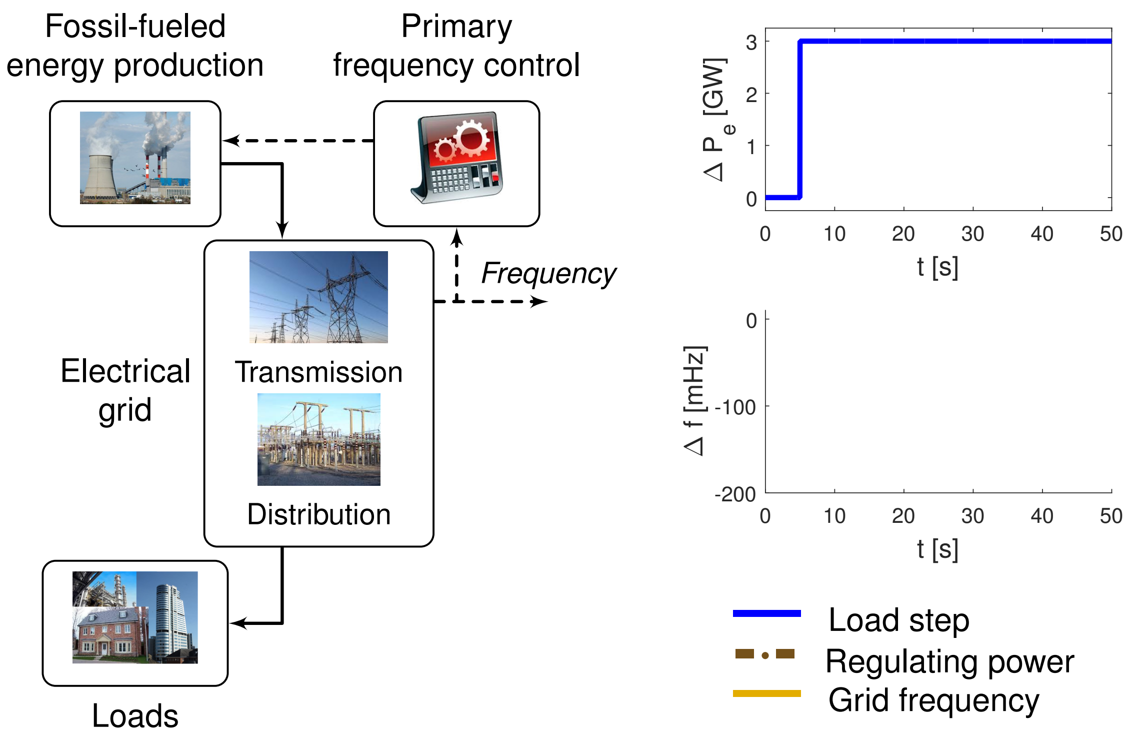

5 / 31

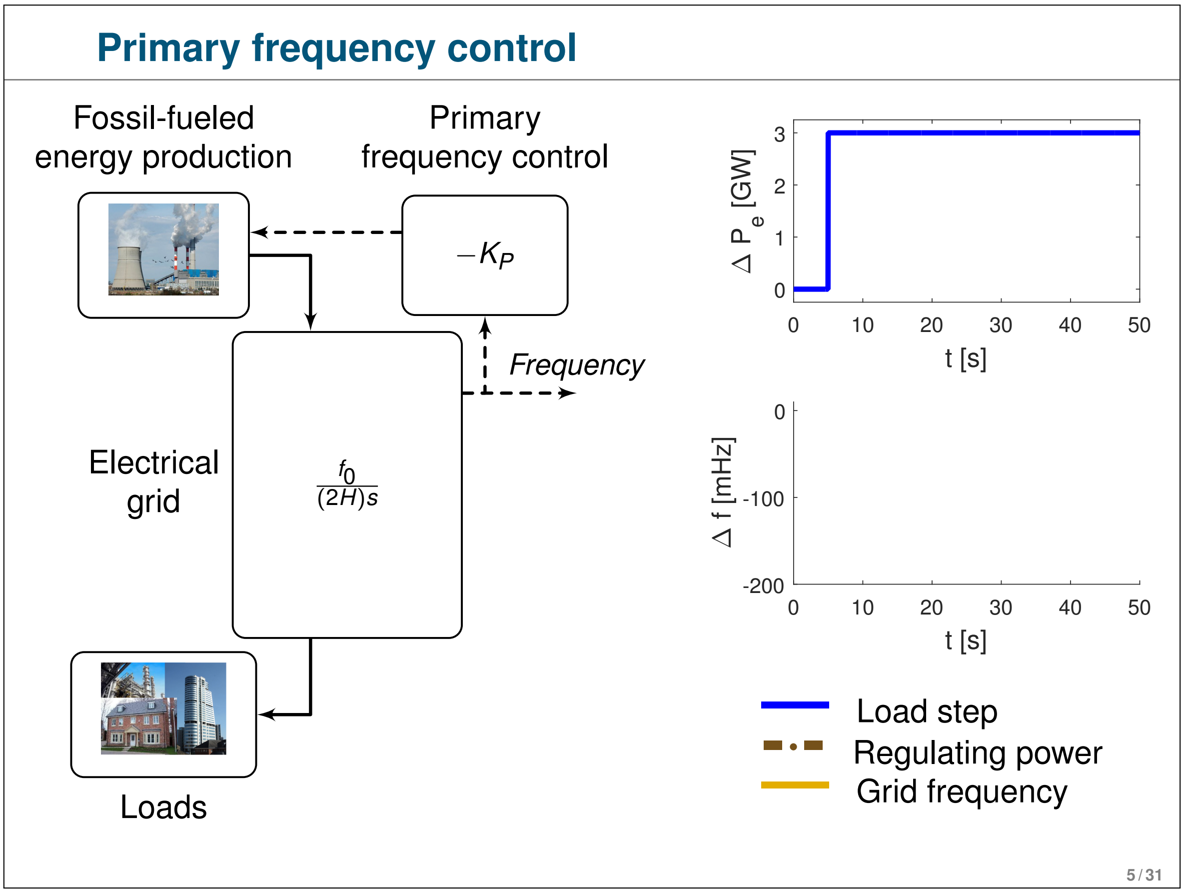
Primary frequency control
Fossil-fueled energy production
Primary frequency control
$-K_P$
Frequency
Electrical grid
$\frac{f_0}{(2H)s}$
Loads
Δ P_e [GW]
t [s]
Δ f [mHz]
t [s]
Load step
Regulating power
Grid frequency
5 / 31

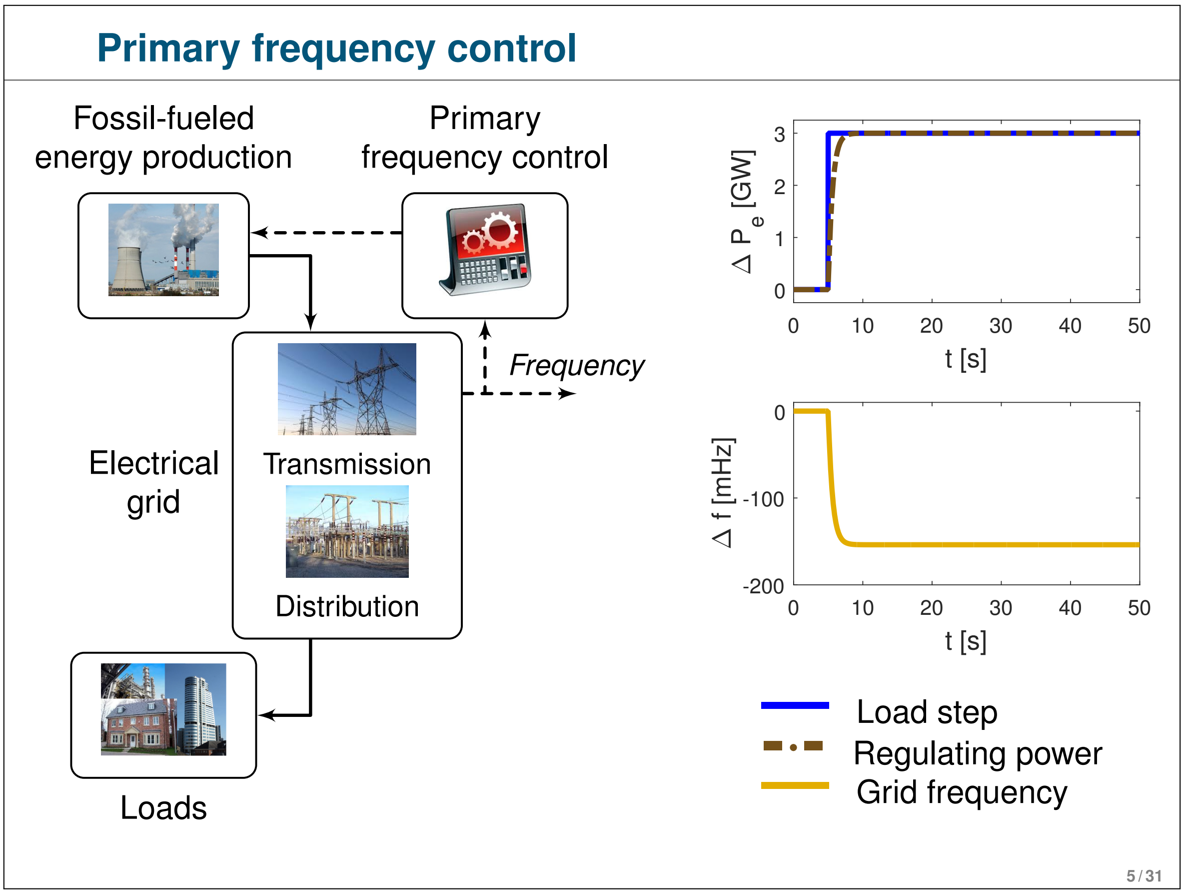
Primary frequency control
Fossil-fueled energy production
Primary frequency control
Frequency
Electrical grid
Transmission
Distribution
Loads
Δ P_e [GW]
t [s]
Δ f [mHz]
t [s]
Load step
Regulating power
Grid frequency
5 / 31

Secondary frequency control

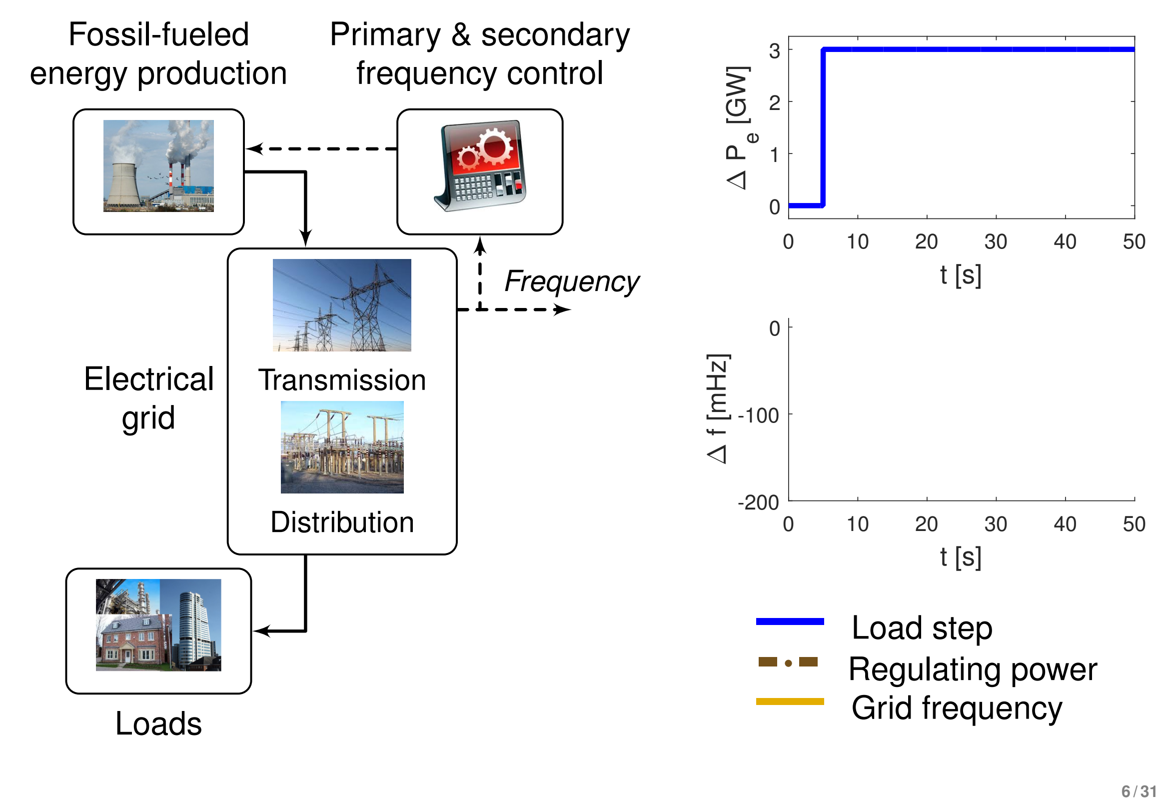

Secondary frequency control

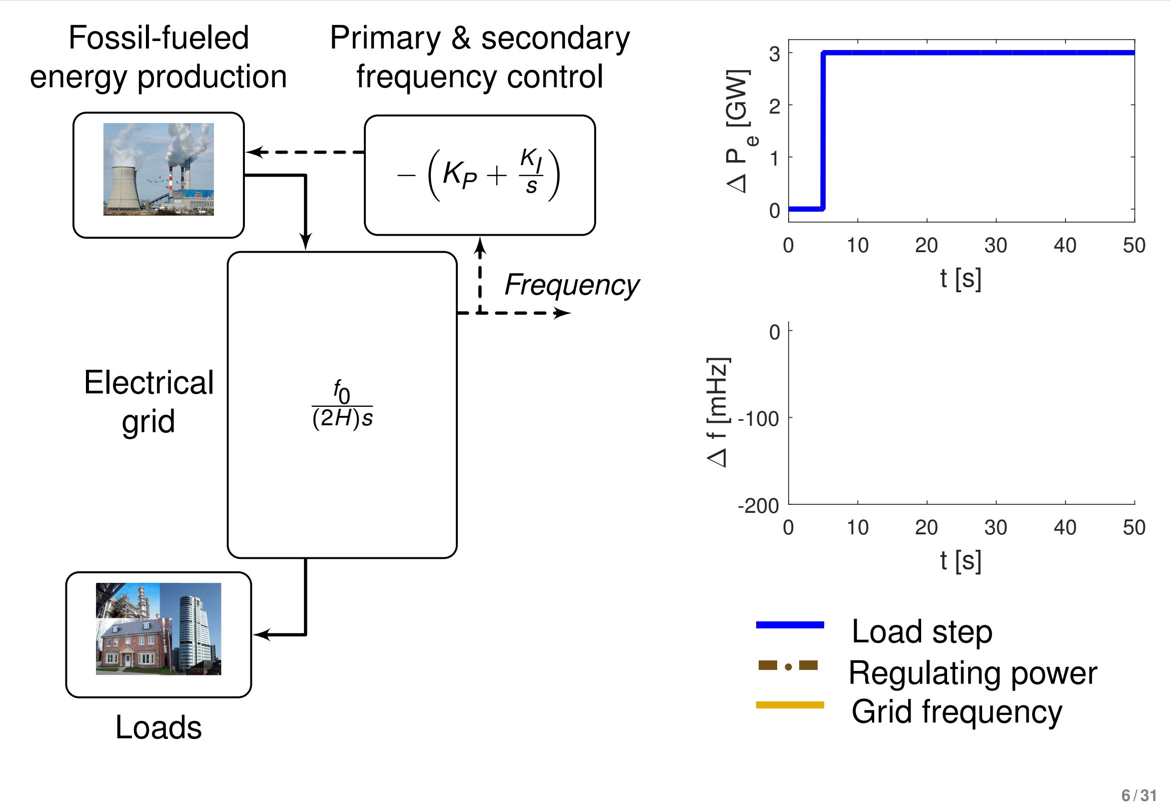

Secondary frequency control

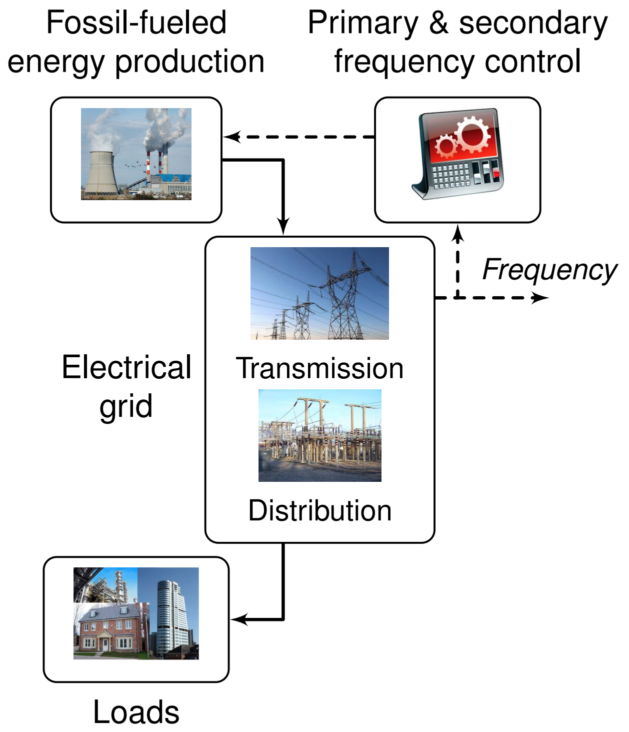

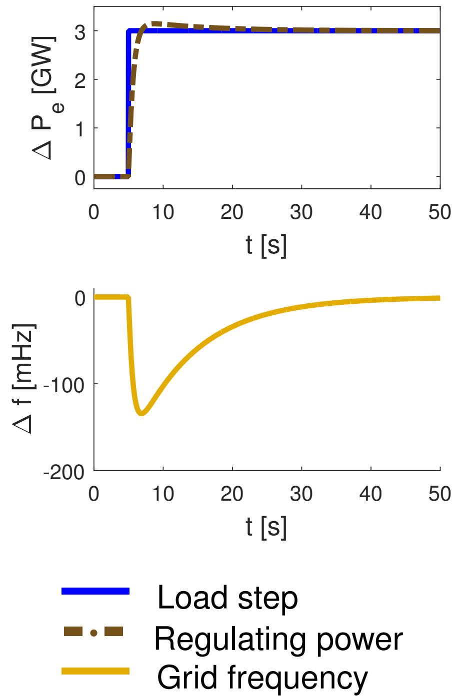

6 / 31

Frequency control in future power systems

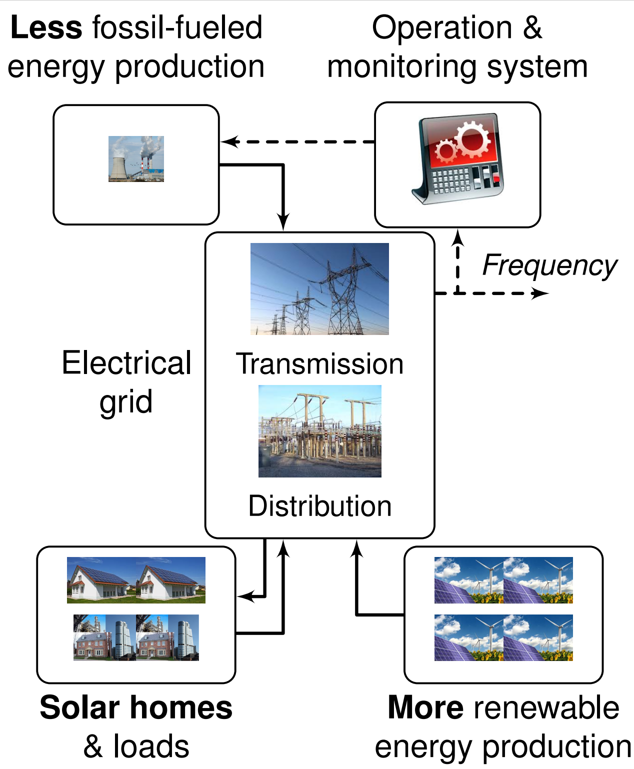

- Reduction of fossil-fueled power plants
- Increasing amount of renewable energy plants at distribution level
- Increasing amount of solar homes

7 / 31

Frequency control in future power systems

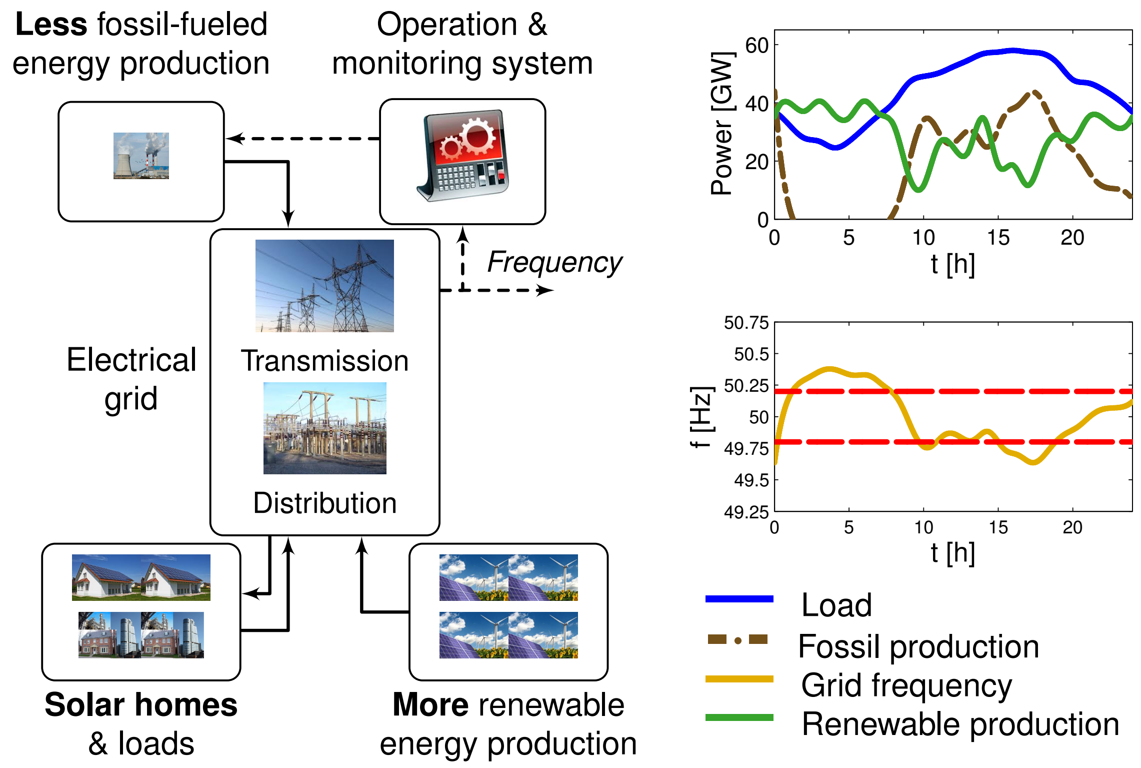

Frequency control in future power systems

Need to integrate renewables into frequency control!

This requires faster, smarter and more flexible network control technologies

Secondary frequency control

Power system model

- Heterogeneous generation pool: rotational synchronous generators (SGs) and inverter-interfaced units
- Dynamics of the generation unit at i-th node

$$\dot{\theta}_i = \omega_i,$$
$$M_i \dot{\omega}_i = -D_i(\omega_i - \omega^d) + P_i^d - P_i + u_{\text{sec},i}$$

- Active power flow at i-th node

$$P_i = G_{ii} V_i^2 + \sum_{k \in \mathcal{N}_i} |B_{ik}| V_i V_k \sin(\theta_i - \theta_k)$$

$\mathcal{N} = \{1, 2, \ldots, n\}$	set of network nodes
$\mathcal{N}_i = \{k \in \mathcal{N} \mid B_{ik} \neq 0\}$	set of neighboring nodes of i-th node

θ_i	phase angle
ω_i	frequency
M_i	inertia constant
D_i	damping constant
ω^d	frequency setpoint
P_i^d	active power setpoint
$u_{\text{sec},i}$	secondary control input

9 / 31

Detailed modeling of inverter-interfaced units

Automatica 74 (2016) 135–150

Contents lists available at ScienceDirect

Automatica

journal homepage: www.elsevier.com/locate/automatica

Survey paper

A survey on modeling of microgrids—From fundamental physics to phasors and voltage sources ☆

Johannes Schiffer [a,1], Daniele Zonetti [b], Romeo Ortega [b], Aleksandar M. Stanković [c], Tevfik Sezi [d], Jörg Raisch [e,f]

[a] School of Electronic and Electrical Engineering, University of Leeds, Leeds LS2 9JT, UK
[b] Laboratoire des Signaux et Systémes, École Supérieure d'Electricité (SUPELEC), Gif-sur-Yvette 91192, France
[c] Tufts University, Medford, MA 02155, USA
[d] Siemens AG, Smart Grid Division, Energy Automation, Humboldtstr. 59, 90459 Nuremberg, Germany
[e] Technische Universität Berlin, Einsteinufer 11, 10587 Berlin, Germany
[f] Max-Planck-Institut für Dynamik komplexer technischer Systeme, Sandtorstr. 1, 39106 Magdeburg, Germany

ARTICLE INFO

Article history:
Received 17 May 2016
Received in revised form
17 May 2016
Accepted 21 June 2016

Keywords:
Microgrid modeling
Microgrid analysis
Smart grid applications
Inverters

ABSTRACT

Microgrids have been identified as key components of modern electrical systems to facilitate the integration of renewable distributed generation units. Their analysis and controller design require the development of advanced (typically model-based) techniques naturally posing an interesting challenge to the control community. Although there are widely accepted reduced order models to describe the dynamic behavior of microgrids, they are typically presented without details about the reduction procedure—hampering the understanding of the physical phenomena behind them. Preceded by an introduction to basic notions and definitions in power systems, the present survey reviews key characteristics and main components of a microgrid. We introduce the reader to the basic functionality of DC/AC inverters, as well as to standard operating modes and control schemes of inverter-interfaced power sources in microgrid applications. Based on this exposition and starting from fundamental physics, we present detailed dynamical models of the main microgrid components. Furthermore, we clearly state the underlying assumptions which lead to the standard reduced model with inverters represented by controllable voltage sources, as well as static network and load representations, hence, providing a complete modular model derivation of a three-phase inverter-based microgrid.

Steady-state power balance

- *Net power balance* in synchronized state

$$\underbrace{\sum\nolimits_{i\in\mathcal{N}} D_i(\omega^* - \omega^d)}_{\text{primary control}} = \underbrace{\sum\nolimits_{i\in\mathcal{N}} P_i^d}_{\text{injection setpoints}} + \underbrace{\sum\nolimits_{i\in\mathcal{N}} u^*_{\mathrm{sec},i}}_{\text{secondary control}}$$

- Power setpoints P_i^d are usually not known exactly

$\rightarrow$ $\omega^* = \omega^d$ only if secondary control inputs compensate for load uncertainty

Secondary frequency control - Problem statement

Problem (Optimal secondary control)

Design a control law for the control inputs $u_{sec,i}$ such that the following performance objectives are satisfied.

1. *Zero steady-state frequency deviation, that is,*

$$\lim_{t\to\infty} \|\omega_i - \omega^d\| = 0, \quad \forall i \in \mathcal{N}, \quad \omega^d \in \mathbb{R}_{>0}.$$

2. *Optimal steady-state resource allocation, that is,*

$$\begin{aligned} \text{minimize}_{u^*_{sec}} & \textstyle\sum_{i\in\mathcal{N}} A_i (u^*_{sec,i})^2, \quad A_i \in \mathbb{R}_{>0}, \\ \textit{subject to} & \textstyle\sum_{i\in\mathcal{N}} u^*_{sec,i} + \sum_{i\in\mathcal{N}} P^d_i = 0, \end{aligned}$$

where $A_i > 0$ is the cost coefficient for source $i \in \mathcal{N}$.

Distributed averaging integral (DAI) frequency control

$$\begin{aligned} u_{\mathrm{sec},i} &= -p_i, \\ \dot{p}_i &= K_i(\omega_i - \omega^d) - K_i A_i \sum_{k\in\mathcal{C}_i} a_{ik}(A_i p_i - A_k p_k), \quad i = 1, \dots, n \end{aligned}$$

- $\mathcal{C}_i$ set of neighboring nodes of i-th node in communication network
- DAI frequency control first proposed by J. Simpson-Porco et al. (Automatica'13)

Consensus-based distributed ctrl in power systems

Secondary Frequency and Voltage Control of Islanded Microgrids via Distributed Averaging

John W. Simpson-Porco, *Student Member, IEEE*, Qobad Shafiee, *Member, IEEE*, Florian Dörfler, *Member, IEEE*, Juan C. Vasquez, *Senior Member, IEEE*, Josep M. Guerrero, *Fellow, IEEE*, and Francesco Bullo, *Fellow, IEEE*

IEEE TRANSACTIONS ON CONTROL SYSTEMS TECHNOLOGY

Distributed Reactive Power Sharing Control for Microgrids With Event-Triggered Communication

Yuan Fan, Guoqiang Hu, *Member, IEEE*, and Magnus Egerstedt, *Fellow, IEEE*

A modular design of incremental Lyapunov functions for microgrid control with power sharing

C. De Persis and N. Monshizadeh

. . . and many more

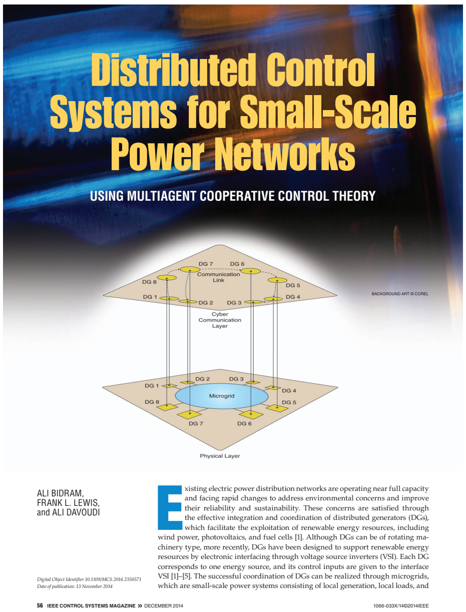
Distributed Control Systems for Small-Scale Power Networks

USING MULTIAGENT COOPERATIVE CONTROL THEORY

ALI BIDRAM, FRANK L. LEWIS, and ALI DAVOUDI

Existing electric power distribution networks are operating near full capacity and facing rapid changes to address environmental concerns and improve their reliability and sustainability. These concerns are satisfied through the effective integration and coordination of distributed generators (DGs), which facilitate the exploitation of renewable energy resources, including wind power, photovoltaics, and fuel cells [1]. Although DGs can be of rotating machinery type, more recently, DGs have been designed to support renewable energy resources by electronic interfacing through voltage source inverters (VSI). Each DG corresponds to one energy source, and its control inputs are given to the interface VSI [1]–[5]. The successful coordination of DGs can be realized through microgrids, which are small-scale power systems consisting of local generation, local loads, and

Digital Object Identifier 10.1109/MCS.2014.2350571
Date of publication: 13 November 2014

56 IEEE CONTROL SYSTEMS MAGAZINE » DECEMBER 2014 — 1066-033X/14©2014IEEE

Nominal closed-loop system

$$\begin{aligned}
\dot{\theta} &= \omega, \\
M\dot{\omega} &= -D(\omega - \mathbb{1}_n\omega^d) + P^d - P - p, \\
\dot{p} &= K(\omega - \mathbb{1}_n\omega^d) - KA\mathcal{L}Ap
\end{aligned}$$

- $\mathcal{L} = \mathcal{L}^\top \in \mathbb{R}^{n\times n}$ . . . Laplacian matrix of undirected and connected communication graph induced by communication network

$$\begin{aligned}
\theta &= \mathrm{col}(\theta_i) \in \mathbb{R}^n \\
\omega &= \mathrm{col}(\omega_i) \in \mathbb{R}^n \\
M &= \mathrm{diag}(M_i) \in \mathbb{R}^{n\times n} \\
D &= \mathrm{diag}(D_i) \in \mathbb{R}^{n\times n} \\
K &= \mathrm{diag}(K_i) \in \mathbb{R}^{n\times n} \\
P^d &= \mathrm{col}(P_i^d) \in \mathbb{R}^n \\
P &= \mathrm{col}(P_i) \in \mathbb{R}^n \\
p &= \mathrm{col}(p_i) \in \mathbb{R}^n \\
A &= \mathrm{diag}(A_i) \in \mathbb{R}^{n\times n}
\end{aligned}$$

Steady-state optimality with DAI

Definition (Synchronized motion)

The power system admits a synchronized motion if it has a solution for all $t \geq 0$ of the form

$$\theta^*(t) = \theta_0^* + \omega^* t, \quad \omega^* = \omega^s \mathbb{1}_n, \quad p^* \in \mathbb{R}^n,$$

where $\omega^s \in \mathbb{R}$ and $\theta_0^* \in \mathbb{R}^n$ such that

$$|\theta_{0,i}^* - \theta_{0,k}^*| < \frac{\pi}{2} \quad \forall i \in \mathcal{N}, \ \forall k \in \mathcal{N}_i.$$

Lemma (Synchronized motion, JS & F. Dörfler'16)

- *DAI-controlled power system possesses at most one synchronized motion*
- *This synchronized motion satisfies*

$$\omega^* = \mathbb{1}_n \omega^d, \ \ p^* = cA^{-1}\mathbb{1}_n, \ \ c = \frac{\mathbb{1}_n^\top P^d}{\mathbb{1}_n^T A^{-1} \mathbb{1}_n}$$

- p^* *is unique minimizer of optimal resource allocation problem*

Robustness of DAI control with respect to communication uncertainties

Impact of communication uncertainties

$$\begin{aligned}\dot{\theta} &= \omega,\\ M\dot{\omega} &= -D(\omega - \mathbb{1}_n\omega^d) + P^d - P - p,\\ \dot{p} &= K(\omega - \mathbb{1}_n\omega^d) - KA\mathcal{L}Ap\end{aligned}$$

- DAI is distributed protocol

→ Need information exchange between units

How do uncertainties on cyber and communication layer affect robustness and performance of DAI-controlled power systems?

Communication uncertainties in DAI control (1)

1) Link failures and packet losses

- Model: dynamic communication network with switched communication topology $\mathcal{G}_{\sigma(t)}$
- $\sigma : \mathbb{R}_{\geq 0} \to \mathcal{M}$ is switching signal
- $\mathcal{M} = \{1, 2, \ldots, \nu\}$, $\nu \in \mathbb{R}_{>0}$, is index set
- Laplacian matrix corresponding to index $\ell = \sigma(t) \in \mathcal{M}$
  $\mathcal{L}_\ell = \mathcal{L}_\ell^\top = \mathcal{L}(\mathcal{G}_\ell) \in \mathbb{R}^{n \times n}$

Assumption (Uniformly connected communication topologies)

The communication topology $\mathcal{G}_{\sigma(t)}$ is undirected and connected for all $t \in \mathbb{R}_{\geq 0}$.

Communication uncertainties in DAI control (2)

2) Communication delays

- Model: message sent by generation unit $k \in \mathcal{N}$ to generation unit $i \in \mathcal{N}$ over communication channel (i.e., edge) $\{i, k\}$ is affected by fast-varying delay $\tau_{ik} : \mathbb{R}_{\geq 0} \rightarrow [0, \bar{h}]$, $\bar{h} \in \mathbb{R}_{\geq 0}$

$\rightarrow$ Resulting control error e_{ik} is then computed as

$$e_{ik}(t) = A_{ii} p_i(t - \tau_{ik}(t)) - A_{kk} p_k(t - \tau_{ik}(t)),$$

i.e., protocol is only executed after message from node k arrives at node i

- We allow for $\tau_{ik}(t) \neq \tau_{ki}(t)$

Closed-loop system with communication uncertainties

- Switched nonlinear delay-differential system

$$\begin{aligned}
\dot{\theta} &= \omega, \\
M\dot{\omega} &= -D(\omega - \omega^d \mathbb{1}_n) + P^d - P - p, \\
\dot{p} &= K(\omega - \mathbb{1}_n \omega^d) - KA \left(\sum_{m=1}^{2|\mathcal{E}_\ell|} T_{\ell,m} A p(t - \tau_m) \right)
\end{aligned}$$

- Matrices $T_{\ell,m}$ describe delayed information flow and satisfy

$$\mathcal{L}_\ell = \sum_{m=1}^{2|\mathcal{E}_\ell|} T_{\ell,m}$$

Problem: Robust stability of DAI frequency control

Problem (Conditions for robust stability)

Given $\bar{h}_i \in \mathbb{R}_{\geq 0}$, $i = 1, \ldots, 2\bar{\mathcal{E}}$, $\bar{\mathcal{E}} = \max_{\ell \in \mathcal{M}} |\mathcal{E}_\ell|$, derive conditions under which the solutions of the secondary-controlled power system converge asymptotically to a synchronized motion.

22 / 31

Proposed solution

- Three main challenges:
  - Time delays
  - Time-varying dynamics
  - Positive semidefiniteness of Laplacian matrix $\mathcal{L}$ results in non-strict $\dot{V}$ in standard Lyapunov approaches

Eliminate invariant subspace of system dynamics via coordinate transformation

↓

Construct strict Lyapunov function for nominal system

Lyapunov-Krasosvkii method

↓

Construct a suitable *strict* common Lyapunov-Krasovskii functional

23 / 31

Main result

Proposition (Robust stability)

- *Fix A and D as well as some* $\bar{h}_m \in \mathbb{R}_{\geq 0}$, $m = 1, \ldots, 2\bar{\mathcal{E}}$
- *Select K such that for all* $\mathcal{T}_{\ell,m}$ *and* $\bar{\mathcal{L}}_\ell$, $\ell = 1, \ldots, |\mathcal{M}|$, *there exist matrices* $S_m > 0 \in \mathbb{R}^{(n-1)\times(n-1)}$, $R_m > 0 \in \mathbb{R}^{(n-1)\times(n-1)}$ *and* $S_{12,m} \in \mathbb{R}^{(n-1)\times(n-1)}$ *satisfying*

$$\Psi(S, R, S_{12}) = \begin{bmatrix} \Psi_{11}(K, \bar{h}) & \Psi_{12}(K, \bar{h}) & \mathbb{0} & \Psi_{14}(K, \bar{h}) \\ * & \Psi_{22}(\bar{h}) & \Psi_{23} & \Psi_{24}(\bar{h}) \\ * & * & R + S & S_{12} + S \\ * & * & * & R + S + \Psi_{44}(\bar{h}) \end{bmatrix} > 0,$$

$R = \text{blockdiag}(R_m),\ S = \text{blockdiag}(S_m),\ S_{12} = \text{blockdiag}(S_{12,m})$

and

$$\begin{bmatrix} R & S_{12} \\ * & R \end{bmatrix} \geq 0$$

- *Then the equilibrium* $z^* = \mathbb{0}_{(3n-1)}$ *is locally uniformly asymptotically stable for all fast-varying delays* $\tau_m(t) \in [0, \bar{h}_m]$

Trading off controller performance for robust stability

Corollary (Performance-robustness-trade-off)

- *Fix A and D as well as some* $\bar{h} \in \mathbb{R}_{\geq 0}$
- *Suppose that* $\tau_m(t) = \tau(t) \in [0, \bar{h}]$
- *Set* $K = \kappa\mathcal{K}$, *where* $\kappa \in \mathbb{R}_{\geq 0}$ *and* $\mathcal{K} \in \mathbb{R}^{n\times n}_{>0}$ *is a diagonal matrix with positive diagonal entries*
- *Then there is* $\kappa > 0$ *sufficiently small, such that the equilibrium* $z^* = \mathbb{0}_{(3n-1)}$ *is locally uniformly asymptotically stable for all fast-varying delays* $\tau(t) \in [0, \bar{h}]$

Example - Kundur's two-area-four-machine system

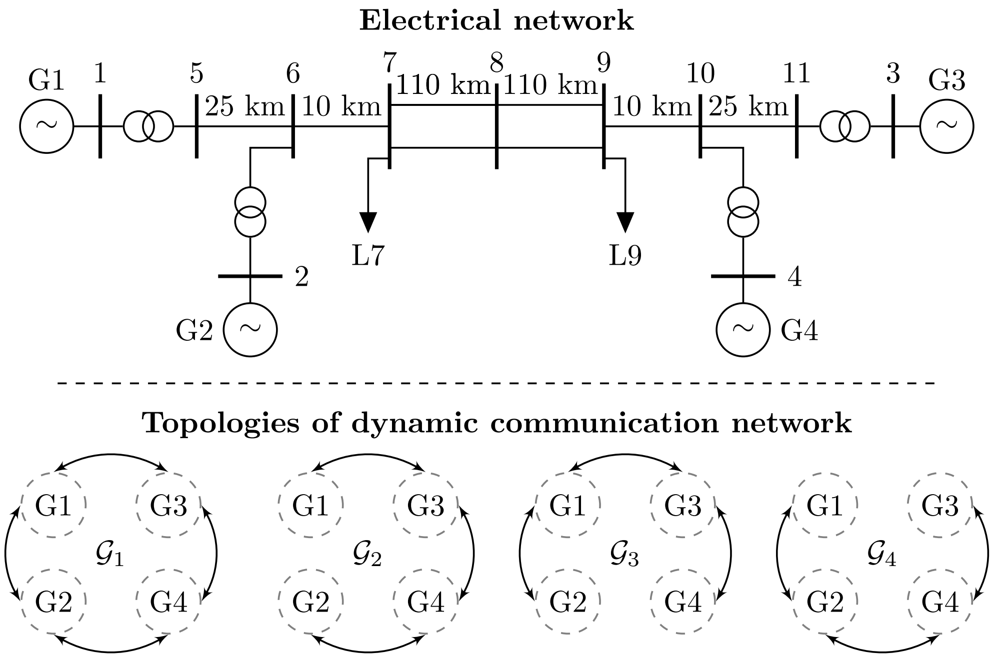

Example - Numerical evaluation

- $\tau_m \in [0, \bar{h}_m]$s, $\bar{h}_m = 2$s, $m = 1, \ldots, 2\bar{\mathcal{E}}$
- $K = \kappa\mathcal{K}$, where $\mathcal{K} = 0.05A^{-1}$
- Obtained feasible gain with *guaranteed* robust stability is $\kappa_{\text{feas}} = 1.544$

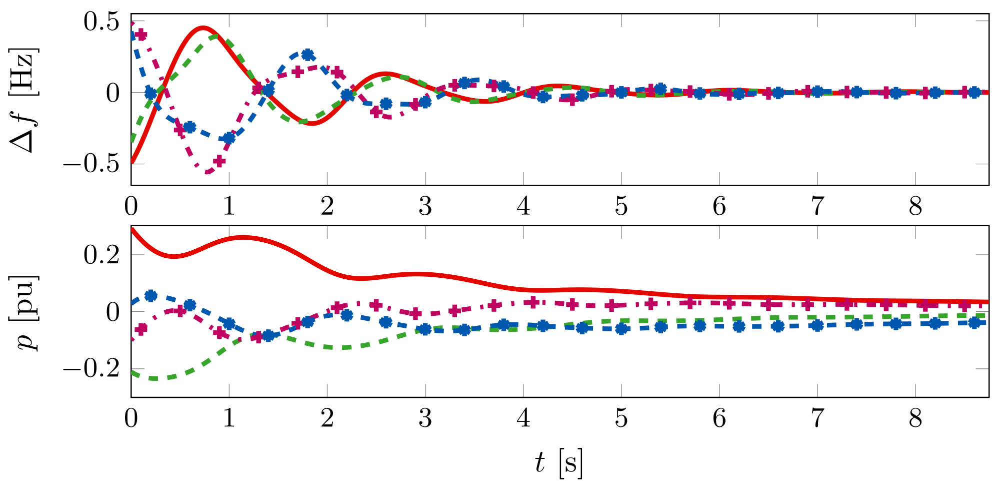

Example - Conservativeness of the conditions (1)

- Robust stability conditions are *equilibrium-independent*

→ If feasible they guarantee (local) stability of any equilibrium point satisfying standard requirement of equilibrium angle differences being contained in an arc of length $\pi/2$

- We consider three different operating points

$\theta^{*,1}$ [rad]	$[0.224, 0.117, -0.076, -0.189] \cdot \pi/2$
$\theta^{*,2}$ [rad]	$[0.3, -0.4, -0.5, 0.4] \cdot 3\pi/8$
$\theta^{*,3}$ [rad]	$[0.3, -0.4, -0.5, 0.4] \cdot \pi/2$

Example - Conservativeness of the conditions (2)

Operating point	Max. feasible gain in simulation	Ratio to analytically predicted gain κ
1	$\kappa_{\text{feas,sim}} = 6.330$	4.1
2	$\kappa_{\text{feas,sim}} = 2.856$	1.85
3	$\kappa_{\text{feas,sim}} = 1.698$	1.1

Conclusions

- Time delays and communication uncertainties pose significant threat to power system stability
- Main focus in this talk: robust stability of DAI-secondary-frequency-controlled power systems
- Considered phenomena: fast-varying delays, link failures and packet losses
- Proposed approach: delay-dependent stability assessment based on common Lyapunov-Krasovskii functional
- Verification of conditions does not require knowledge of operating point
- Future extensions
  - Include voltage and reactive power dynamics + controllers
  - Consider structure-preserving models
  - Relax uniform connectivity assumption

30 / 31

Selected publications

J. Schiffer, F. Dörfler and E. Fridman
Cyber-Physical Aspects of Distributed Averaging Control in Power Systems: Time Delays & Dynamic Communication Topology
Automatica, 80:261-271, 2017

J. Schiffer, D. Zonetti, R. Ortega, A. Stankovic, T. Sezi and J. Raisch
A Survey on Modeling of Microgrids - From Fundamental Physics to Phasors and Voltage Sources
Automatica, 74 (12):135-150, 2016

J. Schiffer, E. Fridman, R. Ortega and J. Raisch
Stability of a Class of Delayed Port-Hamiltonian Systems with Application to Microgrids with Distributed Rotational and Electronic Generation,
Automatica, 74 (12):71-79, 2016

J. Schiffer, R. Ortega, A. Astolfi, J. Raisch and T. Sezi
Conditions for Stability of Droop-Controlled Inverter-Based Microgrids
Automatica, 50 (10):2457-2469, 2014

J. Schiffer, T. Seel, J. Raisch and T. Sezi
Voltage Stability and Reactive Power Sharing in Inverter-Based Microgrids with Consensus-Based Distributed Voltage Control
IEEE Transactions on Control Systems Technology, 24 (1):96-109, 2016

D. Efimov, J. Schiffer and R. Ortega
Robustness of Delayed Multistable Systems with Application to Droop-Controlled Inverter-Based Microgrids
International Journal of Control, 89 (5):909-918, 2016

J. Schiffer, C.A. Hans, T. Kral, J. Raisch and R. Ortega
Modelling, Analysis and Experimental Validation of Clock Drift Effects in Low-Inertia Power Systems
IEEE Transactions on Industrial Electronics, Special Section on Power-Electronics-Enabled Autonomous Power Systems (in press), 2017

C. De Persis, N. Monshizadeh, J. Schiffer and F. Dörfler
A Lyapunov Approach to Control of Microgrids with a Network-Preserved Differential-Algebraic Model
55th IEEE Conference on Decision and Control, pp. 2595-2600, Las Vegas, NV, USA, 2016

31 / 31

Fractional-Order Observer for Integer-Order LTI Systems

Christoph Weise[a] **Kai Wulff**[a] **Johann Reger**[a]

We consider a completely observable n-order LTI system

$$\Sigma_{\mathrm{IO}}: \begin{cases} \dot{x}(t) = Ax(t) + Bu(t) & \text{(1a)} \\ y(t) = Cx(t) & \text{(1b)} \end{cases}$$

with initial condition $x(t_0) = x_0$. The solution of the free system ($u \equiv 0$) is given by the well-known matrix exponential function

$$\Phi(t, t_0) = \exp\left(A(t - t_0)\right) \tag{2}$$

as transition matrix, i.e. $x(t) = \Phi(t, t_0)\, x_0$. A fractional order system with a pseudo-state representation may be understood as an extension of the integer-order case. It takes the form

$$\Sigma_{\mathrm{FO}}: \begin{cases} \mathcal{D}^\alpha \tilde{x}(t) = A\tilde{x}(t) + Bu(t) & \text{(3a)} \\ \tilde{y}(t) = C\tilde{x}(t) & \text{(3b)} \end{cases}$$

with n states, the order of differentiation $\alpha \in (0, 2)$ and the initial conditions $\tilde{x}(t_0) = \tilde{x}_0$. In this equation, $\mathcal{D}$ is the fractional-order derivative using Caputo's definition [3, 1]. Since this fractional differential operator is not local, the pseudo transition matrix given by the Mittag-Leffler-function $\mathcal{E}$ reads

$$\tilde{\Phi}(t, t_0) = \mathcal{E}_{\alpha,1}(A(t - t_0)^\alpha) = \sum_{i=0}^{\infty} \frac{(A(t - t_0)^\alpha)^i}{\Gamma(\alpha i + 1)} \tag{4}$$

and depends on the complete past of the system, see [1]. In opposition to the exponential function the scalar Mittag-Leffler-functions exhibits an algebraic decay [2] which leads to a slow convergence for large times. At initial time t_0, however, the derivative is unbounded.

Our aim is to exploit this property for designing observers that show a faster convergence of the estimation error.

Main result

The connection of fractional-order systems with some class of time-varying integer-order systems has been discussed in previous works [4, 5]. However, in this contribution we derive a fractional-order system associated with the integer-order system to be observed, that is

$$\mathcal{D}^\alpha z(t) = \underbrace{\begin{pmatrix} 0 & I & 0 & \cdots & 0 \\ 0 & 0 & I & \cdots & 0 \\ \vdots & \vdots & \vdots & \ddots & \vdots \\ 0 & 0 & 0 & \cdots & I \\ A & 0 & 0 & \cdots & 0 \end{pmatrix}}_{\bar{A}} z(t) + \underbrace{\begin{pmatrix} 0 \\ 0 \\ \vdots \\ 0 \\ B \end{pmatrix}}_{\bar{B}} \bar{u}(t)\,, \tag{5}$$

[a]Fachgebiet Regelungstechnik, Technische Universität Ilmenau, Helmholtzplatz 5, D-98693 Ilmenau, E-Mail: {`christoph.weise,johann.reger`}`@tu-ilmenau.de`

where $\alpha^{-1} = k \in \mathbb{N}$ is the rational order of differentiation and the new input is defined by a fractional-order integral with respect to the original input $\bar{u}(t) = \mathcal{I}^{(k-1)\alpha}u(t) = \mathcal{I}^{1-\alpha}u(t)$. The extended state z then contains the original state and its fractional order integrals, i.e.

$$z(t) = \begin{pmatrix} z_1(t) \\ z_2(t) \\ \vdots \\ z_{k-1}(t) \\ z_k(t) \end{pmatrix} = \begin{pmatrix} \mathcal{I}^{(k-1)\alpha}x(t) \\ \mathcal{I}^{(k-2)\alpha}x(t) \\ \vdots \\ \mathcal{I}^{\alpha}x(t) \\ x(t) \end{pmatrix}. \tag{6}$$

Choosing matching initial conditions

$$z(0)^\top = \begin{pmatrix} 0 & 0 & \cdots & 0 & x_0^\top \end{pmatrix}^\top \tag{7}$$

we conclude that $z_k(t) = x(t)$, thus the trajectories are identical. When initializing properly, this associated fractional-order system captures various properties of the original integer-order LTI system, e.g. system (5) inherits to be stable, observable or controllable if the original system (1) exhibits the corresponding property. We can also formulate a direct connection of the eigenvalues of the integer-order and associated fractional-order system.

Using this system we obtain an observer that shows a very fast convergence immediately after initialization and a poor convergence for large times. In order to overcome the latter problem we propose two strategies:

- Reinitialization of the observer in short intervals may lead to a convergence faster than exponential.
- The concept of impulsive observers [6] can be extended to fractional-order systems such that the observer converges in fixed time and the performance is increased in the first time interval.

[1] C. Monje, Y. Chen, B. Vinagre, D. Xue, and V. Feliu-Batlle, *Fractional-order Systems and Controls: Fundamentals and Applications.* Springer, 2010.

[2] F. Mainardi and R. Gorenflo, "On Mittag-Leffler-type functions in fractional evolution processes," *Journal of Computational and Applied Mathematics*, vol. 118, no. 1–2, pp. 283–299, Jun. 2000.

[3] I. Podlubny, *Fractional Differential Equations: An Introduction to Fractional Derivatives, Fractional Differential Equations, to Methods of Their Solution and Some of Their Applications.* Academic Press, 1999.

[4] B. Bandyopadhyay and S. Kamal, *Stabilization and Control of Fractional Order Systems: A Sliding Mode Approach.* Springer, 2014.

[5] C. Weise, K. Wulff, and J. Reger, "Exponentially Converging Observer for a Class of FO-LTI Systems," in *IEEE Multi-conference on Systems and Control (MSC)*, Sept 2016.

[6] T. Raff, *Impulsive Observers for Continuous Time Systems and Global Output Feedback Control.* VDI-Verlag, 2010.

Fachgebiet Regelungstechnik

TECHNISCHE UNIVERSITÄT ILMENAU

Fractional-Order Observer for Integer-Order LTI Systems

Christoph Weise*

christoph.weise@tu-ilmenau.de

* Control Engineering Group, TU Ilmenau, Germany

12th September 2017

20. Styrian Workshop on Automatic Control, Retzhof

Outline

Motivating Questions

1. How are integer-order LTI systems connected to fractional-order LTI systems?
2. How can we use this connection for state estimation of integer-order LTI systems?

Fractional-Order Operators

To generalize the derivative to non-integer order, the fractional-order integral is needed for $t > 0$:

$$\mathcal{I}^\alpha f(t) = \frac{1}{\Gamma(\alpha)} \int_0^t (t-\tau)^{\alpha-1} f(\tau)\,\mathrm{d}\tau, \qquad \mathcal{L}\{\mathcal{I}^\alpha f(t)\} = \frac{\mathcal{L}\{f(t)\}}{s^\alpha}$$

CAPUTO'S definition combines the integer-order derivative and the fractional-order integral:

$$\mathcal{D}^\alpha f(t) = \frac{1}{\Gamma(m-\alpha)} \int\limits_0^t \frac{f^{(m)}(\tau)}{(t-\tau)^{\alpha-m+1}}\,\mathrm{d}\tau, \qquad m-1 < \alpha < m$$

$$\mathcal{L}\{\mathcal{D}^\alpha f(t)\} = s^\alpha \mathcal{L}\{f(t)\} - \sum_{k=0}^{m-1} s^{\alpha-k-1} f^{(k)}(0)$$

Properties

$$\mathcal{D}^{\alpha} f(t) = \frac{1}{\Gamma(m-\alpha)} \int_0^t \frac{f^{(m)}(\tau)}{(t-\tau)^{\alpha-m+1}} \,\mathrm{d}\tau, \qquad m-1 < \alpha < m$$

Properties:

- Identity $\alpha = 0$: $\mathcal{D}^0 f(t) = f(t)$ (by LEIBNIZ' rule)
- Integer-order case $\alpha = 1$: $\mathcal{D}^1 f(t) = \dot{f}(t)$
- Linear: $a\mathcal{D}^{\alpha} f_1(t) + b\mathcal{D}^{\alpha} f_2(t) = \mathcal{D}^{\alpha}\left(af_1(t) + bf_2(t)\right)$
- Composition – in general: $\mathcal{D}^{\beta}(\mathcal{D}^{\alpha} f(t)) \neq \mathcal{D}^{\alpha+\beta} f(t)$
- Scaling: $\mathcal{D}^{\alpha} f(\gamma t) = \gamma^{\alpha}\mathcal{D}^{\alpha} f(t)$

Fractional Order LTI System

$$\Sigma_{\mathrm{FO}} : \begin{cases} \mathcal{D}^{\alpha} x(t) = Ax(t) + Bu(t)\,, & x(0) = x_0 \\ y(t) = Cx(t) + Du(t) \end{cases}$$

with: state $x(t) \in \mathbb{R}^n$, input $u(t) \in \mathbb{R}^q$, output $y(t) \in \mathbb{R}^p$, order of differentiation $\alpha \in (0, 2)$ and fitting real-valued matrices A, B, C and D.

The solution to the initial value problem is given by

$$x(t) = \mathcal{E}_{\alpha,1}(At^{\alpha})x_0 + \int_0^t (t-\tau)^{\alpha-1}\mathcal{E}_{\alpha,\alpha}(A(t-\tau)^{\alpha})Bu(\tau)\,\mathrm{d}\tau$$

with the MITTAG-LEFFLER-Function

$$\mathcal{E}_{\alpha,\beta}(z) = \sum_{k=0}^{\infty} \frac{z^k}{\Gamma(\alpha k + \beta)}, \qquad \alpha, \beta > 0.$$

Properties of the Mittag-Leffler-Function – I

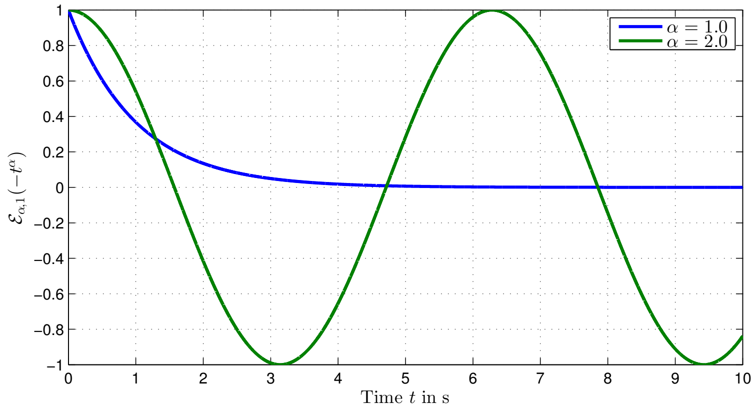

- Generalisation of the matrix-exponential function: $\mathcal{E}_{1,1}(At) = e^{At}$
- Oscillations for $\alpha > 1$: $\mathcal{E}_{2,1}(-\lambda t) = \cos(\lambda t)$

Properties of the Mittag-Leffler-Function – II

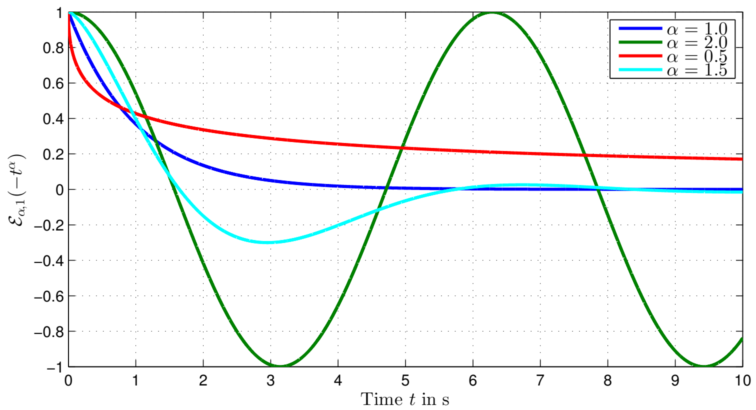

- Infinite derivative at the initial time $t = 0$ for $\alpha \in (0, 1)$:

$$\dot{\mathcal{E}}_{\alpha,1}(\lambda t^\alpha) = t^{-1} \sum_{k=1}^{\infty} \frac{\alpha k (\lambda t^\alpha)^k}{\Gamma(\alpha k + 1)}, \qquad \lambda < 0\,.$$

- Algebraic decay for $\alpha \in (0, 1)$: $\mathcal{E}_{\alpha,1}(-t^\alpha) \sim t^{-\alpha}/\Gamma(1-\alpha)$.

Stability

Theorem (Stability Condition [Monje et al., 2010])

The origin of the system $\mathcal{D}^{\alpha} x(t) = A\, x(t)$ is asymptotically stable (in the sense of Lyapunov) if and only if

$$|\arg(\lambda_i(A))| > \alpha\pi/2, \quad \forall i = 1, 2, \ldots, n,$$

where $\lambda_i(A)$ denotes the i-th eigenvalue of A.

Observability

Definition (Observability [Matignon and d'Andréa-Novel, 1996])

System Σ_{FO} or the pair (C, A) is completely observable on the interval $[t_0, t_1]$ if any initial state $x(t_0)$ can be uniquely determined from knowledge of $y(t)$ and $u(t)$ on the interval $t \in [t_0, t_1]$, only.

Theorem (Observability [Matignon and d'Andréa-Novel, 1996])

System Σ_{FO} or the pair (C, A) is observable iff the observability matrix $\mathcal{O}$ has full rank, i. e. $\operatorname{rank}(\mathcal{O}) = n$, where $\mathcal{O}$ is given by

$$\mathcal{O} = \begin{pmatrix} C \\ CA \\ \vdots \\ CA^{n-1} \end{pmatrix}.$$

Associated Fractional-Order System

For an integer-order LTI system an associated fractional-order LTI system with $\alpha^{-1} = k \in \mathbb{N}$ is given by

$$\mathcal{D}^\alpha z(t) = \underbrace{\begin{pmatrix} 0 & I & 0 & \cdots & 0 \\ 0 & 0 & I & \cdots & 0 \\ \vdots & \vdots & \vdots & \ddots & \vdots \\ 0 & 0 & 0 & \cdots & I \\ A & 0 & 0 & \cdots & 0 \end{pmatrix}}_{\bar{A} \in \mathbb{R}^{kn \times kn}} z(t) + \underbrace{\begin{pmatrix} 0 \\ 0 \\ \vdots \\ 0 \\ B \end{pmatrix}}_{\bar{B} \in \mathbb{R}^{kn \times p}} \bar{u}(t)$$

With the new input $\bar{u}(t) = \mathcal{I}^{(k-1)\alpha} u(t) = \mathcal{I}^{1-\alpha} u(t)$ and initial conditions $z(0) = \begin{pmatrix} 0 & 0 & \cdots & 0 & x_0^\top \end{pmatrix}^\top$ such that:

$$\begin{pmatrix} 0 & 0 & \cdots & 0 & I \end{pmatrix} z(t) = x(t) \qquad \forall t \geq 0$$

Sketch of a Proof

The choice of the extended state $z(t)$

$$z(t) = \begin{pmatrix} z_1(t) \\ \vdots \\ z_{k-1}(t) \\ z_k(t) \end{pmatrix} = \begin{pmatrix} \mathcal{I}^{(k-1)\alpha} x(t) \\ \vdots \\ \mathcal{I}^{\alpha} x(t) \\ x(t) \end{pmatrix}$$

guarantees: $z_i(0) = 0$ for $i = 1, 2, \ldots, k-1$ such that

$$\mathcal{L}\{\mathcal{D}^\alpha z_i(t)\} = s^\alpha Z_i(s) - s^{\alpha-1} z_i(0) = s^\alpha Z_i(s) = Z_{i+1}(s)$$

and for $i = k$

$$\begin{aligned} \mathcal{L}\{\mathcal{D}^\alpha z_k\} = s^\alpha Z_k(s) - s^{\alpha-1} z_k(0) &= A Z_1(s) + B s^{-(1-\alpha)} U(s) \quad \Big| \cdot s^{1-\alpha} \\ s Z_k(s) - z_k(0) &= A s^{1-\alpha} Z_1(s) + B U(s) \\ &= A Z_k(s) + B U(s) \end{aligned}$$

Associated FO-System – Eigenvalues

Theorem (Eigenvalues)

Let λ_i denote some eigenvalue of A. Then $\bar{\lambda}_l$ is an eigenvalue of $\bar{A}$ iff

$$\bar{\lambda}_l^k = \lambda_i, \qquad \text{with:} \qquad \begin{aligned} i &= 1, 2, \ldots, n \\ l &= (i-1)k + 1, \ldots, ik \end{aligned}$$

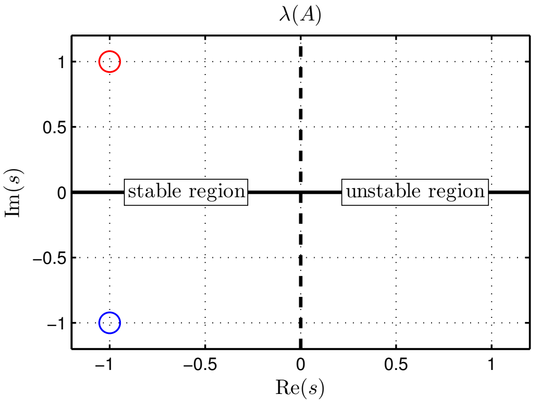

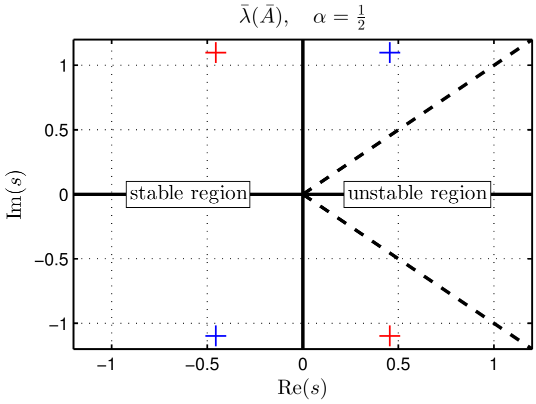

Associated FO-System – Eigenvalues – Proof

We compute the characteristic polynomial of $\bar{A}$ with $\Lambda = \lambda I - \bar{A}$:

$$\left(\begin{array}{c|ccccc} \bar{\lambda} I & -I & 0 & \cdots & 0 \\ 0 & \bar{\lambda} I & -I & \cdots & 0 \\ \vdots & \vdots & \ddots & \ddots & \vdots \\ 0 & 0 & 0 & \ddots & -I \\ \hline -A & 0 & 0 & \cdots & \bar{\lambda} I \end{array}\right) = \left(\begin{array}{c|c} \Lambda_{11} & \Lambda_{12} \\ \hline \Lambda_{21} & \Lambda_{22} \end{array}\right) = \begin{pmatrix} \Lambda_{12} & 0 \\ \Lambda_{22} & I \end{pmatrix} \begin{pmatrix} \Lambda_{12}^{-1}\Lambda_{11} & I \\ \Lambda_{21} - \Lambda_{22}\Lambda_{12}^{-1}\Lambda_{11} & 0 \end{pmatrix}$$

$$\begin{aligned} \det(\Lambda) &= \det(\Lambda_{12}) \det\left(A + \Lambda_{22}\Lambda_{12}^{-1}\Lambda_{11}\right) \\ &= (-1)^{n(k-1)} \det\left(A + \bar{\lambda}^2 \begin{pmatrix} 0 & \cdots & 0 & I \end{pmatrix} \Lambda_{12}^{-1} \begin{pmatrix} I & 0 & \cdots & 0 \end{pmatrix}^\top\right) \\ &= (-1)^{n(k-1)} \det(A - \bar{\lambda}^k I). \end{aligned}$$

Associated FO-System – Eigenvalues

Consequences

- Theorem allows to relate eigenvalues of integer- and fractional order systems although the order of differentiation is different
- The associated system Σ_{FO} inherits its stability properties from the integer-order system Σ_{IO}.
- We might identify integer-order dynamics in disguise.
- For fractional-order systems we can reduce the case $\alpha \in (1, 2)$ to $\bar{\alpha} \in (0, 1)$ regarding stability analysis.

Associated FO-System – Observability

With the output equation:

$$y(t) = \begin{pmatrix} 0 & 0 & \cdots & 0 & C \end{pmatrix} z(t) = \bar{C} z(t)$$

Theorem (Observability – Associated FO System)

The associated FO system Σ_{FO} is completely observable iff the original IO-LTI system Σ_{IO} with $\operatorname{rank}(A) = n$ is completely observable.

The proof uses the observability matrix of the pair $(\bar{C}, \bar{A})$:

$$\bar{\mathcal{O}} = \begin{pmatrix} & \bar{C} & \\ I_k & \otimes & CA \\ I_k & \otimes & CA^2 \\ & \vdots & \\ \begin{pmatrix} I_{k-1} & 0 \end{pmatrix} & \otimes & CA^n \end{pmatrix}$$

$$\operatorname{rank}(\bar{\mathcal{O}}) = \operatorname{rank}(\operatorname{diag}(\mathcal{O}A, \ldots, \mathcal{O}A, \mathcal{O})) = kn \iff \operatorname{rank}(\mathcal{O}) = n$$

Observer Design

The observer design uses the associated fractional-order system:

$$\mathcal{D}^{\alpha}\hat{z}(t) = \bar{A}\hat{z}(t) + \bar{B}\bar{u}(t) + \bar{L}\left(y(t) - \bar{C}\hat{z}(t)\right), \qquad \begin{aligned} \alpha^{-1} &= k \in \mathbb{N} \\ \bar{L} &\in \mathbb{R}^{kn\times q} \end{aligned}$$

This leads to

$$\mathcal{D}^{\alpha} e_z(t) = \left(\bar{A} - \bar{L}\bar{C}\right) e_z(t)$$

of the extended error $e_z(t) = z(t) - \hat{z}(t)$ if the poles of $\left(\bar{A} - \bar{L}\bar{C}\right)$ are placed such that $\bar{\lambda}_l \neq \sqrt[k]{\lambda^\star}$ with $l = 0, 1, \ldots, k-1$ and $\lambda^\star \in \mathbb{C}$.

The extended initial state is partially known:

$$\hat{z}(0)^\top = \begin{pmatrix} 0 & \cdots & 0 & \hat{x}_0^\top \end{pmatrix}^\top \implies e_z(0)^\top = \begin{pmatrix} 0 & \cdots & 0 & e_0^\top \end{pmatrix}^\top$$

To keep the computational costs low we use: $\alpha = \frac{1}{2}$.

Simulation Example

$$\dot{x}(t) = \begin{pmatrix} 0 & 1 \\ -1 & -2 \end{pmatrix} x(t) + \begin{pmatrix} -1 \\ 0.5 \end{pmatrix} \sin(2t) \qquad x(0) = \begin{pmatrix} -2 \\ 3 \end{pmatrix}$$

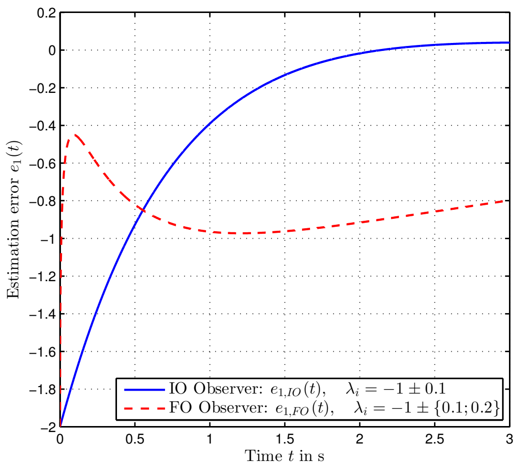

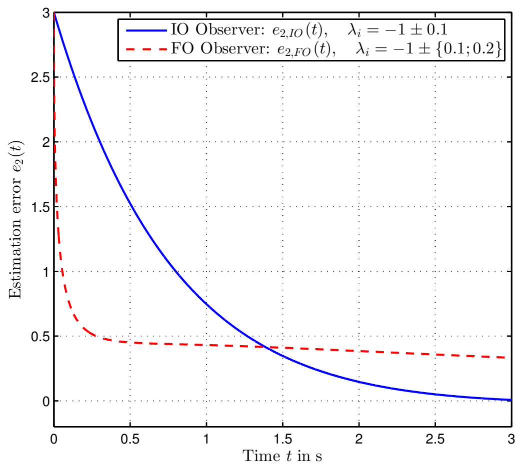

Algebraic Decay Compensation - Reinitialization

The system Σ_{IO} is time-invariant and the observer can be reinitialized:

$$\hat{z}(t_k^+) = \begin{pmatrix} 0 & 0 \\ 0 & I \end{pmatrix} \hat{z}(t_k^-), \qquad t_{k+1} - t_k = \delta > t_{\min}$$

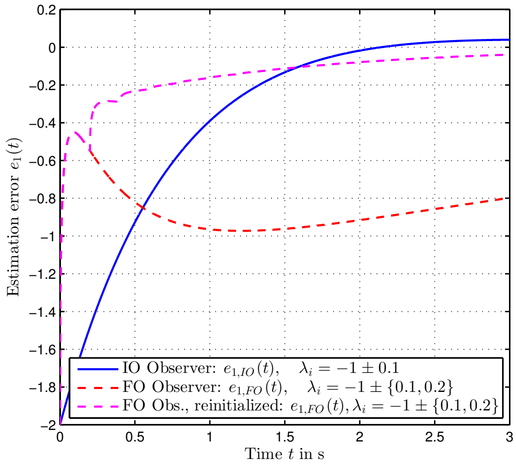

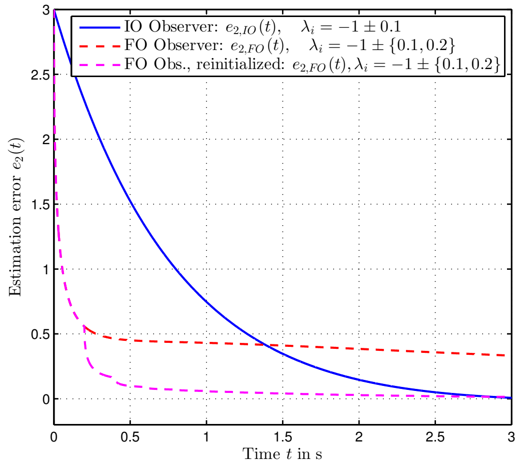

Algebraic Decay Compensation - Impulsive Observer

We use 2 observers with $\alpha = \frac{1}{2}$ in parallel with the estimation error:

$$e_{z,i}(\delta) = \mathcal{E}_{\alpha,1}(\bar{F}_i \delta^\alpha) e_{z,i}(0), \quad \bar{F}_i = \bar{A} - \bar{L}_i \bar{C}, \qquad i = 1, 2$$

Changing to the original coordinates:

$$\underbrace{\begin{pmatrix} I_{2n} & -\mathcal{E}_{\alpha,1}(\bar{F}_1 \delta^\alpha) \\ I_{2n} & -\mathcal{E}_{\alpha,1}(\bar{F}_2 \delta^\alpha) \end{pmatrix}}_{\Omega} \begin{pmatrix} z(\delta) \\ z(0) \end{pmatrix} = \begin{pmatrix} \hat{z}_1(\delta) - \mathcal{E}_{\alpha,1}(\bar{F}_1 \delta^\alpha) \hat{z}_1(0) \\ \hat{z}_2(\delta) - \mathcal{E}_{\alpha,1}(\bar{F}_2 \delta^\alpha) \hat{z}_2(0) \end{pmatrix} = \begin{pmatrix} \tilde{z}_1(\delta) \\ \tilde{z}_2(\delta) \end{pmatrix}$$

Ω^{-1} can be computed off-line and the state is estimated in fixed time δ.
With $z(0) = \begin{pmatrix} 0 & x_0^\top \end{pmatrix}^\top$ the dimension of Ω can be reduced:

$$\tilde{\Omega} = T \Omega T^\top \qquad \text{with} \qquad T = \begin{pmatrix} I & 0 & 0 & 0 \\ 0 & I & 0 & 0 \\ 0 & 0 & 0 & I \end{pmatrix}$$

Algebraic Decay Compensation - Impulsive Observer

$$\mathcal{D}^{\frac{1}{2}} \hat{z}_i(t) = \bar{F}_i \hat{z}(t) + \bar{B}\bar{u}(t) + \bar{L}_i y(t), \qquad t \neq \delta, \quad \hat{z}_i(t_0) = \begin{pmatrix} 0 & \hat{x}_0^\top \end{pmatrix}^\top$$

$$\hat{z}_i(\delta^+) = \begin{pmatrix} 0 & 0 & 0 \\ 0 & I & 0 \end{pmatrix} \tilde{\Omega}^{-1} T \begin{pmatrix} \tilde{z}_1(\delta^-) \\ \tilde{z}_2(\delta^-) \end{pmatrix}, \qquad t = \delta, \quad \hat{x}(t) = \begin{pmatrix} I & 0 \end{pmatrix} \hat{z}_1(t)$$

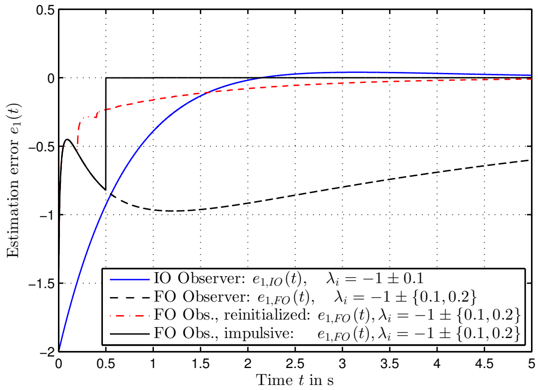

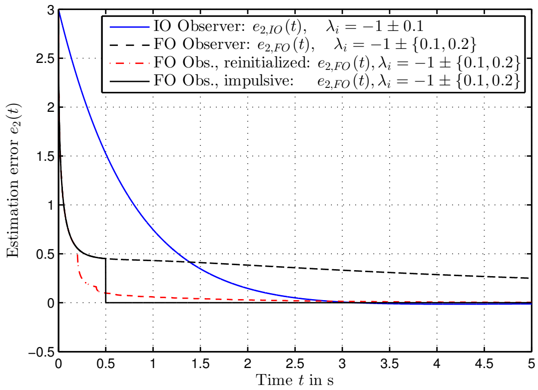

Conclusions & Future Work

Conclusions

- The associated FO system captures the relevant properties of Σ_{IO} (stability, observability, controllability)
- The new observer guarantees a fast convergence short after $t = 0$ (without increasing the peaking phenomenon).
- The algebraic decay for $t \gg 0$ can be avoided (via re-initialization).

Future Work

- Investigation of the observer's robustness
- Optimal choice of the observer gain $\bar{L}$
- Reinitialization time-span: $t_{\min} < \delta < t_{\max}$ for fast convergence

Matignon, D. and d'Andréa-Novel, B. (1996).
Some results on controllability and observability of finite-dimensional fractional differential systems.
In *Proceedings of CESA'96*, volume 2, pages 952–956.

Monje, C., Chen, Y., Vinagre, B., Xue, D., and Feliu-Batlle, V. (2010).
Fractional-order Systems and Controls: Fundamentals and Applications.
Springer.

Podlubny, I. (1999).
Fractional Differential Equations: An Introduction to Fractional Derivatives, Fractional Differential Equations, to Methods of Their Solution and Some of Their Applications.
Aca. Press.

Raff, T. (2010).
Impulsive Observers for Continuous Time Systems and Global Output Feedback Control.
VDI-Verlag.

Weise, C., Wulff, K., and Reger, J. (2016).
Exponentially Converging Observer for a Class of FO-LTI Systems.
In *MSC*, pages 723–729.

Weise, C., Wulff, K., and Reger, J. (2017).
Fractional-Order Observer for Integer-Order LTI Systems.
In *submitted to ASCC 2017*.

Longitudinal tunnel ventilation control: Dynamic feedforward control and non-linear disturbance observation

Nikolaus Euler-Rolle[a] **Stefan Jakubek**[a]

New constructions or refurbishments of road tunnels impose increasingly tight safety requirements on the electrotechnical tunnel equipment such as the ventilation system, as well as on its operation. Particularly in the event of an incident with fire and smoke spreading in the tunnel, adequate safety measures have to be taken without delay to protect life and health of the tunnel users. The main goal is to guarantee a minimum amount of time for persons in the tunnel to safely follow the escape routes with sufficient visibility available. For this purpose, tunnels exceeding a certain minimum length are equipped with ventilation systems.

In this contribution, non-linear longitudinal ventilation control is considered holistically in case of an emergency, where jet fans are used to induce fresh air into the tunnel through one portal and exhaust the smoke through the other. Since the spread of smoke in the tunnel cannot be measured, it is assumed that a safe condition is achieved by maintaining a prescribed average air flow velocity in the tunnel, which is high enough to convey smoke out of the tunnel, but not too high to save the naturally occurring smoke stratification from being destroyed. In this context, control is especially challenging for short tunnels due to their low inertia and the resulting highly dynamic behaviour. In particular, two key elements are investigated. First, the enhancement of classic linear control with a non-linear dynamic feedforward control of the jet fans is considered. Second, the observation and rejection of disturbances is treated. As there are several disturbance influences such as vehicles in the tunnel, buoyancy of hot gases, wind load onto the portals or meteorological pressure differences influencing the flow velocity, a sufficiently fast disturbance rejection capability is required to compensate the quickly changing air flow velocity in the tunnel. For this purpose, the dynamic feedforward control is expanded with the ability to take into account estimated disturbances that are fed back from a non-linear unknown input observer. Non-linear disturbance observation of external influences is achieved by applying a specially structured non-linear observer. Deviations between the measured flow velocity and its estimation are exclusively attributed to external disturbances. As a consequence, the proposed observer has a unique structure that allows to show the stability of the observer for a specific implementation for the open- and closed-loop system with few restrictive assumptions. Based on Lyapunov theory the convergence and stability of the implemented observer is independent of the control scheme. Simulations show significant improvements in the control performance with active disturbance rejection.

The proposed approach to obtain the dynamic feedforward control is based on feedback linearisation as a non-linear system transformation. Feedback linearisation is applied to the air flow model, and the resulting non-linear input transformation is used as model inverse

[a]Institute of Mechanics and Mechatronics, Division of Control and Process Automation, TU Wien, Getreidemarkt 9/E325/A5, 1060 Vienna, Austria, E-mail: `nikolaus.euler-rolle@tuwien.ac.at`, `stefan.jakubek@tuwien.ac.at`

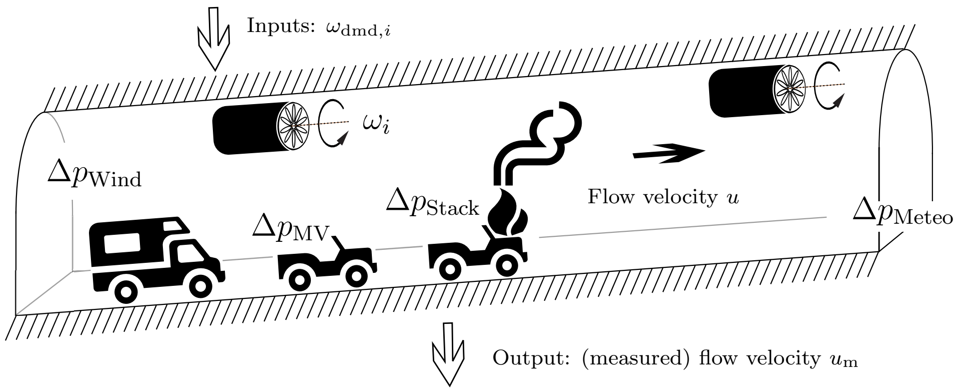

Figure 1: Schematic overview of the air flow model showing the inputs, the output and the individual sources and losses of momentum.

for feedforward control of the rotational speeds of the jet fans. In Figure 1 a schematic overview of the air flow model and the individual sources of momentum in form of equivalent pressure differences is given. The controlled input $\omega_{\mathrm{dmd},i}$ into the model is the demanded rotational speed of each jet fan and the output is the measured air flow velocity u_{m}. However, when applying feedback linearisation, controllability issues in combination with a bifurcation characteristic caused by the absolute values in the Bernoulli equation occasionally lead to implausible control signals. Thus, for a flawlessly robust operation in different conditions, these issues require a modified evaluation of the feedforward control. Instead of the original expression resulting from feedback linearisation, a modified robustness-oriented feedforward control is based on the state transformation for trajectory evaluation in combination with control loops to actuate the individual jet fans.

Both, the proposed non-linear dynamic feedforward control and the disturbance observer have been implemented and tested in the St. Ruprecht motorway tunnel on the Austrian Semmering motorway S6 in course of an encompassing tunnel refurbishment and modernisation. Thus, experiments could have been carried out while the tunnel was closed to traffic. During the final commissioning also a test with an actual fire has been conducted. All results show excellent control performance with significantly reduced correcting feedback control action. Further details and results can be found in [1] and [2].

[1] N. Euler-Rolle, M. Fuhrmann, M. Reinwald, and S. Jakubek. Longitudinal tunnel ventilation control. Part 1: Modelling and dynamic feedforward control. *Control Engineering Practice*, 63:91–103, 2017.

[2] M. Fuhrmann, N. Euler-Rolle, M. Killian, M. Reinwald, and S. Jakubek. Longitudinal tunnel ventilation control. Part 2: Non-linear observation and disturbance rejection. *Control Engineering Practice*, 63:44–56, 2017.

Model Predictive Control with Flatness Based Linear Programming for the Single Mast Stacker Crane

Anastasiia Galkina[a] **Kurt Schlacher**[a]

Introduction

This paper deals with model predictive control (MCP) for a stabilization of a time-optimal motion of a single mast stacker crane (SMC) (see Fig. 1), which is used for an automatic storage or retrieval of payloads in automated warehouses. The mathematical model of the plant is a distributed parameter one, but it admits an excellent approximation by a flat lumped parameter system. To reduce a working time and to increase the SMC productivity a time-optimal strategy is chosen. It is shown that the approximated system can be simplified further and a linear time-varying system can be considered for the control design. MPC is chosen to stabilize the trajectory and fulfill certain state and input constraints. MPC is derived by implementing linear parametric optimization, where flatness of the model is exploited. The linear time-varying model is parametrized by the flat output. The optimization task for the MPC is formulated in a form of a linear program, which is solved by means of an open-source optimization software LPSOLVE. Finally, simulation results are presented.

Modeling and time-optimal trajectory

Model of the SMC is presented in [4] and [3]. Although the system under consideration is a distributed parameter one, we use a lumped parameter system derived by help of the Rayleigh–Ritz approximation. According to this method the mast deflection $w\,(Y,\,t)$ is approximated by the first-order Ritz ansatz function

$$w^*\,(Y,\,t) = x_c\,(t) + \varPhi_1\,(Y)\,\bar{q}^1\,(t)\,,$$

with the new generalized coordinate $\bar{q}_1$, and the spatial basis function

$$\varPhi_1\,(Y) = 6\,(Y/L)^2 - 4\,(Y/L)^3 + (Y/L)^4\,.$$

The nonlinear approximating equations of motion are

$$\mathbf{M}(\mathbf{q})\ddot{\mathbf{q}} + \mathbf{C}(\mathbf{q},\ddot{\mathbf{q}}) = \mathbf{G}\mathbf{u}, \tag{1}$$

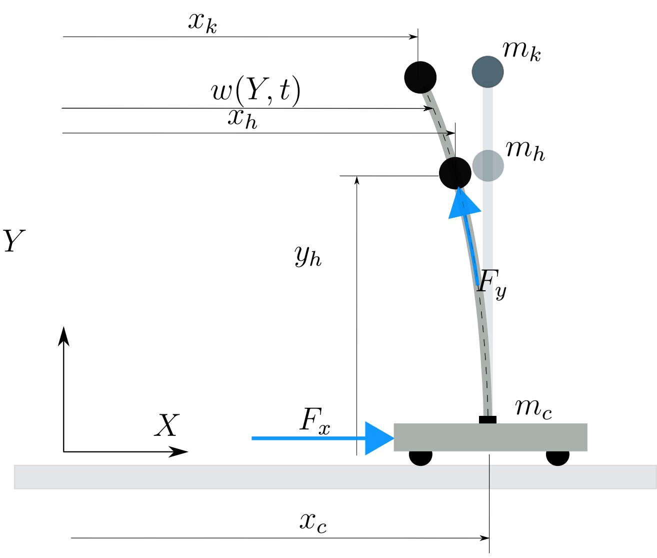

Abbildung 1: Single mast stacker crane

[a]Institute of Automatic Control and Control Systems Technology, Johannes Kepler University Linz, Altenberger Strasse 69, 4040 Linz, Austria, E-mail: anastasiia.galkina@jku.at

Here $\mathbf{q} = [x_c \quad \bar{q}_1 \quad y_h]^T$ are the generalized coordinates. Assuming $\partial_Y \Phi_1 (y_h) = 0$ and $\partial_Y^2 \Phi_1 (y_h) = 0$, the nonlinear model (1) is simplified further. This simplification results in the linear time-varying system

$$\begin{aligned} \dot{\bar{\mathbf{x}}} &= \mathbf{A}_1(y_{h,d})\bar{\mathbf{x}} + \mathbf{b}_1(y_{h,d})F_x, \\ \dot{\bar{\mathbf{y}}} &= \mathbf{A}_2\bar{\mathbf{y}} + \mathbf{b}_2\bar{v}, \end{aligned} \tag{2}$$

with $\bar{\mathbf{x}} = [x_c \quad \bar{q}_1 \quad \dot{x}_c \quad \dot{\bar{q}}_1]^T$, $\bar{\mathbf{y}} = [y_h \quad \dot{y}_h]^T$, $\bar{v} = (F_y - gm_h)/m_h$ and the optimal trajectory $(y_{h,d}, \dot{y}_{h,d}, \ddot{y}_{h,d})$.

Model predictive control with linear programming

The model (2) can be considered as two interconnected subsystems, where the first subsystem is a linear time-varying one and the second is a linear time-invariant one. The formulation of the optimization task for the MPC is based on the method, which was implemented in [1]. The subsystems of (2) are parametrized by the flat output $\mathbf{h} = [h_1 \quad h_2]^T$ using an exact time discretization and a transformation into the Brunovsky canonical form. The optimization task for the MPC in a form of a linear program (see e.g. [2]) can be divided into two independent optimization tasks corresponding to the subsystems of (2) and is given by

$$\min_{\bar{\mathbf{h}}^1} \quad \varepsilon_1 + \varepsilon_2 + \varepsilon_3$$

$$\begin{aligned} |M_{b,k}(\bar{\mathbf{h}}^1) - M_{b,d,k}| &\leq \varepsilon_1 \quad k = 1, ..., N \\ |F_{x,k}(\bar{\mathbf{h}}^1) - F_{x,d,k}| &\leq \varepsilon_2 \quad k = 1, ..., N \\ |x_{h,k}(\bar{\mathbf{h}}^1) - x_{h,d,k}| &\leq \varepsilon_3 \quad k = 1, ..., N \end{aligned}$$

$$\min_{\bar{\mathbf{h}}^2} \quad \varepsilon_4 + \varepsilon_5$$

$$\begin{aligned} |y_{h,k}(\bar{\mathbf{h}}^2) - y_{h,d,k}| &\leq \varepsilon_4 \quad k = 1, ..., N \\ |F_{y,k}(\bar{\mathbf{h}}^2) - F_{y,d,k}| &\leq \varepsilon_5 \quad k = 1, ..., N \end{aligned}$$

where ε_i with $i = 1, ..5$ are some positive values, $(M_{b,d,k}, F_{x,d,k}, x_{h,d,k})$ and $(y_{h,d,k}, F_{y,d,k})$ - desired optimal trajectory, $\bar{\mathbf{h}}^1 = [\varepsilon_1 \quad \varepsilon_2 \quad \varepsilon_3 \quad h_1]^T$ and $\bar{\mathbf{h}}^2 = [\varepsilon_4 \quad \varepsilon_5 \quad h_2]^T$ are optimization vectors and N is an optimization horizon. An open-source optimization software LPSOLVE is used for solving both optimization tasks. Finally, simulation results of the trajectory stabilization for the nonlinear model (1), subject to parameter uncertainties and measurement noises are presented.

[1] A. Galkina, I. Gafur, and K. Schlacher. Model predictive control with linear programming for the strip infeed in hot rolling mills. In *Proceedings of the 20th World Congress of the International Federation of Automatic Control*, 2017.

[2] D. Luenberger and Y. Ye. *Linear and Nonlinear Programming.* Springer, 233 Spring Street, New York, NY 10013, USA, 4 edition, 2008.

[3] H. Rams, M. Schöberl, and K. Schlacher. Optimal control of a single mast stacker crane. *IEEE Transactions on Control System Technology*, 2017.

[4] M. Staudecker, K. Schlacher, and R. Hansl. Passivity based control and time optimal trajectory planning of a single mast stacker crane. In *Proceedings of the 17th IFAC World Congress*, 2008.

MODEL PREDICTIVE CONTROL WITH FLATNESS BASED LINEAR PROGRAMMING FOR THE SINGLE MAST STACKER CRANE

20. Styrian Workshop on Automatic Control

A. Galkina,[1] K. Schlacher[1]

September 12, 2017

[1] Institute of Automatic Control and Control Systems Technology
Johannes Kepler University Linz

JOHANNES KEPLER UNIVERSITY LINZ

LINZ CENTER OF MECHATRONICS GMBH

Outline

- Problem Statement
- State of the Art
- Model of the Single Mast Stacker Crane (SMC)
- Flatness Analysis and System Simplification
- Flatness Based Parameterization for Model Predictive Control
- Model Predictive Control with Flatness Based Linear Programming
- Simulation results

1/36

PROBLEM STATEMENT

Problem Statement

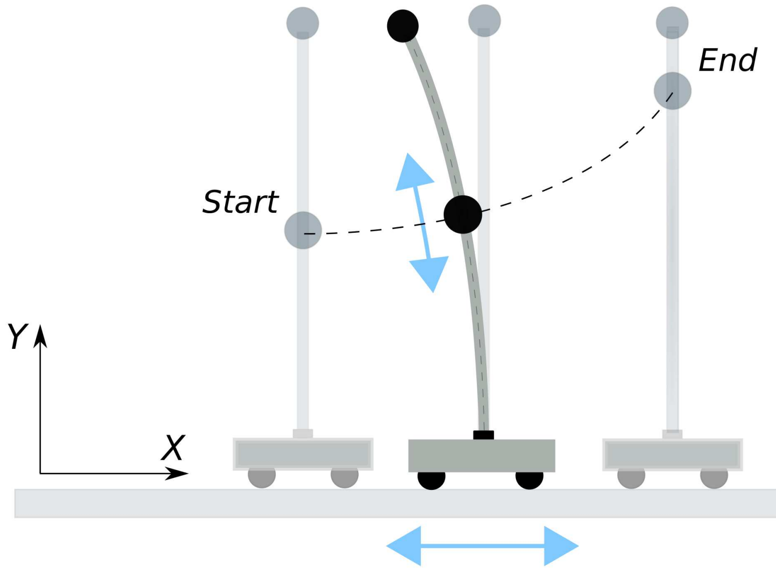

2/36

State of the art: Modeling

- Payload is fixed during positioning of the carriage
  - M. Bachmayer, H. Ulbrich, J. Rudolph. Flatness-based control of a horizontally moving erected beam with a point mass. *Mathematical and Computer Modelling of Dynamical Systems*, 17(1):49-69, 2011.
  - G. Kostin, H. Aschemann, A. Rauh, V. Saurin. Optimal Real-Time Control of Flexible Rack Feeders Using the Method of Integrodifferential Relations. *Proceedings of the 7th Vienna International Conference on Mathematical Modelling*, 1147-1153, 2012.
- Moving of the payload during the carriage transportation
  - M. Staudecker, K. Schlacher, R. Hansl. Passivity Based Control and Time Optimal Trajectory Planning of a Single Mast Stacker Crane. *Proceedings of the 17th IFAC World Congress*, 875-880, 2008.
  - H. Rams, M. Schöberl, K. Schlacher. Optimal Motion Planning and Energy-Based Control of a Single Mast Stacker Crane. *IEEE Transactions on Control System Technology*, 1-9, 2017.
- Control-oriented model
  - H. Aschemann, D. Schindele. Model Predictive Trajectory Control for High-Speed Rack Feeders. *Model Predictive Control*, InTech, 183-198, 2010.

3/36

State of the art: Control

- Flatness-based and optimal feedforward control
  - M. Bachmayer, H. Ulbrich, J. Rudolph. Flatness-based control of a horizontally moving erected beam with a point mass. *Mathematical and Computer Modelling of Dynamical Systems*, 17(1):49-69, 2011.
  - G. Kostin, H. Aschemann, A. Rauh, V. Saurin. Optimal Real-Time Control of Flexible Rack Feeders Using the Method of Integrodifferential Relations. *Proceedings of the 7th Vienna International Conference on Mathematical Modelling*, 1147-1153, 2012.
- Passivity-based and energy-based feedback control
  - M. Staudecker, K. Schlacher, R. Hansl. Passivity Based Control and Time Optimal Trajectory Planning of a Single Mast Stacker Crane. *Proceedings of the 17th IFAC World Congress*, 875-880, 2008.
  - H. Rams, M. Schöberl, K. Schlacher. Optimal Motion Planning and Energy-Based Control of a Single Mast Stacker Crane.[1] *IEEE Transactions on Control System Technology*, 1-9, 2017.

[1] B. Kolar, H. Rams, K. Schlacher. Time-optimal flatness based control of a gantry crane. *Control Engineering Practice*, 60, 18-27, 2017.

4/36

State of the art: Control

- Model predictive control
  - H. Aschemann, D. Schindele. Model Predictive Trajectory Control for High-Speed Rack Feeders. *Model Predictive Control*, InTech, 183-198, 2010.

5/36

Implemented Model and Optimal Trajectory

- To take the structural vibrations into account, the model of Staudecker et al. will be used
  - M. Staudecker, K. Schlacher, R. Hansl. Passivity Based Control and Time Optimal Trajectory Planning of a Single Mast Stacker Crane. *Proceedings of the 17th IFAC World Congress*, 875-880, 2008.
- To increase the productivity, the optimal trajectory derived by Rams et al. will be used
  - H. Rams, M. Schöberl, K. Schlacher. Optimal Motion Planning and Energy-Based Control of a Single Mast Stacker Crane. *IEEE Transactions on Control System Technology*, 1-9, 2017.

6/36

MODEL OF THE SINGLE MAST STACKER CRANE (SMC)

Single Mast Stacker Crane

Mast can be considered as a beam satisfying the Euler-Bernoulli hypothesis, having length L, uniform mass density ρ, uniform cross section surface A and uniform flexural rigidity EI.

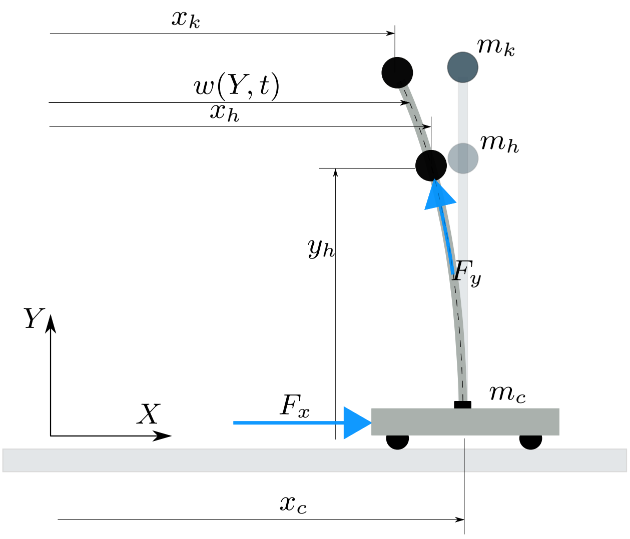

System Energy

- Kinetic energy

$$E_k = \frac{1}{2}\left(m_c \dot{x}_c^2 + m_h \left(\dot{x}_h^2 + \dot{y}_h^2\right) + m_k \dot{x}_k^2 + \rho A \int_0^L \left(\partial_t w\right)^2 \mathrm{d}Y \right)$$

- Potential energy

$$E_p = m_h g y_h^2 + \frac{1}{2} EI \int_0^L \left(\partial_Y^2 w\right)^2 \mathrm{d}Y$$

- External forces

$$E_{ext} = x_c F_x + y_h F_y$$

Apply the extended Hamilton's principle on the Lagrangian action functional

$$\mathcal{L} = \int_{t_1}^{t_2} \left(E_k - E_p + E_{ext}\right) \mathrm{d}t + \lambda_1 \left(x_h - w\left(y_h,\, t\right)\right) + \lambda_2 \left(x_k - w\left(L,\, t\right)\right), \quad (1)$$

which is extended by the mechanical restrictions, namely, $x_h = w\left(y_h,\, t\right)$ and $x_k = w\left(L,\, t\right)$, based on the technique of Lagrangian multipliers.

Mixed-dimensional system

One partial differential equation

$$\rho A \partial_t^2 w \quad = \quad -EI\partial_Y^4 w \tag{2}$$

Set of ordinary differential equations

$$\begin{aligned} m_c \ddot{x}_c &= F_x - EI\partial_Y^3 w\,(0,\,t) \\ m_h \ddot{y}_h &= F_y - m_h g - m_h \ddot{x}_h \partial_Y w\,(y_h,\,t) \\ m_h \ddot{x}_h &= EI\left(\partial_Y^3 w\left(y_h^-,\,t\right) - \partial_Y^3 w\left(y_h^+,\,t\right)\right) \\ m_k \ddot{x}_k &= EI\partial_Y^3 w\,(L,\,t) \end{aligned} \tag{3}$$

Boundary conditions

$$\begin{aligned} &w\,(0,\,t) = x_c\,,\ \partial_Y w\,(0,\,t) = 0\,,\ w\,(y_h,\,t) = x_h\,, \\ &w\,(L,\,t) = x_k\,,\ \partial_Y^2 w\,(L,\,t) = 0\,,\ \partial_Y^2 w\left(y_h^-,\,t\right) = \partial_Y^2 w\left(y_h^+,\,t\right). \end{aligned} \tag{4}$$

The values y_h^+ and y_h^- denote the right-hand and the left-hand limit of y_h.

9/36

System approximation with Rayleigh-Ritz method

The mast deflection $w\,(Y,\,t)$ is approximated by the first-order Ritz ansatz function

$$w^*\,(Y,\,t) = x_c\,(t) + \Phi_1\,(Y)\,\bar{q}^1\,(t)\,, \tag{5}$$

with the new generalized coordinate $\bar{q}_1$, and an appropriately chosen spatial basis function

$$\Phi_1\,(Y) = 6\,(Y/L)^2 - 4\,(Y/L)^3 + (Y/L)^4\,.$$

Substituting the Ritz ansatz function (5) into

$$\mathcal{L} = \int_{t_1}^{t_2} (E_k - E_p + E_{ext})\,\mathrm{d}t + \lambda_1\,(x_h - w^*\,(y_h,\,t)) + \lambda_2\,(x_k - w^*\,(L,\,t))$$

and again applying the extended Hamilton's principle, we get the approximated equations of motion.

10/36

ODE

The approximated equations of motions are

$$\mathbf{M}(\mathbf{q})\,\ddot{\mathbf{q}} + \mathbf{C}(\mathbf{q},\,\dot{\mathbf{q}}) = \mathbf{G}\mathbf{u} \tag{6}$$

with the generalized coordinate $\mathbf{q} = \begin{bmatrix} x_c & \bar{q}^1 & y_h \end{bmatrix}^T$ and the control input $\mathbf{u} = \begin{bmatrix} F_x & F_y \end{bmatrix}^T$.

$$\mathbf{M} = \begin{bmatrix} m_{11} & m_{12} + m_h \Phi_1(y_h) & m_h \bar{q}^1 \partial_Y \Phi_1(y_h) \\ \vdots & m_{22} + m_h \Phi_1^2(y_h) & m_h \bar{q}^1 \Phi_1(y_h)\, \partial_Y \Phi_1(y_h) \\ \text{sym.} & \dots & m_h + m_h \left(\bar{q}^1 \partial_Y \Phi_1(y_h)\right)^2 \end{bmatrix},$$

$$\mathbf{C} = \begin{bmatrix} 2m_h \dot{y}_h \dot{\bar{q}}^1 \partial_Y \Phi_1(y_h) + m_h \dot{y}_h^2 \bar{q}^1 \partial_Y^2 \Phi_1(y_h) \\ C_1 \Phi_1(y_h) + EI\bar{q}^1 \int_0^L \left(\partial_Y^2 \Phi_1\right)^2 \mathrm{d}Y \\ m_h g + C_1 \dot{\bar{q}}^1 \partial_Y \Phi_1(y_h) \end{bmatrix}, \qquad \mathbf{G} = \begin{bmatrix} 0 & 0 & 1 \\ 1 & 0 & 0 \end{bmatrix}^T,$$

with $m_{11} = m_c + m_h + m_k + \rho A L$, $m_{12} = m_k \Phi_1(L) + \int_0^L \rho A \Phi_1 \mathrm{d}Y$ and $m_{22} = m_k \Phi_1^2(L) + \int_0^L \rho A \Phi_1^2 \mathrm{d}Y$.

11/36

ODE

The approximated equations of motions are

$$\mathbf{M}(\mathbf{q})\,\ddot{\mathbf{q}} + \mathbf{C}(\mathbf{q},\,\dot{\mathbf{q}}) = \mathbf{G}\mathbf{u}$$

with the generalized coordinate $\mathbf{q} = \begin{bmatrix} x_c & \bar{q}^1 & y_h \end{bmatrix}^T$ and the control input $\mathbf{u} = \begin{bmatrix} F_x & F_y \end{bmatrix}^T$.

$$\mathbf{M} = \begin{bmatrix} m_{11} & m_{12} + m_h \Phi_1(y_h) & m_h \bar{q}^1 \partial_Y \Phi_1(y_h) \\ \vdots & m_{22} + m_h \Phi_1^2(y_h) & m_h \bar{q}^1 \Phi_1(y_h)\, \partial_Y \Phi_1(y_h) \\ \text{sym.} & \dots & m_h + m_h \left(\bar{q}^1 \partial_Y \Phi_1(y_h)\right)^2 \end{bmatrix}$$

$$\mathbf{C} = \begin{bmatrix} 2m_h \dot{y}_h \dot{\bar{q}}^1 \partial_Y \Phi_1(y_h) + m_h \dot{y}_h^2 \bar{q}^1 \partial_Y^2 \Phi_1(y_h) \\ C_1 \Phi_1(y_h) + EI\bar{q}^1 \int_0^L \left(\partial_Y^2 \Phi_1\right)^2 \mathrm{d}Y \\ m_h g + C_1 \dot{\bar{q}}^1 \partial_Y \Phi_1(y_h) \end{bmatrix}, \qquad \mathbf{G} = \begin{bmatrix} 0 & 0 & 1 \\ 1 & 0 & 0 \end{bmatrix}^T.$$

12/36

FLATNESS ANALYSIS AND SYSTEM SIMPLIFICATION

Flatness and System Decomposition

Assuming that $y_h = h^2$ is a flat output, it can be concluded that the desired trajectory $y_{h,d}\left(t\right) = h_d^2\left(t\right)$ and its time derivatives are known.

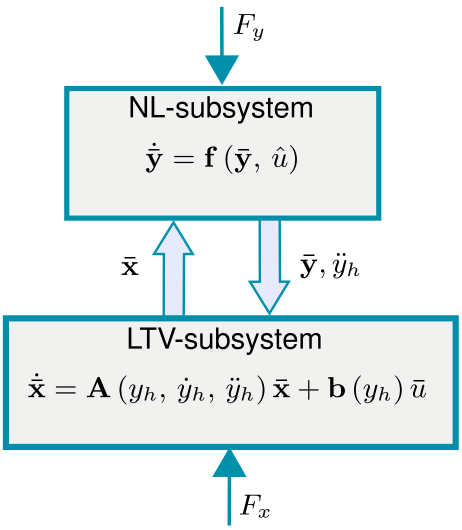

$$
\begin{aligned}
\bar{\mathbf{x}} &= \begin{bmatrix} x_h & \bar{q}^1 & \dot{x}_h & \dot{\bar{q}}^1 \end{bmatrix}^T, \\
\bar{u} &= F_x, \\
\bar{\mathbf{y}} &= \begin{bmatrix} y_h & \dot{y}_h \end{bmatrix}^T, \\
\hat{u} &= \begin{bmatrix} x_h & \bar{q}^1 & \dot{x}_h & \dot{\bar{q}}^1 & F_y \end{bmatrix}^T.
\end{aligned}
$$

Hence, the methods and approaches for the linear time-varying system can be implemented to the LTV-subsystem.

13/36

System Simplification

- For linear systems the properties of flatness and controllability are equivalent. Hence, we may obtain a flat ouput by transforming LTV-subsystem into a time-varying controllability canonical form
- The linear time-varying transformation $h^1 = T_j^1(t)\,\bar{x}^j$ in general is a function of the corresponding time derivatives of $\mathbf{b}(t)$ and $\mathbf{A}(t)$

Futher assumption

$$\partial_Y \Phi_1(y_h) = 0$$

$$\partial_Y^2 \Phi_1(y_h) = 0$$

- The linear time-varying transformation will be reduced to the simpler rule for the time-invariant transformation: all the corresponding time derivatives of $\mathbf{b}(t)$, $\mathbf{A}(t)$ and $\mathbf{T}(t)$ will disappear
- NL-subsystem is reduced to the linear time-invariant system

$$\dot{\bar{\mathbf{y}}} = \begin{bmatrix} 0 & 1 \\ 0 & 0 \end{bmatrix} \bar{\mathbf{y}} + \begin{bmatrix} 0 \\ 1 \end{bmatrix} \bar{v}$$

with the input $\bar{v} = (F_y - gm_h)/m_h$

Simplified System

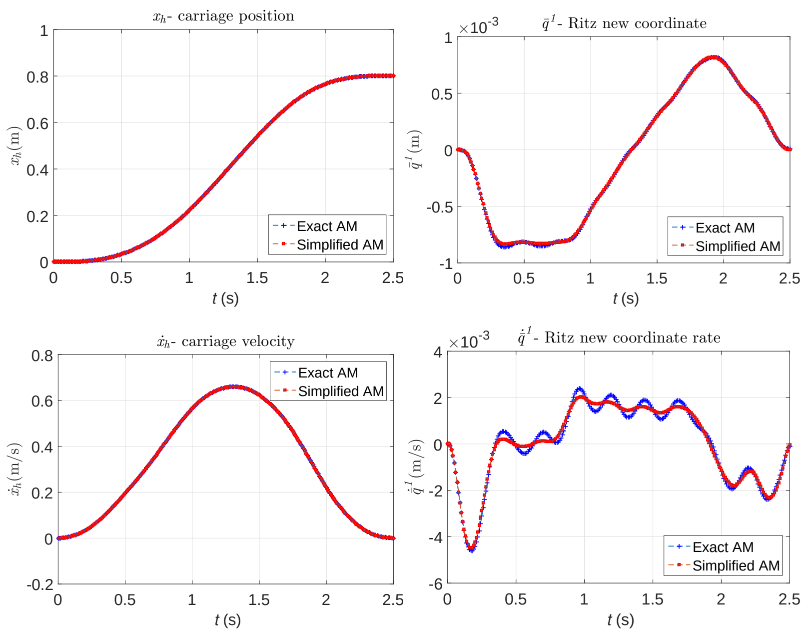

Figure: Simplified and exact approximated model (AM) of SMC

Simplified System

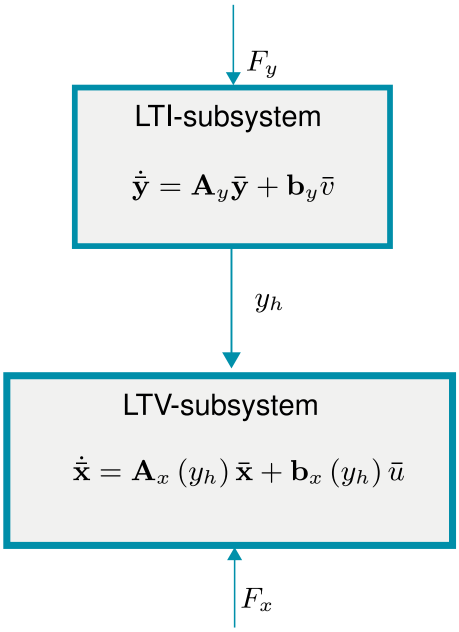

16/36

Simplified System with Optimal Trajectory

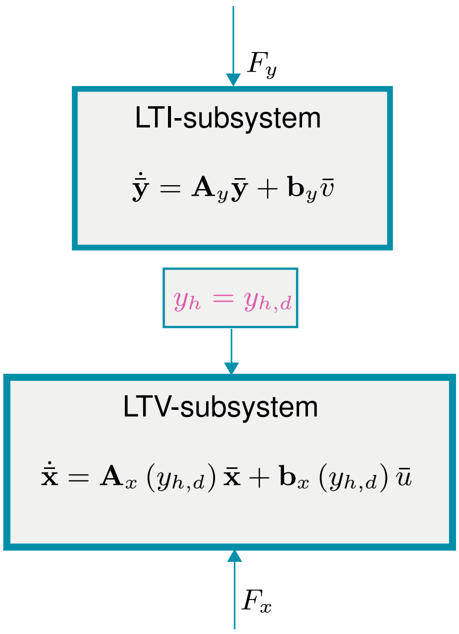

17/36

Parametrization by Flat Outputs

- Parameterization by a flat output

$$\tilde{\mathbf{x}}_k = \mathbf{A}_1 \left(y_{h,d}\right) \tilde{\mathbf{h}}_k^1$$
$$\tilde{\mathbf{y}}_k = \mathbf{A}_2 \tilde{\mathbf{h}}_k^2$$

where

$$\begin{aligned}
\tilde{\mathbf{x}}_k &= \begin{bmatrix} x_{h,k} & \bar{q}_k^1 & \dot{x}_{h,k} & \dot{\bar{q}}_k^1 & F_{x,k} \end{bmatrix}^T, \\
\tilde{\mathbf{y}}_k &= \begin{bmatrix} y_{h,k} & \dot{y}_{h,k} & F_{y,k} \end{bmatrix}^T, \\
\tilde{\mathbf{h}}_k^1 &= \begin{bmatrix} \hat{h}_k^1 & \hat{h}_{k+1}^1 & \hat{h}_{k+2}^1 & \hat{h}_{k+3}^1 & \hat{h}_{k+4}^1 \end{bmatrix}^T, \\
\tilde{\mathbf{h}}_k^2 &= \begin{bmatrix} \hat{h}_k^2 & \hat{h}_{k+1}^2 & \hat{h}_{k+2}^2 \end{bmatrix}^T
\end{aligned}$$

- General discrete-time linear system

$$\mathbf{z}_{k+1} = \mathbf{A}\mathbf{z}_k + \mathbf{b}u_k$$

with the solution for $k = N$

$$\mathbf{z}_N = \mathbf{A}^N \mathbf{z}_0 + \mathbf{H}_N u_{[0,N-1]}$$

where $\mathbf{H}_N = \begin{bmatrix} \mathbf{A}^{N-1}\mathbf{b} & \dots & \mathbf{A}\mathbf{b} & \mathbf{b} \end{bmatrix}$, $u_{[0,N-1]} = \begin{bmatrix} u_0 & \dots & u_{N-1} \end{bmatrix}^T$

18/36

Structure of the Jacobian Matrix for the Optimization Program

- $\mathbf{J} = \begin{bmatrix} X & X & X & 0 & 0 & 0 & 0 & 0 \\ 0 & X & X & X & 0 & 0 & 0 & 0 \\ 0 & 0 & X & X & X & 0 & 0 & 0 \\ 0 & 0 & 0 & X & X & X & 0 & 0 \\ 0 & 0 & 0 & 0 & X & X & X & 0 \\ 0 & 0 & 0 & 0 & 0 & X & X & X \end{bmatrix}$

- $\mathbf{J} = \begin{bmatrix} X & 0 & \dots & 0 & 0 \\ X & X & \dots & 0 & 0 \\ \vdots & \dots & \ddots & \dots & \vdots \\ X & X & \dots & X & 0 \\ X & X & \dots & X & X \end{bmatrix}$

19/36

Parametrization by Flat Outputs

- Transformation into controllability canonical form is carried out by $\bar{\mathbf{h}}^1 = \mathbf{T}(y_h)\,\bar{\mathbf{x}}$, which results in

$$\dot{\bar{\mathbf{h}}}^1 = \mathbf{A}_R(y_h)\,\bar{\mathbf{h}} + \mathbf{b}_R\bar{u}$$

with $\bar{\mathbf{h}}^1 = \begin{bmatrix} h^1 & \dot{h}^1 & \ddot{h}^1 & h^{1,(3)} \end{bmatrix}^T$

- Transforming the input by $\bar{u} = \sum_{i=0}^{n_x} a_i(\mathbf{A}_R)\,\bar{h}^{1,(i)}$ with the coefficients of the characteristical polynomial a_i of $\mathbf{A}_R(y_h)$ into Brunovsky canonical form
- Another flat output $y_h = h^2$.
- LTI-subsystem is already in Brunovsky canonical form

LTV-subsystem

$$\dot{\bar{\mathbf{x}}} = \mathbf{A}_x(y_h)\,\bar{\mathbf{x}} + \mathbf{b}_x(y_h)\,\bar{u}$$

$\Downarrow$ $\bar{\mathbf{h}}^1 = \mathbf{T}(y_h)\,\bar{\mathbf{x}}$

CCF

$$\dot{\bar{\mathbf{h}}}^1 = \mathbf{A}_R(y_h)\,\bar{\mathbf{h}}^1 + \mathbf{b}_R\bar{u}$$

$\Downarrow$ $\bar{u} = \sum_{i=0}^{n_x} a_i(\mathbf{A}_R)h^{1,(i)}$

Brunovsky CF

$$\dot{\bar{\mathbf{h}}}^1 = \mathbf{A}_B\bar{\mathbf{h}}^1 + \mathbf{b}_R h^{1,(4)}$$

20/36

Exact Discretization

Then we discretize both subsystems with the sampling time $T_a = 20$ ms

$$\bar{\mathbf{h}}^1_{k+1} = \begin{bmatrix} 1 & T_a & \frac{T_a^2}{2} & \frac{T_a^3}{6} \\ 0 & 1 & T_a & \frac{T_a^2}{2} \\ 0 & 0 & 1 & T_a \\ 0 & 0 & 0 & 1 \end{bmatrix} \bar{\mathbf{h}}^1_k + \begin{bmatrix} \frac{T_a^4}{24} \\ \frac{T_a^3}{6} \\ \frac{T_a^2}{2} \\ T_a \end{bmatrix} h^1_{k+4},$$

$$\bar{\mathbf{h}}^2_{k+1} = \begin{bmatrix} 1 & T_a \\ 0 & 1 \end{bmatrix} \bar{\mathbf{h}}^2_k + \begin{bmatrix} \frac{T_a^2}{2} \\ T_a \end{bmatrix} h^2_{k+2}.$$

Using the previous approach, the discretized subsystems are transformed into Brunovsky canonical form one more time

$$\begin{bmatrix} \hat{h}^1_{k+1} \\ \hat{h}^1_{k+2} \\ \hat{h}^1_{k+3} \\ \hat{h}^1_{k+4} \end{bmatrix} = \begin{bmatrix} 0 & 1 & 0 & 0 \\ 0 & 0 & 1 & 0 \\ 0 & 0 & 0 & 1 \\ 0 & 0 & 0 & 0 \end{bmatrix} \begin{bmatrix} \hat{h}^1_{k} \\ \hat{h}^1_{k+1} \\ \hat{h}^1_{k+2} \\ \hat{h}^1_{k+3} \end{bmatrix} + \begin{bmatrix} 0 \\ 0 \\ 0 \\ 1 \end{bmatrix} \hat{h}^1_{k+4}$$

$$\begin{bmatrix} \hat{h}^2_{k+1} \\ \hat{h}^2_{k+2} \end{bmatrix} = \begin{bmatrix} 0 & 1 \\ 0 & 0 \end{bmatrix} \begin{bmatrix} \hat{h}^2_{k} \\ \hat{h}^2_{k+1} \end{bmatrix} + \begin{bmatrix} 0 \\ 1 \end{bmatrix} \hat{h}^2_{k+2}.$$

21/36

Parametrization by Flat Outputs

The system states are parametrized with flat output and we have

$$\boxed{\begin{aligned} \tilde{\mathbf{x}}_k &= \mathbf{A}_1\left(y_{h,d,k}\right)\tilde{\mathbf{h}}^1_k, \\ \tilde{\mathbf{y}}_k &= \mathbf{A}_2\tilde{\mathbf{h}}^2_k, \end{aligned}}$$

where

$$\begin{aligned} \tilde{\mathbf{x}}_k &= \begin{bmatrix} x_{h,k} & \bar{q}^1_k & \dot{x}_{h,k} & \dot{\bar{q}}^1_k & F_{x,k} \end{bmatrix}^T, \\ \tilde{\mathbf{y}}_k &= \begin{bmatrix} y_{h,k} & \dot{y}_{h,k} & F_{y,k} \end{bmatrix}^T, \\ \tilde{\mathbf{h}}^1_k &= \begin{bmatrix} \hat{h}^1_k & \hat{h}^1_{k+1} & \hat{h}^1_{k+2} & \hat{h}^1_{k+3} & \hat{h}^1_{k+4} \end{bmatrix}^T, \\ \tilde{\mathbf{h}}^2_k &= \begin{bmatrix} \hat{h}^2_k & \hat{h}^2_{k+1} & \hat{h}^2_{k+2} \end{bmatrix}^T. \end{aligned}$$

22/36

Why do we use this parameterization?

- The system variables $\begin{pmatrix} x_{h,k} & \bar{q}_k^1 & \dot{x}_{h,k} & \dot{\bar{q}}_k^1 & F_{x,k} \end{pmatrix}$ and $\begin{pmatrix} y_{h,k} & \dot{y}_{h,k} & F_{y,k} \end{pmatrix}$ are the linear functions of 5 and 3 free parameters $\tilde{\mathbf{h}}_k^1$ and $\tilde{\mathbf{h}}_k^2$, respectevily, independed on the k

- Due to such parameterization the Jacobian matrix of the optimization problem will have the band structure

MODEL PREDICTIVE CONTROL WITH LINEAR PROGRAMMING

MPC with Linear Programming

Galkina, A., Gafur I., Schlacher K. Model Predictive Control with Linear Programming for the Strip Infeed in Hot Rolling Mills. *The 20th World Congress of the International Federation of Automatic Control*, 2017.

- The system state behaviour is the same comparing to Quadratic Programming
- The computational efficiency is higher comparing to Quadratic Programming

MPC with Linear Programming

If the number of the rest trajectory points $N_T > N$, then

$$\begin{array}{ccccc} & & \min_{\hat{p}_1}\ \epsilon_1+\epsilon_2+\epsilon_3 & & \\ & & \text{subject to} & & \\ |x_c(\hat{p}_1,\,k)-x_{c,d}(k)| & \leq & \epsilon_1 & & k=1,..,N \\ |M_b(\hat{p}_1,\,k)-M_{b,d}(k)| & \leq & \epsilon_2 & & k=1,..,N \\ |F_x(\hat{p}_1,\,k)-F_{x,d}(k)| & \leq & \epsilon_3 & & k=1,..,N \\ 0 & \leq & \epsilon_1 & \leq & |\Delta x_c| \\ 0 & \leq & \epsilon_2 & \leq & |\Delta M_b| \\ 0 & \leq & \epsilon_3 & \leq & |\Delta F_x| \end{array}$$

- optimization vector $\hat{p}_1 = \begin{bmatrix} \epsilon_1 & \epsilon_2 & \epsilon_3 & \hat{h}_0^1 & \ldots & \hat{h}_{N-1}^1 \end{bmatrix}^T$
- planned trajectory $(x_{c,d},\, M_{b,d},\, F_{x,d})\,,\,(y_{h,d},\, \dot{y}_{h,d})$
- MPC prediction horizon N
- $\hat{\mathbf{h}}_0^1$ depends on the initial state of SMC.

MPC with Linear Programming

If the number of the rest trajectory points $N_T > N$, then

$$\begin{array}{ccccc} & & \min_{\hat{p}_2}\ \varepsilon_1 + \varepsilon_2 & & \\ & & \text{subject to} & & \\ |y_h(\hat{p}_2, k) - y_{h,d}(k)| & \leq & \varepsilon_1 & & k = 1,..,N \\ |\dot{y}_h(\hat{p}_2, k) - \dot{y}_{h,d}(k)| & \leq & \varepsilon_2 & & k = 1,..,N \\ 0 & \leq & \varepsilon_1 & \leq & |\Delta y_h| \\ 0 & \leq & \varepsilon_2 & \leq & |\Delta \dot{y}_h| \end{array}$$

- optimization vector $\hat{p}_2 = \begin{bmatrix} \varepsilon_1 & \varepsilon_2 & \hat{h}_0^2 & \ldots & \hat{h}_{N-1}^2 \end{bmatrix}^T$
- planned trajectory $(x_{c,d},\ M_{b,d},\ F_{x,d})$, $(y_{h,d},\ \dot{y}_{h,d})$
- MPC prediction horizon N
- $\hat{\mathbf{h}}_0^2$ depends on the initial state of SMC.

26/36

MPC with Linear Programming

If the number of the rest trajectory points $N_T \leq N$, then

$$\begin{array}{ccccc} & & \min_{\hat{p}_1}\ \epsilon_1 + \epsilon_2 + \epsilon_3 & & \\ & & \text{subject to} & & \\ |x_c(\hat{p}_1, k) - x_{c,d}(k)| & \leq & \epsilon_1 & & k = 1,..,N-n \\ |M_b(\hat{p}_1, k) - M_{b,d}(k)| & \leq & \epsilon_2 & & k = 1,..,N-n \\ |F_x(\hat{p}_1, k) - F_{x,d}(k)| & \leq & \epsilon_3 & & k = 1,..,N-n \\ 0 & \leq & \epsilon_1 & \leq & |\Delta x_c| \\ 0 & \leq & \epsilon_2 & \leq & |\Delta M_b| \\ 0 & \leq & \epsilon_3 & \leq & |\Delta F_x| \end{array}$$

- optimization vector $\hat{p}_1 = \begin{bmatrix} \epsilon_1 & \epsilon_2 & \epsilon_3 & \hat{h}_0^1 & \ldots & \hat{h}_{N-n-1}^1 \end{bmatrix}^T$
- planned trajectory $(x_{c,d},\ M_{b,d},\ F_{x,d})$, $(y_{h,d},\ \dot{y}_{h,d})$
- MPC prediction horizon $N - n$, actual step $n = 0...N - 1$
- $\hat{\mathbf{h}}_0^1$ depends on the initial state of SMC.

27/36

MPC with Linear Programming

If the number of the rest trajectory points $N_T \leq N$, then

$$
\begin{array}{ccccc}
 & & \min_{\hat{p}_2} \varepsilon_1 + \varepsilon_2 & & \\
 & & \text{subject to} & & \\
|y_h(\hat{p}_2, k) - y_{h,d}(k)| & \leq & \varepsilon_1 & & k = 1,..,N-n \\
|\dot{y}_h(\hat{p}_2, k) - \dot{y}_{h,d}(k)| & \leq & \varepsilon_2 & & k = 1,..,N-n \\
0 & \leq & \varepsilon_1 & \leq & |\Delta y_h| \\
0 & \leq & \varepsilon_2 & \leq & |\Delta \dot{y}_h|
\end{array}
$$

- optimization vector $\hat{p}_2 = \begin{bmatrix} \varepsilon_1 & \varepsilon_2 & \hat{h}_0^2 & \ldots & \hat{h}_{N-n-1}^2 \end{bmatrix}^T$
- planned trajectory $(x_{c,d}, M_{b,d}, F_{x,d})$, $(y_{h,d}, \dot{y}_{h,d})$
- MPC prediction horizon $N - n$, actual step $n = 0...N-1$
- $\hat{\mathbf{h}}_0^2$ depends on the initial state of SMC.

28/36

SIMULATION RESULTS WITH LP_SOLVE

Simulation

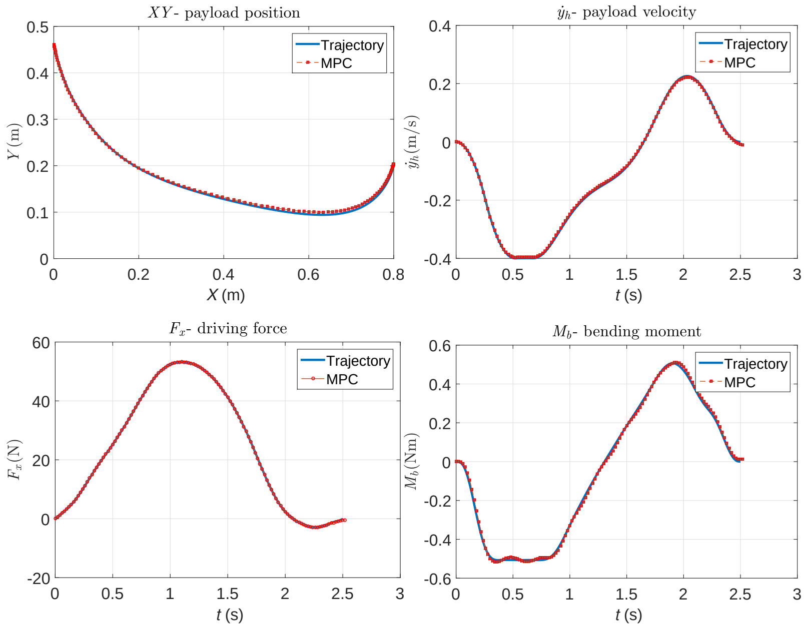

29/36

Optimization time with prediction horizon $N = 40$

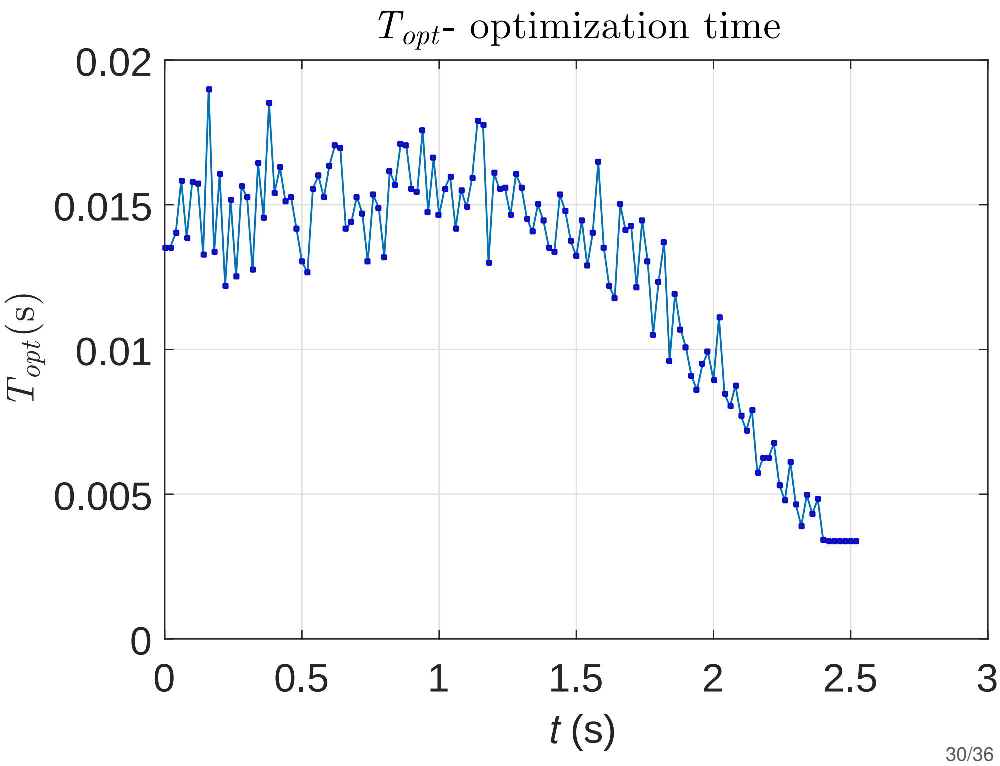

30/36

Simulation Results with Disturbed System without MPC

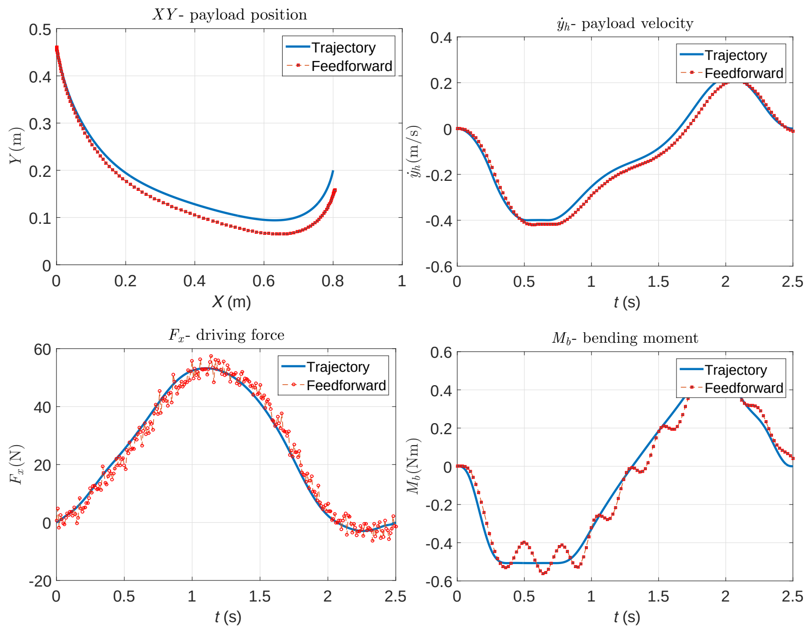

31/36

Simulation Results with Disturbed System with MPC using LP_SOLVE

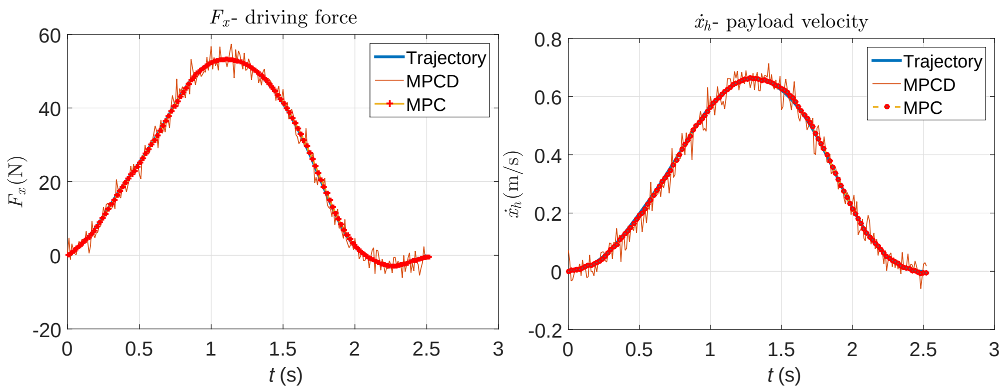

32/36

Simulation Results with Disturbed System with MPC using LP_SOLVE

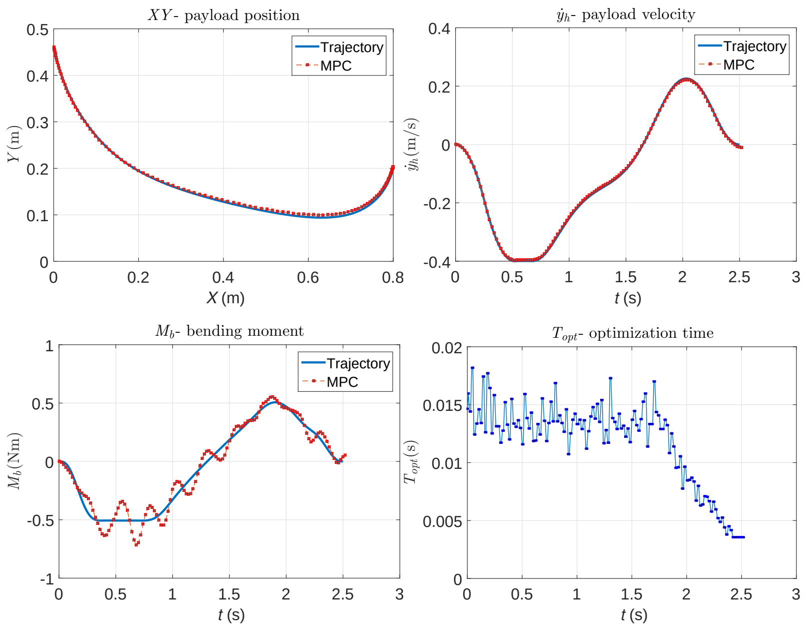

33/36

CONCLUSIONS

Conclusions

- The simplified linear time-varying model can be used to control a single mast stacker crane
- An effective MPC in form of a linear program can be designed using a parametrization by flat output to stabilize the desired trajectory
- The simulation based on nonlinear ODE with MPC in form of a linear program shows very good accuracy in the case of disturbed signals and parameter uncertainties
- The standard free optimizations solver LP_SOLVE can be simply implemented for the tracking problem

34/36

Part II.

Wednesday morning session

New Single-Ended Earthfault Distance Estimation for Compensated Networks

Dr. Gernot Druml, Sprecher Automation GmbH
g.druml@ieee.org
gernot.druml@sprecher-automation.com
Austria

1 Abstract

Due to today´s increased demands on grid operation management, new methods for earth fault localization and detection are needed. The fault localization should be performed as quickly as possible and under the condition, that the fault current at the fault location will not be significantly increased.

The pros and cons of Distance Protection in solid grounded networks are well known. In case of a single-line earthfault, the current via the fault location in solid grounded networks is in the range of some kA.

In compensated networks the residual current I_res via the fault location is, in case of a single line fault, only few ampere.

Very often this current is much smaller than the load current of the feeder. A distinction between load current, circulating currents in meshed networks and fault current is more or less not possible. Therefore, the Earthfault-Distance-Protection in compensated networks is usually switched off.

With the new transient relays, based on the qu2-algorithm, it is possible to detect in the substation very reliable the faulty feeder and the direction of the fault. This statement is also correct for meshed networks.

In a 110-kV-network the distance between two substations is in the range of 50 km to 200 km. Also if the feeder is identified correctly, it is still a challenge to locate the exact fault position on this feeder.

In this paper some new methods for the estimation of the earthfault distance, measured only from one side, with an accuracy of few percentages will be presented. The advantages of the proposed methods are, that they can be implemented in standard distance protection relays. By measurements on both sides of a line, these methods can be improved.

The results of field-test in a 110-kV-network with different fault impedances will be presented.

2 Introduction

In *Fig. 1* the distribution of compensated networks in Germany is shown.

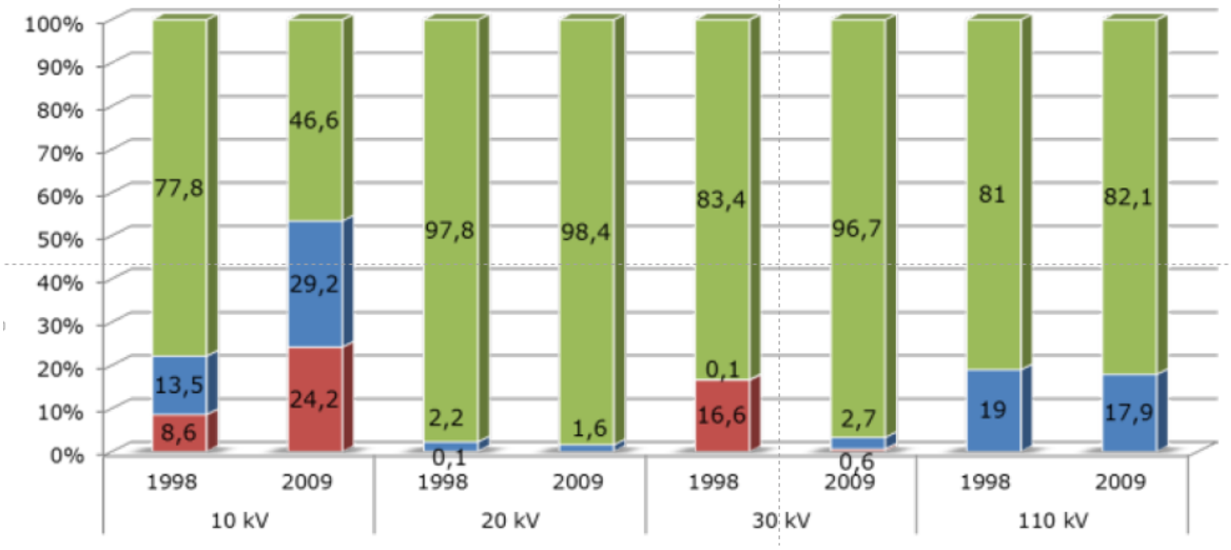

Fig. 1 Neutral Point Treatment in Germany
green: Petersen-Coil
blue: solid grounded
red: isolated

The distribution in Austria and Switzerland is similar. The advantage of compensated networks is, that the customers can be supplied continuously during a single line to earth fault. The duration of operation with one single-line-fault is only limited by the thermal design of the Petersen-Coil.

At the distribution level it is easy to install additional devices in switching stations. In Germany the distance between switching stations is in the range of 0.5 km up to 5 km.

But also in the distribution network a distance estimation of the earthfault, based on sensor measurements, would be an improvement. In this paper also a short preview of these technique and the corresponding requirements will be presented.

The detailed explanation of the qu2-algorithm implemented in the EDIR SW-module can be found in [4] and [5]. This SW-Module is implemented identical in the following devices:

Fig. 2 SW-module EDIR with qu2-algorith implemented in SPRECON-E-P Dxx and SPRECON-EDIR

For the distance estimation a new algorithm was implemented in the SPRECON-E-P device

3 Distance Estimation

3.1 Improved standard-algorithm

The distance protection for earthfaults are working with sufficient accuracy of about two span in solid grounded and low-resistance grounded networks. The standard algorithm is depicted in equation (1)

$$\underline{Z}_L = \frac{\underline{U}_{L1E}}{\underline{I}_{L1} + \underline{I}_{\Sigma} \cdot \underline{k}_0} \tag{1}$$

Z_L	Calculated impedance up to the fault location
U_{L1E}	Phase voltage of the faulty phase
I_{L1}	Current of the faulty phase
I_{Σ}	Residual current
k_0	Earth-fault factor

The deviation of the real line impedance increases with the increase of the fault-impedance [2]. Therefore it is necessary to estimate the fault-current and the fault-impedance as accurate as possible to enable a correction of the standard-algorithm.

In [2] a method by measuring the earth-fault current respectively in [14] by measuring the negative-sequence-current is presented to improve significantly the fault-impedance calculation.

The major influences for the distance estimation in compensated networks are:

- load current
- circulating currents in meshed networks
- tapped lines
- distributed generation
- high capacities of cables
- impedance at the fault location
- dependence of the zero-sequence-system due to the skin depth of the current

For the verification of the new algorithm, extensive field-tests in the 110-kV-network were done. A detailed description of the tests is described in chapter 0.

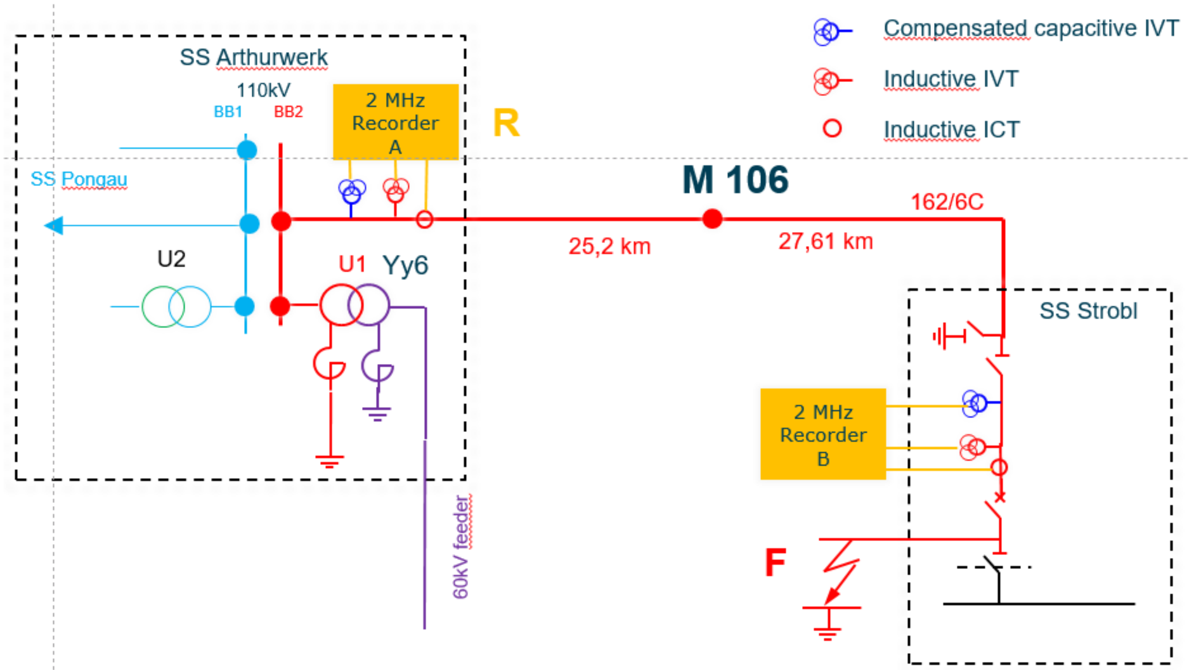

Fig. 3 110-kV-network for the tests

Data of the network:

- length of the OHL: 25.2 km + 27.6 km = 52.81 km
- measured primary zero-sequence-impedance with CPC: 21.1 Ω
- the super structure of both sections are similar

The relays have been started with each earthfault, but the distance estimation was not calculated in all cases. This is related to the measurement window which has not yet been optimized for earth faults. In the actual version the following items are not optimized in the calculation:

- transient effects,
- recharging processes of the capacitances
- variable behavior of fault arcs (quenching and re-ignition of the current, dynamic arc elongation etc.)

The results of the distance estimation of the relay in the substation Arthurwerke are shown in the following table:

Test	Estimated distance km
Solid grounded	50
OHL on meadow within the substation area	48
OHL on meadow outside the substation	52
OHL on 35 cm snow	50
OHL on tree	-
Cable fault (outdoor)	52
Cable fault in the sand-box	52
Arc started with ignition wire	-

The results shows, that the prototype without optimization of the measuring window, makes an estimation of the distance of 52.8 km with a tolerance of less than 10%.

3.2 Travelling waves

The solution of the line differential equation [14] [15] provides the phase velocity γ as a function of the conduction lines *L'* and C' according to equation (2)

$$v = \frac{1}{\sqrt{L'C'}} \tag{2}$$

Simultaneously with the voltage-traveling wave associated current-traveling waves occurs. They always belong together. These are only two different possibilities of representation. In case of a loss-less line the connection between the amplitudes is the surge-impedance according equation (3).

$$Z_W = \frac{u}{i} = \sqrt{\frac{L'}{C'}} \tag{3}$$

Particularly in the case of overhead lines, it must be noted that the inductance of the OHL-earth loop is very large and frequency-dependent. Therefore also the propagation speed becomes frequency-dependent. The propagation speed of the zero-sequence-system is different from the speed of the positive-sequence-system and the negative-sequence-system.

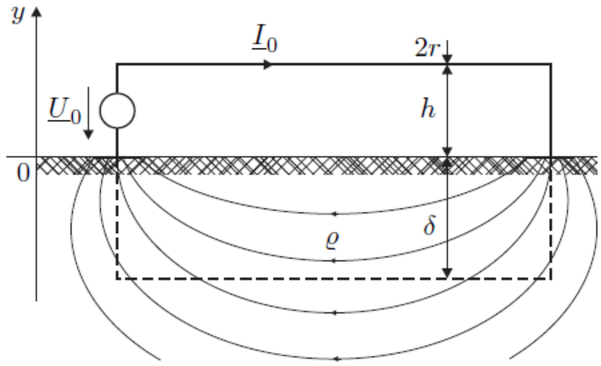

Fig. 4 OHL-ground loop for the calculation of the line-impedance

In case of transient simulations, it must be noted that most simulation programs do not consider this frequency dependency. It is very often simplified with the calculated values at operating frequency, which results in no correct distances.

The strong frequency dependence of the zero system results from the frequency-dependent penetration depth δ of the return current in the earth [8][9].

The advantage of using travelling waves is, that they are robust against some "disturbances" for example:

- load current
- circulating currents in meshed networks
- distributed generation
- dependence of the zero-sequence-system due to the skin depth of the current
- independent of neutral treatment

The disadvantage of travelling waves are:

- Reflexions on each change of the surge impedance for example junction, bus bar, etc.
- Behaviour of connected transformers as large capacitor (5 … 10 nF)
- Measurement equipment
- Measurement with high frequencies in the range of some MHz

In this presentation only the single ended measurement of the travelling wave is under observation. More details can be found in [7] and [5]

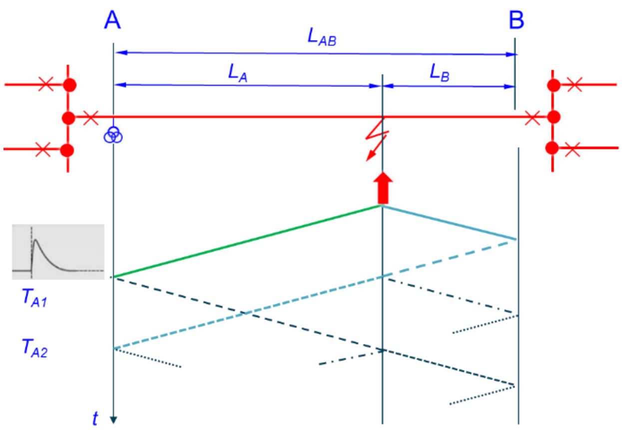

Fig. 5 One side measurement with travelling waves

For the calculation of the propagation velocity of the ground-fault traveling wave *L'* and *C'* must be determined from the network data, taking into account the depth of the earth penetration for very high frequencies. The values for 50 Hz cannot be used. For the experimental network, a value of
$v = v_0 * 0.978$ was obtained for the propagation velocity using the equation(2).

Unfortunately it is in the 110-kV-network not possible to measure with standard inductive ICTs und IVTs in the range of MHz. However, there are new capacitive sensors available that allow a measurement up to the MHz range.

Usually the wavelet analysis is used for the localization of the jump points [9].
But the experiments have shown that other approaches, e.g. a correlation analysis, can provide better results.

From Fig.5 , it can be seen that in the first 359.5 µs the voltage of the traveling wave remains constant. Only when the traveling wave, which is reflected at the fault point, arrives again, the voltage increases. The fast pulses of the earth fault are also visible in the reflected wave. The distance can be calculated from the time of the first fast voltage peak to the first peak of the wave reflected at the short circuit at the fault location.

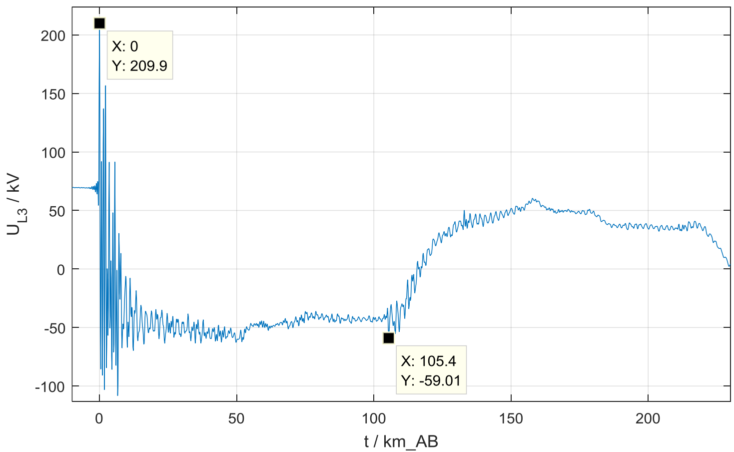

Fig. 5 Travelling waves measured at the relay in Arthurwerke the time is already recalculated as distance in km

The distance to the defect location can be determined by use of suitable filters and a cross-correlation. In this measurement, a distance of 105.4 / 2 = 52.7 km was determined. The desired value is 52.8 km. These results were also observed in all the other earth-faults [7], which caused a larger jump in the faulty phase L3.

4 Description of field tests in the 110-kV-network

To compare the algorithm, extensive field tests were done in a compensated 110-kV-network.The following single line earth fault test cases for the fault location were done:

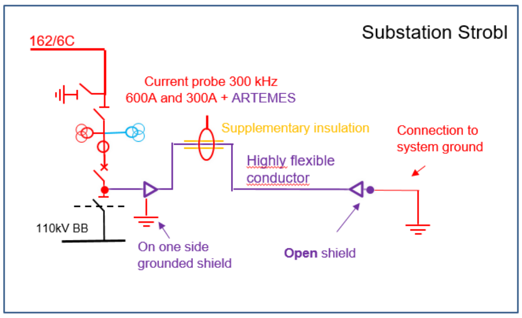

Fig. 5 Solid grounded

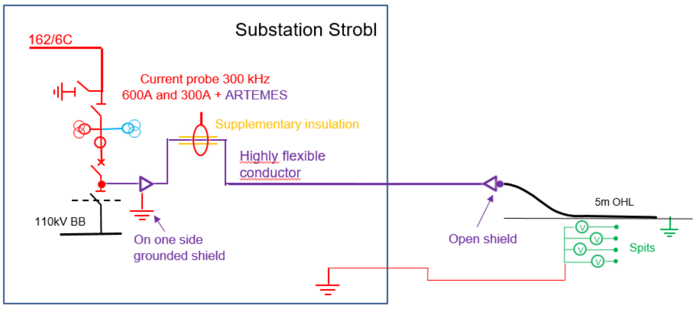

Fig. 6 OHL on meadow

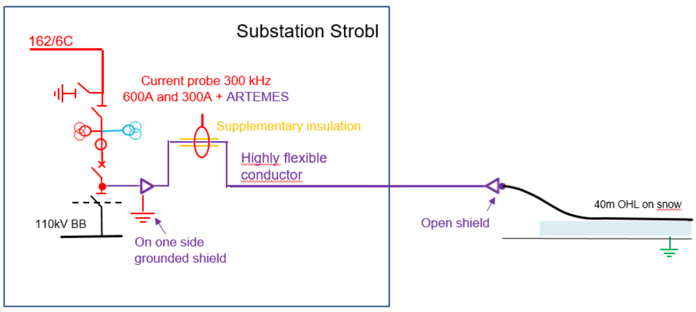

Fig. 7 OHL on 35 cm dry snow

In this test the behaviour of the earth-fault in case of an OHL on dry snow was under investigation.

The arc was ignited after few seconds only on one position. The resulting arc voltage was about 10 kV. This voltage was not high enough to ignite an arc on another location. The change of voltage was high enough for the distance estimation.

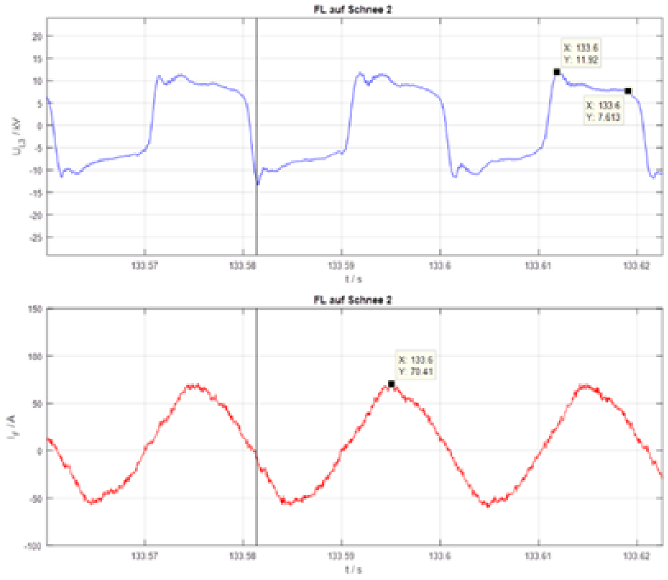

Fig. 8 Voltage and current in the faulty phase in case of OHL on 35 cm dry snow

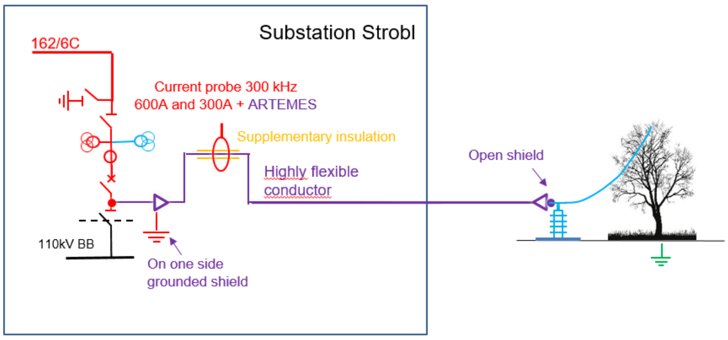

Fig. 9 OHL on tree

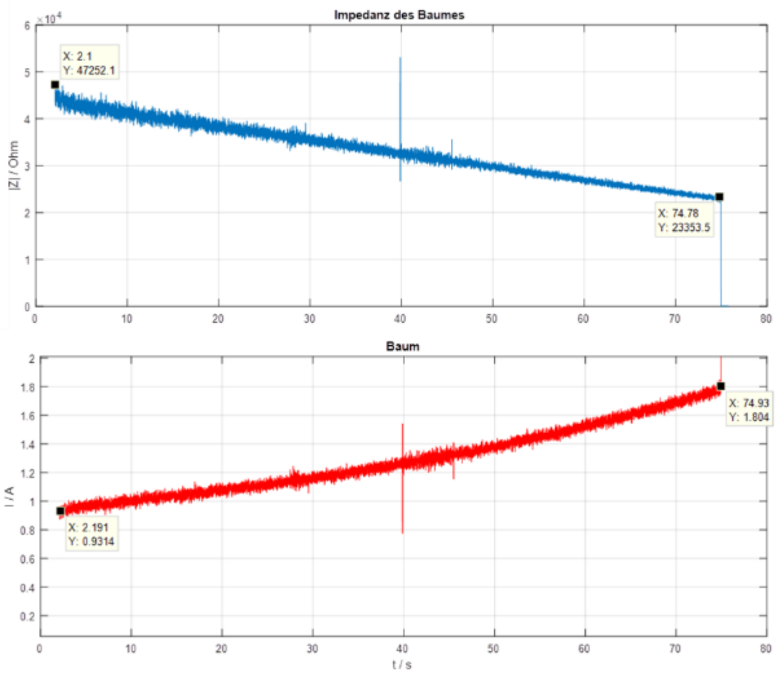

Fig. 10 Impedance of the fault location and earth-fault-current via the tree

The impedance of the tree starts at the beginning of the earth-fault with a value of 48 kΩ and was going down to 23 kΩ after 75 s. It was not possible to detect relevant transients at the beginning of the earth-fault neither in the voltage nor in the current.

The current via the fault location started in the 110-kV-network with 0.9 A and was increasing to 1.8 A at the end of the 75 s.

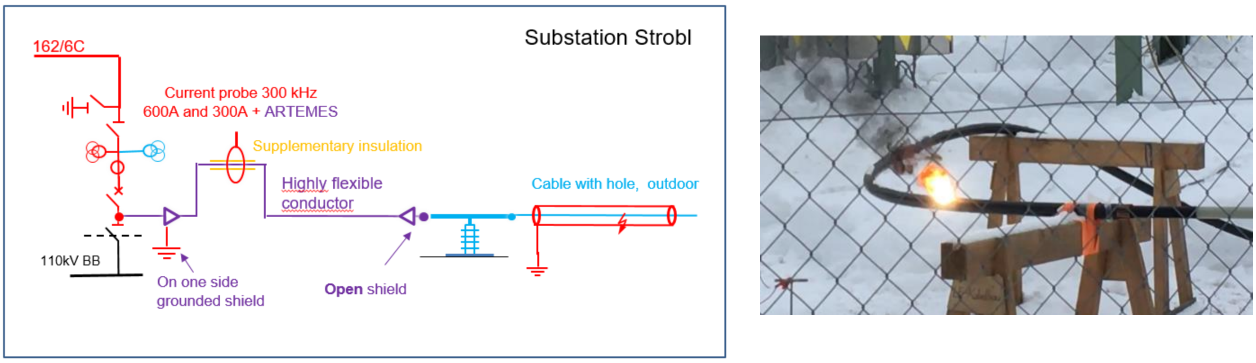

Fig. 11 Earth-fault due to a damaged cable (6 mm hole in the cable)

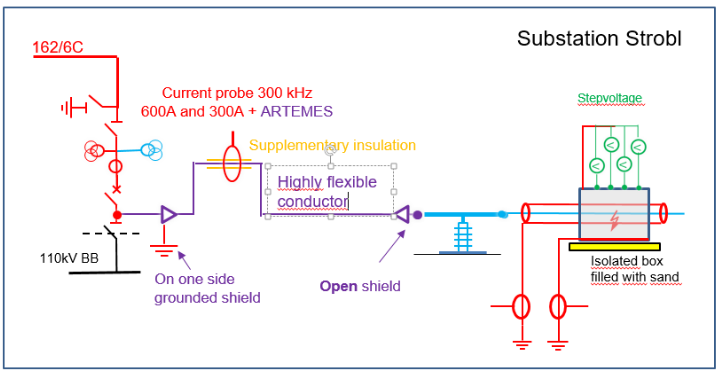

Fig. 12 Earth-fault due to a damaged cable (6 mm hole in the cable), but within a box filled with sand

This test shows, that more or less the whole current is flowing via the shield of the cable. The resulting touch and step-voltages can be neglected. They are in the range of less than 5 V.

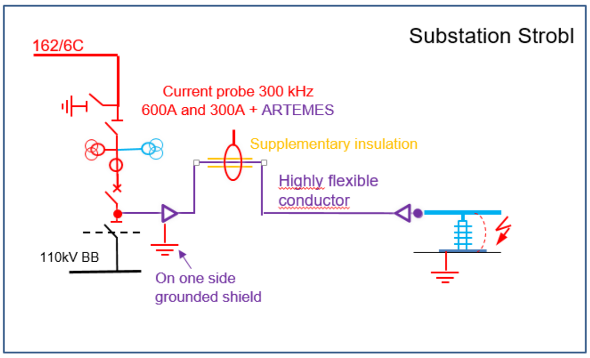

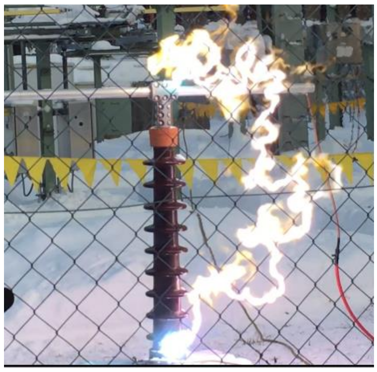

Fig. 13 Earth-fault started with an igniter wire

For the measurement the following equipment were used:

- Transient-recorder from ARTEMES with a synchronous sampling rate of 2 MHz
- ADC with 24 bit resolution
- 4 currents and 4 voltages
- Compensated capacitive voltage divider
- Current Probes with a bandwidth of 300 kHz
- Standard inductive ICT and IVTs for comparison

5 Summary

This publication presents earth-fault tests in the 110-kV-network and the applicability of a new distance protection algorithm. As an alternative results of travelling waves are presented.

Various realistic scenarios were tested in the tests. There were lead wires, cable faults, as well as earth-faults via OHL on tree part of the tests.Due to the new algorithm for an accurate earth fault distance estimation in the range of about 10%, the time to locate the fault location can be reduced, especially in the compensated 110-kV-networks with overhead lines.

The comparison of the voltage measurement with the new capacitive sensors and the standard built-in inductive IVT has clearly shown that the inductive IVT in the 110-kV-network are not suitable for transient measurements.

In the case of nearly homogeneous lines, earthfault-fault distance estimates using travelling waves can be realized with an accuracy in the range of less than 1%.

6 References

[1] A. Aichhorn, B. Etzlinger, R. Mayrhofer, A. Springer, 2016, "*Accurate Clock Synchronization for Power Systems Protection Devices over Packet Switched Networks*", Springer Link, Computer Science - Research and Development, Special Issue Paper, pp. 1-12, Jul. 2016

[2] Achleitner G, 2008, "*Earth Fault Distance Protection"*, Dissertation, Technische Universtität Graz

[3] Achleitner G., Leitner W., Druml G., Simon R., Fickert L., 2017, "*110-kV-Erdschlussversuch und Test eines Erdschlussdistanzschutzes*", *Proccedings ETG Fachtagung STE 2017 Aschaffenburg*, ETG-Fachbericht 151, VDE-Verlag GmbH, Berlin

[4] Druml G., 2013,"*Innovative Methoden zur Erdschlussortung und Petersen-Spulen Regelung*", Thesis at the Institute of Electrical Power System in Graz, Austria

[5] Druml G., Schmidt U., Schegner P.,2016, "*Effects of the nonlinear Arc of a 20-kV-net single-line cable fault on the Earth-Fault-Detection and –Control*", Conference PAC World 2016, Ljubljana, Slovenia

[6] Druml G., Seifert O., Zickler U., Roser M., Fickert L., 2011, "A*uswertung von nichtlinearen Erdschlüssen"*, *Proccedings ETG Fachtagung STE 2011 Erfurt*, ETG-Fachbericht 129, VDE-Verlag GmbH, Berlin Offenbach, 2011

[7] Druml G., Skrbinjek O., Hipp W., Aichhorn A., Schmidt U., Schegner P., 2017, "*Abschätzung der Fehlerentfernung von Erdschlüssen basierend auf Wanderwellen*", *Proccedings ETG Fachtagung STE 2017 Aschaffenburg*, ETG-Fachbericht 151, VDE-Verlag GmbH, Berlin

[8] Herold G., 2008, *Elektrische Energieversorgung II*, J. Schlembach Fachverlag, Weil der Stadt, Germany

[9] Imriš P., 2008, "*Transient based Earth Fault Localisation in 110 kV Subtransmission Networks*", TKK Dissertation, Espoo Finland

[10] Kovács K.P., Raácz I., 1959, *Transiente Vorgänge in Wechselstrommaschinen*, Band 1, Verlag der ungarischen Akademie der Wissenschaften Budapest

[11] Küchler A., 2009: *Hochspannungstechnik, Grundlagen-Technologie-Anwendungen*, 3.Aufl., Springer-Verlag, Berlin,

[12] Melzer H.: 2012, "*Die aktuelle Situation der Sternpunktbehandlung in Netzen bis 110 kV (D-A-CH)*", *ETG-Fachbericht 132*, VDE Verlag GmbH, Berlin Offenbach, 2012

[13] Tengg Ch., Schoass K., Druml G., Schmaranz R., Marketz M., Fickert L., 2013, "*Evaluation of new earth fault localization methods by earth fault experiments*", *CIRED Stockholm 2013*, paper 1317

[14] Wurm M, 2013, "*Vergleich der Bestimmungsmethoden der Fehlerortentfernung beim einpoligen Fehler und Nachweis im praktischen Netzbetrieb*", Dissertation, Technische Universtität Graz

AUTOMATED DESIGN, INSTANTIATION AND QUALIFICATION OF COMPLEX, HIGHLY FAULT TOLERANT AVIONIC SYSTEMS

Florian Kraus[a] **Reinhard Reichel**[a]

MOTIVATION. *The Flexible Platform (fp) technology* reflects its value in the effective development of complex safety-critical fly-by-wire systems, in particular, but not exclusively in the small aircraft domain (CS23) while significantly reducing risks and costs. It is embedded in the *AAA-Process*, which in turn – as the bigger picture – also covers the certification relevant documentation and testing aspect. Both were developed at the University of Stuttgart.

As shown in the submitted presentation, the core idea behind the *fp technology* results in a necessity to adapt generic components to a specific solution. Meeting this challenge emphasizes on use of Domain-Specific Models to represent the system being designed. These models are then used to automatically synthesize executable software code or to generate interfaces for subsequent analysis, documentation or testing purposes.

This presentation covers both, the *Flexible Platform technology* and the *AAA-Process* in general. It will discuss the motivation for

- making use of a platform approach,
- separating the application (e.g. flight control laws) from the platform management,
- embedding the application into a virtual, failure-free and simplex-minded environment and
- describing the system's properties at a very high level of abstraction using a domain-specific modeling language.

Finally the presentation focuses on the multistep refinement process that has proven within the scope of multiple research projects. Applied methods, tools and concepts are presented.

BACKGROUND. The *fp technology* in its core is characterized by a clear separation between the actual application (i.e. flight control laws) and a generic management software layer (*platform management software, plama*). This management layer comprises the whole signal and network communication as well as the entire redundancy management to operate the system in a failure-tolerant way. Complexity, distribution, failure tolerance and redundancy are transparent to the actual application. Once the interface is well defined, both the application and the *plama* can be developed widely independently in accordance with the well-established V-Process whereas the *plama* benefits of its platform based design that ensures a reuse of its generic components.

Adaption to an individual system (e.g. specialization) is done by composition and parametrization of these generic components. This results in many advantages but shifts the development effort towards this specialization. It is a tremendously challenging task since

[a]Institute of Aircraft Systems (ILS), University of Stuttgart, Pfaffenwaldring 27, 70569 Stuttgart, Germany, E-Mail: `florian.kraus@ils.uni-stuttgart.de`, `reinhard.reichel@ils.uni-stuttgart.de`

thousands of parameters have to be set properly and we cannot disregard their strong dependence on the application interface and the actual system's hardware topology. To meet the challenge of specializing the generic *fp* components we make use of the *Model Driven Engineering approach (MDE, also known as MDD)* and share the idea of using a *domain-specific modeling language (DSML, or more general: DSL)* that is tailored to a specific domain of interest, i.e. the Flexible Platform domain. This allows to describe the system's properties at a very high level of abstraction and is an intuitive and efficient way to express (e.g. to model) the system's specification manually. This specification is stored as a domain-specific model and is then used to automatically specialize the *platform management software* in a multi-step refinement process that generates implementation-level parameter data. The refinement process includes several complex model transformations. Those transformations – together with the *DSML* – carry all the system- and software-architectural knowledge required for the specialization task. Model transformations implemented in a traditional high-level, general-purpose programming language (e.g. Python) become inefficient and almost unmanageable in the illustrated case. Dedicated graph transformation languages overcome this problem. In this approach we found a suitable solution that allows the formal specification of model transformations using elements from the source and target domain-specific languages.

In a nutshell, a high-level system specification is used to adapt the platform management software automatically which finally leads to executable software code. The underlying modeling language is tailored to the specific needs of the *fp* respectively fly-by-wire domain and therefore implicates its expressiveness on all levels of abstraction.

University of Stuttgart
Institute of Aircraft Systems (ILS)

ILS Institute of Aircraft Systems Universität Stuttgart
Aviotech

Steirisches Seminar über Regelungstechnik und Prozessautomatisierung
Retzhof, Leibnitz, Austria, Sept. 12-13, 2017

Source: Aviotech GmbH

Automated Design, Instantiation and Qualification of complex, highly fault tolerant Avionics Systems

Reinhard Reichel, Florian Kraus,
Tim Belschner, Rolf-Rekke Riebeling

ILS-Focus: Control Systems for GA

ILS Forschungsflugzeug

SAFAR / EU, Flysmart / LUFO
Source: Diamond Aircraft I.

LAPAZ / LUFO
Source: Stemme AG

Control Categories

OPV	Optionally Piloted Aircraft (manned or unmanned)
UAV	Unmanned Air Vehicle (RPAS)
EPV	Easily Piloted Air Vehicle

Control System

Functions

- Flight Control — Full automatic/autonomous flight incl. ATOL (Automatic Take Off & Landing)
- Vehicle Management — Automatization of the aircraft / utility-systems

Avionics

- Architecture — Integrated
- Loss of Function (Safety) — $10^{-7}..10^{-9}$/h (F/O-…) --- Fly-by-Wire without mech. backup
- Design Assurance Level — DAL B – DAL A

Certification Regulations

- *Compliance with* — *CS23, CS23.1309, ASTM F3061, JARUS AMC RPAS.1309, ARP4754, ARP4761/ ED-135, DO-178C/, DO-297, …*

Exemplary Control System: Fly-by-Wire System for a DA42-OPV

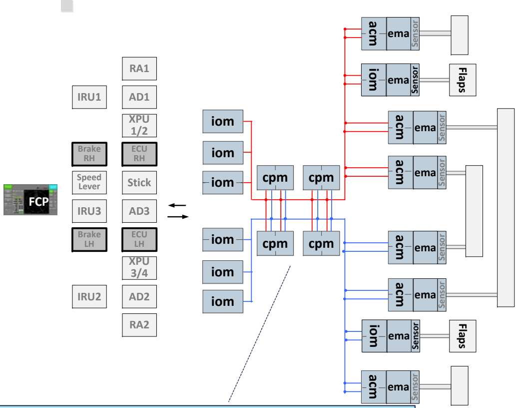

Functions/Laws
APFI allows simplex minded Application Design.
Implemented Applications/Laws:
- Flight Control, Autopilot (4D Trajectory Tracking, ATOL)
- Mission Management (incl. Path-Planning)
- Vehicle Management (NWS, Braking,….)

ILS-Approach Step A: Advanced Integrated Avionics Platform

Basic Idea

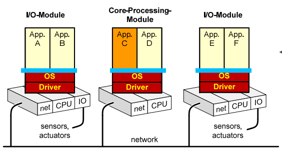

Integrated Avionics Platform IMA
State of the Art at AIRBUS, BOEING

Complexity: System-Management is Part of the Function/Application

Objective: **Plama shall be generated highly automated**

Challenge: **Fly-by-Wire Systems and consequently Plama-Instancies vary significantly.**

Clear Separation of "Laws" and "System-Management"1)

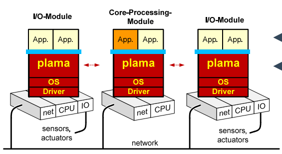

Objective: Laws operate virtually simplex
Complexity: System-Complexity abstracted by plama

Advanced Integrated Avionics Platform APF
Developed by ILS

Note 1) System-Management ≙ Platform-Management (plama)

Advanced Integrated Avionics Platform : Basic Services and PDI

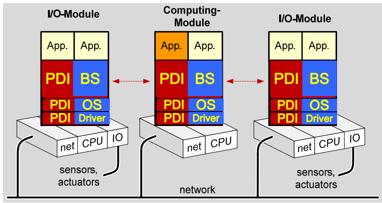

Plama-BS: Basic Service BS (Executable Code)
- is a generic Software-Unit
- has to be developed and qualified only once

Plama-PDI: Parameter Data Items
- specialize the function of any BS-Instance
- define their Data- & Control-Coupling
- have to be generated for any new Platform Instance

OS-PDI: ***OS Configuration Data***

DR-PDI: ***Driver Configuration Data***

Objective: **Plama shall be generated automatically**
➔ Highly automated generation of PDI

Challenge: **100.000 – 1.000.000 PDI-Data per Platform-Instance**

ILS-Approach Step B: AAA-Process (Tool-Suite)

Axx Automatic System-Refinement, SW-Decomposition and PDI-Generation

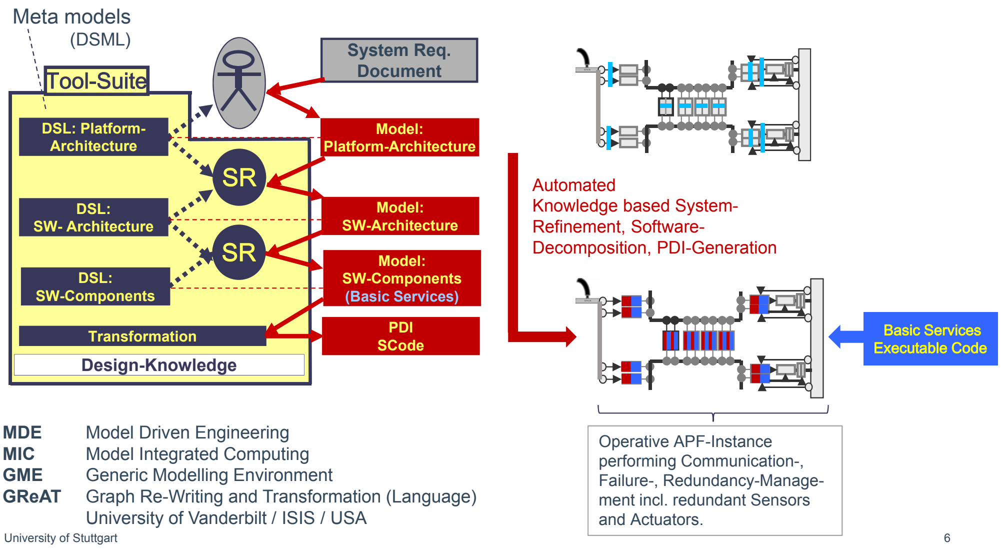

MDE Model Driven Engineering
MIC Model Integrated Computing
GME Generic Modelling Environment
GReAT Graph Re-Writing and Transformation (Language)
University of Vanderbilt / ISIS / USA

Axx-Process --- 1st Step: Generation of the Platform Architecture / DSL

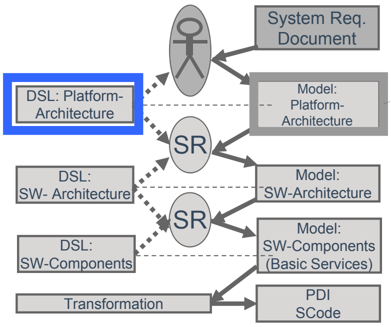

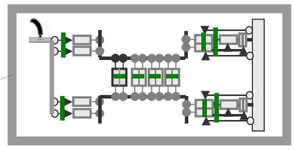

DSL: Aspects
- Hardware Architecture
- IO-Signals
- Granulation of Peripherals
- Data Flow (Virtual Links)
- mapps (composition of laws to multi-apps)
- Allocation of mapps (static)
- Reconfiguration
- Operating Mode

Simplification for the Presentation:
DSL: Aspects
- Hardware Architecture
- IO-Signals
- Data Flow (Virtual Links)
- Allocation of Laws (static)

Platform Architecture: Aspect of Hardware Structure / DSL

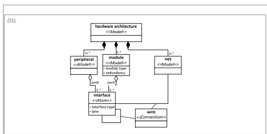

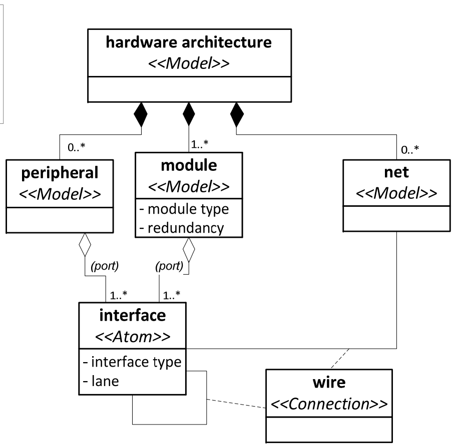

DSL: Aspects
- **Hardware Architecture**
- IO-Signals
- Data Flow
- Allocation of Laws (static)

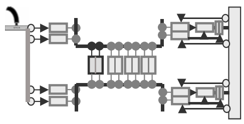

Platform Architecture: Aspect of Hardware Structure / Model Instance

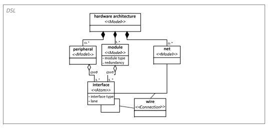

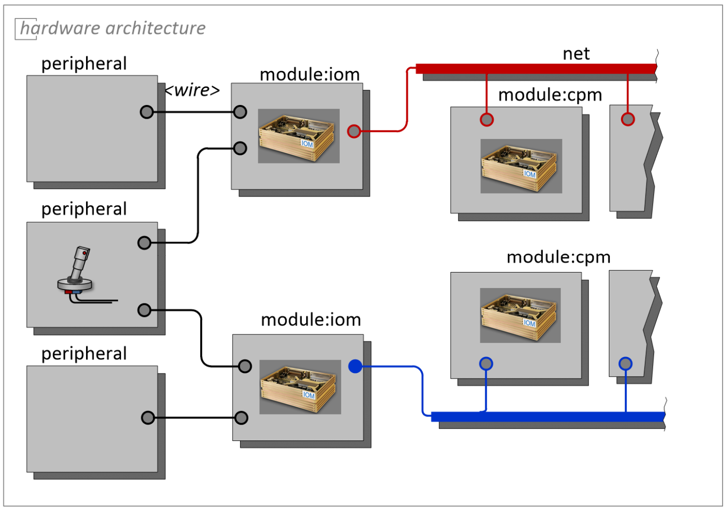

Manual Implementation – Generic Modelling Environment (GME)

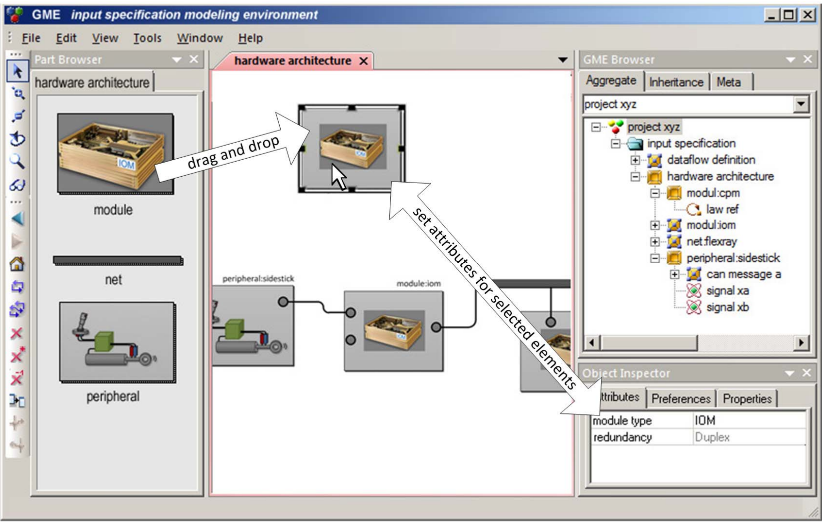

Platform Architecture: Aspect of IO-Signals / DSL

DSL

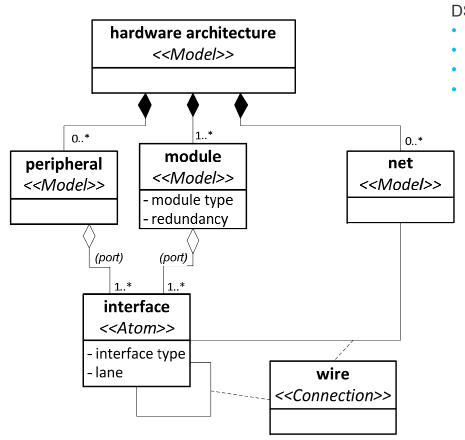

DSL: Aspects

- Hardware Architecture
- **IO-Signals**
- Data Flow
- Allocation of Laws (static)

Platform Architecture: Aspect of IO-Signals / DSL

DSL

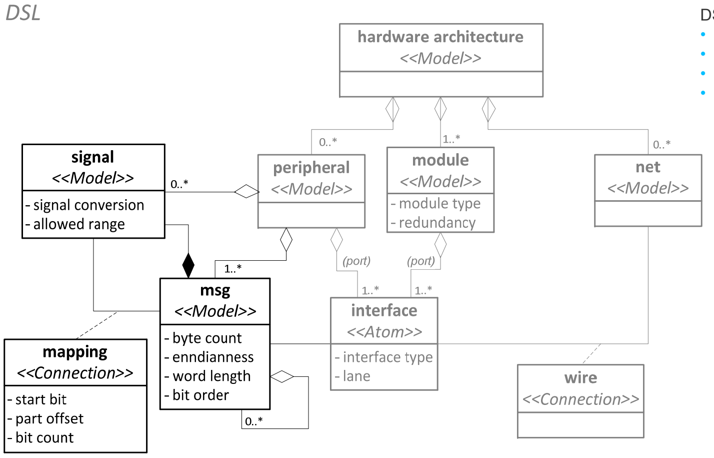

DSL: Aspects

- Hardware Architecture
- **IO-Signals**
- Data Flow
- Allocation of Laws

Platform Architecture: Aspect of IO-Signals / Model Instance

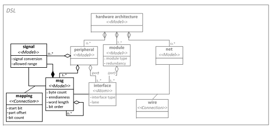
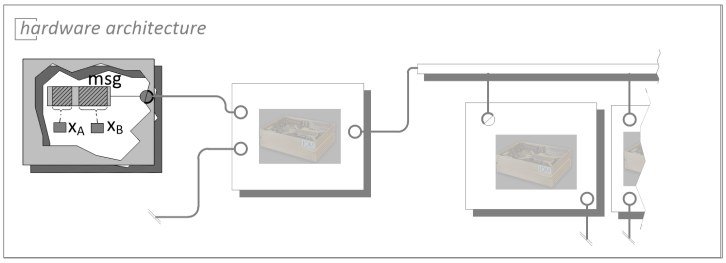

Platform Architecture: Aspect of Data Flow / DSL

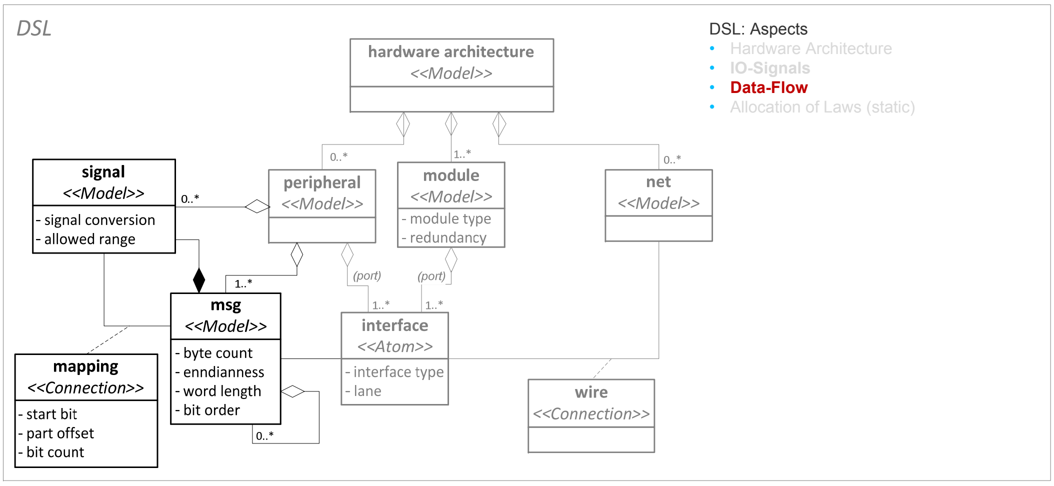

Platform Architecture: Aspect of Virtual Links / DSL

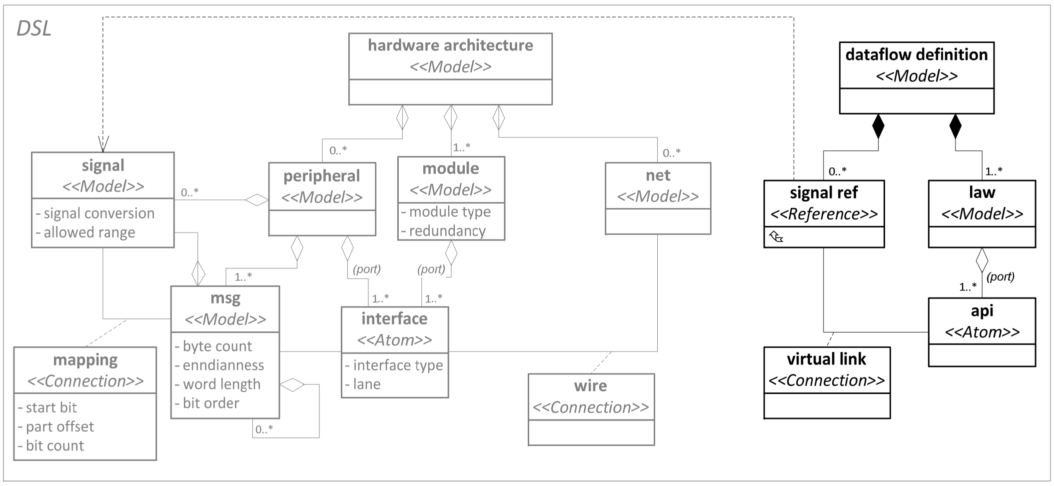

Platform Architecture: Aspect of Virtual Links / Model Instance

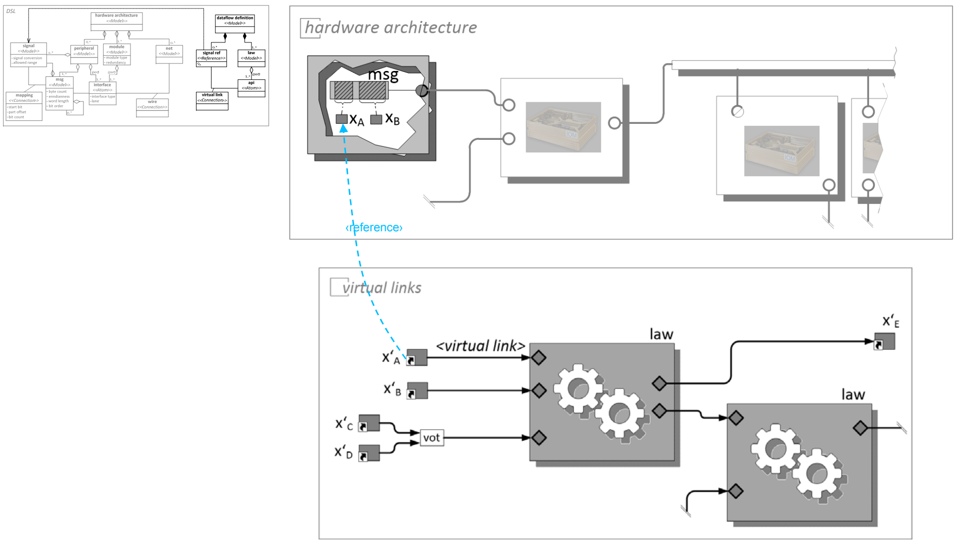

Platform Architecture: Aspect of Allocation of Laws / DSL

DSL: Aspects
- Hardware Architecture
- IO-Signals
- Data Flow
- **Allocation of Laws (static)**

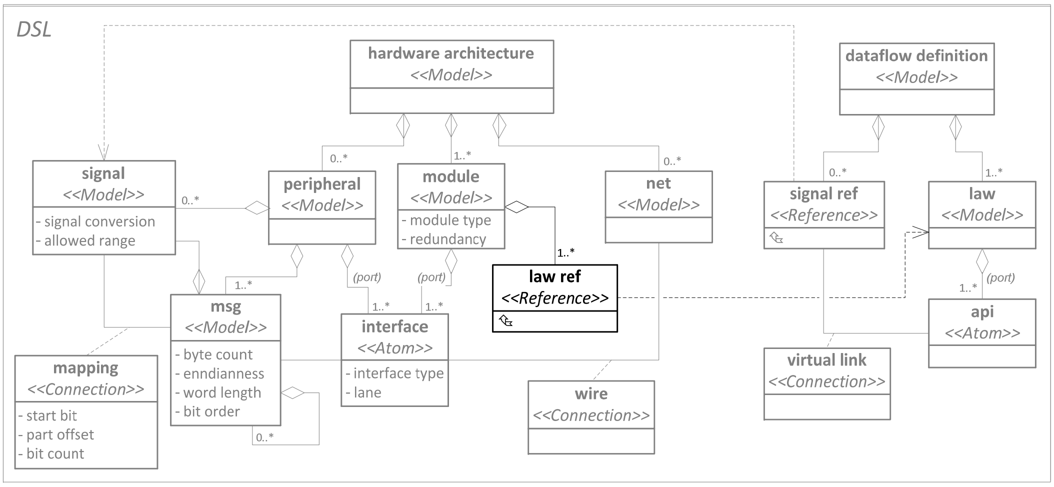

Platform Architecture: Aspect of Allocation of Laws / Model Instance

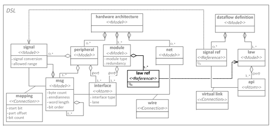

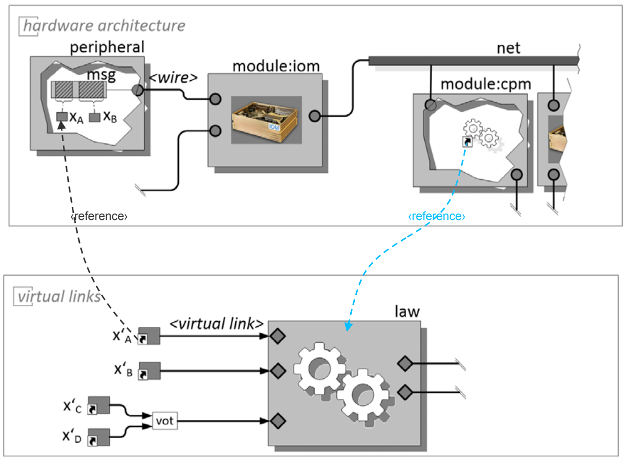

Axx-Process --- 2st Step: Refinement towards Plama-SW-Architecture

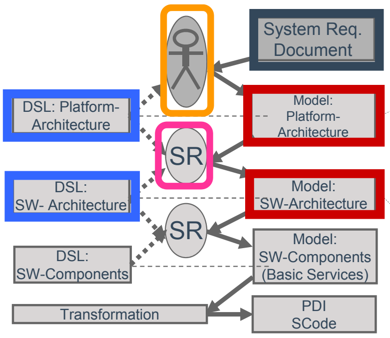

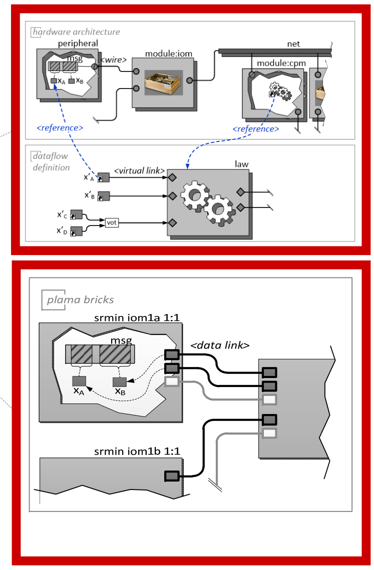

Plama SW Architecture: Synthesis Rules

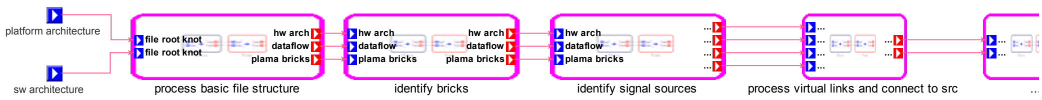

Plama SW Architecture: Synthesis Rules

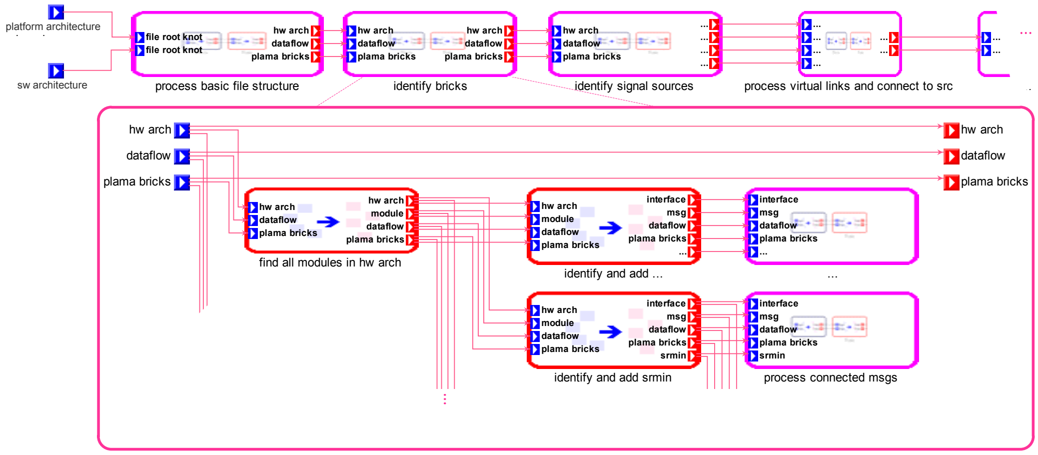

Plama SW Architecture: Synthesis Rules

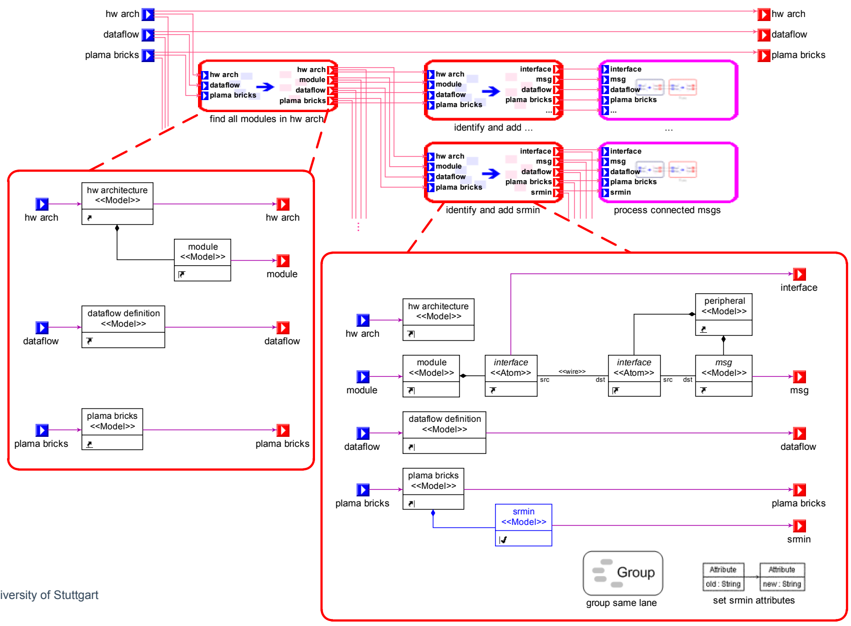

Axx-Process --- 3rd Step: Refinement towards SW Component Configuration

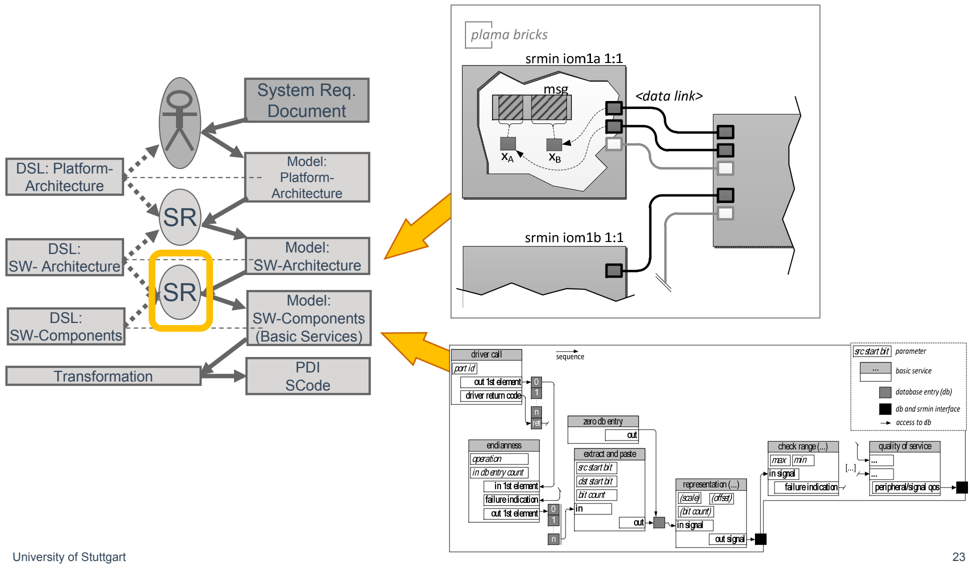

University of Stuttgart

23

Axx-Process --- 4th Step: Tranformation to compilable Source-Code

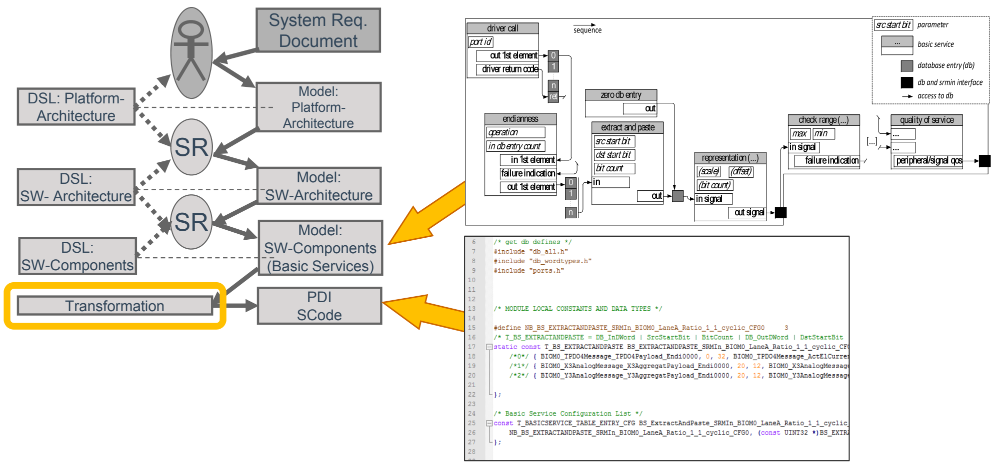

University of Stuttgart

24

AAA-Process (Tool-Suite): Overview

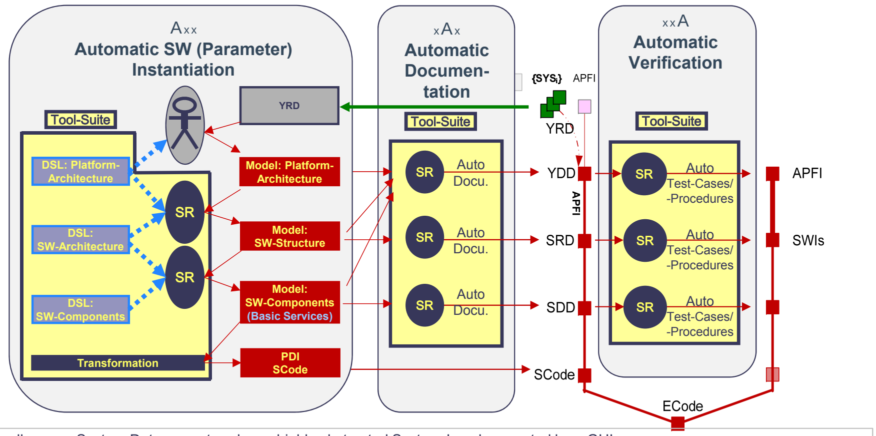

Manually:	System Data are entered on a highly abstracted System-Level supported by a GUI
Automated:	System-Refinement, Software-Decomposition down to BS and automated Generation of PDI
Automated:	Generation of YDD (System Design Document), SRD (Software-Req-Documents), SDD (Software-Design-Documents)
Automated:	Generation of Requirements based Test-Cases resp. Test-Procedures. Test-Scripts can be executed automatically
Certification:	Process is in Accordance with DO178C, DO297 e.a.
Applications:	Development and Pre-Qualification “simplex minded” in a pure Simulation Environment

University of Stuttgart 25

Summary

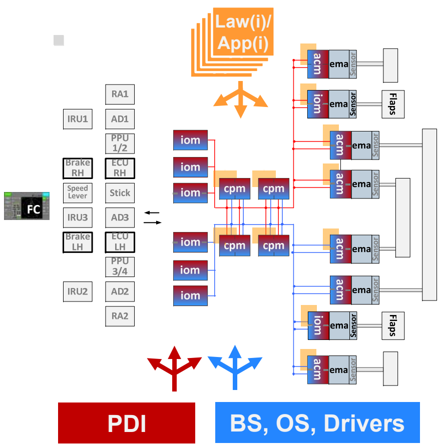

System of Integrated Systems (SIS)

SIS consists of
- an APF-Instance
- multiple Systems (System: Law(s) + Peripheral-Units)

SIS can be incrementally certified:
- BS : Certification Items / Qualification once-only
- APF-Instance : Certification Item / Qualification automated
- Law(i) : Certification Item
  - Prequalified in Simulation Environment
  - Qualified finally by automatic Re-Run of tests in the Simulation Environment on the APFI

University of Stuttgart 26

Multi-sensor data fusion for automated driving

Daniel Watzenig[a]

Automated vehicle technology has the potential to be a game changer on the roads, altering the face of driving as we experience it by today. Many benefits are expected ranging from improved safety, increased energy efficiency, reduced congestion, lower stress for car occupants, and better road utilization due to optimal integration of private and public transport. Automated driving is characterized by a computer-based derivation and execution of appropriate driving maneuvers based on the current traffic situation captured by a multitude of sensors. The basis for evaluating the traffic situation, however, is knowledge about all relevant entities in a vehicle's environment, including traffic participants, road infrastructure (lane markings, traffic signs, traffic lights) or obstacles. For acquiring such knowledge, numerous sensors have to be used that permanently provide relevant data. As effective sensors are, they have some drawbacks such as

- Limited range
- Performance is susceptible to common environmental conditions (rain, fog, varying lighting conditions)
- Range determination not as accurate as required
- Detection of artefacts, so-called "false positives"

In order to overcome these drawbacks, multi-sensor fusion plays an important role in order to increasing reliability and safety and hence user acceptance of automated vehicles. Model-based sensor fusion is the combining of sensory data or data derived from disparate sources such that the resulting information has less uncertainty. The term uncertainty reduction implies

- Increased object classification accuracy (Higher detection rate, fewer false alarms, enhanced level of detail of object description)
- Improved state estimation accuracy
- Improved robustness for instance in adverse weather conditions
- Increased availability
- Enlarged field of view

For many automated driving functions, information from different sensors are required (e.g., the velocity of an object measured by a radar and its class determined by a camera). Model-based sensor fusion inherently combines data from all available sensors in order to provide both a higher quantity and a higher quality of available information. For a single sensor, it is difficult to determine the current error of its measurement. The model-based approach, however, can exploit the redundancy between sensors as well as the model-knowledge to

[a]VIRTUAL VEHICLE Research Center, Inffeldgasse 21a, 8010 Graz, Austria, E-mail: `daniel.watzenig@v2c2.at`

estimate the current estimation errors. Only if the driving functions know about the current expected error of the environmental representation, it can take appropriate decisions. The most common way to describe these uncertainties is by means of probabilistic quantities.

This talk discusses state-of-the-art methods for model-based multi-sensor data fusion for automated driving in order to manage correlated, inconsistent, and imperfect data. Different algorithms (e.g. Bayes estimators, fuzzy reasoning, evidential belief reasoning, adaptive and hybrid techniques…), concepts (high level, intermediate level, low level), and classes (complementary, competitive, cooperative) will be analyzed and investigated in terms of applicability and performance by examples.

Model-based control of hydronic networks using graph theory

Daniel Muschick[a] **Viktor Unterberger**[a b] **Markus Gölles**[a]

Hydronic networks are networks using a liquid heat-transfer medium for heating or cooling purposes. They can range in size from small cooling applications in machines to large district heating networks with many producers and consumers.

Whatever their size, the main control problems always remain the same: heat needs to be transported from sources to sinks while ensuring that certain temperatures, mass flows and pressures in the system remain within given boundaries. The difficulty lies in the fact that the heat to be transported cannot be controlled directly; it depends on both the fluid mass flows and temperature levels in the system. In order to control a hydronic network, it is thus necessary to determine the fluid mass flows which result in the desired behavior; then the hydraulic components have to be controlled in such a way that the desired mass flows are realized. For this the network as a whole has to be considered and the mutual influences of the different components have to be taken into account. Currently, however, the components in hydronic networks are often controlled individually and only their local influence is considered.

This article presents a control architecture that automatically takes into account the links between the hydraulic and the thermal aspects of a hydronic network. The key to handle this issue efficiently and systematically is to represent the hydronic network in a structured way using graph theory. By doing so, it is possible to automatically generate mathematical models of both the stationary heat distribution, used for determining the necessary mass flows, and the hydraulic dynamics used for the control of these mass flows.

The graphs representing the networks consist of nodes $\mathfrak{N}$ connected via edges $\mathfrak{E}$. Each edge corresponds to a component in the network, e.g. a pipe, a heat producer or a valve. Each component has an influence on both the temperatures T and the pressures p in the network. This influence can be described by possibly non-linear functions ΔT for the temperature change and Δp for the pressure change depending on the type of component, the temperatures, the mass flows and the control signals in the case of actuators.

The individual edges and nodes are connected via node and mesh equations

$$\sum_{i\in\mathfrak{N},\,\dot m_{ij}>0} \dot m_{ij} = \sum_{k\in\mathfrak{N},\,\dot m_{jk}>0} \dot m_{jk} \quad \forall j \in \mathfrak{N}, \qquad \sum_{\{i,j\}\in\mathfrak{M}_k} \Delta p_{ij} = 0 \quad \forall\, \mathfrak{M}_k \in \mathfrak{M}, \tag{1}$$

where $\dot m_{ij}$ and Δp_{ij} denote the mass flow from node i to node j respectively the corresponding pressure difference $p_j - p_i$, and $\mathfrak{M}$ denotes the set of all loops or meshes in the network.

[a]BIOENERGY2020+ GmbH, Inffeldgasse 21b, 8010 Graz, Austria, E-mail: `daniel.muschick@bioenergy2020.eu`

[b]Institute of Automation and Control, Graz University of Technology, Inffeldgasse 21b, 8010 Graz, Austria

Assuming constant heat capacities, a similar relation exists for describing the mixing of flows in nodes:

$$\sum_{i \in \mathfrak{N},\, \dot{m}_{ij}>0} \dot{m}_{ij}\left(T_i + \Delta T_{ij}\right) = \Big(\sum_{k \in \mathfrak{N},\, \dot{m}_{jk}>0} \dot{m}_{jk}\Big) T_j \quad \forall j \in \mathfrak{N} \tag{2}$$

The individual component equations can now be combined with these relations and written in a concise way to describe the stationary heat distribution.

Similarly, the hydraulic dynamics can be automatically obtained by combining the node and mesh equations with the simple differential equation

$$\frac{l_{ij}}{A_{ij}} \frac{\mathrm{d}\dot{m}_{ij}}{\mathrm{d}t} = \Delta p_{ij} \tag{3}$$

describing the acceleration of a fluid in every edge representing a pipe with length l_{ij} and cross section A_{ij}.

Finally, the models generated can now be used in the hydronic control strategy, which consists of three parts: First, the model describing the stationary heat distribution is used to calculate the mass flows in such a way that the desired temperature levels are reached and no mass flow limitations are violated. Second, a temperature controller compares the actual temperatures with the desired values and adapts the calculated mass flows $\dot{\mathbf{m}}_{\mathrm{ff}}$ in order to reach the desired values. Third, the resulting desired mass flows $\dot{\mathbf{m}}^*$ are used as references for a hydraulic controller to control all actuators (valves $\mathbf{u}_{\mathrm{V}}$ and pumps $\mathbf{u}_{\mathrm{P}}$) at the same time. A schematic overview of this cascading control structure is shown in Fig. 1.

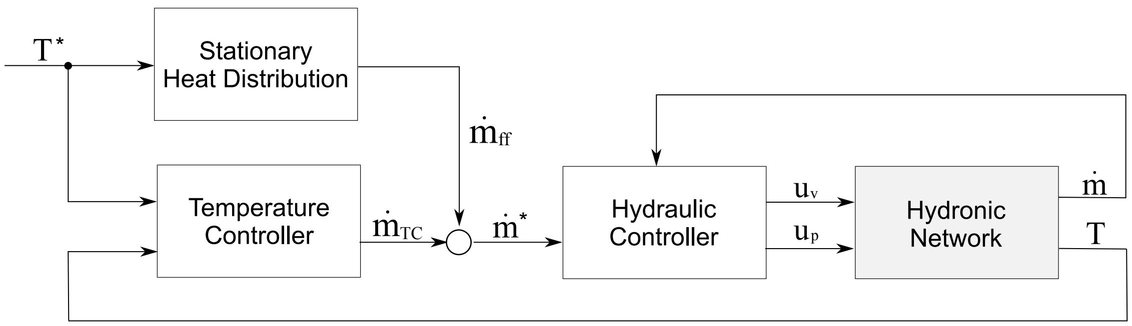

Figure 1: Cascading control structure for a hydronic network.

bioenergy2020+

Model-based control of hydronic networks using graph theory

Daniel Muschick, Viktor Unterberger, Markus Gölles

Retzhof, September 13th, 2017

powered by klima+ energie fonds

FFG

innovations kompetenz

bioenergy2020+

Motivation

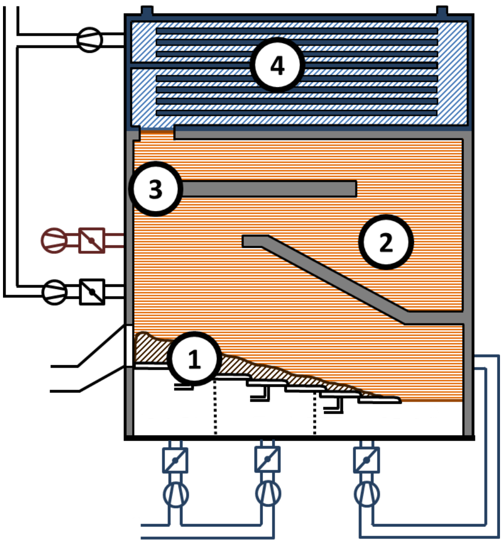

innovations kompetenz

bioenergy2020+

Motivation

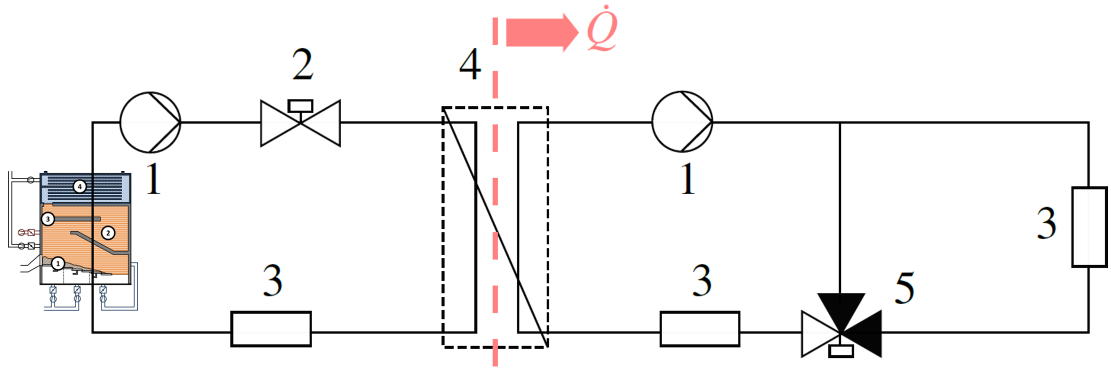

Slide 3
Retzhof, Sept. 13th, 2017

innovations kompetenz

bioenergy2020+

Motivation

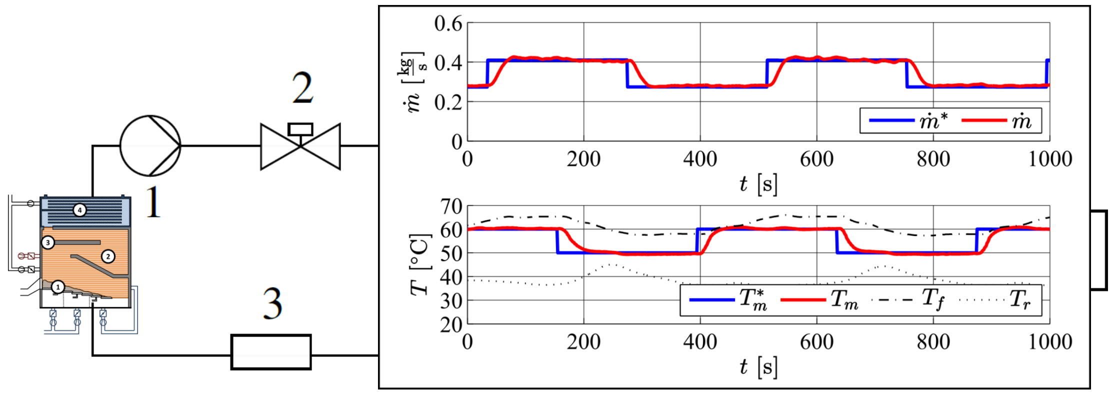

Decoupled control of mass flows and temperatures

Control of heat transfer via heat exchanger

Slide 4
Retzhof, Sept. 13th, 2017

innovations kompetenz

bioenergy2020+

Motivation

- New projects include the control of
  - Solar Collectors
  - Heat Pumps
  - Small-sized Heating Grids
  - Thermal Buffers

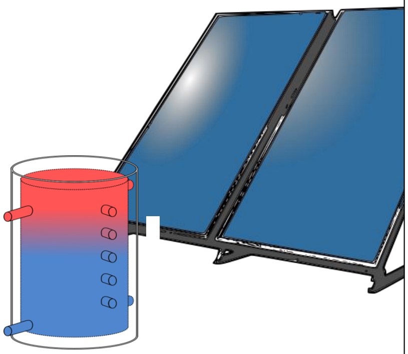

- All connected in **hydronic** (hydraulic+thermal) **networks**

innovations kompetenz

bioenergy2020+

Motivation

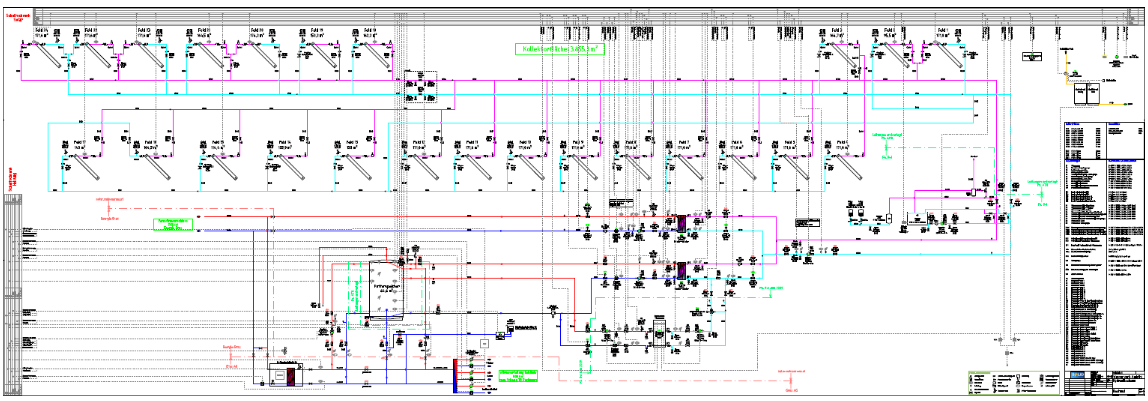

innovations kompetenz

bioenergy2020+

Motivation

- **How can we simulate something like this?**
  - Automatic deduction of hydraulic and thermal simulation models based on a general description of the network
- **What do we need to control in the first place?**
  - Automatic identification of low-level control objectives based on high-level specifications
- **How can we control something like this?**
  - Hierarchical control: heat flow / temperatures / mass flows

bioenergy2020+

Motivation – Hierarchical Hydronic Controller

A **Steady State Optimizer** calculates the mass flows and free heat flows in order to meet high-level objectives and temperature constraints in steady state

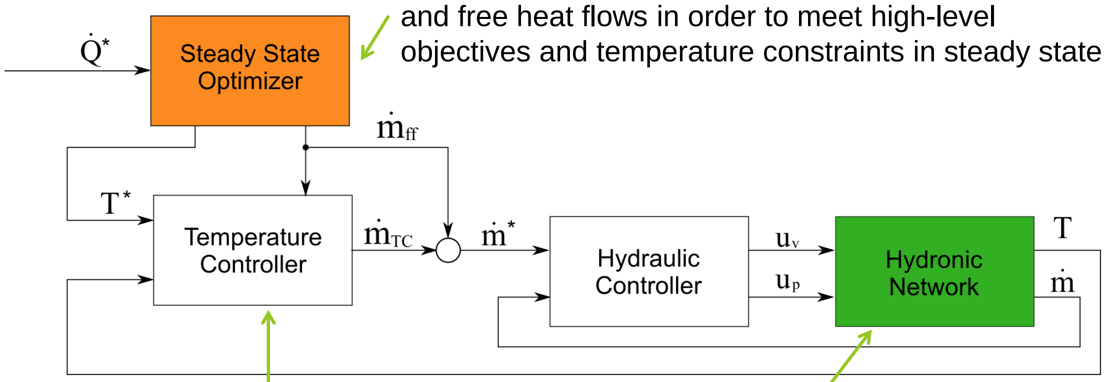

A **Temperature Controller** adjusts the desired mass flows

A **Hydraulic Controller** varies the pump pressures and valve openings to ensure the desired mass flows

bioenergy2020+

Motivation – Goals

- Computer-aided methods should deliver
  - a **dynamic hydraulic model** suitable for simulation and model-based controller design
  - a **static model** of the **temperature distribution** suitable for numeric optimization techniques
- Describing networks by **graphs** makes them accessible to computer algorithms

Slide 9
Retzhof, Sept. 13th, 2017

innovations kompetenz

bioenergy2020+

Overview

- Motivation
- **Graph-based representation of networks**
- **Hydraulic ODE model**
- **Thermal steady state model**
- **Example**
- **Summary**

Slide 10
Retzhof, Sept. 13th, 2017

innovations kompetenz

Graph-based representation of networks

- Networks can be described as directed **graphs** consisting of **nodes** N connected by **edges** E
- Each edge corresponds to an element in the network, e.g. a resistor, inductance, valve, pump…
- The way the nodes are connected can be mathematically represented by the **incidence matrix A**

$$\mathbf{A} = \langle a_{ij} \rangle, \qquad a_{ij} = \begin{cases} 1 & \text{node } i \text{ is end point of edge } j \\ -1 & \text{node } i \text{ is starting point of edge } j \\ 0 & \text{otherwise} \end{cases}$$

Graph-based representation of networks – Electric Example

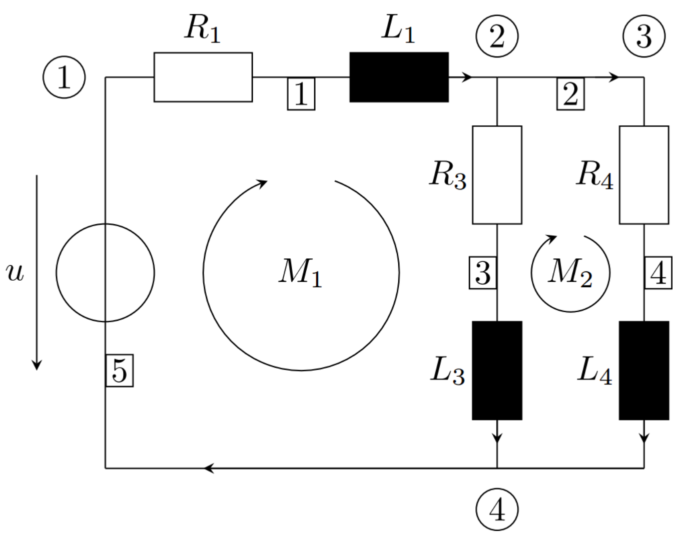

$$\begin{array}{cc} & \text{edges} \\ \text{nodes} & \mathbf{A} = \begin{bmatrix} -1 & 0 & 0 & 0 & 1 \\ 1 & -1 & -1 & 0 & 0 \\ 0 & 1 & 0 & -1 & 0 \\ 0 & 0 & 1 & 1 & -1 \end{bmatrix} \end{array}$$

bioenergy2020+

Graph-based representation of networks – Kirchhoff's Laws

- The mass flows and the pressure changes along the edges must fulfill the hydraulic equivalent of *Kirchhoff*'s laws:
  - Mass conservation

$$\sum_{i \in N,\, \dot{m}_{ij}>0} \dot{m}_{ij} = \sum_{k \in N,\, \dot{m}_{jk}>0} \dot{m}_{jk} \quad \forall j \in N,$$

  - Energy conservation

$$\sum_{j \in M_k} \Delta p_j = 0 \quad \forall\ M_k \in M$$

- The mass conservation law can easily be expressed via the incidence matrix:

$$\mathbf{A}\dot{\mathbf{m}} = \mathbf{0}$$

innovations kompetenz

bioenergy2020+

Graph-based representation of networks – Cycles

- For the energy conservation law, we need the concept of **cycles / loops**
- Cycles can be represented by the cycle-edge-incidence matrix **B**

$$\mathrm{B} = \langle b_{jk} \rangle, \qquad b_{jk} = \begin{cases} 1 & j \in M_k, \text{same orientation} \\ -1 & j \in M_k, \text{opposite orientation} \\ 0 & \text{otherwise.} \end{cases}$$

- The matrix **B** can be automatically generated from the **A** matrix using algorithms from graph theory
- With it, the energy conservation law becomes

$$\mathbf{B}\Delta\mathbf{p} = \mathbf{0}$$

innovations kompetenz

Graph-based representation of networks – Electric Example

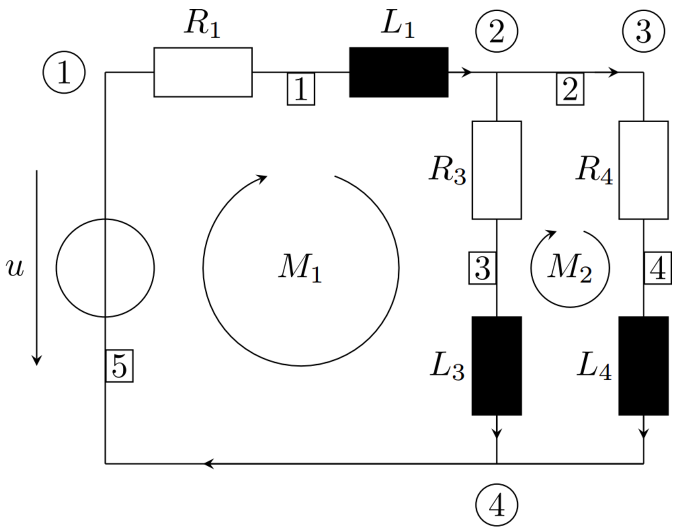

edges

nodes

$$\mathbf{A} = \begin{bmatrix} -1 & 0 & 0 & 0 & 1 \\ 1 & -1 & -1 & 0 & 0 \\ 0 & 1 & 0 & -1 & 0 \\ 0 & 0 & 1 & 1 & -1 \end{bmatrix}$$

cycles

$$\mathbf{B} = \begin{bmatrix} 1 & 0 & 1 & 0 & 1 \\ 0 & 1 & -1 & 1 & 0 \end{bmatrix}$$

$$\mathbf{A}\dot{\mathbf{m}} = \begin{bmatrix} \dot{m}_5 - \dot{m}_1 \\ \dot{m}_1 - \dot{m}_2 - \dot{m}_3 \\ \dot{m}_2 - \dot{m}_4 \\ \dot{m}_3 + \dot{m}_4 - \dot{m}_5 \end{bmatrix} = \mathbf{0}$$

bioenergy2020+

Graph-based representation of networks – Electric Example

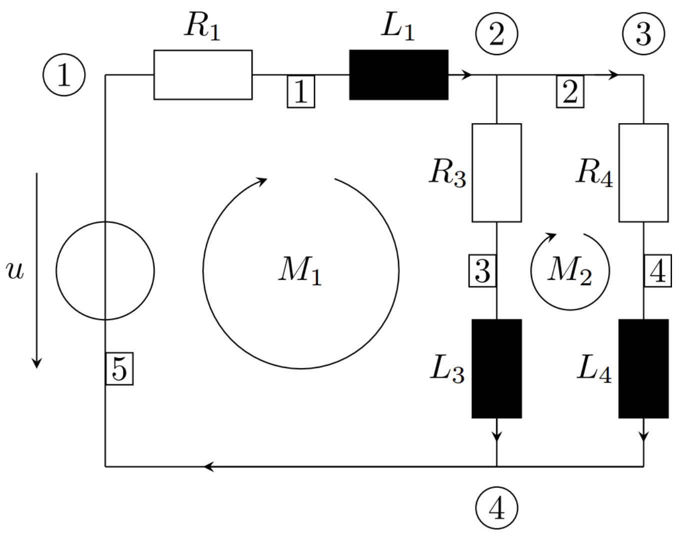

edges

nodes

$$\mathbf{A} = \begin{bmatrix} -1 & 0 & 0 & 0 & 1 \\ 1 & -1 & -1 & 0 & 0 \\ 0 & 1 & 0 & -1 & 0 \\ 0 & 0 & 1 & 1 & -1 \end{bmatrix}$$

cycles

$$\mathbf{B} = \begin{bmatrix} 1 & 0 & 1 & 0 & 1 \\ 0 & 1 & -1 & 1 & 0 \end{bmatrix}$$

$$\mathbf{B}\Delta\mathbf{p} = \begin{bmatrix} \Delta p_1 + \Delta p_3 + \Delta p_5 \\ \Delta p_2 - \Delta p_3 + \Delta p_4 \end{bmatrix} = \mathbf{0}$$

bioenergy2020+

Overview

- Motivation
- Graph-based representation of networks
- Hydraulic ODE model
- Thermal steady state model
- Example
- Summary

Slide 17
Retzhof, Sept. 13th, 2017

innovations kompetenz

bioenergy2020+

Hydraulic ODE Model

- We would like to have an **ODE model** of the form

$$\frac{d\mathbf{x}}{dt} = \mathbf{f}(\mathbf{x}, \mathbf{u})$$

- The **inputs** $\mathbf{u}$ are
  - Pump pressures
  - Valve opening ratios
- What are the **state variables** $\mathbf{x}$?

Slide 18
Retzhof, Sept. 13th, 2017

innovations kompetenz

bioenergy2020+

Hydraulic ODE Model – Single Edge

- The pressure change along any edge can be described by
  - Acceleration of mass in a pipe
  - Pressure drop due to resistance
  - Pressure increase due to pumps

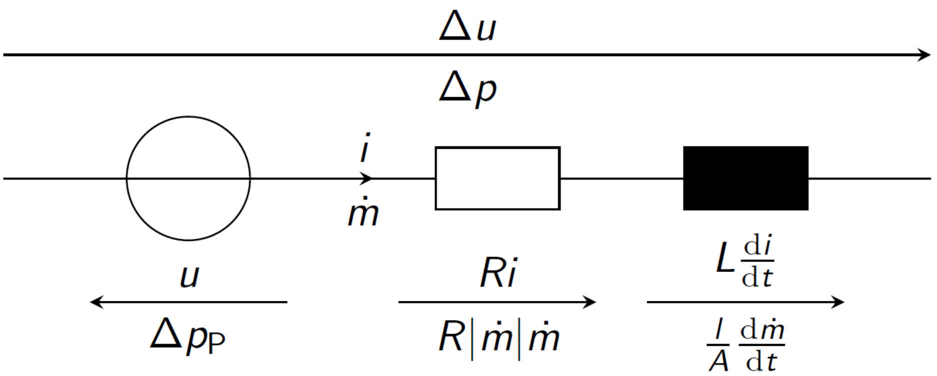

innovations kompetenz

bioenergy2020+

Hydraulic ODE Model – Single Edge

- The pressure change along any edge can be described by
  - Accele
  - Pressu
  - Pressu

$$\Delta p_j = \frac{l_j}{A_j}\frac{d\dot{m}_j}{dt} + R_j|\dot{m}_j|\dot{m}_j - \Delta p_{P,j}$$

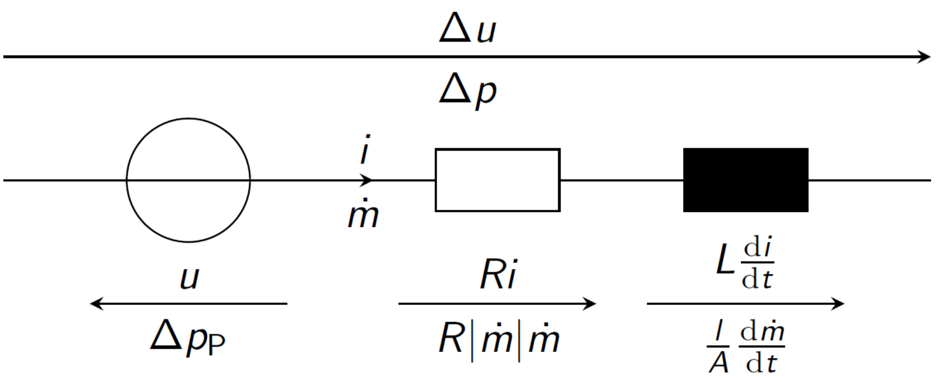

innovations kompetenz

bioenergy2020+

Hydraulic ODE Model – Matrix form

- The individual equations for the $\mathrm{N_j}$ edges

$$\Delta p_1 = \frac{l_1}{A_1}\frac{\mathrm{d}\dot{m}_1}{\mathrm{d}t} + R_1|\dot{m}_1|\dot{m}_1 - \Delta p_{\mathrm{P},1}$$
$$\vdots$$
$$\Delta p_{N_j} = \frac{l_{N_j}}{A_{N_j}}\frac{\mathrm{d}\dot{m}_{N_j}}{\mathrm{d}t} + R_{N_j}\left|\dot{m}_{N_j}\right|\dot{m}_{N_j} - \Delta p_{\mathrm{P},N_j}$$

  can be combined and written in **matrix form**:

$$\Delta\mathbf{p} = \mathrm{diag}\left(\frac{l_i}{A_i}\right)\frac{\mathrm{d}\dot{\mathbf{m}}}{\mathrm{d}t} + \mathrm{diag}(R_i)\mathrm{diag}(|\dot{\mathbf{m}}|)\dot{\mathbf{m}} - \Delta\mathbf{p}_\mathrm{P}$$

- Applying the **energy conservation law** yields

$$\mathbf{B}\Delta\mathbf{p} = 0 = \boxed{\mathbf{B}\Lambda_m}\frac{\mathrm{d}\dot{\mathbf{m}}}{\mathrm{d}t} + \mathbf{B}\Lambda_R\mathrm{diag}(|\dot{\mathbf{m}}|)\dot{\mathbf{m}} - \mathbf{B}\Delta\mathbf{p}_\mathrm{P}$$

Slide 21
Retzhof, Sept. 13th, 2017

innovations kompetenz

bioenergy2020+

Hydraulic ODE Model – Cycle Mass Flows

- The edge mass flows are **not** suitable state variables. They are constrained by the mass conservation law $\mathbf{A}\dot{\mathbf{m}} = \mathbf{0}$
- "**Cycle mass flows**" are independent of each other

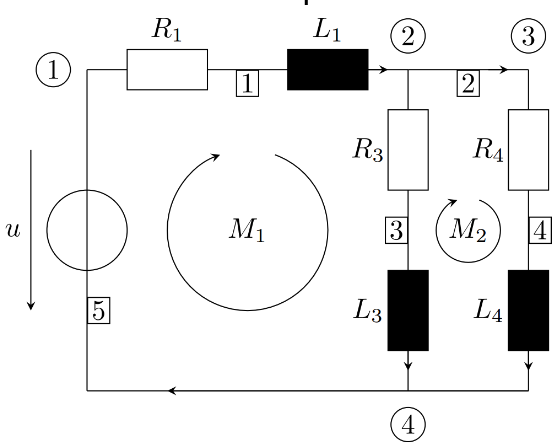

Slide 22
Retzhof, Sept. 13th, 2017

innovations kompetenz

bioenergy2020+

Hydraulic ODE Model – Cycle Mass Flows

- The edge mass flows are **not** suitable state variables. They are constrained by the mass conservation law $\mathbf{A}\dot{\mathbf{m}} = \mathbf{0}$
- "**Cycle mass flows**" are independent of each other
- Edge mass flows can be expressed by cycle mass flows via the edge-cycle incidence matrix

$$\dot{\mathbf{m}} = \mathbf{B}^T \dot{\mathbf{m}}_C$$

The mass conservation law is automatically fulfilled: $\mathbf{A}\mathbf{B}^T = \mathbf{0}$

$$\boxed{\mathbf{B}\Lambda_m\mathbf{B}^T \frac{\mathrm{d}\dot{\mathbf{m}}_C}{\mathrm{d}t} + \mathbf{B}\Lambda_R \mathrm{diag}(|\mathbf{B}^T\dot{\mathbf{m}}_C|)\mathbf{B}^T\dot{\mathbf{m}}_C - \mathbf{B}\Delta\mathbf{p}_P = 0}$$

- If no cycle exists with zero fluid mass, the matrix $\mathbf{B}\Lambda_m\mathbf{B}^T$ is invertible → $\dot{\mathbf{m}}_C$ **is a valid state variable**

innovations kompetenz

bioenergy2020+

Hydraulic ODE Model - Simulation

- Mass flows can be forced to zero (valve closed) or predetermined by a mass flow controller

$$\mathbf{S}_m\dot{\mathbf{m}} = \dot{\mathbf{m}}^*$$

- This reduces the number of free cycle mass flows

$$\dot{\mathbf{m}}_C = \dot{\mathbf{m}}_{C,0} + \mathbf{K}\dot{\mathbf{m}}_f, \quad \mathbf{S}_m\mathbf{B}^T\dot{\mathbf{m}}_{C,0} = \dot{\mathbf{m}}^* \quad \mathbf{S}_m\mathbf{B}^T\mathbf{K} = \mathbf{0}$$

- The **reduced order** dynamic model for the hydraulic part is

$$\mathbf{B}\Lambda_m\mathbf{B}^T\mathbf{K}\frac{\mathrm{d}\dot{\mathbf{m}}_f}{\mathrm{d}t} = -\mathbf{B}\Lambda_R\mathrm{diag}\left(\left|\mathbf{B}^T\left(\dot{\mathbf{m}}_{C,0} + \mathbf{K}\dot{\mathbf{m}}_f\right)\right|\right)\mathbf{B}^T\left(\dot{\mathbf{m}}_{C,0} + \mathbf{K}\dot{\mathbf{m}}_f\right) + \mathbf{B}\Delta\mathbf{p}_P$$

- The matrix on the left can be eliminated by left-multiplication with the pseudo-inverse to give an ODE suitable for controller design and simulation

innovations kompetenz

bioenergy2020+

Overview

- Motivation
- Graph-based representation of networks
- Hydraulic ODE model
- **Thermal steady state model**
- Example
- Summary

innovations kompetenz

bioenergy2020+

Thermal Steady State Model

- The thermal steady state is defined by the temperatures of the fluid in the nodes
- Along the edges, heat is added or subtracted

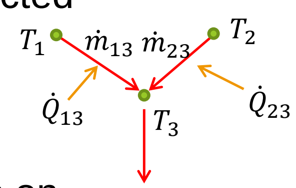

- The amount of heat transported depends on
  - the type of edge (pipe, heat exchanger, storage buffer, …)
  - temperatures and
  - mass flows

innovations kompetenz

bioenergy2020+

Thermal Steady State Model - Components

- Types of edges:
  - Pipe $\dot{Q}_{ij} = -k_{ij}U_{ij}l_{ij}\left[\frac{1}{2}(T_i + T_j) - T_{\mathrm{a}}\right]$

    Ambient temperature
  - Heat Exchanger

    Implicit equation

$$\dot{Q}_{kl} = -\dot{Q}_{ij} = -UA\frac{\left(\frac{1}{c_p\dot{m}_{ij}} - \frac{1}{c_p\dot{m}_{kl}}\right)\dot{Q}_{kl}}{\ln\left(\frac{T_i - T_k - \frac{1}{c_p\dot{m}_{ij}}\dot{Q}_{kl}}{T_i - T_k - \frac{1}{c_p\dot{m}_{kl}}\dot{Q}_{kl}}\right)}$$

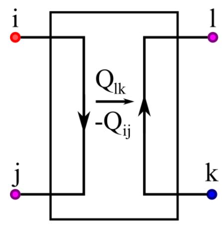

  - Buffer storage $\dot{Q}_{ij} = (T_{\mathrm{out}} - T_i)c_p\dot{m}_{ij}$

    Fixed outlet temperature

innovations kompetenz

bioenergy2020+

Thermal Steady State Model – Enthalpy conservation

- At the nodes, **enthalpy conservation** results in the mixing formula

$$T_j = \frac{\sum_{i,\dot{m}_{ij}>0}\dot{m}_{ij}(T_i + \Delta T_{ij})}{\sum_{i,\dot{m}_{ij}>0}\dot{m}_{ij}}, \quad \Delta T_{ij} = \frac{\dot{Q}_{ij}}{c_p\dot{m}_{ij}}$$

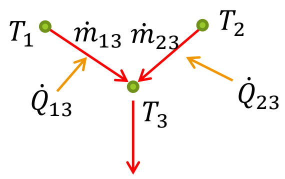

- By combining all node temperatures in a vector $\mathbf{T}$ and all heat flows in a vector $\dot{\mathbf{Q}}$, overall enthalpy conservation can be expressed by the **implicit** equation

$$\mathbf{T} = \mathrm{diag}(c_p\mathbf{S}_{\mathrm{E}}\mathbf{B}^T\dot{\mathbf{m}}_{\mathrm{C}})^{-1}\mathbf{S}_{\mathrm{E}}\left(c_p\mathbf{M}(\dot{\mathbf{m}}_{\mathrm{C}})\mathbf{T} + \dot{\mathbf{Q}}(\dot{\mathbf{m}}_{\mathrm{C}}, \mathbf{T})\right)$$

  - $\mathbf{S}_{\mathrm{E}}$ denotes, for each node, the edges that are incident to it and
  - $\mathbf{M}(\dot{\mathbf{m}}_{\mathrm{C}})$ is used to obtain the products $\dot{m}_{ij}T_i$.
- The solution to this equation describes the **thermal steady state**.

innovations kompetenz

bioenergy2020+

Thermal Steady State Model - Solution

- The solution to the thermal steady state can only be obtained numerically using e.g. *Newton*'s method
  - **Constraints** such as desired temperatures can be integrated as additional equations
  - **Objectives** such as minimum pumping power can be handled by formulating a nonlinear optimization problem

- The solution contains node temperatures, free heat flows, pump pressures and mass flows

$$\mathbf{f}(\mathbf{T}, \dot{\mathbf{m}}_\mathrm{C}, \dot{\mathbf{Q}}_\mathrm{f}, \Delta\mathbf{p}_\mathrm{P}) = \begin{pmatrix} \mathbf{T} - \mathbf{N}\mathbf{S}_\mathrm{E}\left(c_p\mathbf{M}\mathbf{T} + \dot{\mathbf{Q}}\right) \\ \mathbf{B}\Lambda_R \mathrm{diag}(|\mathbf{B}^T\dot{\mathbf{m}}_\mathrm{C}|)\mathbf{B}^T\dot{\mathbf{m}}_\mathrm{C} - \mathbf{B}\Delta\mathbf{p}_\mathrm{P} \end{pmatrix} = \mathbf{0}$$

innovations kompetenz

bioenergy2020+

Thermal Steady State Model - Solution

- Numerical methods require the knowledge of the gradients with respect to the unknown variables
  - Symbolic calculating of these gradients is tedious
  - Automatic Differentiation tools such as CasADi help
  - Alternatively, Algebraic Modelling Languages (AMPL, GAMS) can be used to formulate the problem and handle the connection with the optimization solver

innovations kompetenz

Overview

- Motivation
- Graph-based representation of networks
- Hydraulic ODE model
- Thermal steady state model
- Example
- Summary

Example

- Solar Collector field in the north of Graz

bioenergy2020+

Example – Steady State Optimizer

- The **Steady State Optimizer** uses a solar insolation prediction to determine the optimal usage of different branches in order to **maximize heat output** at the **desired feed temperature**

Slide 33
Retzhof, Sept. 13th, 2017

innovations kompetenz

bioenergy2020+

Example – Steady State Optimizer

- T u p o b **m** **d**

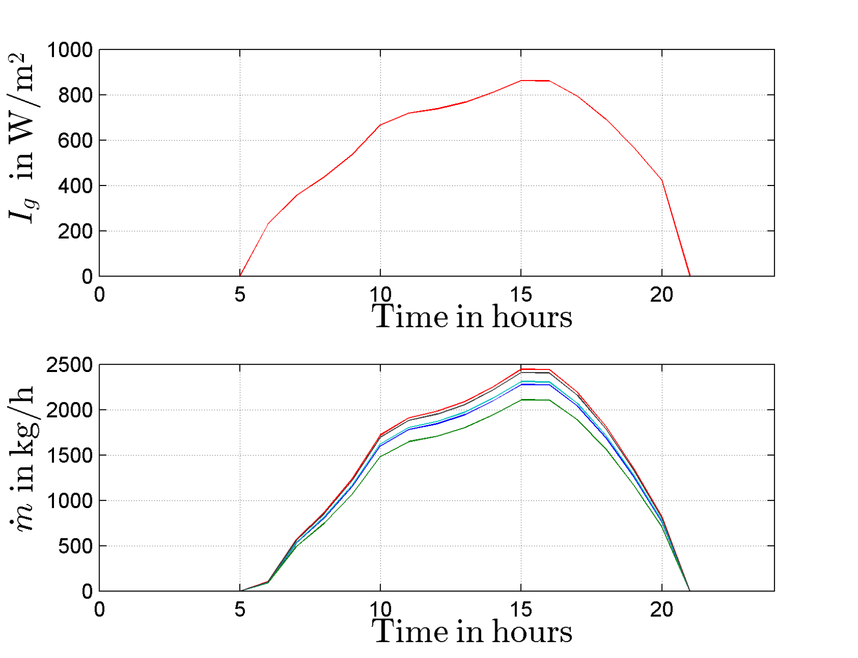

Slide 34
Retzhof, Sept. 13

innovations kompetenz

bioenergy2020+

Example – Temperature Controller

- The desired outlet temperature of each collector branch is controlled by using the thermal model and varying the mass flow

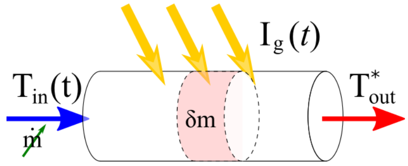

Slide 35
Retzhof, Sept. 13th, 2017

innovations kompetenz

bioenergy2020+

Example – Temperature Controller

- The c
of ea
contr
mode
flow

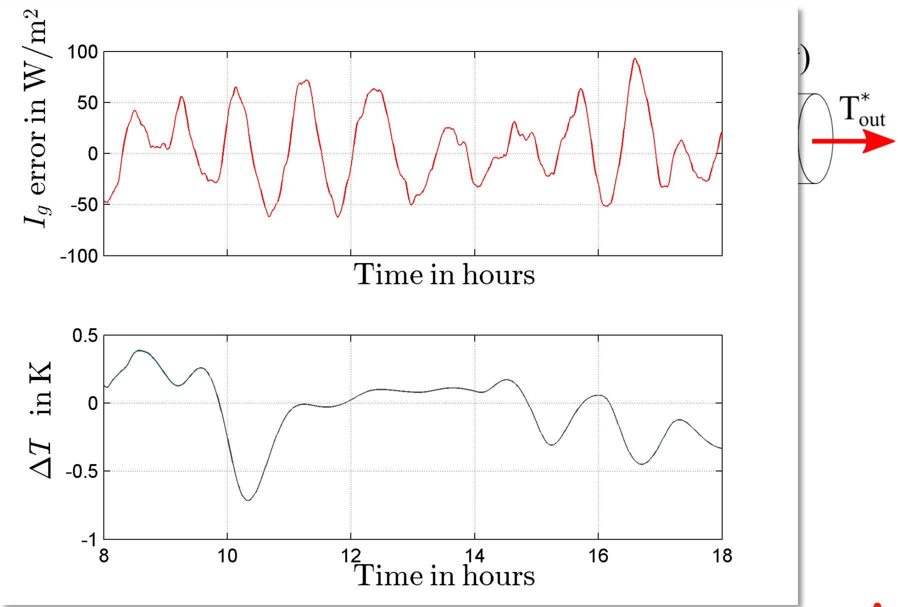

Slide 36
Retzhof, Sept. 13th, 2017

innovations kompetenz

bioenergy2020+

Example – Hydraulic Control

- The hydraulic ODE model describes a non-linear MIMO system affine in the inputs

$$\frac{d\mathbf{x}}{dt} = \mathbf{a}(\mathbf{x}) + \mathbf{b}(\mathbf{x})\mathbf{u}_V + \mathbf{b}_P\mathbf{u}_P$$

$$\mathbf{y} = \mathbf{C}\mathbf{x}$$

- The pump pressure difference $\mathbf{u}_P$ is kept at the value determined by the steady state optimizer
- The mass flow control is done by inverting the nonlinear valve characteristics and using a non-linear MIMO control law, e.g. MIMO FOSM

Slide 37
Retzhof, Sept. 13th, 2017

innovations kompetenz

bioenergy2020+

Overview

- Motivation
- Graph-based representation of networks
- Hydraulic ODE model
- Thermal steady state model
- Example
- **Summary**

Slide 38
Retzhof, Sept. 13th, 2017

innovations kompetenz

bioenergy2020+

Summary

- Based on a general description of the network, it is possible to **automatically**
  - deduce the ODE describing the hydraulic dynamics,
  - calculate the thermal steady state and even
  - determine desired mass flows and heat flows that ensure desired conditions in steady state.

- The resulting models make it possible to use well-known model-based controller designs
  - Flatness based feedforward control
  - State feedback or sliding mode control

innovations kompetenz

Model-Based Reference Shaping for Biomass Grate Boilers

Richard Seeber[a] **Markus Gölles**[b] **Nicolaos Dourdoumas**[a] **Martin Horn**[a]

The use of biomass as a sustainable fuel has become more and more important in recent years. One common use is its combustion in grate boilers ranging from small-scale boilers supplying heat to a single consumer to large-scale district heating plants. A model-based control approach has been shown to greatly improve the efficiency of such boilers' operation [2, 3, 4]. The approach is based on a fourth-order nonlinear model developed in [1, 2]. It consists of an input-output linearization to control relevant outputs in a decoupled manner, of a Kalman filter to reconstruct the plant states therefor required, and of PI-controllers to eliminate constant control deviations.

A challenge with this approach are actuator saturations. When active, nonlinear couplings are reintroduced and possibly undesired output deviations can occur; these may cause emergency shutdowns, reduced efficiency or increased emissions. In this talk a strategy is presented that prevents these effects by an appropriate modification of reference inputs.

For this purpose, an optimization problem is considered that aims for minimizing suitably weighted reference deviations. In general this leads to a nonlinear and non-convex problem; to avoid this a sequential minimization of the deviations is used, with the sequence being determined by requirements of the plant operation. A series of linear-fractional optimization problems is thus obtained that may ultimately be solved using linear programming.

The strategy was implemented and experimentially verified on a biomass grate boiler with a nominal capacity of 180 kW. Figure 1 exemplarily shows one result of this verification obtained by imposing an artificial lower limit on the primary air mass-flow after time t_1, which in a real-world scenario could be caused by an actuator failure. Without reference shaping, a highly undesired permanent deviation of the the hot water feed temperature T_f from its reference occurs. This corresponds to a surplus in power output. With the reference shaping strategy in place this deviation is avoided by instead accepting control deviations of less critical plant outputs such as the air ratio in the fuel bed.

The technique leads to several improvements. Undesired deviations of critical plant outputs such as the discussed surplus in power output or a too small flue-gas oxygen content are avoided to the greatest extent possible. Additionally, windup of the PI-controllers' integrators is mitigated and overall control performance during actuator saturations is improved. As a consequence, by alleviating overshoots, reducing variations and avoiding excessively large values of the flue-gas temperature, thermal stress on the furnace refractory lining is reduced, thus increasing its lifetime. Furthermore, carbon monoxide emissions may also be reduced under certain operating conditions.

[a]Institute of Automation and Control, Graz University of Technology, Inffeldgasse 21/B/I, 8010 Graz, E-Mail: richard.seeber@tugraz.at, nicolaos.dourdoumas@tugraz.at, martin.horn@tugraz.at
[b]Bioenergy 2020+ GmbH, Inffeldgasse 21/B, 8010 Graz, E-Mail: markus.goelles@bioenergy2020.eu

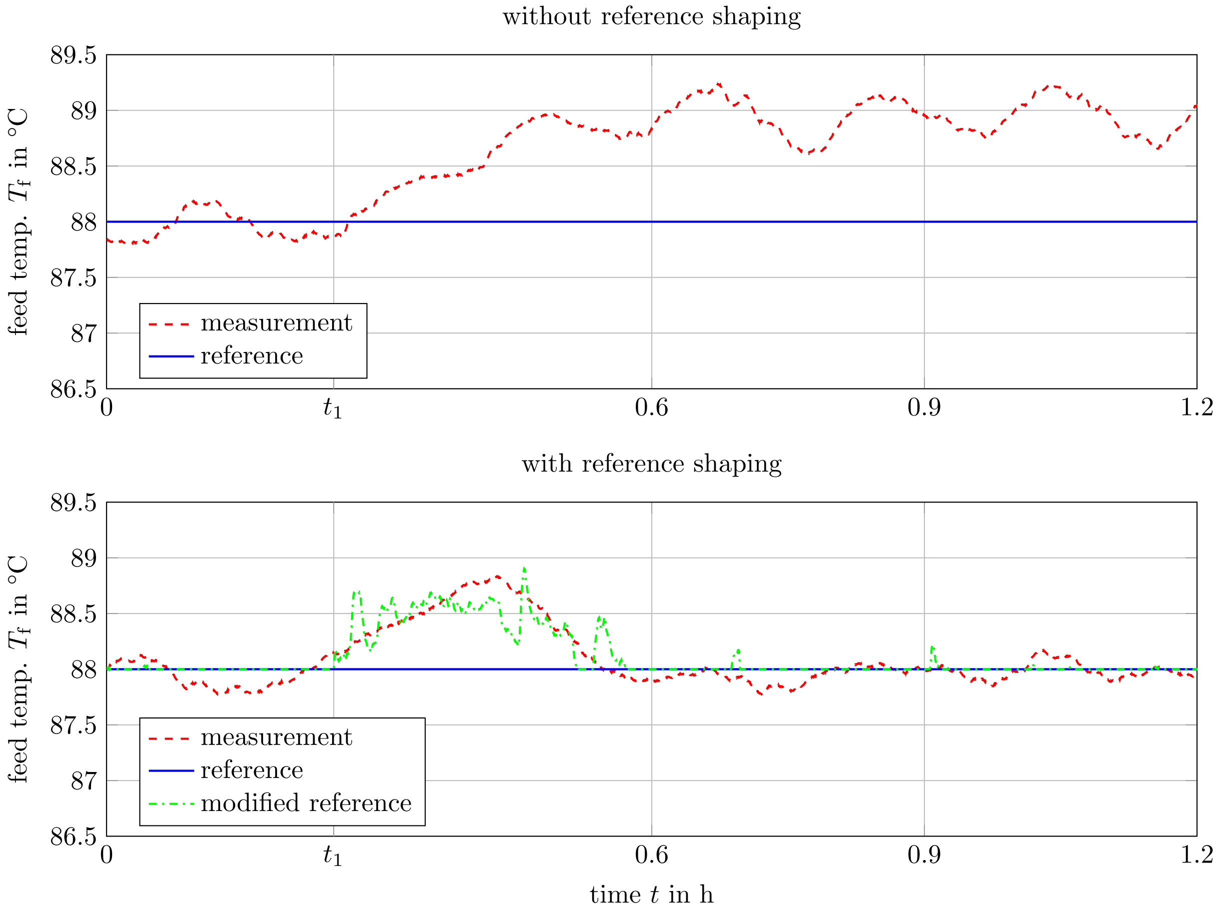

Figure 1: Hot water feed temperature T_f with an artificial upper limit being imposed on the primary air mass-flow starting at time instant t_1

[1] Robert Bauer. *Modelling and Model Based Control Strategies Using the Example of a Biomass Furnace*. Habilitation treatise, Technische Universität Graz, 2009. (in German).

[2] Markus Gölles, Robert Bauer, Thomas Brunner, Nicolaos Dourdoumas, and Ingwald Obernberger. Model based control of a biomass grate furnace. In *European Conference on Industrial Furnaces and Boilers*, April 2011.

[3] Markus Gölles, Stefan Reiter, Thomas Brunner, Nicolaos Dourdoumas, and Ingwald Obernberger. Model based control of a small-scale biomass boiler. *Control Engineering Practice*, 22:94–102, 2014.

[4] Christopher Zemann, Otto Heinreichsberger, Markus Gölles, Thomas Brunner, Nicolaos Dourdoumas, and Ingwald Obernberger. Application of a model based control strategy at a fixed bed biomass district heating plant. In *Proceedings of the 22nd European Biomass Conference and Exhibition*, pages 1698–1705, Hamburg, Germany, June 2014.

W I S S E N ▪ T E C H N I K ▪ L E I D E N S C H A F T

TU Graz

Model-Based Reference Shaping for Biomass Grate Boilers

Richard Seeber*, Markus Gölles‡, Nicolaos Dourdoumas*, Martin Horn*

*Institute of Automation and Control, TU Graz

‡Bioenergy 2020+ GmbH

September 13, 2017

www.irt.tugraz.at

bioenergy2020+

Biomass Grate Boiler

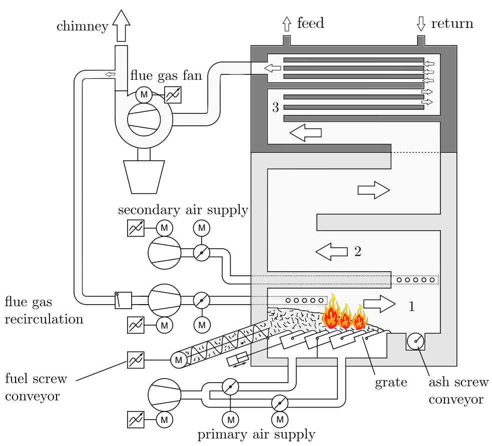

Inputs (mass flows)

- fuel feed $\dot{m}_{\mathrm{ff}}$
- primary air $\dot{m}_{\mathrm{pa}}$
- secondary air $\dot{m}_{\mathrm{sa}}$
- recirculated flue gas $\dot{m}_{\mathrm{rf}}$

Controlled outputs

- air ratio in the fuel bed λ_{fb}
- flue gas oxygen content ν_{ox}
- flue gas temperature in secondary combustion zone T_{fg}
- feed temperature T_{f}

Model

- nonlinear, coupled MIMO system
- 4 inputs, 4 outputs

Existing Control Strategy

Strategy

- control of ν_{ox}, T_{fg}, T_{f} using $\dot{m}_{\mathrm{pa}}$, $\dot{m}_{\mathrm{sa}}$, $\dot{m}_{\mathrm{rf}}$
  - state-feedback input-output linearization
  - linear, decoupled behavior
  - PI-controllers to reject constant disturbances
- control of air ratio λ_{fb} using $\dot{m}_{\mathrm{ff}}$
  - feedback linearization not possible due to large delay
  - feedforward control with steady-state fuel feed $\dot{m}_{\mathrm{ff,s}}$
  - P-controller for stabilization

Structure

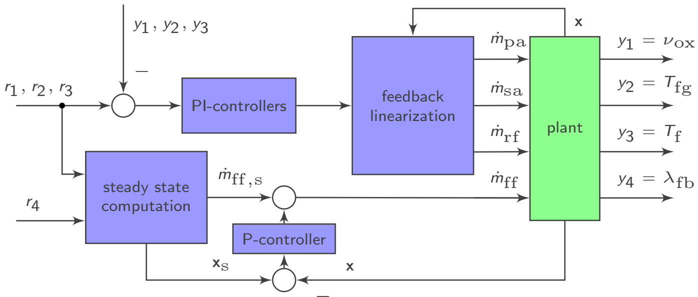

Problem

Actuator limitations

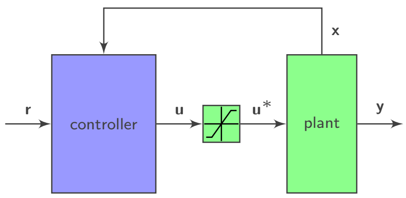

- limited mass flows
- feedback linearization, steady state computation only valid if $\mathbf{u} = \mathbf{u}^*$

Problems on actuator saturation

- nonlinear behaviour
- possibly undesired deviations of outputs
- windup of PI-controllers

Problem – Windup

First attempt for anti-windup strategy

- stop certain integrators on actuator saturation, based on process insight
- example:
  - recirculated flue-gas $\dot{m}_{\mathrm{rf}}$ primarily used for cooling the flue-gas
  - $\rightarrow$ on saturation of $\dot{m}_{\mathrm{rf}}$, stop integrator for flue-gas temperature T_{fg}

Flue-gas temperature during load changes $120\,\mathrm{kW} \rightarrow 60\,\mathrm{kW} \rightarrow 180\,\mathrm{kW}$

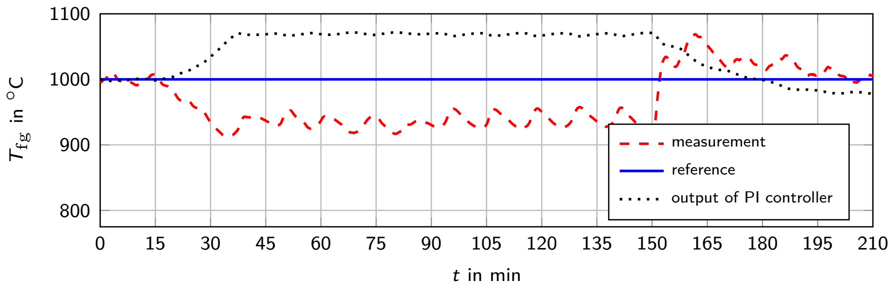

- $\dot{m}_{\mathrm{rf}}$ at lower limit for $37 \leq t \leq 150$ (operation at $60\,\mathrm{kW}$) $\rightarrow$ integrator is stopped
- other actuators saturated starting at $t = 15$ $\rightarrow$ some wind-up still persists

New Strategy

Reference shaping

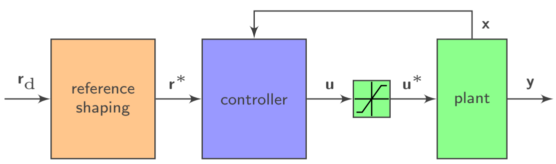

Given a desired reference $\mathbf{r}_{\mathrm{d}}$ find a modified reference $\mathbf{r}^*$, such that

- the resulting control action $\mathbf{u}$ obeys the actuator limitations

$$\mathbf{u}_{\min} \leq \mathbf{u} \leq \mathbf{u}_{\max}$$

- the reference $\mathbf{r}^*$ obeys given limitations (e.g. lower limit on flue gas oxygen content ν_{ox})

$$\mathbf{r}_{\min} \leq \mathbf{r}^* \leq \mathbf{r}_{\max}$$

- the difference between desired reference $\mathbf{r}_{\mathrm{d}}$ and modified reference $\mathbf{r}^*$ is as small as possible

$$\mathbf{r}^* = \arg\min_{\mathbf{r}} J(\mathbf{r}, \mathbf{r}_{\mathrm{d}})$$

$\Rightarrow$ optimization problem

New Strategy – Structure

Instances of reference shaping

- 2 sets of references
  - references for feedback linearization $\mathbf{r} = [r_1 \quad r_2 \quad r_3]^\mathrm{T}$
  - references for steady-state computation $\mathbf{r}_s = [r_{s,1} \quad r_{s,2} \quad r_{s,3} \quad r_{s,4}]^\mathrm{T}$
- have to be treated separately: for example, high power-demand that is ...
  - not sustainable in steady-state (limited fuel mass-flow $\dot{m}_\mathrm{ff}$)
  - but sustainable for a short time (if enough fuel is in the fuel bed)

  $\rightarrow$ only steady-state references should be modified
- 2 instances of reference shaping

New structure (without P- and PI-controllers)

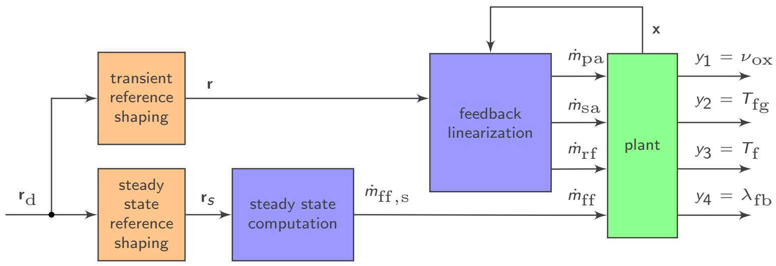

Optimization Problem – Prerequisites

Connection between u and r

- state-feedback control law $\mathbf{u} = \mathbf{h}(\mathbf{x}, \mathbf{r})$
- steady-state equations $\mathbf{u}_\mathrm{s} = \mathbf{h}_\mathrm{s}(\mathbf{r}_\mathrm{s})$
- can in both cases be written as: $\mathbf{r} = \mathbf{g}(\mathbf{x}, \mathbf{u})$
  - state-feedback case: $\mathbf{g} = \mathbf{h}^{-1}$
  - steady state case: $\mathbf{g} = \mathbf{h}_\mathrm{s}^{-1}$
- for the considered nonlinear model these equations have the structure

$$r_i = g_i(\mathbf{x}, \mathbf{u}) = \frac{\mathbf{a}_i^T \mathbf{u} + b_i}{\mathbf{c}_i^T \mathbf{u} + d_i}$$

  (in state-feedback case, coefficients $\mathbf{a}_i^T$, b_i, $\mathbf{c}_i^T$ and d_i depend on $\mathbf{x}$)
- eliminate $\mathbf{r}$ from the optimization problem

$$\min_{\mathbf{u}} J(\mathbf{g}(\mathbf{u}), \mathbf{r}_\mathrm{d})$$

$$\text{s.t.}$$

$$\mathbf{u}_\mathrm{min} \leq \mathbf{u} \leq \mathbf{u}_\mathrm{max}$$

$$\mathbf{r}_\mathrm{min} \leq \mathbf{g}(\mathbf{u}) \leq \mathbf{r}_\mathrm{max}$$

Optimization Problem – Constraints

Constraints on $\mathbf{u}$

$$\mathbf{u}_{\min} \leq \mathbf{u} \leq \mathbf{u}_{\max}$$

linear constraints on $\mathbf{u}$

Constraints on $\mathbf{r}$

$$r_i = \frac{\mathbf{a}_i^T \mathbf{u} + b_i}{\mathbf{c}_i^T \mathbf{u} + d_i} \leq r_{\max,i}$$

assuming a positive denominator:

$$\mathbf{a}_i^T \mathbf{u} + b_i \leq r_{\max,i} \mathbf{c}_i^T \mathbf{u} + r_{\max,i} d_i$$

linear constraints on $\mathbf{u}$

Result

- constraints are linear, and can be written as
$$\mathbf{A}\mathbf{u} \leq \mathbf{b}$$
- optimization problem
$$\min_{\mathbf{u}} J(\mathbf{g}(\mathbf{u}), \mathbf{r}_{\mathrm{d}})$$
s.t.
$$\mathbf{A}\mathbf{u} \leq \mathbf{b}$$

Optimization Problem – Cost Function (I)

Considerations for choosing a cost function $J(\mathbf{r}, \mathbf{r}_{\mathrm{d}})$

- procedural requirements
- cost function should be convex
to ensure that all optima are global

Idea

controlled variables have different priorities, e.g.

- power output (feed temperature T_{f}):
avoid deviations at all cost
- increased air ratio λ_{fb} acceptable
if oxygen content ν_{ox} can be reduced instead (higher efficiency)

$\Rightarrow$ Sequential Optimization of Multiple Cost Functions

Optimization Problem – Cost Function (II)

Cost functions

deviations between $\mathbf{r}$ and $\mathbf{r}_\mathrm{d}$

- upper deviation

$$q_{i^+} = \begin{cases} |r_i - r_{\mathrm{d},i}| & r_i > r_{\mathrm{d},i} \\ 0 & \text{otherwise} \end{cases}$$

- lower deviation

$$q_{i^-} = \begin{cases} |r_i - r_{\mathrm{d},i}| & r_i < r_{\mathrm{d},i} \\ 0 & \text{otherwise} \end{cases}$$

in general: cost functions q_j with

$$j \in \{1^+, 1^-, 2^+, 2^-, \ldots\}$$

Illustration

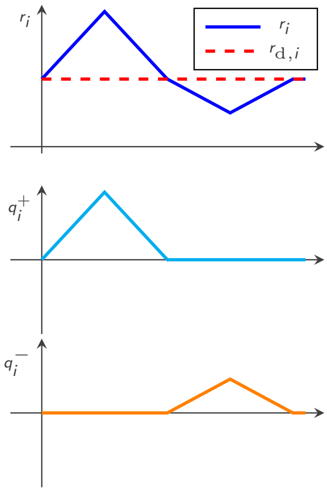

Optimization Problem – Resulting Problems

Sequential Optimization

- choose sequence of cost functions $J_1(\mathbf{u}) = q_{j_1}(\mathbf{u}), \ldots, J_m(\mathbf{u}) = q_{j_m}(\mathbf{u})$
- find $J_1^* = \min\limits_{\mathbf{u}} J_1(\mathbf{u})$ s.t. $\mathbf{Au} \leq \mathbf{b}$
- find $J_2^* = \min\limits_{\mathbf{u}} J_2(\mathbf{u})$ s.t. $\mathbf{Au} \leq \mathbf{b}, J_1(\mathbf{u}) = J_1^*$
- find $J_3^* = \min\limits_{\mathbf{u}} J_3(\mathbf{u})$ s.t. $\mathbf{Au} \leq \mathbf{b}, J_1(\mathbf{u}) = J_1^*, J_2(\mathbf{u}) = J_2^*$
- ...
- find $J_m^* = \min\limits_{\mathbf{u}} J_m(\mathbf{u})$ s.t. $\mathbf{Au} \leq \mathbf{b},\ J_k(\mathbf{u}) = J_k^*$ for $k < m$

Parameters

- optimization sequence $\mathcal{S} = (j_1, j_2, \ldots, j_m)$ with $j_k \in \{1^+, 1^-, 2^+, \ldots\}$
- hard reference constraints $\mathbf{r}_\mathrm{min}$, $\mathbf{r}_\mathrm{max}$

Optimization Problem – Optimization Sequence

Steady-state references $\mathbf{r}_s{}^*$

- constraints
  - upper bound T_f by reference $\rightarrow$ no excess power output
  - lower bound ν_ox by reference
  - reasonable bounds for other quantities
- optimization sequence

  $\mathcal{S} = (2^-, 3^-, 4^-, 2^+, 1^+, 4^+)$

State-feedback references $\mathbf{r}^*$

- for consistency $\mathbf{r}^* \overset{!}{=} \mathbf{r}_s{}^*$ has to hold in steady state
- same or relaxed constraints
- no hard upper bound on T_f: $\rightarrow$ temporary surplus in power output permitted
- optimization sequence

  $\mathcal{S} = (3^+, 2^-, 3^-, 2^+, 1^+)$

Steady-state constraints and optimization sequence

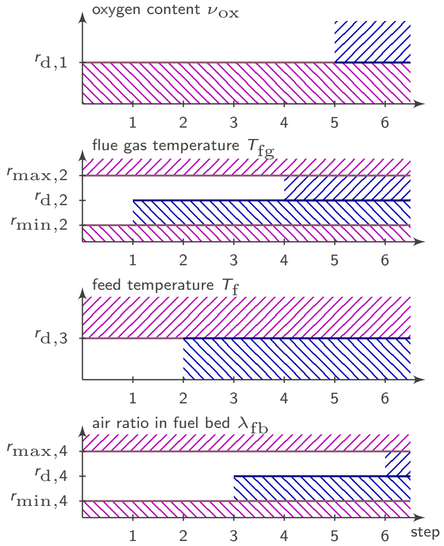

Optimization Problem – Individual Problems

Individual optimization problems (for upper deviation)

$$J^* = \min_{\mathbf{u}} g(\mathbf{u}) - r_\mathrm{d} = \min_{\mathbf{u}} \frac{\mathbf{a}^\mathsf{T}\mathbf{u} + b}{\mathbf{c}^\mathsf{T}\mathbf{u} + d} - r_\mathrm{d}$$

s.t.

$$\tilde{\mathbf{A}}\mathbf{u} \le \tilde{\mathbf{b}}$$

- abbreviations: $J^* := J_k^*$, $r_\mathrm{d} := r_{\mathrm{d},j_k}$, $g := g_{j_k}$, $\mathbf{a}^\mathsf{T} := \mathbf{a}_{j_k}^T$, $b := b_{j_k}$, ...

Constraints

linear constraints $\tilde{\mathbf{A}}\mathbf{u} \le \tilde{\mathbf{b}}$ contain

- mass-flow constraints $\mathbf{u}_\mathrm{min} \le \mathbf{u} \le \mathbf{u}_\mathrm{max}$
- reference constraints $\mathbf{r}_\mathrm{min} \le \mathbf{g}(\mathbf{u}) \le \mathbf{r}_\mathrm{max}$
- constraints from previous optimizations $J_1(\mathbf{u}) = J_1^*, \ldots, J_{k-1}(\mathbf{u}) = J_{k-1}^*$

Properties

- linear-fractional optimization problem
- nonconvex cost function

Optimization Problem – Solution

Individual optimization problem

$$J^* = \min_{\mathbf{u}} \frac{\mathbf{a}^\mathsf{T}\mathbf{u} + b}{\mathbf{c}^\mathsf{T}\mathbf{u} + d} - r_\mathrm{d}$$

s.t.

$$\tilde{\mathbf{A}}\mathbf{u} \leq \tilde{\mathbf{b}}$$

Change of variables

$$\mathbf{u} =: \frac{\mathbf{z}}{\sigma} \quad \text{with } \sigma > 0$$

- optimum is the same for all $\sigma > 0$
- new degree of freedom σ permits constraint on denominator

$$\sigma \cdot (\mathbf{c}^\mathsf{T}\mathbf{u} + d) = 1$$

Transformed problem

$$J^* = \min_{\mathbf{z},\sigma} \left(\mathbf{a}^\mathsf{T}\mathbf{z} + b\sigma\right) - r_\mathrm{d}$$

s.t.

$$\tilde{\mathbf{A}}\mathbf{z} - \tilde{\mathbf{b}}\sigma \leq \mathbf{0}$$
$$\mathbf{c}^\mathsf{T}\mathbf{z} + d\sigma = 1$$
$$\sigma \geq 0$$

$\Rightarrow$ Linear Program, may be solved by state-of-the-art techniques algorithm

Resulting Structure

Structure of feedback linearization control loop

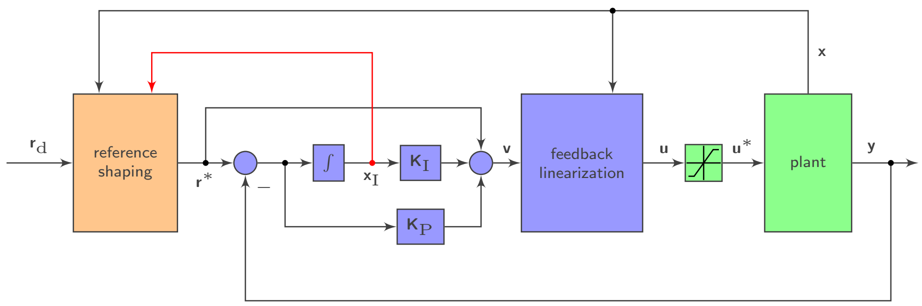

Wind-up prevention

- conditioning technique by Hanus, et al.: use of realizable references avoides wind-up
- modify reference shaping: take PI-controllers into account in function $\mathbf{g}(\mathbf{u})$ (requires integrator state $\mathbf{x}_\mathrm{I}$ in addition to $\mathbf{x}$)
- no actutator saturation with modified reference $\mathbf{r}^*$, i.e. $\mathbf{u} = \mathbf{u}^*$ $\Rightarrow$ no integrator windup

Results

Setup

- competence centre Bioenergy 2020+
- 180 kW pilot-scale grate boiler

Experiments

- selective limitation of mass flows
  - upper limit on $\dot{m}_{\mathrm{pa}}$
  - lower limit on $\dot{m}_{\mathrm{pa}}$
  - upper limit on $\dot{m}_{\mathrm{sa}}$
  - upper limit on $\dot{m}_{\mathrm{rf}}$
- fast load changes

Results – Lower Limit on Primary Air: $\dot{m}_{\mathrm{pa}} \geq 55\,\mathrm{kg/h}$

Feed temperature T_{f}

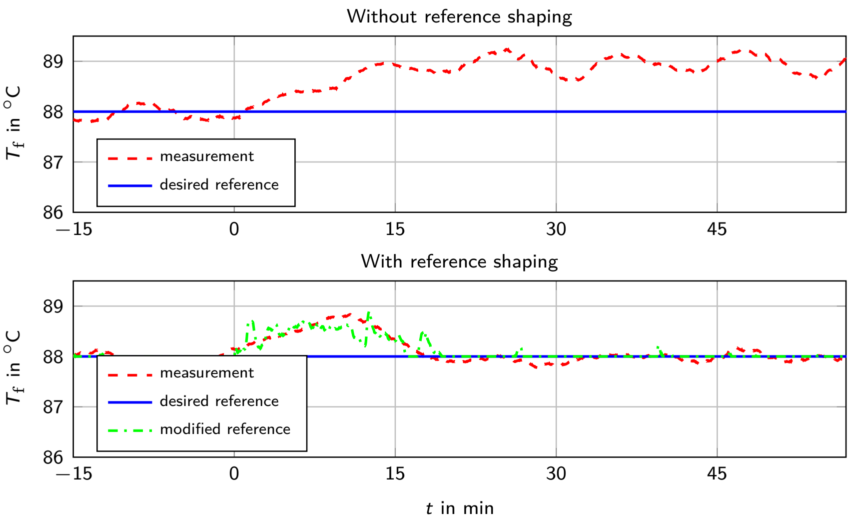

no excess power output ...

Results – Lower Limit on Primary Air: $\dot{m}_{\mathrm{pa}} \geq 55\,\mathrm{kg/h}$

Air ratio in the fuel bed λ_{fb}

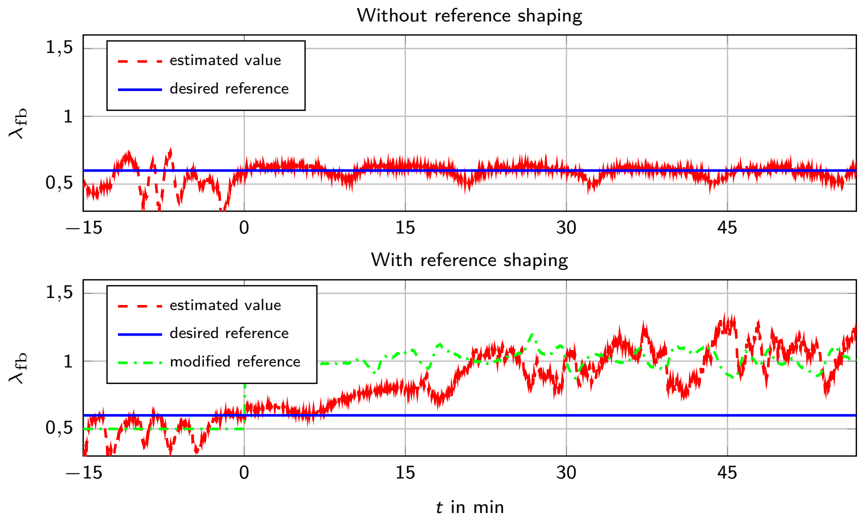

. . . by increasing the air ratio in the fuel bed

Results – Upper Limit on Primary Air: $\dot{m}_{\mathrm{pa}} \leq 140\,\mathrm{kg/h}$

Flue-gas temperature T_{fg}

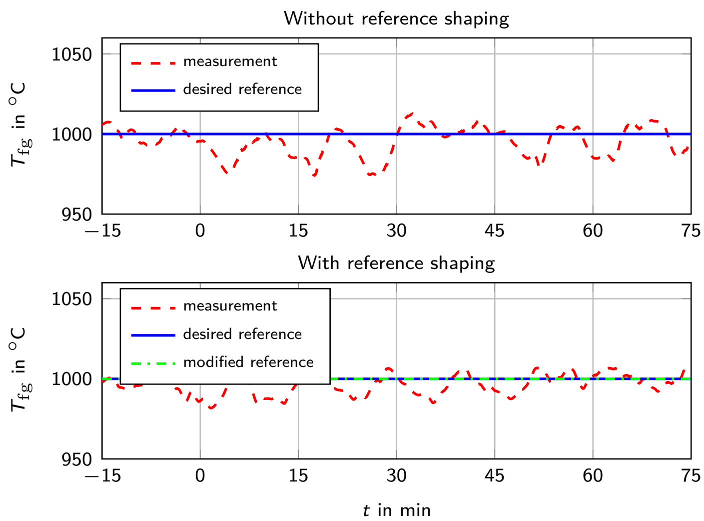

reduced combustion temperature variations due to improved decoupling . . .

Results – Upper Limit on Primary Air: $\dot{m}_{\mathrm{pa}} \leq 140\,\mathrm{kg/h}$

Carbon monoxide emissions ν_{co}

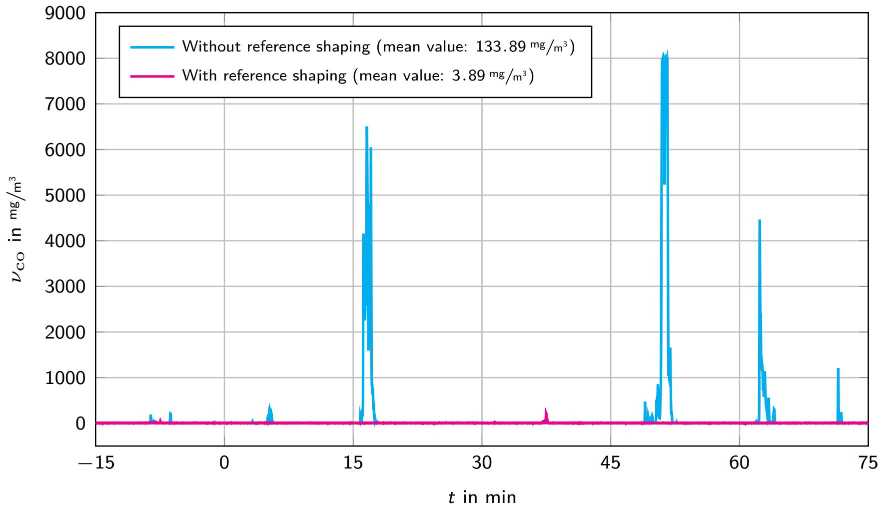

. . . along with a reduction of CO-emissions

www.irt.tugraz.at

Results – Upper Limit on Secondary Air: $\dot{m}_{\mathrm{sa}} \leq 150\,\mathrm{kg/h}$

Flue-gas oxygen content ν_{ox}

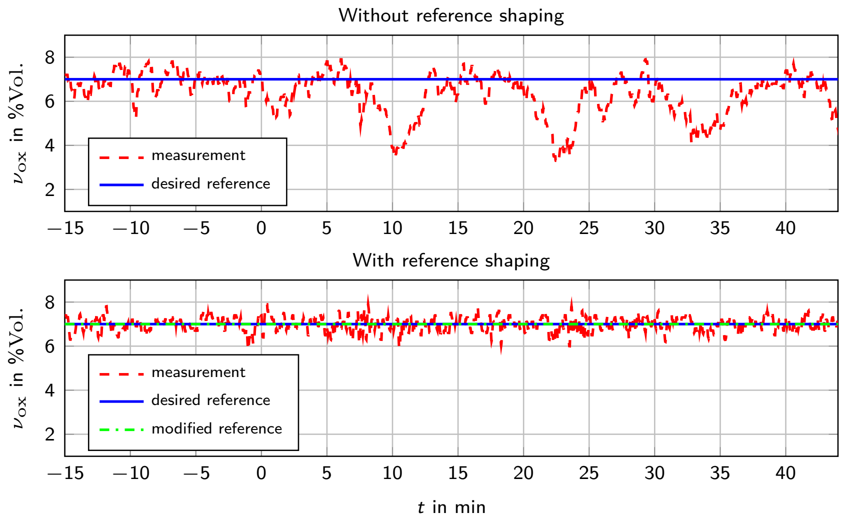

oxygen content kept above prescribed minimum . . .

Results – Upper Limit on Secondary Air: $\dot{m}_{\mathrm{sa}} \leq 150\,\mathrm{kg/h}$

Feed temperature T_{f}

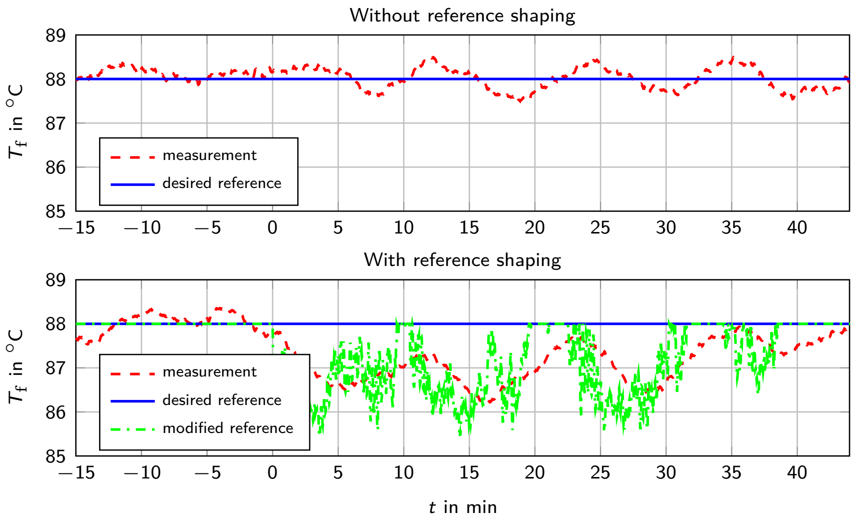

…by reducing the power output if necessary

Results – Fast Load Increase from 60 kW to 180 kW

Flue-gas temperature T_{fg}

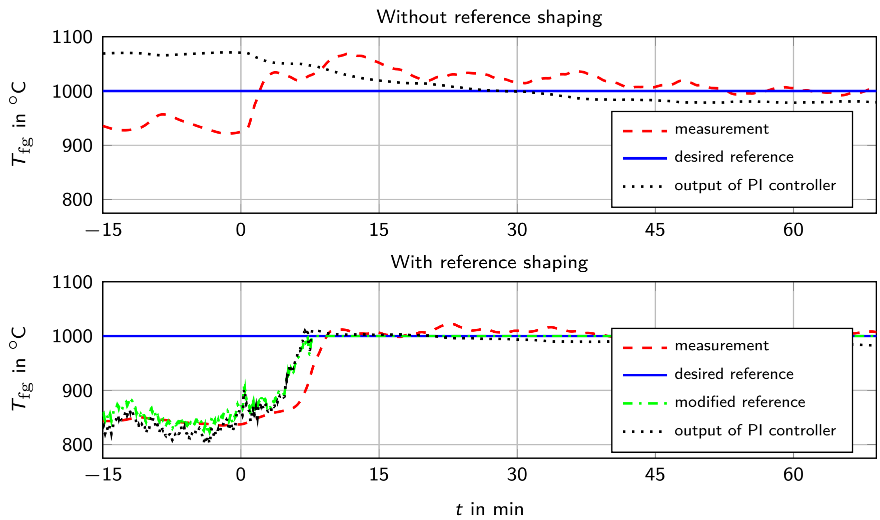

reduced overshoot by avoiding integrator windup

Summary

- problems caused by mass flow limitations
- anti-windup by halting integrators did not solve all problems
- design of a reference shaping strategy using sequential optimization
- use of conditioning technique prevents integrator windup
- implementation at a 180 kW pilot-scale biomass grate boiler
- performance improvements and reduced emissions

References

[1] R. Bauer, M. Gölles, T. Brunner, N. Dourdoumas, and I. Obernberger.
Dynamic modelling of the heat transfer in a gas tube heat exchanger.
at – Automatisierungstechnik, 56:513–520, 2008 (in German).

[2] R. Bauer, M. Gölles, T. Brunner, N. Dourdoumas, and I. Obernberger.
Modelling of grate combustion in a medium scale biomass furnace for control purposes.
Biomass and Bioenergy, 34(4):417–427, 2010.

[3] M. Gölles, R. Bauer, T. Brunner, N. Dourdoumas, and I. Obernberger.
Model based control of a biomass grate furnace.
In *European Conference on Industrial Furnaces and Boilers*, April 2011.

[4] R. Seeber, M. Gölles, T. Brunner, N. Dourdoumas, and I. Obernberger.
Improvement of a model based control strategy for biomass furnaces.
at – Automatisierungstechnik, 62(12):891–902, 2014 (in German).

[5] C. Schörghuber, M. Reichhartinger, M. Horn, M. Gölles, and R. Seeber.
Control of a biomass-furnace based on input-output-linearization.
In *2015 European Control Conference (ECC)*, pages 3508–3513. IEEE, 2015.

[6] A. Charnes and W. W. Cooper.
Programming with linear fractional functionals.
Naval Research Logistics Quarterly, 9:181–186, 1962.

[7] R. Hanus, M. Kinnaert, and J.-L. Henrotte.
Conditioning technique, a general anti-windup and bumpless transfer method.
Automatica, 23(6):729–739, 1987.

Part III.

Wednesday afternoon session

Is It Reasonable to Substitute Discontinuous SMC by Continuous HOSMC?

Leonid Fridman[a]

Professor Utkin proposed an example showing that the amplitude of chattering caused by the presence of parasitic dynamics in systems governed by First- Order Sliding-Mode Control (FOSMC) is lower than the obtained using Super-Twisting Algorithm (STA). This example served to motivate this research reconsidering the problem of comparison of chattering magnitude in systems governed by FOSMC that produces a discontinuous control signal and by STA that produces a continuous one, using Harmonic Balance (HB) methodology. With this aim the Averaged Power (AP) criteria for chattering measurements is revisited. The STA gains are redesigned to minimize amplitude or AP of oscillations predicted by HB. The comparison of the chattering produced by FOSMC and STA with redesigned gains is analyzed taking into account their amplitudes, frequencies and values of AP allowing to conclude that:

(a) for any value of upper bound of disturbance and Actuator Time Constant (ATC) there exist a bounded disturbance for which the amplitude and AP of chattering produced by FOSMC is lower than the caused by STA

(b) if the upper bound of disturbance and upper bound of time-derivative disturbance are given, then for all sufficiently small values of ATC the amplitude of chattering and AP produced by STA will be smaller than the caused by FOSMC

(c) critical values of ATC are predicted by HB for which the parameters, amplitude of chattering and AP, produced by FOSMC and STA are the same. Also the frequency of self exited oscillations caused by FOSMC is always grater than the produced by STA.

[a]Departamento de Ingenierıa de Control y Robotica Facultad de Ingenierıa, UNAM, Mexico, E-mail: fridman@unam.mx

Analysis of Sliding Mode Controllers in the Frequency Domain

Leonid Fridman
lfridman@unam.mx

Facultad de Ingeniería
National Autonomous University of Mexico (UNAM)

Outline

Introduction DF

DF technique is:

- Applied to nonlinear systems where the nonlinear part can be separated from the linear part.
- Based on the hypothesis of law pass filter. i.e. that the input of the nonlinear part is sinusoidal.

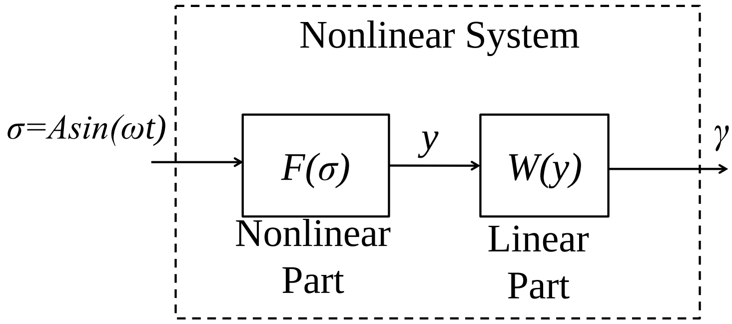

Introduction DF

- Based on the Fourier series representation of the nonlinearity.

$$y = F(A\sin\omega t) = \frac{a_0}{2} + \Sigma_{n=1}^{\infty}(a_n\cos n\omega t + b_n \sin n\omega t)$$

$$\begin{aligned} a_0 &= \frac{\omega}{\pi}\int_0^{2\pi/\omega} F(A\sin\omega t)dt; \\ a_n &= \frac{\omega}{\pi}\int_0^{2\pi/\omega} F(A\sin\omega t)\cos n\omega t dt; \\ b_n &= \frac{\omega}{\pi}\int_0^{2\pi/\omega} F(A\sin\omega t)\sin n\omega t dt. \end{aligned}$$

Introduction DF

Main hypothesis: Linear part is a low pass filter.

Closed loop system, the output can be approximated

$$y = F(A\sin\omega t) \quad \approx \quad \frac{a_0}{2} + \Sigma_{n=1}^{\infty}(a_1\cos\omega t + b_1\sin\omega t)$$

$$a_2, a_3, \ldots \approx 0 \quad ; \quad b_2, b_3, \ldots \approx 0$$

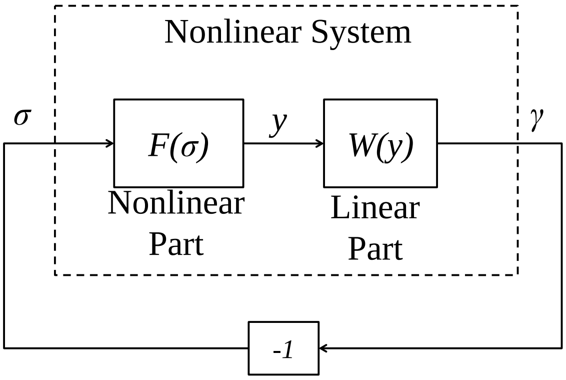

Introduction DF

DF is an equivalent complex gain of the nonlinear part

$$F(\sigma) = N(A,\omega)\sigma$$

For symmetric nonlinearities

$$N(A,\omega) = \frac{\omega}{\pi A}\int_0^{2\pi/\omega} F(A\sin\omega t)\sin\omega t dt + j\frac{\omega}{\pi A}\int_0^{2\pi/\omega} F(A\sin\omega t)\cos\omega t dt$$

DF and Harmonic Balance

Harmonic Balance condition

$$1 + W(j\omega)N(A,\omega) = 0; \qquad W(j\omega) = -\frac{1}{N(A,\omega)}$$

- Identify oscillations
- Find frequency ω and amplitude A of the oscillations

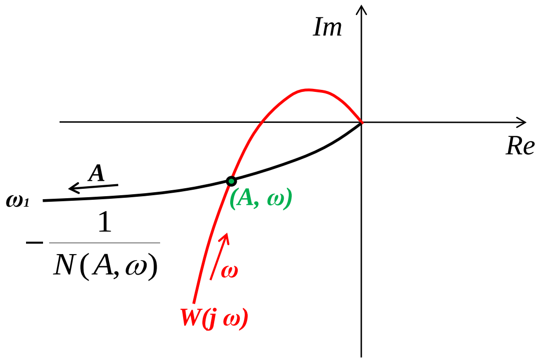

Oscillations in SMC systems

NO ONE MODEL TAKES INTO ACCOUNT ALL SYSTEM DYNAMICS!!!
The phenomenon of **chattering** is caused by the inevitable existence of un-modeled dynamics.

The principal dynamics are the dynamics of the plant is a model that are used for controller design.

The un-modeled dynamics are not accounted during the SMC design; delays, actuators, sensors, etc.

The relative degree increases and the real sliding mode emerges, where the sliding variable contains a limit cycle (chattering) with **finite frequency** and **finite amplitude**.

DF in SMC

Systems driven by SMC can be analyzed by the frequency domain, when the un-modeled dynamics are taken into account.

DF-HB technique is applied to identify limit cycles (chattering) and estimate their parameters, **amplitude** and **frequency**.

$$N(A,\omega) = \frac{\omega}{\pi A}\int_0^{2\pi/\omega} u(t)\sin\omega t dt + j\frac{\omega}{\pi A}\int_0^{2\pi/\omega} u(t)\cos\omega t dt$$

$N(A,\omega)$ is the DF of SMC algorithm.

Conventional SMC: DF Analysis

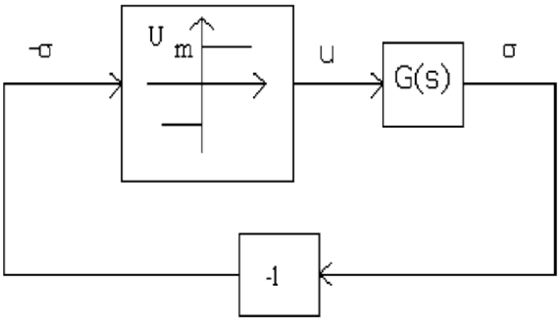

Figure: Block diagram of a linear system with relay control and ideal sliding

Replace the Laplace variable s by $j\omega$,

$$-\sigma = A_c \sin\omega_c t, \tag{1}$$

ω_c is frequency

Conventional SMC: DF Analysis

Amplitude A_c and Frequency ω_c have to satisfy the Harmonic Balance (HB) eq.

$$G(j\omega) = -\frac{1}{N(A,\omega)}. \tag{2}$$

For conventional SMC, $N(A,\omega)$ DOES NOT DEPEND ON ω

$$N(A) = \frac{4U_m}{\pi A} \tag{3}$$

Leonid Fridman *lfridman@unam.mx* (UNAM) Analysis of Sliding Mode Controllers in the Frequency 11 / 54

Conventional SMC:DF analysis

Example of **Ideal SMC**

$$\begin{aligned} \dot{x}_1 &= x_2 \\ \dot{x}_2 &= -x_1 - x_2 + u \\ \sigma &= x_1 + x_2 \end{aligned} \tag{4}$$

with control

$$u = -\mathrm{sign}(\sigma) \tag{5}$$

Transfer function

$$G(s) = \frac{s+1}{s^2+s+1} \tag{6}$$

HB eq.

$$\mathrm{Re}\,[G(j\omega] = -\frac{\pi A}{4U_m} \tag{7}$$

Leonid Fridman *lfridman@unam.mx* (UNAM) Analysis of Sliding Mode Controllers in the Frequency 12 / 54

Conventional SMC: DF analysis

Example of **Ideal SMC**

Real part

$$\frac{1-\omega+\omega^2}{(1-\omega^2)^2+\omega^2} = -\frac{\pi A}{4U_m} \tag{8}$$

Imaginary part

$$\frac{\omega^2}{(1-\omega^2)^2+\omega^2} = 0 \tag{9}$$

Ideal sliding-mode

$$A_c = 0,\ \omega_c \to \infty \tag{10}$$

Conventional SMC: DF analysis

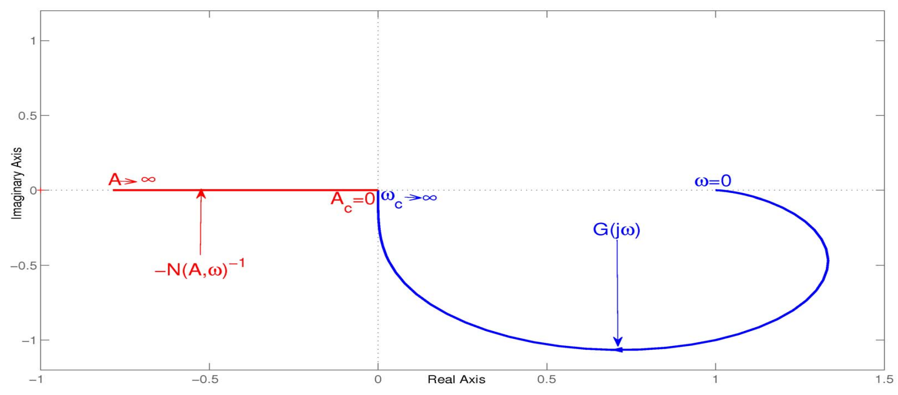

Figure: Graphical solution of the harmonic balance equation for system $G(s)$

Phase deficit is 90 grade. Finite time convergence!

Conventional SMC: DF analysis

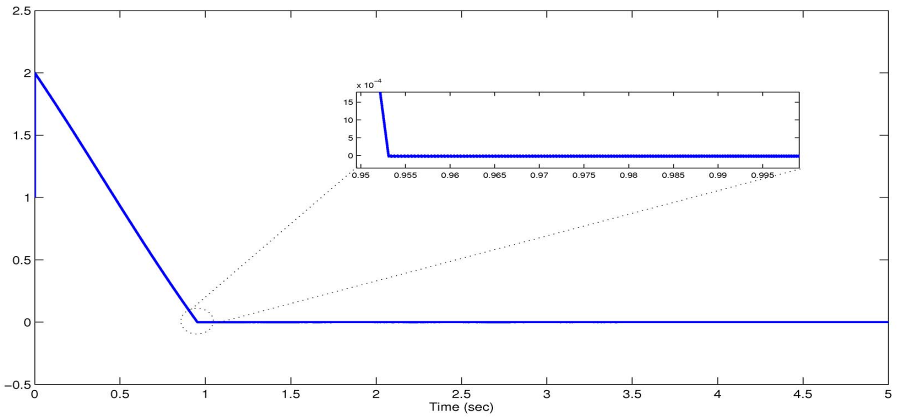

Figure: Surface

Phase deficit is 90 grade. Finite time convergence!

Conventional SMC: DF analysis

Example of **Real SMC**

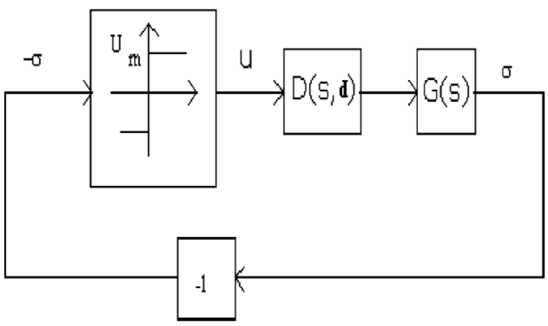

Figure: Block diagram of a linear system with Real SMC

$$D(j\omega, \mathbf{d})G(j\omega) = -\frac{1}{N(A,\omega)}, \quad N(A,\omega) = \frac{4U_m}{\pi A} \tag{11}$$

$D(j\omega, \mathbf{d})$ un-modelled dynamics

Conventional SMC: DF analysis

Example of **Real SMC**

Plant

$$\begin{aligned}\dot{x}_1 &= x_2;\\ \dot{x}_2 &= -x_1 - x_2 + u_a;\end{aligned}$$

Actuator

$$0.01\dot{u}_a = -u_a + u;$$

Sliding surface

$$\sigma = x_1 + x_2;$$

Conventional SMC

$$u = -\mathrm{sign}(\sigma) \quad (12)$$

Transfer function

$$D(s,d)G(s) = \frac{s+1}{(0.01s+1)(s^2+s+1)} \quad (13)$$

Conventional SMC: DF analysis

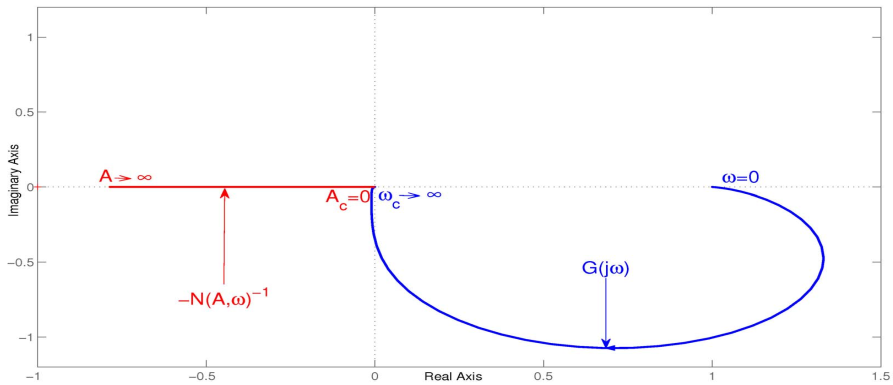

Figure: Graphical solution of the HB eq for system $D(s,d)G(s)$ plus 1st order actuator

The phase dificit is 0. Only asymptotic converence.

Conventional SMC: DF analysis

The phase dificit is 0. Only asymptotic converence.

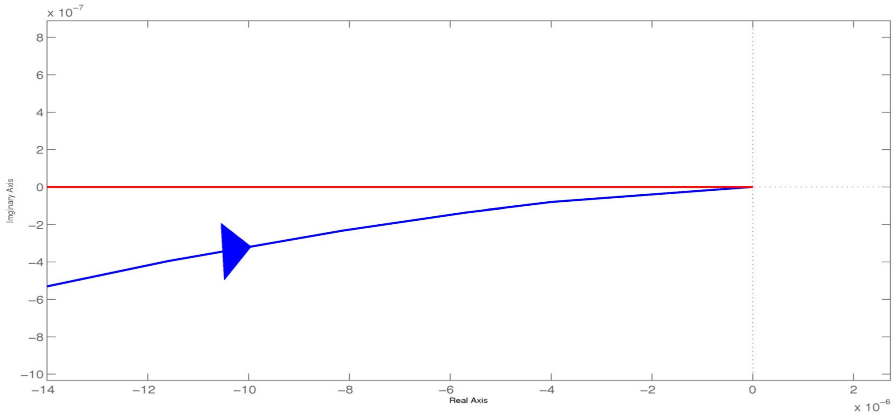

Figure: Zoom

Conventional SMC: DF analysis

The phase dificit is 0. Only asymptotic converence.

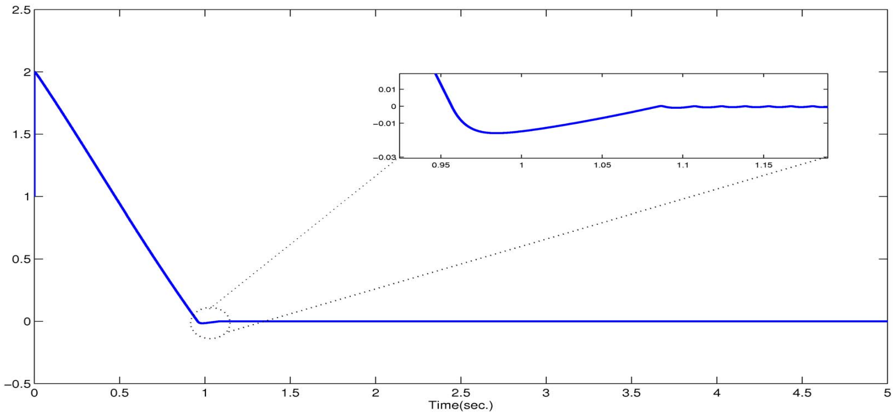

Figure: Surface

Conventional SMC: DF analysis

Plant plus 2nd order actuator

$$\dot{x}_1 = x_2 \quad ; \quad 0.0001\ddot{u}_a = -0.01\dot{u}_a - u_a + u$$
$$\dot{x}_2 = -x_1 - x_2 + u_a \quad ; \quad \sigma = x_1 + x_2$$
$$u = -\text{sign}(\sigma)$$

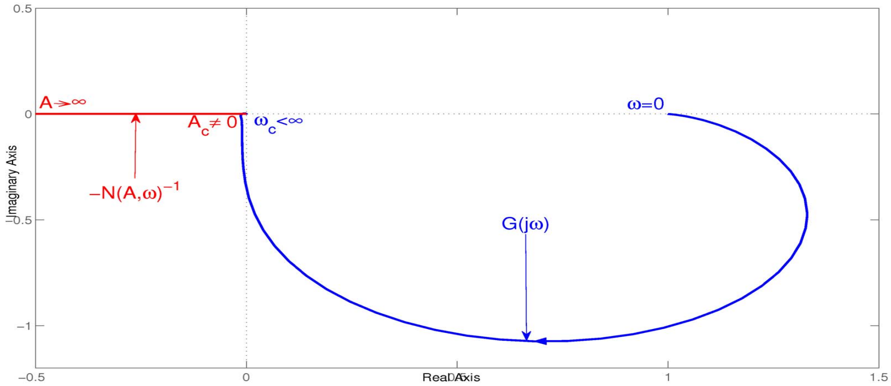

Figure: Graphical solution of the HB eq for system $D(s,d)G(s)$ plus 2nd order actuator

Conventional SMC: DF analysis

Plant plus 2nd order actuator

$$\dot{x}_1 = x_2 \quad ; \quad 0.0001\ddot{u}_a = -0.01\dot{u}_a - u_a + u$$
$$\dot{x}_2 = -x_1 - x_2 + u_a \quad ; \quad \sigma = x_1 + x_2$$
$$u = -\text{sign}(\sigma)$$

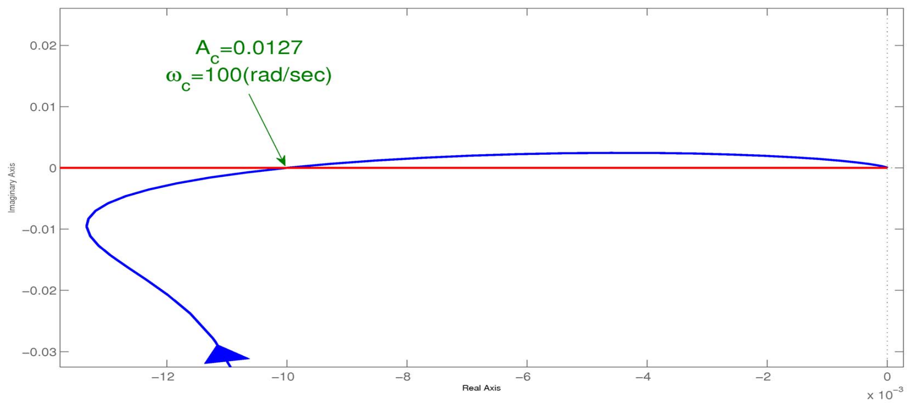

Figure: Zoom

Conventional SMC: DF analysis

Plant plus 2nd order actuator

$$\dot{x}_1 = x_2 \quad ; \qquad 0.0001\ddot{u}_a = -0.01\dot{u}_a - u_a + u$$
$$\dot{x}_2 = -x_1 - x_2 + u_a \quad ; \qquad \sigma = x_1 + x_2$$
$$u = -\text{sign}(\sigma)$$

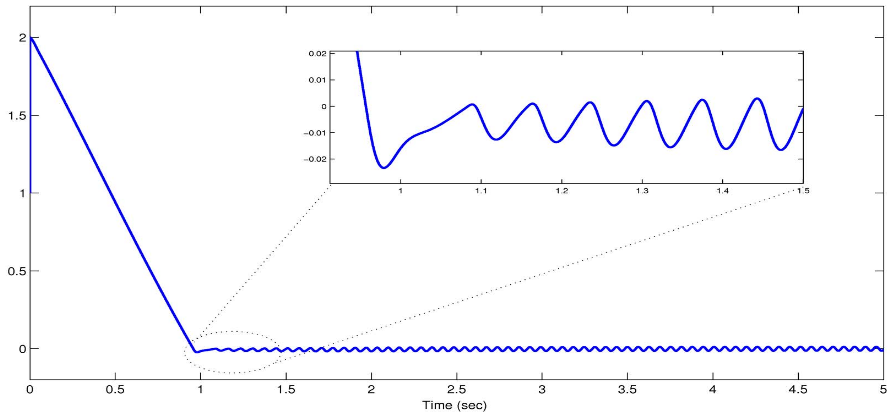

Figure: Surface

Twisting and its DF

Twisting Algorithm

$$\ddot{x} = u;$$
$$u = -c_1 sign(x) - c_2 sign(\dot{x}),$$

with $c_1 > c_2 > 0$.

DF

$$N(A) = N_1 + sN_2 = \frac{4}{\pi A}(c_1 + jc_2),$$

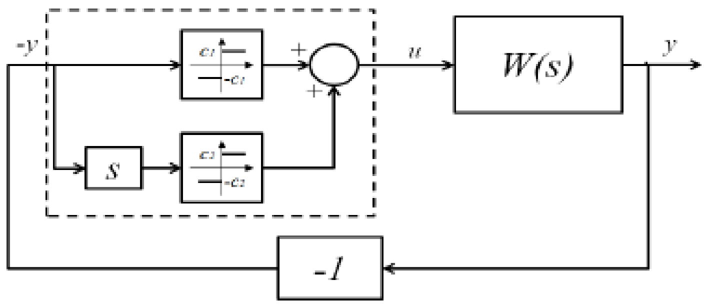

Twisting and its DF

HB eq.

$$W(j\omega) = \pi A \frac{-c_1 + jc_2}{4(c_1^2 + c_2^2)},$$

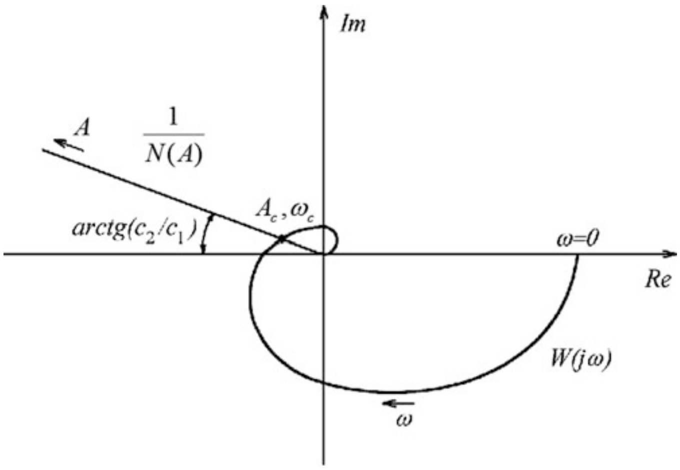

The phase dificit is $arctg(c_2/c_1)$. Finite-time convergence

Super-twisting and its DF

ST algorithm

$$\begin{aligned} \dot{x} &= u; \\ u &= -\beta|\sigma|^{1/2} sign(\sigma) + u_s, \\ \dot{u}_s &= -\alpha sign(\sigma), \end{aligned}$$

DF

$$N(A, \omega) = \frac{4\alpha}{\pi A j\omega} + \frac{1.1128\beta}{\sqrt{A}},$$

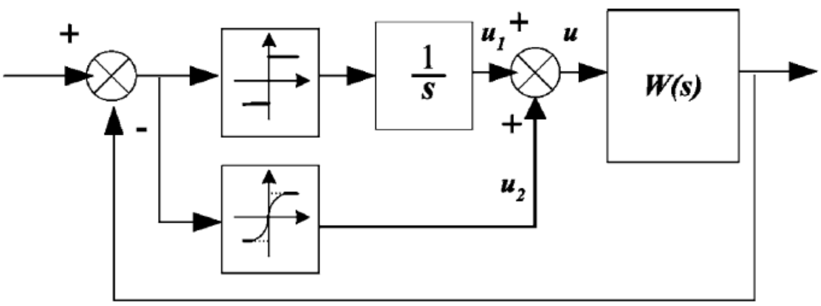

Super-twisting and its DF

HB eq.

$$W(j\omega) = -\frac{0.8986\frac{\sqrt{A}}{\beta} + j1.1329\frac{\alpha}{\beta^2\omega}}{1 + 1.3092\frac{\alpha^2}{\beta^2 A\omega^2}}$$

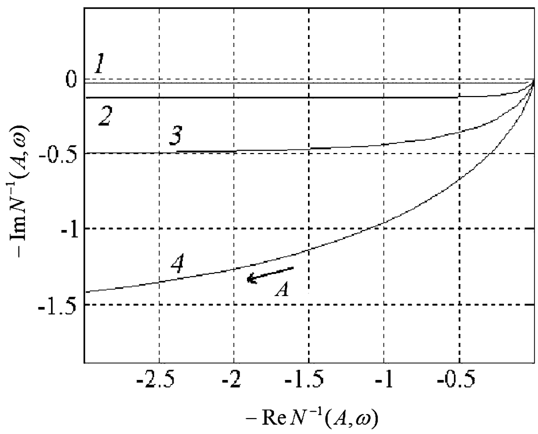

Super-twisting and its DF

Existence of the periodic solutions

Write HB eq. as: $N(A) = -W^{-1}(j\omega)$,

$$\frac{4\gamma}{\pi A}\frac{1}{j\omega} + 1.1128\frac{\lambda}{\sqrt{A}} = -W^{-1}(j\omega). \tag{14}$$

Consider the real part of both sides

$$1.1128\frac{\lambda}{\sqrt{A}} = -\operatorname{Re} W^{-1}(j\omega) \tag{15}$$

Eliminating A from eqs. (14)-(15),

$$\Psi(\omega) = \frac{4\gamma}{\pi\omega}\frac{1}{\operatorname{Im} W^{-1}(j\omega)} - \left(\frac{1.1128\lambda}{\operatorname{Re} W^{-1}(j\omega)}\right)^2 = 0. \tag{16}$$

Eq. (16) has ONLY one unknown variable, ω.

Super-twisting and its DF

Existence of the periodic solutions

Once ω is obtained from Eq. (16).

Amplitude, A_c can be computed as:

$$A_c = \frac{4\gamma}{\pi\omega_c} \frac{1}{\mathrm{Im}\, W^{-1}(j\omega_c)}. \tag{17}$$

Is It Reasonable to Substitute Discontinuous SMC by Continuous HOSMC?

Motivation Example. Relative Degree One

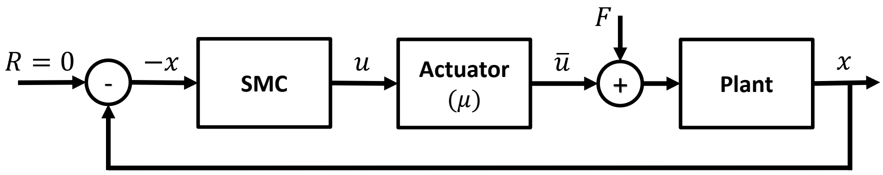

Plant

$$\dot{x}(t) = \bar{u}(t) + F(t)$$

Actuator

$$\dot{z}(t) = \begin{bmatrix} 0 & 1 \\ -\frac{1}{\mu^2} & -\frac{2}{\mu} \end{bmatrix} z(t) + \begin{bmatrix} 0 \\ \frac{1}{\mu^2} \end{bmatrix} u(t)$$

$$\bar{u}(t) = \begin{bmatrix} 1 & 0 \end{bmatrix} z(t)$$

Assumption 1

The parasitic dynamics (Actuator) is not required for the design of the SMC/HOSMC gains and its effects can be measured through the ATC μ.

Considered SMC and Disturbances

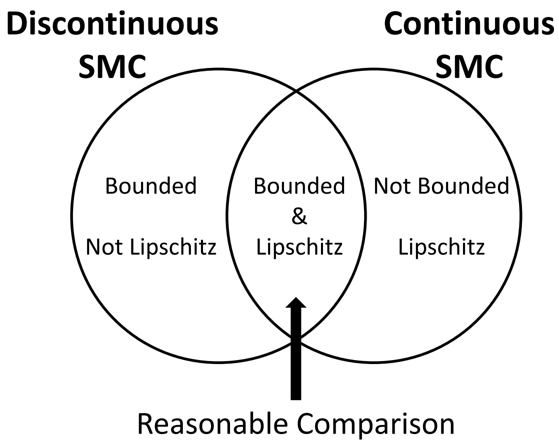

Disturbance form

$$F(t) = \alpha \sin(\Omega t)$$

where the upperbounds

$$\begin{array}{ccccc} |F| & \leq & \alpha & = & \delta \\ |\dot{F}| & \leq & \alpha\Omega & = & \Delta \end{array}$$

are assumed known.

FOSMC

$$u = -M \,\mathrm{sign}(x)$$

with $M = 1.1\delta$.

Twisting Filter

$$\dot{u} = -c_1 \,\mathrm{sign}(x) - c_2 \,\mathrm{sign}(\dot{x})$$

with $c_1 = 2.3\Delta,\ c_2 = 1.1\Delta$.

STA

$$\begin{aligned} u &= -k_1 |x|^{1/2} \,\mathrm{sign}(x) + v \\ \dot{v} &= -k_2 \,\mathrm{sign}(x) \end{aligned}$$

with $k_1 = 1.5\Delta^{1/2},\ k_2 = 1.1\Delta$.

Simulations Results for Some Values of ATC and Increasing Ω

Control \ Ω		1	10	100
Discontinuous Control				
FOSMC	$\mu = 10^{-1}$	1.366×10^{-1}	1.692×10^{-1}	0.934×10^{-1}
	$\mu = 10^{-2}$	1.092×10^{-2}	1.361×10^{-2}	1.692×10^{-2}
	$\mu = 10^{-3}$	1.064×10^{-3}	1.096×10^{-3}	1.362×10^{-3}
Continuous Control				
STA	$\mu = 10^{-1}$	1.243×10^{-1}	8.663×10^{-1}	6.4041
	$\mu = 10^{-2}$	9.431×10^{-4}	1.302×10^{-2}	8.694×10^{-2}
	$\mu = 10^{-3}$	8.915×10^{-6}	9.445×10^{-5}	1.343×10^{-3}

Table: Sliding-Mode Amplitude Accuracy

Discussion Aspects

Professor V. Utkin Hypothesis

Simulations confirms that for any value of ATC there exist a **bounded disturbance** for which the amplitude of possible oscillations produced by FOSMC is **lower** than the obtained applying STA.

Hypothesis 2

It should exists a value of ATC for which the amplitude of chattering produced by FOSMC and STA are **the same**.

Hypothesis 3

For any bounded and Lipschitz disturbance, the amplitude of possible oscillations produced by STA may be less than the obtained using FOSMC if the actuator dynamics is **fast enough**.

Methodology

The parameters that characterizes the chattering of the steady-state behavior of the nominal system ($F(t) = 0$) are:

1. Amplitude of periodic motion (A)
2. Frequency of periodic motion (ω)
3. Average power (P)

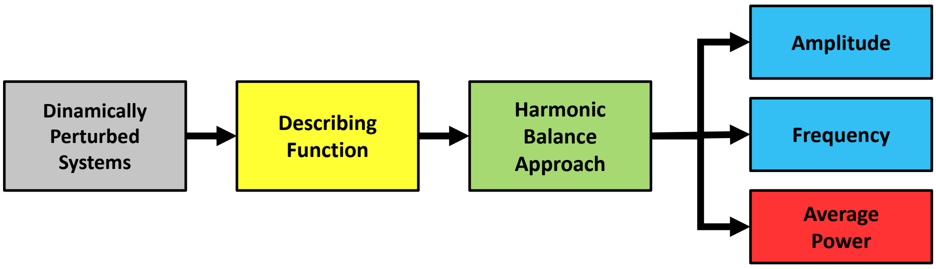

DF Analysis

Assumption 2 (Low pass filter hypothesis)

The dynamically perturbed system (Actuator-Plant) $W(s)$ has *low pass filter* characteristics with respect to the higher harmonics of the output $x(t)$. Hence the output of the system converges to a periodic motion [Gelb (1968)], [Boiko (2009)], which can be well-approximated by its first-harmonic,

$$\begin{aligned} x(t) &= A\sin(\omega t), \\ \dot{x}(t) &= A\omega\cos(\omega t). \end{aligned}$$

Harmonic Balance Approach

Parameters of a possible periodic motion, amplitude A and frequency ω, can be found by solving the Harmonic Balance equation (see for example [Gelb (1968)], [Atherton (1975)])

$$N(A,\omega)W(j\omega) = -1$$

where $N(A,\omega)$ is the DF of the non-linearity (SMC algorithm).

Average Power Approach

L_p-chattering [Levant (2010)]

$$\text{chatt}_{L_p}(x) = \left(\int_0^T \dot{x}^p(\tau)d\tau\right)^{1/p}$$

Drawbacks

- There is no chattering in ideal sliding-mode motion!
- How to compute chatt_{L_p}?

$$\Downarrow$$

A novel approach: Average (Real) Power

$$\text{P} = \frac{1}{T}\int_0^T \bar{u}(\tau)x(\tau)d\tau = \frac{\omega}{2\pi}\int_0^{\frac{2\pi}{\omega}} \frac{A^2\omega}{2}\sin(2\omega\tau)d\tau = \frac{4A^2\omega}{\pi}$$

Preliminaries

Let the dynamically perturbed system (actuator-plant)

$$W(s) = \frac{1}{s(\mu s + 1)^2}$$

FOSMC

$$u = -M \operatorname{sign}(x)$$

Twisting Filter

$$\dot{u} = -c_1 \operatorname{sign}(x) - c_2 \operatorname{sign}(\dot{x})$$

STA

$$\begin{aligned} u &= -k_1 |x|^{1/2} \operatorname{sign}(x) + v \\ \dot{v} &= -k_2 \operatorname{sign}(x) \end{aligned}$$

DF

$$N(A) = \frac{4M}{\pi A}$$

DF

$$N(A, \omega) = \frac{4}{\pi A \omega} (c_2 - j c_1)$$

DF

$$N(A, \omega) = \frac{2\alpha_1 k_1}{\pi A^{1/2}} - j \frac{4k_2}{\pi A \omega}$$

with $\alpha_1 = 1.748$.

Chattering Parameters Estimated by HB

FOSMC

$$A = \mu \left(\frac{2M}{\pi} \right)$$

$$\omega = \frac{1}{\mu}$$

$$P = \mu \left(\frac{16M^2}{\pi^3} \right)$$

Twisting Filter

$$A = \mu^2 \left(\frac{2c_2^4}{\pi(\sqrt{c_1^2 + c_2^2} - c_1)^3} \right)$$

$$\omega = \frac{1}{\mu} \left(\frac{\sqrt{c_1^2 + c_2^2} - c_1}{c_2} \right)$$

$$P = \mu^3 \left(\frac{16c_2^7}{\pi^3(\sqrt{c_1^2 + c_2^2} - c_1)^5} \right)$$

STA

$$A = \mu^2 \left(\frac{\alpha_1^2 k_1^2 + 4\pi k_2}{\pi \alpha_1 k_1} \right)^2$$

$$\omega = \frac{1}{\mu} \left(\frac{\alpha_1^2 k_1^2}{\alpha_1^2 k_1^2 + 4\pi k_2} \right)^{1/2}$$

$$P = \mu^3 \left(\frac{4(\alpha_1^2 k_1^2 + 4\pi k_2)^{7/2}}{\pi^5 \alpha_1^3 k_1^3} \right)$$

Chattering Parameters as Function of μ

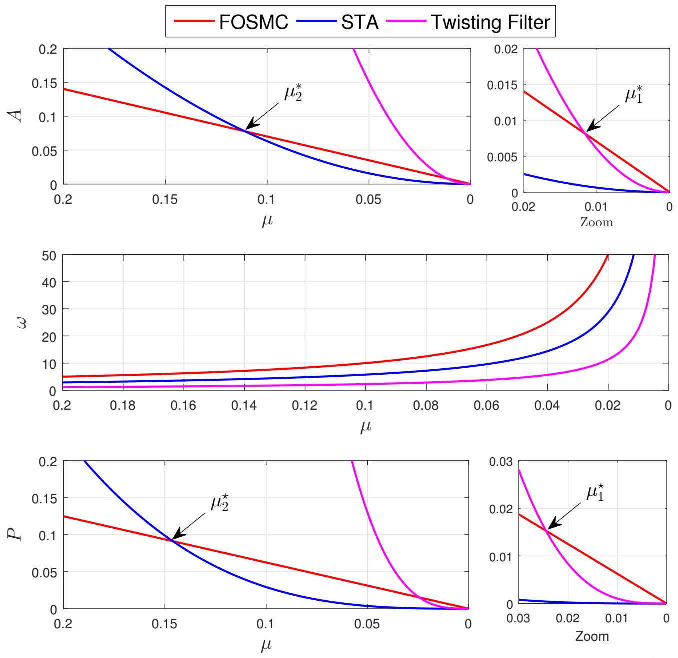

Figure: Chattering Parameters as Function of ATC $\mu \to 0$, with $\delta = \Delta = 1$.

Amplitude Discussion

Result 1

There exist a value of the ATC for which the amplitude of oscillations caused by FOSMC is equal that the produced by Twisting Filter,

$$\mu_1^* = \frac{M(\sqrt{c_1^2 + c_2^2} - c_1)^3}{c_2^4}$$

Result 2

There exist a value of the ATC for which the amplitude of oscillations caused by FOSMC is equal that the produced by STA,

$$\mu_2^* = \frac{2\pi M(\alpha_1 k_1)^2}{\left((\alpha_1 k_1)^2 + 4\pi k_2\right)^2}$$

Frequency Discussion

Result 3

The frequency of oscillations caused by STA is always lower than the produced by FOSMC.

Result 4

The frequency of oscillations caused by Twisting Filter is always lower than the produced by FOSMC.

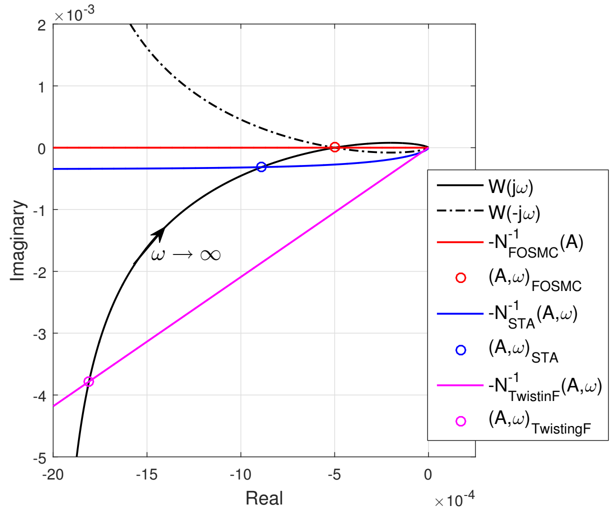

Figure: Graphical Solution of HB equation

Average Power Discussion

Result 5

There exist a value of the ATC for which the average power of oscillations caused by FOSMC is equal that the produced by Twisting Filter,

$$\mu_1^\star = \frac{M(\sqrt{c_1^2 + c_2^2} - c_1)^{5/2}}{c_2^{7/2}}$$

Result 6

There exist a value of the ATC for which the average power of oscillations caused by FOSMC is equal that the produced by STA,

$$\mu_2^\star = \frac{2\pi M(\alpha_1 k_1)^{3/2}}{\left((\alpha_1 k_1)^2 + 4\pi k_2\right)^{7/2}}$$

Selection of STA Gains to Minimize the Amplitude of Chattering

Minimum Amplitude for a given $k_2 > \Delta$

$$k_1 = \left(\frac{4\pi k_2}{\alpha_1^2}\right)^{1/2} = 2.028\sqrt{k_2}$$

Proposed STA Gains†

$$k_1 = 2.127\sqrt{\Delta}$$
$$k_2 = 1.1\Delta$$

† Sufficient stability conditions are satisfied:

$$k_1 > 1.449\sqrt{\Delta}$$
$$k_2 = 1.1\Delta$$

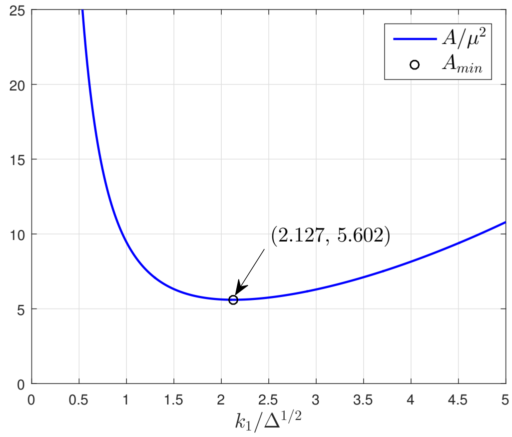

Figure: Amplitude as Function of k_1

Selection of STA Gains Minimize the Average Power

Minimum Average Power for a given $k_2 > \Delta$

$$k_1 = \left(\frac{3\pi k_2}{\alpha_1^2}\right)^{1/2} = 1.756\sqrt{k_2}$$

Proposed STA Gains†

$$k_1 = 1.842\sqrt{\Delta}$$
$$k_2 = 1.1\Delta$$

† Sufficient stability conditions are satisfied:

$$k_1 > 1.449\sqrt{\Delta}$$
$$k_2 = 1.1\Delta$$

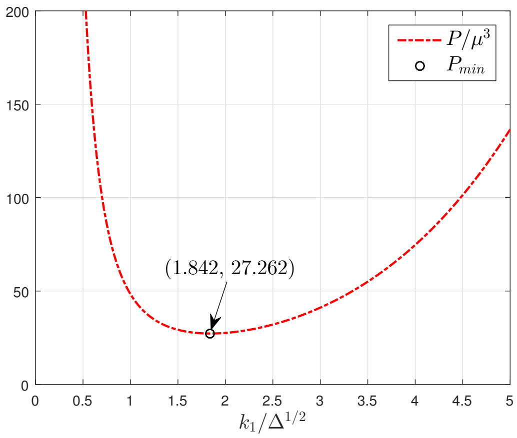

Figure: Average Power as Function of k_1

Motivation Example. Relative Degree Two

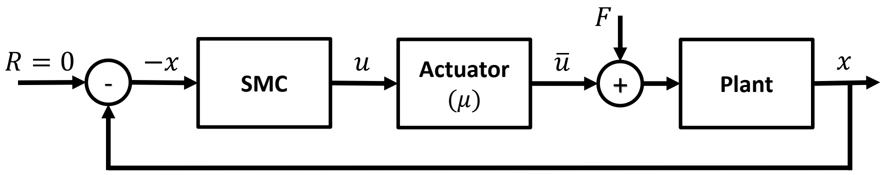

Plant

$$\ddot{x}(t) = \bar{u}(t) + F(t)$$

Actuator

$$\dot{z}(t) = \begin{bmatrix} 0 & 1 \\ -\frac{1}{\mu^2} & -\frac{2}{\mu} \end{bmatrix} z(t) + \begin{bmatrix} 0 \\ \frac{1}{\mu^2} \end{bmatrix} u(t)$$

$$\bar{u}(t) = \begin{bmatrix} 1 & 0 \end{bmatrix} z(t)$$

Assumption 1

The parasitic dynamics (Actuator) is not required for the design of the SMC/HOSMC gains and its effects can be measured through the ATC μ.

Considered SMC and Disturbances

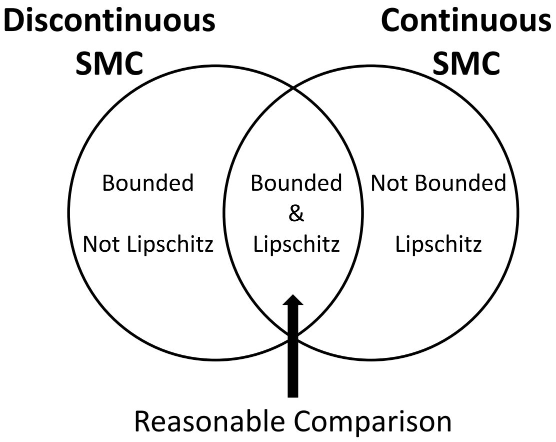

Disturbance form

$$F(t) = \alpha \sin(\Omega t)$$

where the upperbounds

$$\begin{array}{rcccl} |F| & \leq & \alpha & = & \delta \\ |\dot{F}| & \leq & \alpha\Omega & = & \Delta \end{array}$$

are assumed known.

Twisting

$$u = -c_1 \operatorname{sign}(x) - c_2 \operatorname{sign}(\dot{x})$$

with $c_1 = 2.3\delta$, $c_2 = 1.1\delta$.

CTA

$$\begin{aligned} u &= -k_1|x|^{1/2}\operatorname{sign}(x) - k_2|\dot{x}|^{1/2}\operatorname{sign}(\dot{x}) + v \\ \dot{v} &= -k_3 \operatorname{sign}(x) - k_4 \operatorname{sign}(\dot{x}) \end{aligned}$$

with $k_1 = 1.5\Delta^{2/3}$, $k_2 = 2.3\Delta^{1/2}$, $k_3 = 1.1\Delta$, $k_4 = 0$.

Average Power Approach

L_p-chattering [Levant (2010)]

$$\text{chatt}_{L_p}(x) = \left(\int_0^T \dot{x}^p(\tau)d\tau \right)^{1/p}$$

Drawbacks

- There is no chattering in ideal sliding-mode motion!
- How to compute chatt_{L_p}?

$$\Downarrow$$

A novel approach: Average (Kinetic) Power

$$\text{P} = \frac{1}{T}\int_0^T \dot{x}^2(\tau)d\tau = \frac{\omega}{2\pi}\int_0^{\frac{2\pi}{\omega}} A^2\omega^2\cos^2(\omega\tau)d\tau = \frac{A^2\omega^2}{2}$$

Preliminaries

Let the dynamically perturbed system (actuator-plant)

$$W(s) = \frac{1}{s^2(\mu s+1)^2}$$

Twisting

$$u = -c_1\,\text{sign}(x) - c_2\,\text{sign}(\dot{x})$$

CTA

$$\begin{aligned} u &= -k_1|x|^{1/2}\,\text{sign}(x) - k_2|\dot{x}|^{1/2}\,\text{sign}(\dot{x}) + v \\ \dot{v} &= -k_3\,\text{sign}(x) - k_4\,\text{sign}(\dot{x}) \end{aligned}$$

DF

$$N(A) = \frac{4}{\pi A}(c_1 + jc_2)$$

DF

$$N(A,\omega) = \frac{2\alpha_1 k_1}{\pi A^{2/3}} + \frac{4k_4}{\pi A\omega} + j\left[\frac{2\alpha_2 k_2\omega^{1/2}}{\pi A^{1/2}} - \frac{4k_3}{\pi A\omega}\right]$$

with $\alpha_1 = 1.821$, $\alpha_2 = 1.748$.

Chattering Parameters Estimated by HB

Twisting

$$A = \mu^2 \left(\frac{2c_2^4}{\pi(\sqrt{c_1^2 + c_2^2} - c_1)^3} \right)$$

$$\omega = \frac{1}{\mu} \left(\frac{\sqrt{c_1^2 + c_2^2} - c_1}{c_2} \right)$$

$$P = \mu^2 \left(\frac{2c_2^6}{\pi^2(\sqrt{c_1^2 + c_2^2} - c_1)^4} \right)$$

CTA with $k_4 = 0$

Solve the non-linear equality for the frequency ω,

$$\frac{k_2}{k_1^{3/4}}(1 - \mu^2\omega^2)^{3/4} - \frac{k_3}{k_1^{3/2}}(1 - \mu^2\omega^2)^{3/2} = 2\mu\,\omega$$

Then, substitute on the amplitude expression,

$$A = \left[\frac{2\alpha_1 k_1}{\pi\omega^2(1 - \mu^2\omega^2)} \right]^{3/2}$$

Chattering Parameters as Function of μ

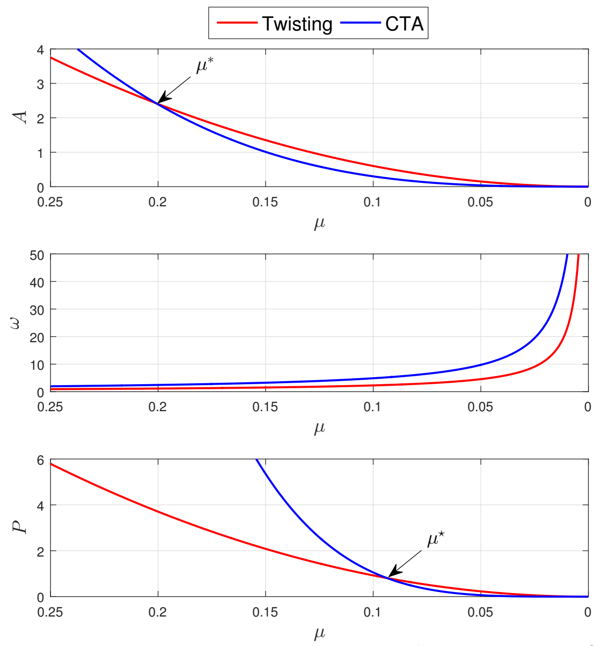

Figure: Chattering Parameters as Function of ATC $\mu \to 0$, with $\delta = 1$, $\Delta = 10$.

Amplitude Discussion

Result 1

There exist a value of the ATC for which the amplitude of oscillations caused by Twisting is equal that the produced by CTA. For the example

$$\mu^* = 0.2$$

Frequency Discussion

Result 2

The frequency of oscillations caused by Twisting is always lower than the produced by CTA.

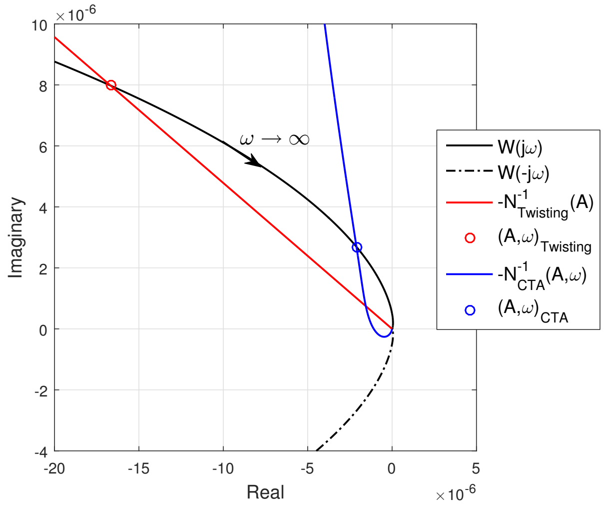

Figure: Graphical Solution of HB equation

Average Power Discussion

Result 3

There exist a value of the ATC for which the average power of oscillations caused by Twisting is equal that the produced by CTA. For the example

$$\mu^{\star} = 0.093$$

Selection of CTA Gains to Minimize the Amplitude of Chattering

Proposed CTA Gains†

Given

$$k_1 = 1.5\Delta^{2/3}$$
$$k_3 = 1.1\Delta$$
$$k_4 = 0$$

the value of k_2 that minimize the amplitude is

$$k_2 = 3.744\Delta^{1/2}$$

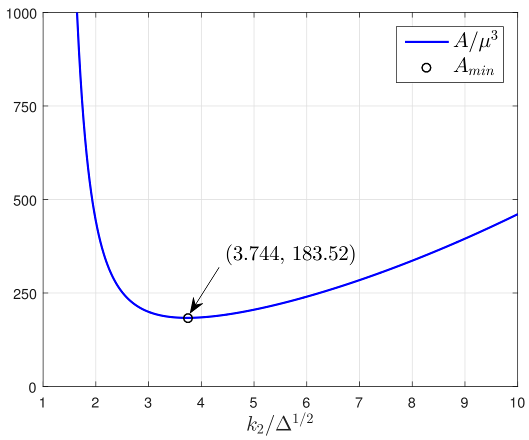

Figure: Amplitude as Function of k_1

Selection of CTA Gains Minimize the Average Power

Proposed CTA Gains†

Given

$$k_1 = 1.5\Delta^{2/3}$$
$$k_3 = 1.1\Delta$$
$$k_4 = 0$$

the value of k_2 that minimize the average power is

$$k_2 = 3.104\Delta^{1/2}$$

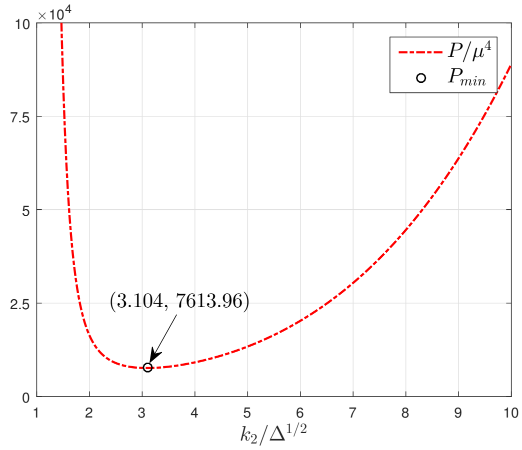

Figure: Average Power as Function of k_2

References

D.P. Atherton, *Nonlinear Control Engineering-Describing Function Analysis and Design*, Van Nostrand Reingold: New York and London, 1975.

I. Boiko, *Frequency-Domain Analysis and Design*, Birkhäuser Basel, 2009.

A. Gelb and W.E. Vander Velde, *Multiple-Input Describing Functions and Nonlinear System Design*, McGraw Hill, 1968.

A. Levant, *Sliding order and sliding accuracy in sliding mode control*, International journal of control, vol. 58, no.6, pp. 1247–1263, Taylor & Francis, 1993.

A. Levant, *Robust exact differentiation via sliding mode technique*, Automatica, vol. 34, no.3, pp. 379–384, Elsevier, 1998.

A. Levant, *Chattering analysis*, Automatic Control, IEEE Transactions on, vol. 55, no.6, pp. 1380–1389, 2010.

References

- J. A. Moreno and M Osorio, *Strict Lyapunov functions for the super-twisting algorithm*, IEEE Transactions on Automatic Control, vol. 57, no. 4, pp. 1035–1040, IEEE, 2012.
- U. Pérez-Ventura and L. Fridman, *Chattering measurement in SMC and HOSMC*, 2016 14th International Workshop on Variable Structure Systems (VSS), pp. 108–113, IEEE, 2016.
- R. Seeber and M. Horn, *Stability proof for a well-established Super-Twisting parameter setting*, Automatica, 2017.
- A. Swikir and V. Utkin, *Chattering analysis of conventional and super twisting sliding mode control algorithm*, 2016 14th International Workshop on Variable Structure Systems (VSS), pp. 98–102, IEEE, 2016.
- V. Utkin, *Sliding modes in optimization and control problems*, Springer Verlag, New York, 1992.
- V. Utkin, *Discussion Aspects of High Order Sliding Mode Control*, Automatic Control, IEEE Transactions on, vol. 61, pp. 829–833, IEEE, 2016.

Adaptive Extension for Higher Order Sliding Mode Controllers

Alexander Barth[a] **Johann Reger**[a]

This contribution deals with nonlinear systems given by

$$\begin{aligned} \dot{x}_i &= x_{i+1}, i = 1, ..., n-1, \\ \dot{x}_n &= f(x) + g(x)\big(\Delta(x,t) + u\big) \end{aligned} \tag{1}$$

where $x(t) \in \mathbb{R}^n$ is the state, $u(t) \in \mathbb{R}$ a scalar control input, f and g are known vector fields. The uncertainty $\Delta(x,t)$ is a composition of two terms

$$\Delta(x,t) = \Delta_{\mathrm{s}}(x) + \Delta_{\mathrm{u}}(x,t) = \Theta^{\mathrm{T}}\phi(x,t) + \Delta_{\mathrm{u}}(x,t)\,, \tag{2}$$

namely the structured uncertainty $\Delta_{\mathrm{s}}(x) = \Theta^{\mathrm{T}}\phi(x,t)$ with an unknown parameter vector Θ and known regressor $\phi(x,t)$. The term $\Delta_{\mathrm{u}}(x,t)$ represents an unstructured uncertainty.

The control objective is to find a suitable control law u such that substituted in (1) the origin is stable even in the presence of the uncertainties in shape of (2).

Sliding-mode control is an established design method to achieve this goal. In general it requires little knowledge about the system or the uncertainties and therefore may simplify the controller design. The main idea is to define a manifold such that the corresponding sliding variable has relative degree one with respect to the control input u. The sliding mode controller ensures that the state of system (1) is forced to this manifold in finite time. Due to a suitable selection of the manifold, the internal dynamics is stable and the state converges to the origin.

Various design approaches [3, 5], including adaptive controllers [6, 1, 2], have been presented to solve this task.

Recently in [4], Moreno proposed a class of control designs that do not require the relative degree one condition and allow the stabilization of the overall system (1) in finite time. These controllers require the cumulative uncertainty to be bounded by

$$|\Delta(x,t)| \leq \Omega_\Delta \tag{3}$$

for some $\Omega_\Delta > 0$.

Main result: We extend the approach by Moreno by an adaptive part to improve the robustness of the proposed class of controllers. The structurally known part $\Theta^{\mathrm{T}}\phi(x,t)$ is compensated by an adaptive extention separately from the unstructured part. As a result, the requirements (3) on the uncertainty may be relaxed to

$$|\Delta_{\mathrm{u}}(x,t)| \leq \Omega_u \tag{4}$$

[a]Fachgebiet Regelungstechnik, Technische Universität Ilmenau, Helmholtzplatz 5, D-98693 Ilmenau, E-Mail: {alexander.barth,johann.reger}@tu-ilmenau.de

with $\Omega_u > 0$ such that the sliding mode part has to handle only the unstructured part of uncertainty.

Exemplarily for a second order system we show the respective design method. However, the method can be extended to an arbitrary order system.

The controller including the adaptation law is given by

$$\begin{aligned} u &= -k_2 \,\mathrm{sign}\left(\lceil x_2 \rfloor^2 + k_1 \, x_1\right) - \hat{\Theta}^{\mathrm{T}} \phi(x,t) \\ \dot{\hat{\Theta}} &= \gamma \, g(x) \, \left(\lceil x_2 \rfloor^2 + k_1^2 \lceil x_1 \rfloor^2\right) \phi(x,t) \end{aligned} \tag{5}$$

with $\hat{\Theta}(0) = \hat{\Theta}_0$ for some $\hat{\Theta}_0$, parameters $k_1, k_2, \gamma > 0$ and $\lceil x \rfloor^\rho = \mathrm{sign}\,(x)\; |x|^\rho$.

The stability of the origin in the closed-loop system is proofed using the Lyapunov function

$$V(x_1, x_2, \hat{\Theta}) = \frac{2}{3}|x_1|^{\frac{3}{2}} + \frac{2}{3}|x_2|^{\frac{3}{2}} + k_1^{\frac{1}{2}} \lceil x_1 \rfloor^{\frac{1}{2}} \, x_2 + \frac{2\, k_1^{\frac{3}{2}}}{3}|x_1|^{\frac{3}{2}} + \frac{1}{2\,\gamma}\left(\Theta - \hat{\Theta}\right)^{\mathrm{T}} \left(\Theta - \hat{\Theta}\right), \tag{6}$$

orininally proposed by Moreno in [4], and extending it by a quadratic term regarding the estimation error $\Theta - \hat{\Theta}$. In view of the certainty equivalence principle, we may then obtain the adaptation law shown in (5).

Since the sliding mode part only has to cover the unstructured part of the uncertainty, we expect to significantly reduce the gains k_1 and k_2 of the controller (5) compared to the conventional approach if $\Omega_{\mathrm{u}} << \Omega_{\Delta}$. Moreover, the aproach does not require a fixed upper bound on the structured uncertainty $\Delta_{\mathrm{s}}(x,t)$, which allows to compensate larger class of uncertainties.

[1] Barth, A., Reichhartinger, M., Reger, J., Horn, M., and Wulff, K.: *Lyapunov-Design for a Super-Twisting Sliding-Mode Controller using the Certainty-Equivalence Principle.* In 1st MICNON, St. Petersburg, Russia, 2015.

[2] Barth, A. , Reichhartinger, M., Reger, J., Horn, M., Wulff, K.: Certainty-equivalence based super-twisting control using continuous adaptation laws. In *Proceedings of the 14th IEEE VSS*, pages 92–97 (2016)

[3] Levant, A.: *Sliding order and sliding accuracy in sliding mode control.* IJC, 58(6), 1247–1263, 1993.

[4] Li, S., Yu, X., Fridman, L., Man, Z., and Wang, X.: *Advances in Variable Structure Systems and Sliding Mode Control.* Springer, New York, 2017.

[5] Orlov, Y.: *Finite time stability and robust control synthesis of uncertain switched systems.* SIAM Journal on Control and Optimization, 43(4), 1253–1271, 2005.

[6] Shtessel, Y., Moreno, J., Plestan, F., Fridman, L. and Poznyak, A.: *Super-twisting adaptive sliding mode control: A lyapunov design.* In 49th IEEE CDC, 5109–5113, 2010.

Fachgebiet Regelungstechnik

TECHNISCHE UNIVERSITÄT ILMENAU

Adaptive Extension for Higher Order Sliding Mode Controllers

Alexander Barth[†], Johann Reger

alexander.barth@tu-ilmenau.de

[†] Control Engineering Group, TU Ilmenau, Germany

13th September 2017

20. Styrian Workshop on Automatic Control

Outline

Introduction - Classical Sliding Mode Control

System

$$\dot{x} = f(x) + g(x)\,(u + \delta(t))$$

- State $x \in \mathbb{R}^n$, Input $u \in \mathbb{R}$

Sliding Surface $\quad \sigma : \sigma(x) = 0$

- relative Degree 1 w.r.t u
- stable Zero-Dynamics

Dynamics for σ

$$\dot{\sigma} = \omega + \Delta(t)$$

- Disturbance $\Delta(t) \in \mathbb{R}$, $|\Delta| < \bar{\Delta}$
- new Input $\omega := \frac{\partial \sigma(x)}{\partial x} f(x) + \frac{\partial \sigma(x)}{\partial x} g(x)\, u$

Control Law

$$\omega = -K \operatorname{sign}(\sigma)$$

with $K > \bar{\Delta}$

Problem Statement

System:

$$\dot{x}_i = \dot{x}_{i-1}, i = 1, \dots, n-1$$

$$\dot{x}_n = \Delta(t,x) + \Theta^{\mathrm{T}}\omega(t,x) + u$$

- Initial Condition: $x_j(0) = x_{0,j} \quad \forall j = 1...n$
- Uncertainty $\Delta(t,x)$
  bounded by $|\Delta(t,x)| \le C : \forall t \in \mathbb{R}, \forall x \in \mathbb{R}^n$
- Parametric Uncertainty $\Theta^{\mathrm{T}}\omega(t,x)$
  - unknown constant Parameter Vector $\Theta \in \mathbb{R}^p$
  - known Regressor $\omega(t,x) : \mathbb{R} \times \mathbb{R}^n \to \mathbb{R}^p$

Objective: stabilize $x_1 = x_2 = ... = x_n = 0$

Control Law

$$u = \varphi(x_1, x_2, \cdots, x_n) + \hat{\Theta}^{\mathrm{T}}\,\omega(t,x)$$

Homogeneity

- Function $V : \mathbb{R}^n \to \mathbb{R}$ or Vector Field $f : \mathbb{R}^n \to \mathbb{R}^n$
- Dilation Operator: $\Delta_\varepsilon^r x := (\varepsilon^{r_1} x_1, ..., \varepsilon^{r_n} x_n)\,, \quad \forall \varepsilon \in \mathbb{R} : \varepsilon > 0$
- Vector $\mathbf{r} = (r_1, ..., r_n)^{\mathrm{T}}$ with $r_i > 0 \quad \forall i = 1, ..., n$

Function is called $\mathbf{r}$-homogeneous of degree l [Zubov, 1964]:

- Scalar Function $V(\Delta_\varepsilon^r x) = \varepsilon^l V(x)$
- Vector field $f : \mathbb{R}^n \to \mathbb{R}^n : f(\Delta_\varepsilon^r x) = \varepsilon^l \Delta_\varepsilon^r f(x)$
- Homogeneous Sphere: $\mathcal{S} = \{x \in \mathbb{R}^n : \|x\|_{\mathbf{r},p} = 1\}$
- with: $\|x\|_{\mathbf{r},p} := \left(\Sigma_{i=1}^n |x_i|^{\frac{p}{r_i}}\right)^{\frac{1}{p}}$

Notation

- Symbol $\lceil z \rfloor^p = |z|^p \operatorname{sign}(z)$ with $z, p \in \mathbb{R}$
- Derivative:
  $\frac{d}{dz}\lceil z \rfloor^p = p\,|z|^{p-1}$ and
  $\frac{d}{dz}|z|^p = p\lceil z \rfloor^{p-1}$
  almost everywhere for z
- Note: $\lceil z \rfloor^2 = |z|^2 \operatorname{sign}(z) \neq z^2$
- Multiplication: $\lceil z \rfloor^p \lceil z \rfloor^q = |z|^{p+q}$

Design Procedure

- Identify unstructured, parametric uncertainty
- Design a Controller for the nominal System (e.g. Parameters are know) including a Lyapunov Function
- Extend the Lyapunov Function by the Parameter Estimation Error
- Obtain the Adaptation Law using the Derivative of the Lyapunov Function

Example: 2nd Order System - Nominal Design

System

$$\dot{x}_1 = x_2$$
$$\dot{x}_2 = \Delta(t, x_1, x_2) + u$$

- System Order: $n = 2$
- Disturbance $\Delta(t, x) \leq C$, $C > 0$ const.
- States $x_1, x_2 \in \mathbb{R}$
- Input $u \in \mathbb{R}$

Nominal Control Law [Levant, 2005]:

$$u(x_1, x_2) = -k_2 \,\mathrm{sign}\left(\lceil x_2 \rfloor^{2+\alpha} + k_1 \lceil x_1 \rfloor^{\frac{2+\alpha}{2}}\right)$$

- $k_1, k_2, \alpha > 0$ constant
- $\mathbf{r}$ - homogeneous of degree: $l = 0$ with $\mathbf{r} = (r_1, r_2)^{\mathrm{T}} = (2, 1)^{\mathrm{T}}$

Solutions in the Sense of Filippov [Filippov, 1988]

Stability Proof

Lyapunov Function [Moreno, 2017]

$$V(x_1,x_2) = V_1(x_1) + W_2(x_1,x_2)$$
$$V_1(x_1) = \frac{2}{m}|x_1|^{\frac{m}{2}}$$
$$W_2(x_1,x_2) = \frac{1}{m}|x_2|^m - \lceil \nu_1(x_1)\rfloor^{m-1} x_2 + \left(1-\frac{1}{m}\right)|\nu_1(x_1)|^m$$

with

$$m = 2n + \alpha$$
$$\nu_1(x_1) = -k_1\lceil x_1 \rfloor^{\frac{1}{2}}$$

- V : $\mathbf{r}$-homogeneous degree m with $\mathbf{r} = (r_1, r_2)^{\mathrm{T}} = (2,1)^{\mathrm{T}}$
- Is W_2 positive definite?

Controller Design

Definiteness of $W_2(x_1,x_2)$

$$W_2(x_1,x_2) = \frac{2-1}{m}|x_2|^m - \lceil \nu_1(x_1)\rfloor^{m-1} x_2 + \left(1-\frac{1}{m}\right)|\nu_1(x_1)|^m$$

Young's Inequality [Hardy et al., 1952]

$$a\lceil b\rfloor^{\beta} \le \frac{1}{\gamma}|a|^{\gamma} + \left(1-\frac{1}{\gamma}\right)|b|^{\beta\frac{\gamma}{\gamma-1}}$$

with $a = x_2,\ b = \nu_1(x_1),\ \beta = m-1,\ \gamma = m$

it follows $W_2(x_1,x_2) \ge 0$

Controller Design

Derivation of Lyapunov Function

$$\dot{V} = \frac{\partial V(x_1, x_2)}{\partial x_1} x_2 + \frac{\partial V(x_1, x_2)}{\partial x_2} \left(\Delta(t, x_1, x_2) + u\right)$$

with

$$\frac{\partial V(x_1, x_2)}{\partial x_2} = \lceil x_2 \rfloor^{m-1} - \lceil \nu_1(x_1) \rfloor^{m-1}$$

$$= \lceil x_2 \rfloor^{m-1} + k_1^{m-1} \lceil (x_1) \rfloor^{\frac{m-1}{2}} := s_{2,d}$$

Note that:

$$\{x \in \mathbb{R}^n | s_{2,d}(x_1, x_2) = 0\} = \left\{x \in \mathbb{R}^n | \lceil x_2 \rfloor^{2+\alpha} + k_1 \lceil x_1 \rfloor^{\frac{2+\alpha}{2}} = 0\right\}$$

Control Law

$$u = -k_2 \operatorname{sign}\left(\lceil x_2 \rfloor^{2+\alpha} + k_1 \lceil x_1 \rfloor^{\frac{2+\alpha}{2}}\right)$$

$$\Rightarrow u = -k_2 \operatorname{sign}(s_{2,d})$$

Controller Design

Derivation of Lyapunov Function

$$\dot{V} = \frac{\partial V(x_1, x_2)}{\partial x_1} x_2 + s_{2,d} \left(\Delta(t, x_1, x_2) - k_2 \operatorname{sign}(s_{2,d})\right)$$

with $|\Delta(t, x)| \leq C$ and $k_2 > C$:

$$\dot{V} \leq \frac{\partial V(x_1, x_2)}{\partial x_1} x_2 - (k_2 - C) |s_{2,d}|$$

Controller Design

Case 1: $s_{2,d} \neq 0$

$$\dot{V} \leq \frac{\partial V(x_1, x_2)}{\partial x_1} x_2 - (k_2 - C)\,|s_{2,d}| < 0$$

select k_2 such:

$$k_2 > \left(\frac{\frac{\partial V(x_1,x_2)}{\partial x_1} x_2}{|s_{2,d}|} + C \right)$$

with $\frac{\partial V(x_1,x_2)}{\partial x_1} = \frac{\partial V_1(x_1)}{\partial x_1} + \frac{\partial W_2(x_1,x_2)}{\partial x_1}$

$$\frac{\partial V_1(x_1)}{\partial x_1} = \lceil x_1 \rfloor^{\frac{m-2}{2}}$$

$$\frac{\partial W_2(x_1, x_2)}{\partial x_1} = -\frac{m-1}{2} k_1^{m-1} |x_1|^{\frac{m-3}{2}} s_2$$

Controller Design

$$\frac{\partial V_1(x_1)}{\partial x_1} = \lceil x_1 \rfloor^{\frac{m-2}{2}}$$

$$\frac{\partial W_2(x_1, x_2)}{\partial x_1} = -\frac{m-1}{2} k_1^{m-1} |x_1|^{\frac{m-3}{2}} s_2$$

Homogeneous Degree $(r_1 = 2, r_2 = 1)$:

$$\frac{\partial V}{\partial x_1} x_2 = \frac{\partial V_1(x_1)}{\partial x_1} x_2 + \frac{\partial W_2(x_1, x_2)}{\partial x_1} x_2 \qquad \Rightarrow l = m - 1$$

$$s_{2,d} = \lceil x_2 \rfloor^{m-1} + k_1^{m-1} \lceil x_1 \rfloor^{\frac{m-1}{2}} \qquad \Rightarrow l = m - 1$$

results in:

$$\frac{\frac{\partial V(x_1,x_2)}{\partial x_1} x_2}{|s_{2,d}|}$$

$\Rightarrow$ Homogeneous Degree $l = 0$

Controller Design

$$\dot{V} \leq \frac{\partial V(x_1, x_2)}{\partial x_1} x_2 - (k_2 - C)\,|s_{2,d}| < 0$$

Case 1: $s_{2,d} \neq 0$

- $\dfrac{\frac{\partial V(x_1,x_2)}{\partial x_1} x_2}{|s_{2,d}|}$ hom. Degree 0
- Inequality:

$$k_2 > \left(\frac{\frac{\partial V(x_1,x_2)}{\partial x_1} x_2}{|s_{2,d}|} + C \right)$$

- Maximum can be found at $\mathcal{S} = \{x \in \mathbb{R}^n : \|x\|_{\mathbf{r},p} = 1\}$

What happens at $s_{2,d} = 0$?

Controller Design

Case 2: $s_{2,d} = 0$

$$s_{2,d} := \lceil x_2 \rfloor^{m-1} + k_1^{m-1} \lceil (x_1) \rfloor^{\frac{m-1}{2}}$$
$$s_2 := x_2 + k_1^{m-1} \lceil (x_1) \rfloor^{\frac{1}{2}}$$

if $s_{2,d} = 0$:

$$\{x \in \mathbb{R}^n | s_{2,d}(x_1, x_2) = 0\} = \{x \in \mathbb{R}^n | s_2(x_1, x_2) = 0\}$$

Results in:

- $x_2 = -k_1 \lceil x_1 \rfloor^{\frac{1}{2}}$
- $\frac{\partial V(x_1,x_2)}{\partial x_1} x_2 = \lceil x_1 \rfloor^{\frac{m-2}{2}} x_2 = -k_1 |x_1|^{\frac{m-1}{2}} < 0, \forall x_1, x_2 \neq 0$

$\Rightarrow$ Closed Loop System is asymptotically stable

Stability Proof

Recursive Function [Moreno, 2017]

for $i = 2, ..., n$:

$$V_1(x_1) = \frac{n}{m}|x_1|^{\frac{m}{n}}, \cdots, V_i(\bar{x}_i) = V_{i-1}(\bar{x}_{i-1}) + W_i(\bar{x}_i)$$

$$W_i(\bar{x}_i) = \frac{r_i}{m}|x_i|^{\frac{m}{r_i}} - \lceil \nu_{i-1}(\bar{x}_{i-1}) \rfloor^{\frac{m-r_i}{r_i}} x_i + \left(1 - \frac{r_i}{m}\right) |\nu_{i-1}(\bar{x}_{i-1})|^{\frac{m}{r_i}}$$

with $m \geq \max\limits_{1 \leq i \leq n} \{2\,n + 1 + \alpha_{i-1} - i\}$ constant

$$\nu_1(x_1) = -k_1 \lceil \sigma_1 \rfloor^{\frac{r_2}{n+\alpha_1}} = -k_1 \lceil x_1 \rfloor^{\frac{n-1}{n}}$$

$$\nu_i(x_i) = -k_i \lceil \sigma_i(\bar{x}_i) \rfloor^{\frac{r_{i+1}}{n+\alpha_i}}$$

$$\sigma_1(x_1) = \lceil x_1 \rfloor^{\frac{n+\alpha_1}{n}}, ..., \sigma_i(\bar{x}_i) = \lceil x_i \rfloor^{\frac{p+\alpha_i}{n-i+1}} - k_{i-1}^{\frac{n+\alpha_i}{n-1+1}} \lceil \sigma_{i-1}(\bar{x}_{i-1}) \rfloor^{\frac{p+\alpha_i}{n+\alpha_{i-1}}}$$

Adaptive Extension

System

$$\dot{x}_1 = x_2$$

$$\dot{x}_2 = \Delta(t, x_1, x_2) + \Theta^{\mathrm{T}}\,\omega(t, x) + u$$

$$x_1(0) = x_{0,1}, \qquad x_2(0) = x_{0,2},$$

- $x_1, x_2, u \in \mathbb{R}$, $x = (x_1, x_2)^{\mathrm{T}}$
- unknown constant $\Theta \in \mathbb{R}^p$
- known Regressor $\omega(t, x) : \mathbb{R} \times \mathbb{R}^n \to \mathbb{R}^p$
- disturbance $|\Delta(t, x_1, x_2)| \leq C$

New Control Law

$$u = -k_2 \operatorname{sign}\left(\lceil x_2 \rfloor^{2+\alpha} + k_1 \lceil x_1 \rfloor^{\frac{2+\alpha}{2}} \right) - \hat{\Theta}^{\mathrm{T}}\,\omega(t, x)$$

- constant $k_1, k_2, \alpha > 0$
- Parameter Estimation $\hat{\Theta} \in \mathbb{R}^p$

Adaptation Law

Extended Lyapunov Function

$$V_{\mathrm{ext}}(x, \tilde{\Theta}) = V(x) + \frac{1}{2\,\Gamma}\tilde{\Theta}^{\mathrm{T}}\tilde{\Theta}$$

- $\Gamma \in \mathbb{R} : \Gamma > 0$
- estimation error $\tilde{\Theta} := \Theta - \hat{\Theta}$

Derivation of Lyapunov Function

$$\begin{aligned} \dot{V}_{\mathrm{ext}} &= \dot{V}(x) + (\Theta^{\mathrm{T}} - \hat{\Theta}^{\mathrm{T}})\,\omega(t,x)\,s_{2,d}(x) + \frac{1}{\Gamma}\tilde{\Theta}^{\mathrm{T}}\,\dot{\tilde{\Theta}} \\ &= \dot{V}(x) + \tilde{\Theta}^{\mathrm{T}}\,\omega(t,x)\,s_{2,d}(x) - \frac{1}{\Gamma}\tilde{\Theta}^{\mathrm{T}}\,\dot{\hat{\Theta}} \end{aligned}$$

- Note that: $\dot{\tilde{\Theta}} = \dot{\Theta} - \dot{\hat{\Theta}} = -\dot{\hat{\Theta}}$
- Adapation Law $\dot{\hat{\Theta}} = \Gamma\,\omega(t,x)\,s_{2,d}(x)$ renders $\dot{V}_{\mathrm{ext}}$ neg. semi-definite
- No Parameter Convergence (error is bounded)

Simulation Results

System

$$\begin{aligned} \dot{x}_1 &= x_2 \\ \dot{x}_2 &= \Delta(t, x_1, x_2) + \Theta^{\mathrm{T}}\,\omega(t, x_1, x_2) + u \\ x_1(0) = 1, &\qquad x_2(0) = 1, \end{aligned}$$

- $\Theta = 4$ and $\omega(t, x_1, x_2) = x_1$
- $\Delta(t, x_1, x_2) = 2\,\sin(t)$

Control Law

- HOSM: $u_{\mathrm{hosm}} = -k_2\,\mathrm{sign}\left(\lceil x_2 \rfloor^{2+\alpha} + k_1\,\lceil x_1 \rfloor^{\frac{2+\alpha}{2}}\right)$
- AHOSM: $u_{\mathrm{ahosm}} = -k_2\,\mathrm{sign}\left(\lceil x_2 \rfloor^{2+\alpha} + k_1\,\lceil x_1 \rfloor^{\frac{2+\alpha}{2}}\right) - \hat{\Theta}^{\mathrm{T}}\,\omega(t,x)$
- Adaptation Law: $\dot{\hat{\Theta}} = \Gamma\,\omega(t,x)\,\left(\lceil x_2 \rfloor^{m-1} + k_1^{m-1}\lceil(x_1)\rfloor^{\frac{m-1}{2}}\right)$
- Parameter $k_1 = 2$, $k_2 = 5$, $\Gamma = 1, \alpha = 1$

Simulation Results

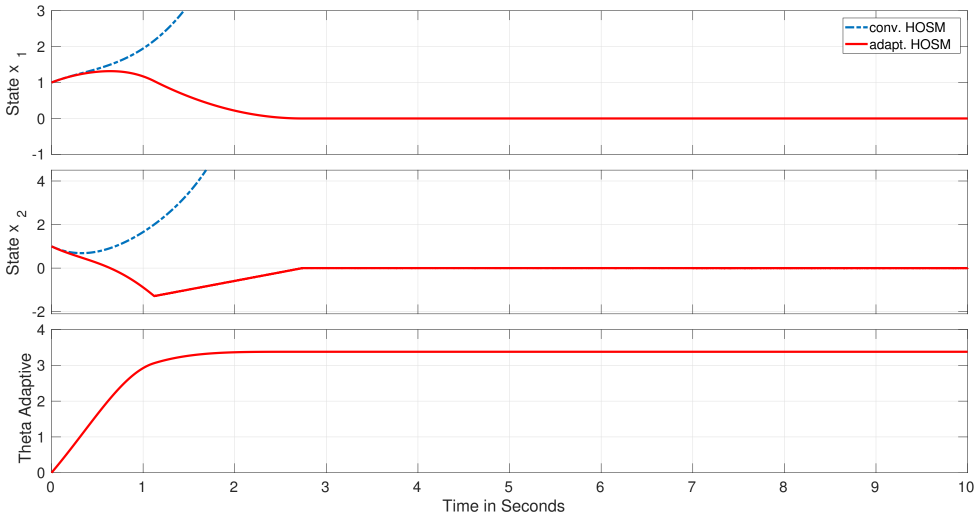

Conclusion

- robust, adaptive Controller handles disturbances, parametric uncertainties
- extended Class of uncertainty compared to conventional approaches
- Design via Lyapunov Function

Outlook

- Adaptive Output Feedback
- Parameter Convergence Properties

Barth, A., Reichhartinger, M., Reger, J., Horn, M., and Wulff, K. (2015).
Lyapunov-design for a super-twisting sliding-mode controller using the certainty-equivalence principle.
In *1st IFAC MICNON*, pages 860–865.

Barth, A., Reichhartinger, M., Reger, J., Horn, M., and Wulff, K. (2016).
Certainty-equivalence based super-twisting control using continuous adaptation laws.
In *14th IEEE VSS*, pages 92–97.

Barth, A., Reichhartinger, M., Wulff, K., Reger, J., Koch, S., and Horn, M. (2017).
Indirect adaptive sliding-mode control using the certainty-equivalence principle.
In Li, S., Yu, X., Friedman, L., Man, Z., and Wang, X., editors, *Advances in Variable Structure Systems and Sliding Mode Control – Theory and Applications*, volume 115 of *Studies in Systems, Decision and Control*, pages 165–191. Springer International Publishing.

Filippov, A. F. (1988).
Differential equations with discontinuous righthand sides.
Mathematics and its applications. Kluwer Academic Publ, Dordrecht.

Hardy, G., Littlewood, J., and Pólya, G. (1952).
Inequalities.
Cambridge Mathematical Library. Cambridge University Press.

Levant, A. (2005).
Homogeneity approach to high-order sliding mode design.
Automatica, 41(5):823 – 830.

Moreno, J. A. (2017).
Lyapunov-based design of homogeneous high-order sliding modes.
In Li, S., Yu, X., Friedman, L., Man, Z., and Wang, X., editors, *Advances in Variable Structure Systems and Sliding Mode Control – Theory and Applications*, volume 115 of *Studies in Systems, Decision and Control*, pages 3–38. Springer International Publishing.

Zubov, V. I. (1964).
Methods of A.M. Lyapunov and their application.
Groningen : P. Noordhoff.

Design of Saturated Sliding Mode Control with Continuous Actuating Signal

Mohammad Ali Golkani[a] **Markus Reichhartinger**[a] **Martin Horn**[a]

Having applied a sliding mode control scheme, a closed-loop's satisfactory robust performance is achieved despite the presence of a particular class of plant uncertainties and external disturbances. Conventional sliding mode control, i.e. first-order sliding mode approach, guarantees a saturated and discontinuous control input. Second-order sliding mode techniques such as the twisting as well as super-twisting algorithms provide absolutely continuous control signals in the case that the relative degree of the system with respect to a defined sliding function is one [3]. Furthermore, the continuous twisting controller introduces a continuous actuating signal if this relative degree is two [4]. In general, these high-order sliding mode algorithms improving the sliding accuracy of the standard sliding mode are able to counteract perturbations, which are Lipschitz continuous, and recorded in the literature as the chattering attenuation strategies. However, for systems with saturating actuators, it is difficult to tune the aforementioned controllers such that the control inputs do not exceed given saturation bounds. Moreover, in the case that a state variable is not measurable and therefore a high-order sliding mode observer is also applied, fairly restrictive assumptions need to be made. It is revealed exemplarily in this presentation that the super-twisting controller based on the high-order sliding mode observer, which is considered in [1] to implement the control system with a mathematical justification, cannot be employed in some scenarios.

This talk presents a twisting-based control law, in which estimate information provided by a second-order robust exact differentiator is incorporated [2]. The class of uncertainties and disturbances dealt with here is much larger than in [1]. It is shown that the actuating signal is Lipschitz continuous and its absolute value is bounded by a known constant. Results of further investigations, which have been conducted into how other algorithms can be adopted in order to introduce saturated signals, are discussed.

[1] A. Chalanga, S. Kamal, L. M. Fridman, B. Bandyopadhyay, and J. A. Moreno. Implementation of super-twisting control: Super-twisting and higher order sliding-mode observer-based approaches. *IEEE Transactions on Industrial Electronics*, 63(6):3677–3685, June 2016.

[2] M. A. Golkani, L. Fridman, S. Koch, M. Reichhartinger, and M. Horn. Observer-based saturated output feedback control using twisting algorithm. In *14th International Workshop on Variable Structure Systems (VSS)*, pages 246–250, June 2016.

[3] Yuri Shtessel, Christopher Edwards, Leonid Fridman, and Arie Levant. *Sliding mode control and observation*. Springer, 2014.

[a]Institute of Automation and Control, Graz University of Technology, Inffeldgasse 21b/I, 8010 Graz, Austria, E-mail: `golkani@tugraz.at`, `markus.reichhartinger@tugraz.at`, `martin.horn@tugraz.at`

[4] V. Torres-González, L. M. Fridman, and J. A. Moreno. Continuous twisting algorithm. In *54th IEEE Conference on Decision and Control (CDC)*, pages 5397–5401, Dec 2015.

Design of Saturated Sliding Mode Control with Continuous Actuating Signal

Mohammad Ali Golkani, Institute of Automation and Control

Retzhof, 13. Sept. 2017

www.irt.tugraz.at

Outline

1. Saturated Super-twisting Algorithm
2. Observer-based Saturated Control
   – Control Strategy Using Twisting Algorithm
3. Saturated Continuous Twisting Algorithm
4. Summary
5. References

First-order system with disturbances

$$\frac{dx}{dt} = u + a(t) \tag{1}$$

- Assumptions:

$$|a(t)| \leq a_M \qquad \left|\frac{da}{dt}\right| \leq L_a$$

- It is aimed to design a control law such that
  - the system state drives to the origin in a finite time;
  - the control signal is absolutely continuous and saturated by

$$\sup|u| \leq \rho \quad \forall t$$

- First-order sliding mode approach guarantees a saturated and **discontinuous** actuating signal

$$u = -k\,\mathrm{sgn}(x) \qquad k > a_M \tag{2}$$

  - The precision is proportional to the sampling time τ ($O(\tau)$).

- Since the relative degree of the system is one, the super-twisting algorithm can be employed to introduce a continuous control signal

$$u = -k_1|x|^{1/2}\,\mathrm{sgn}(x) + \nu \qquad k_1 > 0 \tag{3a}$$

$$\frac{d\nu}{dt} = -k_2\,\mathrm{sgn}(x) \qquad k_2 > 3L_a + 2\left(\frac{L_a}{k_1}\right)^2 \tag{3b}$$

  - The sliding accuracy is improved by $O(\tau^2)$, i.e.
$\exists T(x_0): \sup_{t\in[T(x_0),\infty)} |x| \leq \gamma\tau^2$

- The conventional super-twisting algorithm **cannot guarantee** that the absolute value of control input *u* is bounded by ρ

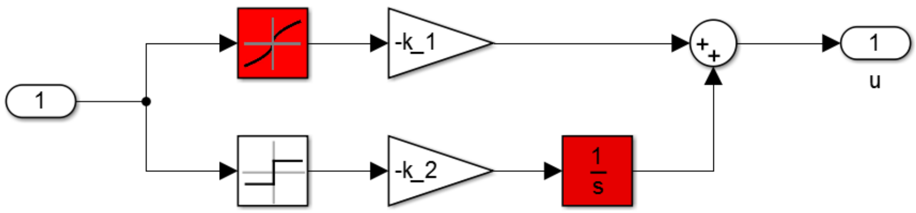

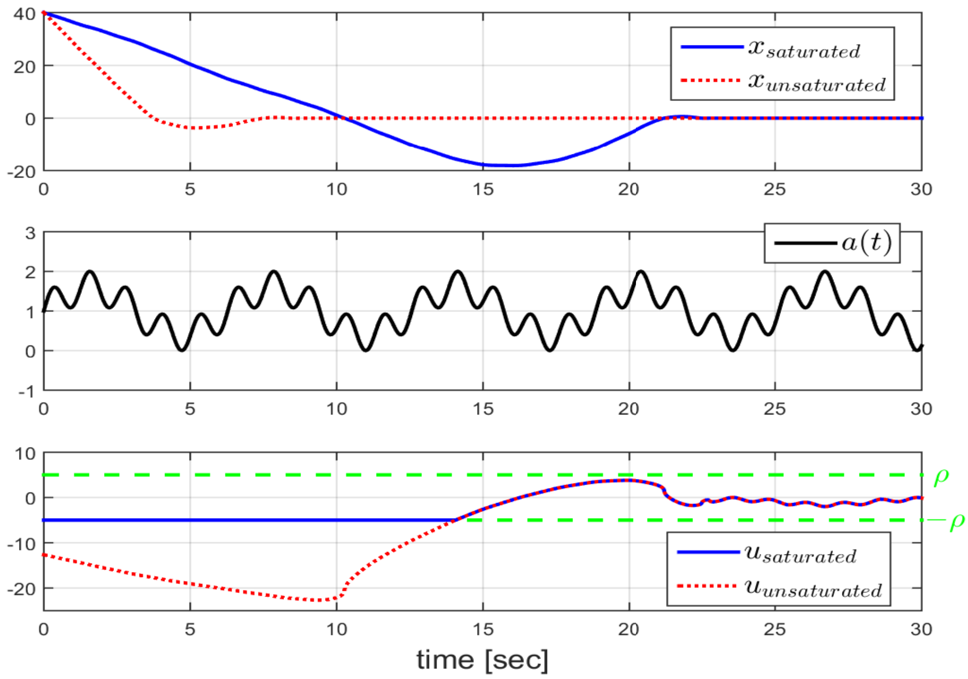

Saturated super-twisting control law

$$u = -k_1 \operatorname{sat}_\epsilon \left\{ |x|^{1/2} \operatorname{sgn}(x) \right\} + \nu \tag{4a}$$

$$\frac{d\nu}{dt} = -k_2 \operatorname{sgn}(x) - k_3 \nu \tag{4b}$$

where

$$\operatorname{sat}_\epsilon \left\{ |x|^{1/2} \operatorname{sgn}(x) \right\} = \begin{cases} |x|^{1/2} \operatorname{sgn}(x) & \text{for } |x|^{1/2} < \epsilon \\ \epsilon \operatorname{sgn}(x) & \text{for } |x|^{1/2} \geq \epsilon \end{cases}$$

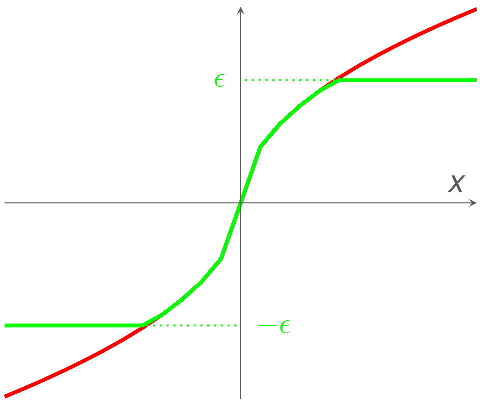

Saturated Super-twisting Algorithm

Saturated super-twisting control law

$$u = -k_1 \operatorname{sat}_\epsilon \left\{ |x|^{1/2} \operatorname{sgn}(x) \right\} + \nu \tag{4a}$$

$$\frac{d\nu}{dt} = -k_2 \operatorname{sgn}(x) - k_3 \nu \tag{4b}$$

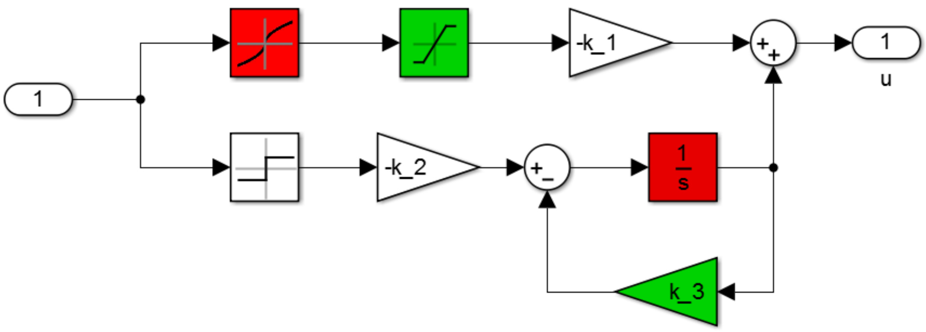

Mohammad Ali Golkani, Institute of Automation and Control
Retzhof, 13. Sept. 2017

Saturated super-twisting control law

$$u = -k_1 \,\mathrm{sat}_\epsilon \left\{|x|^{1/2}\mathrm{sgn}(x)\right\} + \nu \tag{4a}$$

$$\frac{d\nu}{dt} = -k_2\mathrm{sgn}(x) - k_3\nu \tag{4b}$$

- It becomes evident

$$\|\nu\|_\infty \le \nu_M = \frac{k_2}{k_3}$$

where ν_0 is selected such that $|\nu_0| \le \nu_M$ holds.

- Therefore, for any initial condition $x_0 \in \mathbb{R}$, the continuous control signal is bounded by

$$|u| \le k_1\epsilon + \frac{k_2}{k_3}$$

- The accuracy level is the same as the conventional super-twisting ($O(\tau^2)$).

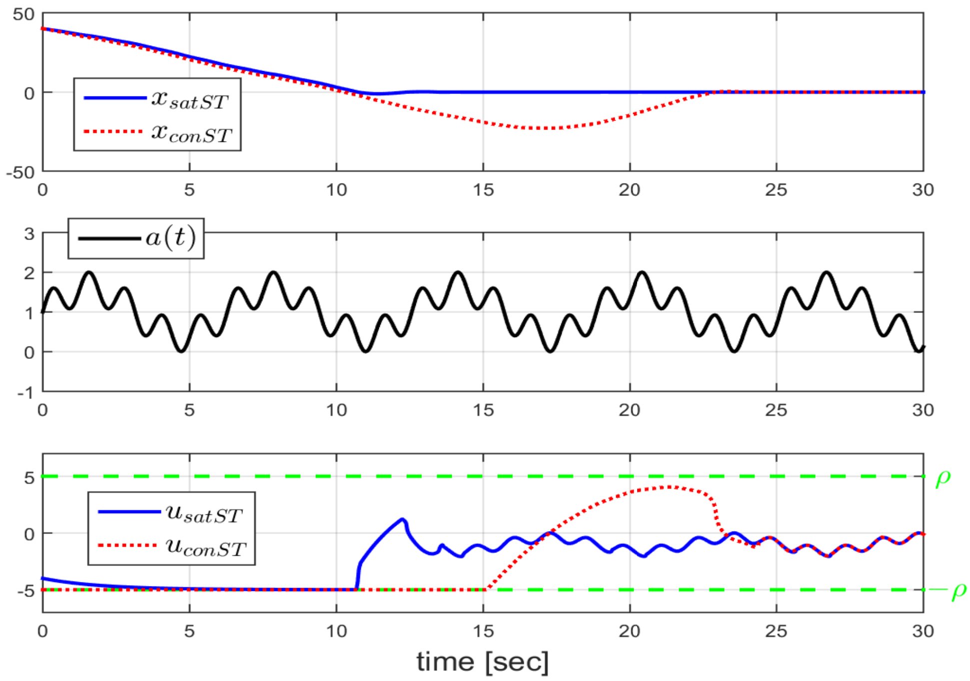

Stability analysis of conventional super-twisting

$$\frac{dx_1}{dt} = -k_1|x_1|^{1/2}\operatorname{sgn}(x_1) + x_2 \tag{5a}$$
$$\frac{dx_2}{dt} = -k_2\operatorname{sgn}(x_1) + \phi(t) \tag{5b}$$

where $\tilde{\boldsymbol{x}} = \begin{bmatrix} x_1 & x_2 \end{bmatrix}^{\mathrm{T}} = \begin{bmatrix} x & \nu + a(t) \end{bmatrix}^{\mathrm{T}}$ and $\phi(t) = \frac{da}{dt}$

- The quadratic Lyapunov functions $V = \zeta^{\mathrm{T}}\boldsymbol{P}\zeta$ are proposed in the literature [Moreno and Osorio(2012)] considering

$$\zeta = \begin{bmatrix} \zeta_1 & \zeta_2 \end{bmatrix}^{\mathrm{T}} = \begin{bmatrix} |x_1|^{1/2}\operatorname{sgn}(x_1) & x_2 \end{bmatrix}^{\mathrm{T}}$$

  - For instance, in the unperturbed case, it is possible to compute constant matrices for the Algebraic Lyapunov Equation $\boldsymbol{A}^{\mathrm{T}}\boldsymbol{P} + \boldsymbol{P}\boldsymbol{A} = -\boldsymbol{Q}$, where

$$\frac{d\zeta}{dt} = \frac{1}{|x_1|^{1/2}}\underbrace{\begin{bmatrix} -k_1/2 & 1/2 \\ -k_2 & 0 \end{bmatrix}}_{\boldsymbol{A}}\zeta \qquad k_1 > 0 \qquad k_2 > 0$$

Stability analysis of saturated super-twisting

$$\frac{dx_1}{dt} = -k_1\operatorname{sat}_\epsilon\left\{|x_1|^{1/2}\operatorname{sgn}(x_1)\right\} + x_2 \tag{6a}$$
$$\frac{dx_2}{dt} = -k_2\operatorname{sgn}(x_1) - k_3x_2 + \phi(t) \tag{6b}$$

where $\tilde{\boldsymbol{x}} = \begin{bmatrix} x_1 & x_2 \end{bmatrix}^{\mathrm{T}} = \begin{bmatrix} x & \nu + a(t) \end{bmatrix}^{\mathrm{T}}$ and perturbations $\phi(t) = k_3a(t) + \frac{da}{dt}$ are bounded by

$$\left|\phi(t)\right| \leq \phi_M = k_3a_M + L_a$$

Remark

Since the sat function and the linear term $-k_3x_2$ are incorporated into the closed-loop dynamics, matrix $\boldsymbol{A}$ is not constant any more and therefore the Algebraic Lyapunov Equation cannot be applied.

Proposition

In the nominal case, i.e. $\phi(t) = 0$, the origin $\tilde{\boldsymbol{x}} = \mathbf{0}$ is globally finite-time stable if

$$k_1 > 0 \qquad \epsilon > 0$$
$$k_3 > 0 \qquad k_2 > 0$$

- A proof can be provided introducing a strict and Lipschitz Lyapunov function candidate as

$$V_n = |x_1| + \frac{1}{2k_2}x_2^2 \tag{7}$$

  - It is shown that the globally negative definiteness of $\dfrac{dV_n}{dt}$ is ensured by the positive control parameters.

Proposition

For the closed-loop system in the presence of disturbances ($\phi(t) \neq 0$), the variables x_1 and x_2 tend to zero in a finite time if

$$k_1 > 0 \qquad k_2 > 4\phi_M + \frac{9\phi_M^2}{2k_1^2} + \frac{k_1^2}{2}$$
$$k_3 > 0 \qquad \epsilon > \frac{k_2}{k_3^2} + \frac{2k_2}{6k_2 + k_1^2}$$

- In order to give the proof, two quadratic functions are incorporated into the Lyapunov function

$$V_d = \zeta^{\mathrm{T}}\boldsymbol{P}\zeta + \tilde{\boldsymbol{x}}^{\mathrm{T}}\tilde{\boldsymbol{P}}\tilde{\boldsymbol{x}}$$

$$\boldsymbol{P} = \frac{1}{2}\begin{bmatrix} 6k_2 + k_1^2 & -k_1 \\ -k_1 & 1 \end{bmatrix} \qquad \tilde{\boldsymbol{P}} = \frac{1}{2}\begin{bmatrix} k_3^2 & k_3 \\ k_3 & 2 \end{bmatrix} \tag{8}$$

where $\tilde{\boldsymbol{x}} = \begin{bmatrix} x & \nu + a(t) \end{bmatrix}^{\mathrm{T}}$ and $\zeta = \begin{bmatrix} |x_1|^{1/2}\operatorname{sgn}(x_1) & x_2 \end{bmatrix}^{\mathrm{T}}$

Perturbed second-order system

$$\frac{dx_1}{dt} = x_2 \quad (9a)$$
$$\frac{dx_2}{dt} = u + a(t) \quad (9b)$$
$$y = x_1 \quad (9c)$$

- Assumptions:
  - $|a(t)|$ is bounded by a_M and it is Lipschitz continuous with L_a.
  - System output y is just measurable.
- It is aimed to design an observer-based control law such that
  - an asymptotic convergence of the system states to zero is achieved;
  - the actuating signal is continuous and its absolute value is bounded by ρ.

State observer using high-order sliding mode algorithm

$$e_1 = x_1 - \tilde{x}_1 \quad (10a)$$
$$\frac{d\tilde{x}_1}{dt} = \mu_1 |e_1|^{2/3} \operatorname{sgn}(e_1) + \hat{x}_2 \quad (10b)$$
$$\frac{d\hat{x}_2}{dt} = u + \mu_2 |e_1|^{1/3} \operatorname{sgn}(e_1) + \tilde{x}_2 \quad (10c)$$
$$\frac{d\tilde{x}_2}{dt} = \mu_3 \operatorname{sgn}(e_1) \quad (10d)$$

- $\hat{x}_2$ and $\tilde{x}_2$ start tracking x_2 and $a(t)$ in a finite time if the observer is tuned suitably.

Remark

*This observer is considered in the literature to implement a **super-twisting** controller with a mathematical justification [Chalanga et al.(2016)]. However, estimates information obtained through it might be exploited to build up a controller using the **twisting** algorithm.*

- The saturated super-twisting algorithm is not helpful any more

$$u = -\left(\boxed{\lambda \hat{x}_2} + k_1 \mathrm{sat}_\epsilon \left\{ |\sigma|^{1/2} \mathrm{sgn}(\sigma) \right\} - \nu \right) \tag{11a}$$

$$\frac{d\nu}{dt} = -\left(k_2 \mathrm{sgn}(\sigma) + \mu_3 \mathrm{sgn}(e_1) + k_3 \nu \right) \tag{11b}$$

where

$$\sigma = \hat{x}_2 + \lambda x_1$$

- Suppose that $k_1 \epsilon + \frac{k_2 + \mu_3}{k_3} \leq \rho$ is satisfied, it **cannot** be concluded that $u \in [-\rho, \rho] \ \ \forall x_0 \in \mathbb{R}$.

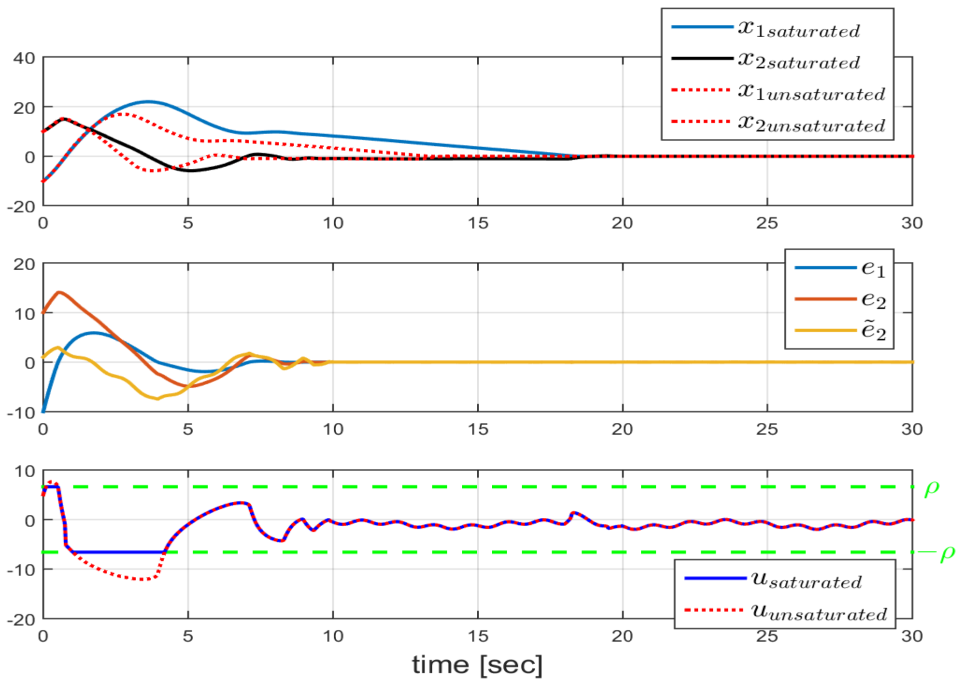

- The twisting algorithm can guarantee a saturated and **discontinuous** control signal for the system of relative degree two

$$u = -k\left(\operatorname{sgn}(x_1) + \frac{1}{2}\operatorname{sgn}(\hat{x}_2)\right) \qquad k > 2a_M \tag{12}$$

  - The accuracy level of output y is $(O(\tau^2))$.

- However, a Lipschitz continuous actuating signal can be introduced if the relative degree of the system with respect to a defined sliding function, e.g. $\sigma_1 = \hat{x}_2 + \lambda x_1$, is one.

  - The asymptotic stability of the system states is implied.

Proposed control law adopting twisting algorithm

$$\frac{du}{dt} = -\left[k\left(\operatorname{sgn}(\sigma_1) + \frac{1}{2}\operatorname{sgn}(\sigma_2)\right) + \mu_3\operatorname{sgn}(e_1) + \lambda u\right] \tag{13}$$

where

$$\sigma_1 = \hat{x}_2 + \lambda x_1 \qquad \sigma_2 = u + \tilde{x}_2 + \lambda\hat{x}_2$$

Remark

This contributes significantly to avoidance of two dangerous chattering classes known as bounded and unbounded [Levant(2010)].

Proposed control law adopting twisting algorithm

$$\frac{du}{dt} = -\left[k\left(\operatorname{sgn}(\sigma_1) + \frac{1}{2}\operatorname{sgn}(\sigma_2)\right) + \mu_3 \operatorname{sgn}(e_1) + \lambda u\right] \qquad (13)$$

where

$$\sigma_1 = \hat{x}_2 + \lambda x_1 \qquad \sigma_2 = u + \tilde{x}_2 + \lambda \hat{x}_2$$

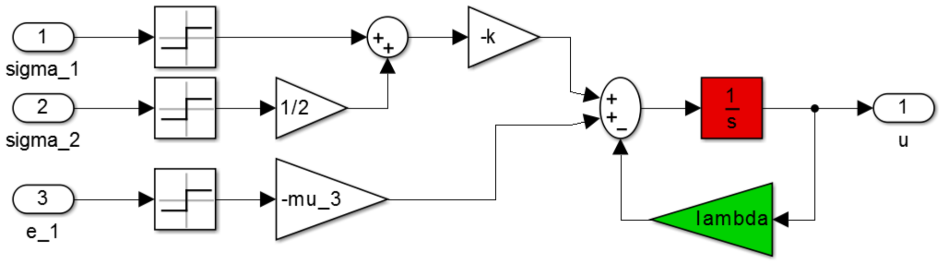

Proposed control law adopting twisting algorithm

$$\frac{du}{dt} = -\left[k\left(\operatorname{sgn}(\sigma_1) + \frac{1}{2}\operatorname{sgn}(\sigma_2)\right) + \mu_3 \operatorname{sgn}(e_1) + \lambda u\right] \qquad (13)$$

where

$$\sigma_1 = \hat{x}_2 + \lambda x_1 \qquad \sigma_2 = u + \tilde{x}_2 + \lambda \hat{x}_2$$

- The control signal and its time derivative are bounded by

$$\|u\|_\infty \le u_M = \frac{3k + 2\mu_3}{2\lambda}$$

$$\left|\frac{du}{dt}\right| \le \frac{3k}{2} + \mu_3 + \lambda u_M = 2\lambda u_M$$

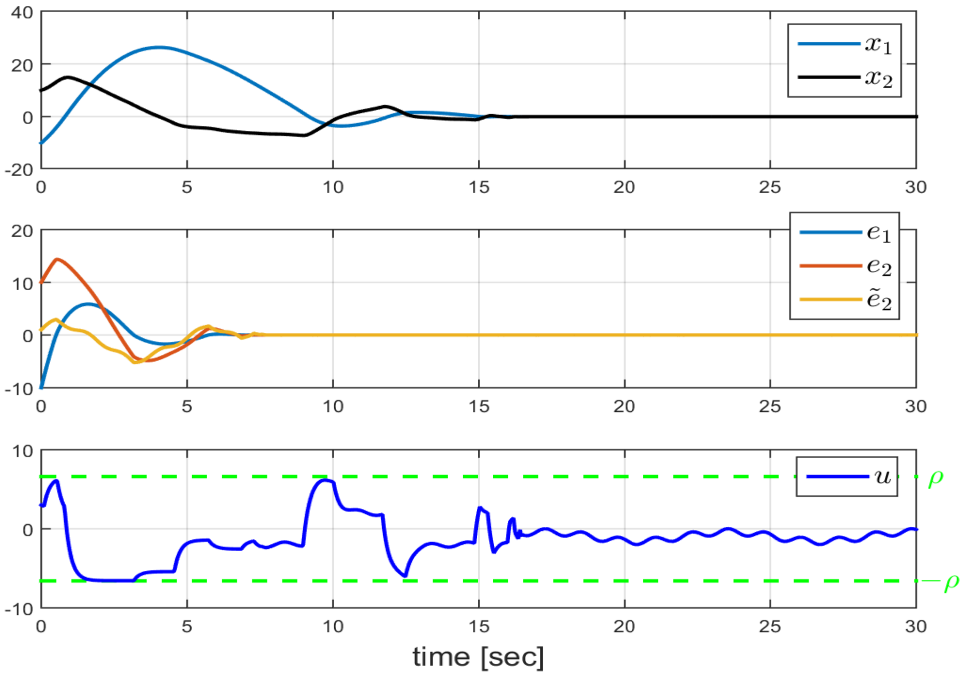

- Introducing $e_2 = x_2 - \hat{x}_2$ and $\tilde{e}_2 = a - \tilde{x}_2$ gives the closed-loop

$$\frac{d\sigma_1}{dt} = \sigma_2 + \mu_2 |e_1|^{1/3} \operatorname{sgn}(e_1) + \lambda e_2 \tag{15a}$$

$$\begin{aligned} \frac{d\sigma_2}{dt} &= -k\left(\operatorname{sgn}(\sigma_1) + \frac{1}{2}\operatorname{sgn}(\sigma_2)\right) \\ &\quad + \lambda\left(\mu_2 |e_1|^{1/3} \operatorname{sgn}(e_1) - \tilde{e}_2 + a\right) \end{aligned} \tag{15b}$$

$$\boxed{\begin{aligned} \frac{de_1}{dt} &= -\mu_1 |e_1|^{2/3} \operatorname{sgn}(e_1) + e_2 && (15c) \\ \frac{de_2}{dt} &= -\mu_2 |e_1|^{1/3} \operatorname{sgn}(e_1) + \tilde{e}_2 && (15d) \\ \frac{d\tilde{e}_2}{dt} &= -\mu_3 \operatorname{sgn}(e_1) + \frac{da}{dt} && (15e) \end{aligned}}$$

  - The driving subsystem is globally asymptotically stable if the observer gains are chosen appropriately.

- Introducing $e_2 = x_2 - \hat{x}_2$ and $\tilde{e}_2 = a - \tilde{x}_2$ gives the closed-loop

$$\boxed{\begin{aligned} \frac{d\sigma_1}{dt} &= \sigma_2 + \mu_2 |e_1|^{1/3} \operatorname{sgn}(e_1) + \lambda e_2 && (15a)\\ \frac{d\sigma_2}{dt} &= -k\left(\operatorname{sgn}(\sigma_1) + \frac{1}{2}\operatorname{sgn}(\sigma_2)\right) \\ &\quad + \lambda\left(\mu_2 |e_1|^{1/3}\operatorname{sgn}(e_1) - \tilde{e}_2 + a\right) && (15b)\end{aligned}}$$

$$\frac{de_1}{dt} = -\mu_1 |e_1|^{2/3}\operatorname{sgn}(e_1) + e_2 \qquad (15c)$$

$$\frac{de_2}{dt} = -\mu_2 |e_1|^{1/3}\operatorname{sgn}(e_1) + \tilde{e}_2 \qquad (15d)$$

$$\frac{d\tilde{e}_2}{dt} = -\mu_3 \operatorname{sgn}(e_1) + \frac{da}{dt} \qquad (15e)$$

- The stability of the driven subsystem is based on integral input-to-state stability.

Proposition

For the aforementioned closed-loop system, a finite time convergence of e_1, e_2, and $\tilde{e}_2$ to zero is achieved and the system states tend to zero asymptotically if positive gains μ_1 and μ_2 are selected large enough, and

$$\mu_3 > L_a$$
$$\lambda > 0 \qquad k > 2\lambda a_M$$

- The continuous twisting algorithm [Torres-González et al.(2017)] also provides a continuous control input for the aforementioned second-order system

$$u = -k_1|x_1|^{1/3}\operatorname{sgn}(x_1) - k_2|\hat{x}_2|^{1/2}\operatorname{sgn}(\hat{x}_2) + \nu \tag{16a}$$

$$\frac{d\nu}{dt} = -k_3\operatorname{sgn}(x_1) \tag{16b}$$

  - The system states drive to zero in a finite time and the accuracy level of output y is improved by ($O(\tau^3)$).

Remark

Considering a separation principle, it is shown that the first-order robust exact differentiator (RED) can be also employed to design the observer.

Saturated continuous twisting control law

$$u = -k_1\,\mathrm{sat}_{\epsilon_1}\left\{|x_1|^{1/3}\operatorname{sgn}(x_1)\right\} - k_2\,\mathrm{sat}_{\epsilon_2}\left\{|\hat{x}_2|^{1/2}\operatorname{sgn}(\hat{x}_2)\right\} + \nu \tag{17a}$$

$$\frac{d\nu}{dt} = -k_3\operatorname{sgn}(x_1) - k_4\nu \tag{17b}$$

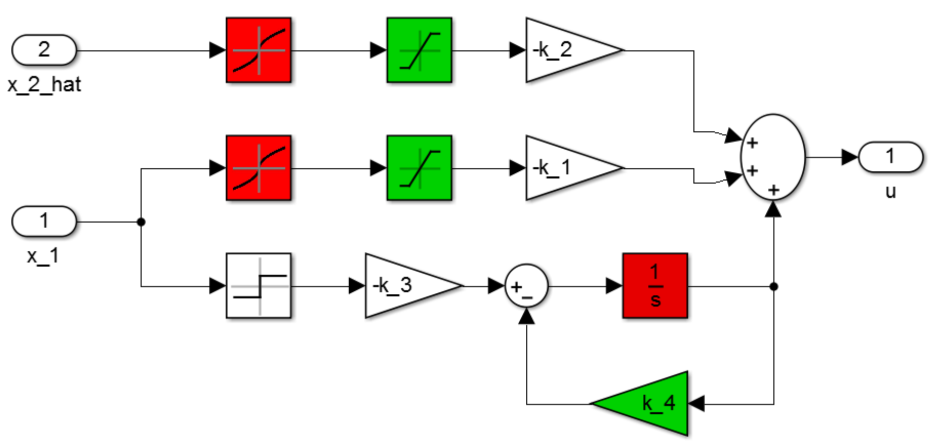

23

Saturated continuous twisting control law

$$u = -k_1 \,\mathrm{sat}_{\epsilon_1}\left\{|x_1|^{1/3}\,\mathrm{sgn}(x_1)\right\} - k_2\,\mathrm{sat}_{\epsilon_2}\left\{|\hat{x}_2|^{1/2}\,\mathrm{sgn}(\hat{x}_2)\right\} + \nu \tag{17a}$$

$$\frac{d\nu}{dt} = -k_3\mathrm{sgn}(x_1) - k_4\nu \tag{17b}$$

- For any initial condition, it becomes evident

$$|u| \leq k_1\epsilon_1 + k_2\epsilon_2 + \frac{k_3}{k_4}$$

24

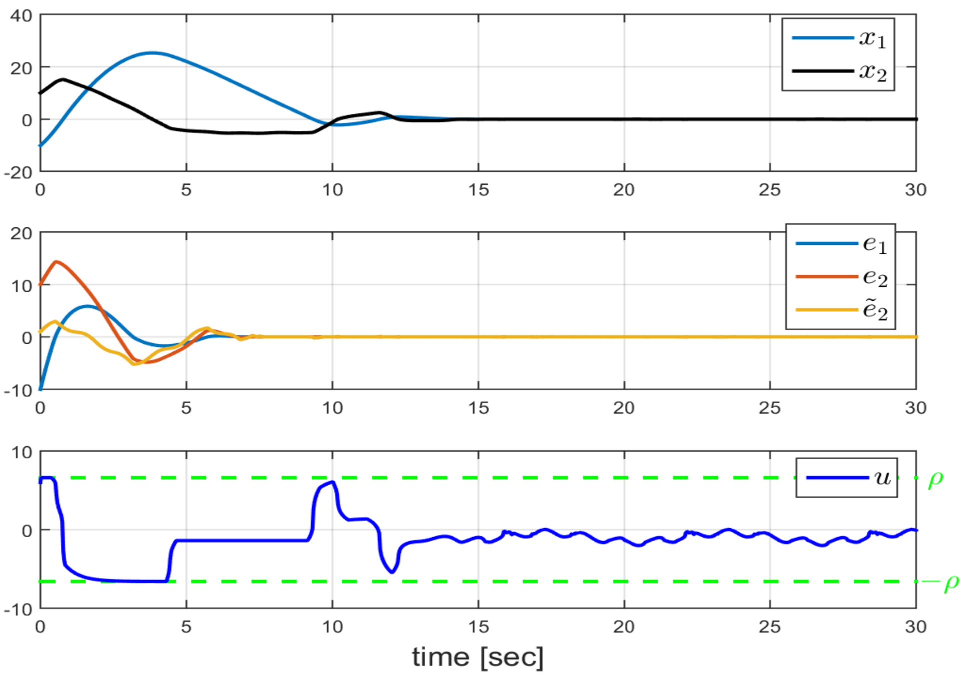

Summary

IRT 25

- Saturated super-twisting control in the case that the relative degree of the system is one.
- An observer-based output feedback control technique for the perturbed system of relative degree two.
- High-order RED is adopted to the observer and the control law is developed using the twisting algorithm.
- The twisting algorithm can be replaced with the continuous twisting one.

Outlook

- Systems of higher relative degree are going to be taken into account.

Mohammad Ali Golkani, Institute of Automation and Control
Retzhof, 13. Sept. 2017

References

IRT 26

A. Chalanga, S. Kamal, L. M. Fridman, B. Bandyopadhyay, and J. A. Moreno, “Implementation of super-twisting control: Super-twisting and higher order sliding-mode observer-based approaches,” IEEE Transactions on Industrial Electronics, vol. 63, no. 6, pp. 3677–3685, June 2016.

M. A. Golkani, L. Fridman, S. Koch, M. Reichhartinger, and M. Horn, “Observer-based saturated output feedback control using twisting algorithm,” in 14th International Workshop on Variable Structure Systems (VSS), June 2016, pp. 246–250.

A. Levant, “Chattering analysis,” Automatic Control, IEEE Transactions on, vol. 55, no. 6, pp. 1380–1389, 2010.

J. A. Moreno and M. Osorio, “Strict lyapunov functions for the super-twisting algorithm,” IEEE Transactions on Automatic Control, vol. 57, no. 4, pp. 1035–1040, April 2012.

Y. Shtessel, C. Edwards, L. Fridman, and A. Levant, Sliding mode control and observation. Springer, 2014.

V. Torres-González, T. Sanchez, L. M. Fridman, and J. A. Moreno, “Design of continuous twisting algorithm,” Automatica, vol. 80, pp. 119 – 126, 2017.

Mohammad Ali Golkani, Institute of Automation and Control
Retzhof, 13. Sept. 2017

A Check of Flatness for time continuous Systems by Computer Algebra Methods

Kurt Schlacher[a] **Markus Schöberl**[a]

Introduction

Since the late 80's of the last century a simple test for time continuous systems is known, whether one can derive an exact linear input to state behavior by static feedback. If this test is met, a system of linear PDEs or equivalently of nonlinear ODEs and a set of nonlinear equations must be solved to derive the linearizing feedback. For the class of systems, which allow a linear behavior by dynamic feedback, several approaches are known, but it is more challenging to derive a test without solving PDEs or nonlinear ODEs. In this contribution we propose a computer algebra approach, with does not require the solution of DEs.

An Old Result

Consider the locally reachable system

$$x_t^i = f^i(t, x, u) \ , \quad i = 1, \dots, n \tag{1}$$

with the vector field $f = \partial_t + f^i \partial_{x^i}$ and the involutive distribution $U = \mathrm{span}\left(\{\partial_{u^1}, \dots, \partial_{u^m}\}\right)$. The system is input to state linearizable by static feedback, iff together with

$$\begin{array}{rclcrcl} D_0 & = & U & \quad & D_k & = & D_{k-1} + [D_{k-1}, f] \\ D_1 & = & D_0 + [D_0, f] & & & \vdots & \\ & \vdots & & & D_{l+1} & = & D_l \end{array}$$

the distributions D_s, $s = 0, \dots, s-1$ are involutive and $\dim(D_l) = n + m$ is met.

Let us consider the first step of this test, where we use the shortcut $B = [U, f]$. Involutivity of D_1 implies $[U, B] \subset D_1$. This is equivalent to the existence of an input transformation $\bar{u} = g(t, x, u)$ to an AI system

$$x_t^i = a^i(t, x) + B_j^i(t, x)\, \bar{u}^j \ , \quad j = 1, \dots, m \ . \tag{2}$$

Involutivity of D_1 implies $[B, B] \subset D_1$, too. This is equivalent to the existence of a state transformation $\bar{x} = h(t, x)$ to an AI system

$$\bar{x}_t^i = a^i(t, x) + \bar{B}_{\bar{j}}^i a_j^{\bar{j}}(t, x)\, \bar{u}^j \ , \quad \bar{j} = 1, \dots, m \ , \tag{3}$$

[a]Institute of Automatic Control and Control Systems Technology, Johannes Kepler University Linz, Altenberger Strasse 69, 4040 Linz, Austria, E-mail: kurt.schlacher@jku.at

where the first $\bar{m} \leq m$ columns of $\left[\bar{B}^{i}_{\bar{j}}\right]$ are unit and the remaining are zero vectors. In addition $\left[a^{\bar{j}}_{j}\right]$ is invertible. Now the system (3) can easily been split into a trivial one and second one that needs further investigations. It is worth mentioning, that the tests here require differentiation and solving linear equations in the ring of e.g. smooth functions, whereas the transformations from (1) to (3) requires the solution of DEs and nonlinear equations. See e.g. [1] for one of the first publications in this topic.

The Dynamic Feedback Case

A necessary condition for a system like (1) to be flat is, one can transform it to a Partial Affine system, or PAI-system, like

$$x^{i}_{t} = a^{i}(t, x, v) + B^{i}_{\alpha_w}(t, x, v)\, w^{\alpha_w} \ . \tag{4}$$

Such an input transformation exists only, iff there exists an involutive distribution $W \subset U$ such that $[W, [W, f]] \subset [W, f] + W$ is met. W corresponds to the variables w_{α_w}, $\alpha_w = 1, \ldots, m_w$ and the involutive complement V, $U = W \oplus V$ to v_{α_v}, $\alpha_v = 1, \ldots, m_v$ with $m_w + m_v = m$. It is worth mentioning that the determination of W is already a non trivial task. To derive V one has to solve DEs and nonlinear equations, but its existence can be shown in a straightforward manner. With help of the distributions $B = \operatorname{span}\left(\left\{B^{i}_{\alpha_w}\partial_{x^i}\right\}\right)$, $\alpha_w = 1, \ldots, m_w$ and $V = \operatorname{span}\left(\left\{\partial_{v^{\alpha_v}}\right\}\right)$, $\alpha_v = 1, \ldots, m_v$ we get further cases.

- Let $[V, B] \subset B + V$ be met, them B has a basis independent on v. If B is involutive, we are back to the previous section, otherwise one has to construct an involutive distribution $\bar{B} \subset B$ and can partially follow the previous steps.
- If $\left[V, \bar{B}\right] \subset \bar{B} + V$ is met for $\bar{B} \subset B$, one applies the previous item to $\bar{B}$.
- Otherwise, we propose to prolong the system (4) in the following trivial manner:

$$\begin{aligned} x^{i}_{t} &= a^{i}(t, x, v) + B^{i}_{\alpha_w}(t, x, v)\, w^{\alpha_w} \\ v^{\alpha_v}_{t} &= v^{\alpha_v}_{1} \ , \end{aligned} \tag{5}$$

  It is shown in [2], how one derives flat outputs by help of the representation (5). But the proposed algorithm requires solving DEs and nonlinear equations.

In this contribution we present a computer algebra approach for a flatness test, which avoids solving DEs and nonlinear equations, whenever it is possible. This is an significant extension of [2]. The algorithms are implemented in the computer algebra System Maple 2016.

[1] Jakubczyk B. and Respondek W.: On linearization of control systems. Bull. Acad. Polonaise Sci., Ser. Sci. Math., 28:517–522, 1980.

[2] Schlacher K., Schöberl M., Kolar B.: A Jet Space Approach to Derive Flat Outputs, Proceedings Modelling, Identification and Control of Nonlinear Systems - 1st MICNON 2015.

A CHECK OF FLATNESS FOR TIME CONTINUOUS SYSTEMS BY COMPUTER ALGEBRA METHODS

K. Schlacher,* M. Schöberl

* Institute of Automatic Control and Control Systems Technology

Johannes Kepler University Linz

20th Styrian Workshop on Automatic Control, September 11 – 13, Schloss Retzhof, Austria

JOHANNES KEPLER UNIVERSITY LINZ

Outlook

A SHORT MOTIVATION

A Very Simple Example

Let us consider the trivial example

$$x_t = x + u^1 + u^2 \ .$$

By help of the input transform

$$\bar{u}^1 = u^1 + u^2 \ , \qquad \bar{u}^2 = u^1 - u^2$$

we get

$$x_t = x + \bar{u}^1 \ ,$$

where $\bar{u}^2$ does not affect the system. We call it a symmetry.

Elimination of the non derivative variable $\bar{u}^1$ leads to the empty system with the additional symmetry x.

With the flat outputs

$$y^1 = x \ , \qquad y^2 = \bar{u}^2$$

one derives

$$x = y^1 \ , \qquad \bar{u}^1 = -y^1 + y^1_1 \ , \qquad y^2 = \bar{u}^2$$

the required parametrization.

JKU

The SISO Case

Let us consider the simple reachable system

$$x_t = Ax + bu$$

together with the transformation

$$\bar{x} = Tx\ , \qquad T = \begin{bmatrix} b^{\perp} \\ b_c^{\perp} \end{bmatrix}\ , \qquad T^{-1} = \begin{bmatrix} b_c & b \end{bmatrix}$$

to

$$\bar{x}_t = TAT^{-1}\bar{x} + e_n u\ .$$

With the projection P to the first $n-1$ components we get

$$\bar{x}_t = TAT^{-1}P\bar{x} + TAb\bar{x}^n + e_n u$$

and

$$P\bar{x}_t = PTAT^{-1}P\bar{x} + PTAb\bar{x}^n$$

after elimination of u. Now we repeat the procedure.

JKU

Controller Design and MIMO Systems

Remark: All input vectors are images of $b, Ab, \ldots, A^{n-2}b$. In the last system before reaching the empty system we get $A^{n-1}b$, which corresponds to a symmetry. The flat output follows from

$$y = cx\ , \qquad c\begin{bmatrix} b & \cdots & A^{n-1}b \end{bmatrix} = e_n^T$$

and a state controller can be derived from

$$\alpha_o y_0 + \cdots + \alpha_{n-1}y_{n-1} + y_n = \alpha_o cx + \cdots \alpha_{n-1}cA^{n-1}x + cA^n x + u = 0\ .$$

In the MIMO case some symmetries may appear before the last step. Let us consider the case of two inputs with the sequences

$$\Delta = b_1, \ldots, A^{n_1-1}b_1\ , \qquad \Lambda = b_2, \ldots, A^{n_2-1}b_2$$

such that with $n_1 > n_2$, $n_1 + n_2 = n$ the set $\{\Delta, \Lambda\}$ forms a basis of $\mathbb{R}^n$ and $A^{n_2}b_2 \in \operatorname{span}\left(\{b_1, \ldots, A^{n_2}b_1, \Lambda\}\right)$ is met.

JKU

MIMO Systems

A choice of flat outputs y^1, y^2 follows from the relations

$$y^1 = c^1 x\ , \qquad c^1\,[\Delta, \Lambda] = e_{n_2}^T\ , \qquad\qquad y^2 = c^2 x\ , \qquad c^2\,[\Delta, \Lambda] = e_n^T$$

and the state controller is given by

$$\alpha_o^1 y_0^i + \cdots + \alpha_{n_i-1}^i y_{n_i-1}^i + y_{n_1} = \alpha_o^i c^i x + \cdots \alpha_{n_i-1}^i c^i A^{n_i-1} x + c^i A^{n_i} x + u^i = 0$$

with $i = 1, 2$.

The characteristic polynomial of the controlled system follows as $\left(\alpha_0^1 + \cdots + s^{n_1}\right)\left(\alpha_0^2 + \cdots + s^{n_2}\right)$. In addition the controller decouples the system into two parts.

Remark: It is straight forward to extend this procedure to more than two inputs.

SINGLE INPUT CASE, NONLINEAR

Elimination

Let us consider the locally reachable nonlinear system

$$x_t = f(x, u) \ .$$

Unfortunately, elimination of u leads to equations nonlinear in x_t.

The implicit function theorem allows us to introduce a new input $\bar{u}$ such that

$$x_t^1 = \bar{f}^1(x, \bar{u}) \ , \qquad x_t^{n-1} = \bar{f}^{n-1}(x, \bar{u}) \ , \qquad x_t^n = \bar{u}$$

is met. Now two cases are of interest:

1. All functions $\bar{f}^i(x, \bar{u})$ are affine in $\bar{u}$, then we can eliminate $\bar{u}$.
2. Otherwise the system is not flat.

A simple test is given by

$$\partial_{\bar{u}}^2 \bar{f}(x, \bar{u}) = 0 \qquad \text{or} \qquad \partial_u^2 f(x, u) \in \operatorname{span}(\{\partial_u f(x, u)\}) \ .$$

JKU

State Transformation

Let us consider the AI system

$$x_t = \bar{f}(x, \bar{u}) = a(x) + \bar{b}(x)\,\bar{u} \ .$$

We derive from the autonomous system

$$\dot{x} = \bar{b}(x)$$

the flow $\varphi_{\bar{x}^n} : \mathcal{M} \times \mathbb{R} \to \mathcal{M}$. Furthermore, we choose a map $\psi : \mathbb{R}^{n-1} \to \mathcal{M}$, such that $x = \phi(\bar{x}) = \varphi_{\bar{x}^n} \circ \psi(\bar{x}^1, \ldots \bar{x}^{n-1})$ is locally invertible. The jacobian and its inverse meet

$$J_\phi(\bar{x}) = \left[\Delta(\bar{x}), \bar{b} \circ \phi^{-1}(\bar{x})\right] \ , \ J^{-1}(\bar{x}) = \begin{bmatrix} \bar{b}^\perp \circ \phi^{-1}(\bar{x}) \\ \bar{b}_c^\perp \circ \phi^{-1}(\bar{x}) \end{bmatrix} \ , \ J_{\phi^{-1}}(x) = \begin{bmatrix} \bar{b}^\perp(x) \\ \bar{b}_c^\perp(x) \end{bmatrix}$$

and we derive a system

$$J_\phi^{-1} x_t = \bar{x}_t = J_\phi^{-1} a \circ \phi + e_n \bar{u} \ ,$$

where the elimination of $\bar{u}$ is straightforward.

JKU

First Results

To continue, we have to determine

$$\partial_{\bar{x}^n} J_\phi^{-1} a \circ \phi = \left[\partial_{\bar{x}^n}, J_\phi^{-1} a \circ \phi\right] = J_\phi^{-1} \left[\bar{b}, a\right] \circ \phi \, .$$

To avoid solving nonlinear equations or determining coordinate transformation, we observe that:

1. Involutivity of the distribution $U + [f, U]$ with $U = \operatorname{span}(\{\partial_u\})$ guarantees that locally one can determine the AI representation.
2. From $\bar{f}(x, u) = a(x) + \bar{b}(x)\, \bar{u}(x, u) = a(x) + b(x, u) = f(x, u)$ we get $\operatorname{span}(\{[f, U]\}) = \operatorname{span}\left(\{\bar{b}\}\right)$ and $[b, a] = [[f, U], a] + v$, $v \in \operatorname{span}(\{[f, U]\})$.
3. From $[b, a] = [b, a + bu]$ we get $[b, a] = [[f, U], f] + v$, $v \in \operatorname{span}(\{[f, U]\})$, or the system admits an AI representation, iff the distribution

$$U + [f, U] + [f, [f, U]] = \operatorname{span}\left(\left\{\operatorname{ad}_f^i \partial_u\right\}_{i=0}^2\right)$$

with $\operatorname{ad}_f^0 v = v$ and $\operatorname{ad}_f^{i+1} v = \left[f, \operatorname{ad}_f^i v\right]$, $i = 0, 1, 2, \ldots$ is involutive.

JKU

Controller Design and MIMO Systems

The previous conditions are, the distributions $\Delta_k = \operatorname{span}\left(\left\{\operatorname{ad}_f^i \partial_u\right\}_{i=0}^k\right)$, $k = 0, \ldots, n-1$ are involutive and meet $\operatorname{rank}(\Delta_k) = k + 1$. Since $\operatorname{ad}_f^{n-1} \partial_u$ corresponds to a symmetry, the flat output follows from the partial differential equations

$$y = c(x) \ , \qquad \mathrm{d}c \rfloor \operatorname{ad}_f^i \partial_u = 0 \ , \quad i = 1, \ldots, n-1 \ , \quad \mathrm{d}c \rfloor \operatorname{ad}_f^n \partial_u = 1 \, .$$

A state controller can be derived from

$$\alpha_o y_0 + \cdots + \alpha_{n-1} y_{n-1} + y_n = \alpha_o L_f^0 c(x)) + \cdots \alpha_{n-1} L_f^{n-1} c(x) + L_f^n c(x) + u = 0 \, .$$

In the MIMO case some symmetries may appear before the last step, which requires additional considerations. In particular the derivation of the partial differential equations requires the alignment of vector fields. Therefore, no simple representation of these equations exists.

JKU

MULTI INPUT CASE, NONLINEAR

Static Feedback

Let us consider the multi input system

$$x_t = f\left(x, u\right) \ .$$

The straightforward extensions from the single to the multi input case are:

1. There exists an input transformation, such that the system can we rewritten in AI -Form
$$x_t = a\left(x\right) + B\left(x\right)\bar{u} \ .$$
2. The vector fields of the input matrix $B = \left[b_1\left(x\right), \ldots, b_m\left(x\right)\right]$ form an involutive distribution or the system can be rewritten in the form
$$\bar{x}_t = \bar{a}\left(\bar{x}\right) + \begin{bmatrix} 0 \\ I \end{bmatrix} \tilde{u} \ .$$

These is met by all systems, iff the distributions

$$\begin{array}{rcl} D_0 & = & \operatorname{span}\left(\left\{\partial_{u^1}, \ldots \partial_{u^{,}}\right\}\right) \\ D_1 & = & D_0 + \left[D_0, f\right] \end{array} \qquad \begin{array}{rcl} & \vdots & \\ D_{l+1} & = & D_l \end{array}$$

are involutive and $\dim\left(D_l\right) = n + m$ is fulfilled.

Flat Systems with Dynamic Feedback

There are two reasons, why the previous test fails.

1. The nonlinear system admits an AI representation, but the involutivity conditions is not met. Obviously, the elimination idea is still applicable, but the number of eliminated variables is smaller.
2. The system does not admit an AI representation but a PAI representation

$$x_t = a(x, v) + B(x, v)\, w \ ,$$

where the system is affine in w only. The elimination idea fails, we are not able to align any field b_j of B. The only exception is, a b_j is independent of v. We will show, how we can overcome this problem by a trivial system extension. In addition it is worth mentioning that this condition is necessary for a system to be flat.

PRELIMINARIES AND NOTATION

Manifolds

$\mathcal{M}$: m-dimensional manifold with local coordinates

$\mathcal{T}(\mathcal{M})$, $\mathcal{T}^*(\mathcal{M})$: tangential , cotangential bundle $\left(z^1,\ldots,z^m,\dot{z}^1,\ldots,\dot{z}^m\right)$, $\left(z^1,\ldots,z^m,\dot{z}_1,\ldots,\dot{z}_m\right)$

Let $f^i(z)$ be m functional independent functions, then $\left\{\mathrm{d}f^1,\ldots,\mathrm{d}f^m\right\}$ and $\left\{\partial_{f^1},\ldots,\partial_{f^m}\right\}$ with

$$\partial_{f^i}\rfloor f^j=\delta_i^j$$

are holonomic bases of $\mathcal{T}^*(M)$, $\mathcal{T}(\mathcal{M})$.

The canonical bases follow from the choice $f^i=z^i$.

Sections of $\mathcal{T}(\mathcal{M})$ are called vector fields. A vector field v is the infinitesimal generator of a flow $\varphi:\mathbb{R}\times\mathcal{M}\to\mathcal{M}$, $\varphi_\varepsilon(x)=\bar{x}$.

Sections of $\mathcal{T}^*(\mathcal{M})$ are called covector fields or 1-forms. If a covector field ω meets $\mathrm{d}g(z)=\omega$, then we get a foliation by $(m-1)$-dimensional submanifolds.

JKU

Bundles, Jet Manifolds

$\mathcal{Z}\xrightarrow{\pi}\mathcal{B}$: denotes a bundle with basis $\mathcal{B}$, total manifold $\mathcal{Z}$ and projection π.

Here: t is the global coordinate of $\mathcal{B}=\mathbb{R}$, $\left(t,z^1,\ldots.z^m\right)$ are local coordinates of $\mathcal{Z}$.

A section $\sigma:\mathcal{B}\to\mathcal{Z}$, $\sigma\in\Gamma(\mathcal{Z})$ of $\mathcal{Z}$ meets

$$z^i \quad=\quad \sigma^i(t)\ .$$

The prolongation $j(\sigma)$ of a section $\sigma\in\Gamma(\mathcal{Z})$ fulfills

$$z_1^{\alpha_z} \quad=\quad \partial_t\sigma^{\alpha_z}(t)\ .$$

The first jet manifold $J(\mathcal{Z})=J^1(\mathcal{Z})$ of $\mathcal{Z}$ with $(t,z^1,\ldots,z^m,z_1^1,\ldots,z_1^m)$ contains all prolonged sections:

$$j(\Gamma(Z)) \quad\subset\quad \Gamma(J(\mathcal{Z}))\ .$$

JKU

A LITTLE BIT OF DIFFERENTIAL GEOMETRY

Total Time Derivative

The first jet bundle $J_0^1(\mathcal{Z})$ is given by $J(Z) \overset{\pi_0^1}{\to} \mathcal{Z}$.

$\pi_0^{1,*}(\mathcal{T}(\mathcal{Z}))$ denotes the pullback of $\mathcal{T}(\mathcal{Z})$ by π_0^1.

On $\pi_0^{1,*}(\mathcal{T}(\mathcal{Z}))$ there we have the distinguished tensor

$$\mathrm{d}t \otimes d_t$$

with the total time derivative

$$d_t \quad = \quad \partial_t + z_1^i \partial_{z^i} \ .$$

Fact: Given a vector field $\partial_t + f(t,z)^i \partial_{z^i}$ the difference

$$\mathrm{d}t \otimes d_t - \mathrm{d}t \otimes f = 0$$

generates the corresponding differential equations $z_1^i = f^i(t,z)$.

Fact: This relation connects geometric objects and free systems. The situation for controlled systems will be different.

Higher time Derivatives

$\mathcal{Y}_\tau$, $\tau = 1, \ldots, l$ denotes a bundle with coordinates (t, y^τ).

$\mathcal{Y} = \mathcal{Y}_1 \times_\mathcal{B} \cdots \times_\mathcal{B} \mathcal{Y}_l$: fibred product

$J^I(\mathcal{Y}) = J^{r_1}(\mathcal{Y}_1) \times_\mathcal{B} \cdots \times_\mathcal{B} J^{r_l}(\mathcal{Y}_l)$: extension to $J^{r_\tau}(\mathcal{Y}_\tau)$ with coordinates $(t, y_0^\tau, \ldots, y_{r_\tau}^\tau)$

I: a sequence $I = r_1, \ldots, r_l$ of numbers r_τ

$y_{[I]}$: all coordinates of $J^I(\mathcal{Y})$ apart from t

y_I: coordinates of the highest derivatives $y_{r_1}^1, \ldots, y_{r_l}^l$.

The total time derivative

$$d_t = \partial_t + y_{\iota_\tau+1}^\tau \partial_\tau^{\iota_\tau} ,$$

$\iota_\tau = 1, \ldots, r_\tau$ generates the tensor $\mathrm{d}t \otimes d_t$ on the jet system $J^I(\mathcal{Y})$.

Remark: The abbreviations $\partial_\tau^{\iota_\tau} = \partial_{y_{\iota_\tau}^\tau}$ are used to increase readability.

JKU

15/37

Distributions and Involutivity

A distribution D is a subspace of the tangential bundle $\mathcal{T}(\mathcal{M})$.

A generator of D is a set $B = \{v_1, \ldots, v_n\}$ with $D = \mathrm{span}(B)$.

A basis of D is a generator of minimal dimension.

An involutive distribution D meets $[D, D] \subset D$.

Any involutive distribution D admits a basis $\tilde{B}$ with $[\tilde{v}_i, \tilde{v}_j] = 0$, which can be derived by transformation of the matrix representation of B to a reduced echelon form:

$$\tilde{B} = \begin{bmatrix} \tilde{B}_1 \\ I \end{bmatrix} .$$

Any involutive distribution D has the matrix representation

$$\tilde{B} = \begin{bmatrix} 0 \\ I \end{bmatrix}$$

in certain coordinates. This requires the determination of flows.

JKU

16/37

Further Properties

The derived system D^+ if D is given by $D^+ = D + [D, D]$.

The sequence of derived systems $D = D_0, \ldots, D_l$ has a last system with $D_{i+1} = D_i^+$, where D_l is involutive.

$S(D)$: denotes the maximal set of symmetries $v_i \in \Gamma(\mathcal{T}((\mathcal{Z}))$, $[v_i, D] \subset D$.

$C(D)$: denotes the (Chauchy) characteristic distribution $\mathrm{span}(S(D)) \cap D$.

The distribution $C(D)$ is involutive.

Let us consider the involutive distributions D, $E \subset D$. Then there exists an involutive complement E_c with $D = E \oplus E_c$.

Fact: The determination of E_c requires flows.

Distributions on Bundles

$\mathcal{Z} \to \mathcal{B}$: A bundle with coordinate t for $\mathcal{B} = \mathbb{R}$ and $\left(t, z^1, \ldots, z^m\right)$ for $\mathcal{Z}$.

$\mathcal{V}(\mathcal{Z}) \subset \mathcal{T}(\mathcal{Z})$: vertical bundle with $\pi_*(\mathcal{V}(\mathcal{Z})) = \mathrm{span}(\{0\})$.

Horizontal bundle H: Choice of a distribution H such that $H + \mathcal{V}(\mathcal{Z}) = \mathcal{T}(\mathcal{Z})$.

$V(D) = D \cap \mathcal{V}(\mathcal{Z})$: Vertical part of D.

A partial assignment $x_1^i = f^i(t, x, u)$, $i = 1, \ldots, n$ for d_t results in

$$f_t \quad = \quad \partial_t + f^i(t, x, u)\, \partial_{x^i} + u_1^j \partial_{u^j}\ , \quad j = 1, \ldots .m.$$

The distribution $\Sigma = H \oplus U$, $U = \{\partial_{u^1}, \ldots, \partial_{u^m}\}$, $H = \mathrm{span}(f_t)$ characterizes a dynamic system with input.

Remark: Because of $f = f^i(t, x, u)$, $f \in \Sigma$ often f is used in calculation only.

Some Results

Local reachability: The last system Σ_l of Σ meets

$$\dim(\Sigma_l) = \dim(x) + \dim(u) + 1 \ .$$

Fact: The only free system contained in Σ_l is the empty system $\partial_t \in \Sigma_l$.

The system Σ admits an AI representation, iff U is a Cauchy characteristic distribution of $U + [f_t, U]$.

The system Σ admits a PAI representation, iff $\tilde{u} = \alpha^j \partial_{u^j}$, $\tilde{U} = \mathrm{span}(\{u\})$ is a Cauchy characteristic distribution of $\tilde{U} + \left[f_t, \tilde{U}\right]$. Because of

$$\begin{aligned} [\tilde{u}, f_t] &= \alpha^j [\partial_{u^j}, f] + u \\ [\tilde{u}, [\tilde{u}, f_t]] &= \alpha^j \alpha^k [\partial_{u^j}, [\partial_{u^j}, f]] + w + \bar{u} \end{aligned}$$

with $u, \bar{u} \in U$ and $w \in \left[f_t, \tilde{U}\right]$, one derives the simple necessary condition

$$\alpha^j \alpha^k [\partial_{u^j}, [\partial_{u^j}, f]] \in U + [f_t, U] \ .$$

JKU

Some Results, ct.

Let the distribution $\tilde{U} \subsetneq U$ contain all solutions of the previous condition, then we simply repeat the procedure to derive the final result.

Remark: For $m = 1$ AI and PAI representation coincide, for $m = 2$ one step is required only.

Fact: Any 1-dimensional subdistribution $F \subset D$ of a distribution D is involutive.

Remark: The construction of higher dimensional involutive subdistributions is more delicate.

A simple approach: Construct a (maximal) subdistribution $F \subset D$ such that $[F, F] \subset D$ is met. Then repeat the procedure with $D = F$.

JKU

REMARKS ON FLATNESS

A Definition

Definition

A dynamic System Σ is flat, iff there is a jet system $J^I(\mathcal{Y})$ with minimal number of coordinates and a submersion $H : J^I(\mathcal{Y}) \to \mathcal{Z}$, $(x,u) = H\left(t, y_{[I]}\right)$ such that

$$d_t\left(H^*\left(x^i\right)\right) = H^*\left(f^i\right)$$

with the total time derivative d_t on $J^I(\mathcal{Y})$ is met. The variables $y = y^1, \ldots, y^l$ are called coordinates of the flat outpus.

Theorem

A necessary condition for a system Σ to be flat is, it admits a PAI representation.

Useful Properties

Fact: The map $(x, u) = \overline{H}_{t,y_{[I-1]}}(y_I)$ is affine.

Theorem

The input distribution of a PAI representation can be written as $W \oplus V$, where W contains a $\bar{m}$-dimensional involutive subdistribution $\bar{m} = \dim(\overline{H})$.

Corollary 1: One can always prolong v^{α_v}, they are independent of y_I. This remains correct for higher order prolongations.

Corollary 2: During the process of elimination one must find variables w^{α_w} and some variables $v_1^{\alpha_v}$ such that both depend on y_I. In this step one can eliminate both.

JKU 22/37

AN ALGORITHM AND EXAMPLES

Algorithm

1) Start: Take $\Sigma = \Sigma_0$.

2) Test 1: If Σ is trivial, stop, Σ is flat.

3) Test 2: If Σ admits an AI representation, goto 6.

4) Test 3: If Σ admits a PAI representation, prolong to determine a AI representation, goto 6. .

5) Stop.

6) Eliminate and simplify, goto 2.

Remark: Input to state linearization with static feedback: Replace 3) by AI representation with involutive input distribution and cancel 4).

JKU

23/37

Example with Transformations

Let us consider the system

$$x_t^1 = \sqrt{u^1 u^2}\,, \quad x_t^2 = u^1\,, \quad x_t^3 = u^2\,,$$

which may be rewritten as

$$\begin{aligned} f_t &= \partial_t + \sqrt{u^1 u^2}\partial_{x^1} + u^1\partial_{x^2} + u^2\partial_{x^3} + u_1^1\partial_{u^1} + u_1^2\partial_{u^2} \\ U &= \operatorname{span}\left((\partial_{u^1}, \partial_{u^2})\right) \\ S &= \left\{\partial_{u_1^1}, \partial_{u_1^2}\right\}\,. \end{aligned}$$

It does not admit an AI representation. With $\tilde{u} = \alpha^1\partial_{u^1} + \alpha^2\partial_{u^2}$ we get

$$\tilde{u} = u^2\partial_{u^1} + u^1\partial_{u^2}\,.$$

With the flow of this field we derive the transformation

$$w^1 = u^1\,, \quad v^1 = \frac{u^1}{u^2}\,.$$

JKU

24/37

Ex. + Ts. 2

Let us start with

$$f_t = \partial_t + \sqrt{v^1} w^1 \partial_{x^1} + v^1 w^1 \partial_{x^2} + w^1 \partial_{x^3} + v_1^1 \partial_{v^1}$$

and $\Sigma = \mathrm{span}\left(\{f_t\}\right) \oplus U$, $U = \mathrm{span}\left(\left\{\partial_{w^1}, \partial_{v_1^1}\right\}\right)$, $C = \mathrm{span}\left(\{0\}\right)$, $S = \{\}$.

The derived system is $\Sigma^+ = \Sigma \oplus [U, f]$, $[U, f] = \mathrm{span}\left(\{a_1, a_2\}\right)$,

$$\begin{aligned} a_1 &= [\partial_{w^1}, f_t] &&= \sqrt{v^1}\partial_{x^1} + v^1 \partial_{x^2} + \partial_{x^3} \\ a_2 &= \left[\partial_{v_1^1}, f_t\right] &&= \partial_{v^1} \ . \end{aligned}$$

The distribution $[U, f]$ is not involutive. With the flow of a_1, see the corollary from above, we get the transformation

$$\bar{x}^1 = x^1 - \sqrt{v^1} x^3 \ , \quad \bar{x}^2 = x^2 - v^1 x^3$$

as well as

$$f = \partial_t - \frac{v_1^1 x^3}{2\sqrt{v^1}} \partial_{x^1} - v_1^1 x^3 \partial_{x^2} + w^1 \partial_{x^3} + v_1^1 \partial_{v^1} \ .$$

JKU

Ex. + Ts. 3

We rewrite the system in the form

$$\begin{aligned} f_t &= \partial_t - \frac{v_1^1 x^3}{2\sqrt{v^1}} \partial_{x^1} - v_1^1 x^3 \partial_{x^2} + v_1^1 \partial_{v^1} \\ U &= \mathrm{span}\left(\left\{\partial_{x^3}, \partial_{v_1^1}\right\}\right) \\ C &= \mathrm{span}\left(\{\partial_{w^1}\}\right) \ . \end{aligned}$$

By help of the transformation

$$\bar{x}^3 = -x^3 v_1^1$$

one gets the simpler representation

$$\begin{aligned} f &= \partial_t + \frac{1}{2\sqrt{v^1}} x^3 \partial_{x^1} + x^3 \partial_{x^2} + v_1^1 \partial_{v^1} \\ U &= \mathrm{span}\left(\left\{\partial_{x^3}, \partial_{v_1^1}\right\}\right) \\ C &= \mathrm{span}\left(\{\partial_{w^1}\}\right) \ . \end{aligned}$$

JKU

Ex. + Ts. 4

The derived system is $\Sigma_d = \Sigma \oplus [U, f]$, $[U, f] = \mathrm{span}(\{a_1, a_2\})$ and

$$\begin{aligned} a_1 &= [\partial_{x^3}, f] &= \tfrac{1}{2\sqrt{v^1}}\partial_{x^1} + \partial_{x^2} \\ a_2 &= \left[\partial_{v_1^1}, f\right] &= \partial_{v^1} \ . \end{aligned}$$

The distribution $[U, f]$ is not involutive. By help of the transformation

$$\bar{x}^1 = 2\sqrt{v^1}x^1 \ , \quad \bar{x}^2 = x^2 - 2\sqrt{v^1}x^1 \ ,$$

derived by the flow of a_1 one gets.

$$f_t = \partial_t + \left(\frac{v_1^1 x^1}{\sqrt{v^1}} + x^3\right)\partial_{x^1} - \frac{v_1^1 x^1}{\sqrt{v^1}}\partial_{x^2} + v_1^1\partial_{v^1} \ .$$

Ex. + Ts. 5

1. With the transformation

$$\bar{x}^3 = \frac{v_1^1 x^1}{\sqrt{v^1}} + x^3$$

one gets the simplified form

$$f_t = \partial_t + x^3\partial_{x^1} - \frac{v_1^1 x^1}{\sqrt{v^1}}\partial_{x^2} + v_1^1\partial_{v^1} \ ,$$

as well as

$$\begin{aligned} f &= \partial_t - \frac{v_1^1 x^1}{\sqrt{v^1}}\partial_{x^2} + v_1^1\partial_{v^1} \\ U &= \mathrm{span}\left(\left\{\partial_{x^1}, \partial_{v_1^1}\right\}\right) \\ C &= \mathrm{span}\left(\{\partial_{x^3}, \partial_{w^1}\}\right) \ . \end{aligned}$$

Ex. + Ts. 6

The transformation

$$\overline{x}^1 = -\frac{v_1^1 x^1}{\sqrt{v^1}}$$

leads to

$$f_t = \partial_t + x^1 \partial_{x^2} + v_1^1 \partial_{v^1} \ .$$

One gets the trivial system

$$\begin{aligned} f &= \partial_t \\ U &= \mathrm{span}\left(\{0\}\right) \\ C &= \mathrm{span}\left(\left\{\partial_{x^1}, \partial_{v_1^1}, \partial_{x^3}, \partial_{w^1}\right\}\right) \\ S &= \{\partial_{x^2}, \partial_{v^1}\} \end{aligned}$$

with $\dim\left(C \oplus \mathrm{span}\left(S\right)\right) = 6$.

Ex. + Ts. 7

The flat outputs are $y^1 = x^2$, $y^2 = v^1$.

They are annihilated by C.

They are adapted to S.

In the original coordinates they are given by:

$$y^1 = v^1 x^3 + x^2 - 2\sqrt{v^1} x^1, \qquad y^2 = v^1 \ .$$

Example with one Transformation

Let us start with

$$\begin{aligned} f_t &= \partial_t + \sqrt{v}w\partial_{x^1} + w\partial_{x^2} + vw\partial_{x^3} + v_1\partial_v + w_1\partial_w \\ U &= \operatorname{span}\left(\{\partial_w, \partial_v\}\right) \\ S &= \{\partial_{w_1}, \partial_{v_1}\} \ . \end{aligned}$$

AI form:

$$\begin{aligned} U &= \operatorname{span}\left(\{\partial_w, \partial_{v_1}\}\right) \\ S &= \{\partial_{w_1}\} \ . \end{aligned}$$

where $[U, f_t]$ is not involutive.

JKU

E. + T. 2

Simplification by elimination of ∂_w:

$$\begin{aligned} U &= \operatorname{span}\left(\left\{\sqrt{v}\partial_{x^1} + \partial_{x^2} + v\partial_{x^3}, \partial_{v_1}\right\}\right) \\ C &= \operatorname{span}\left(\{\partial_w\}\right) \\ S &= \{\partial_{w_1}\} \ . \end{aligned}$$

Again $[U, f]$ is not involutive.

Simplification by elimination of $\sqrt{v}\partial_{x^1} + \partial_{x^2} + v\partial_{x^3}$:

$$\begin{aligned} U &= \operatorname{span}\left(\left\{\partial_{x^1} + 2\sqrt{v}\partial_{x^3}, \partial_{v_1}\right\}\right) \\ C &= \operatorname{span}\left(\left\{\sqrt{v}\partial_{x^1} + \partial_{x^2} + v\partial_{x^3}, \partial_w\right\}\right) \\ S &= \{\partial_{w_1}\} \ . \end{aligned}$$

Now $[U, f]$ is involutive.

JKU

E. + T. 3

Simplification by elimination of U:

$$\begin{aligned} U &= \operatorname{span}\left(\{\partial_{x^3}, \partial_v\}\right) \\ C &= \operatorname{span}\left(\{\partial_{x^1} + 2\sqrt{v}\partial_{x^3}, \partial_{v_1}, \sqrt{v}\partial_{x^1} + \partial_{x^2} + v\partial_{x^3}, \partial_w\}\right) \\ S &= \{\partial_{w_1}\} \end{aligned}$$

where $[U, f]$ is involutive.

Simplification by elimination of U:

$$\begin{aligned} U &= \operatorname{span}\left(\{0\}\right) \\ C &= \operatorname{span}\left(\{\partial_{x^1} + 2\sqrt{v}\partial_{x^3}, \partial_{v_1}, \sqrt{v}\partial_{x^1} + \partial_{x^2} + v\partial_{x^3}, \partial_w\}\right) \\ S &= \{\partial_{x^3}, \partial_v, \partial_{w_1}\} \end{aligned}$$

JKU

33/37

E+T. 4

Remark: The symmetries $\operatorname{span}\left(\{\partial_{x^3}, \partial_v\}\right)$ correspond to states of the last system before reaching the trivial one. In this lucky case their determination is straightforward.

The determination of the flat output requires the determination of the flows of C and these solutions must be aligned to S:

$$\begin{aligned} C &= \operatorname{span}\left(\{\partial_{x^1} + 2\sqrt{v}\partial_{x^3}, \partial_{v_1}, \sqrt{v}\partial_{x^1} + \partial_{x^2} + v\partial_{x^3}, \partial_w\}\right) \\ S &= \{\partial_{x^3}, \partial_v, \partial_{w_1}\} \end{aligned}$$

The result in the original coordinates is

$$y^1 = v\,, \quad y^2 = x^3 + vx^2 - 2\sqrt{v}x^1\,,$$

where the variable w_1 is already eliminated.

JKU

34/37

SUMMARY

Summary

- Systems, which are input to state linearizable by static feedback admit a sequence of simplified systems with AI representation and involutive input distribution. This property can be checked by a classical test based on derived systems.
- From a computer algebra point of view, one works with Lie brackets and checks linear dependency over the ring of smooth functions.
- In the case of flat systems it is admissible, that the input distribution is not involutive. This problem can be handled by choosing an involutive subdistribution.
- If only a PAI representation is possible, then one has to solve certain polynomial equations over the ring of smooth functions and has to make a trivial system extension in special coordinates.
- In both cases flows are required to determine the flat outputs.

References

[1] Schlacher, K.; Schöberl, M.: A Jet Space Approach to Check Pfaffian Systems for Flatness, Proceedings 52nd Conference on Decision and Control (CDC), S. 2576–2581, 2013.

[2] Schlacher, K.; Schöberl, M.: Geometrische Darstellung nichtlinearer Systeme, at–Automatisierungstechnik, 62(7), S. 452–462, 2014.

[3] Schöberl, M.; Schlacher, K.: Eine Normalform für eine spezielle Klasse flacher nichtlinearer Mehrgrößensysteme in Pfaffscher Systemdarstellung, at-Automatisierungstechnik, 62(7) S. 463-474, 2014.

[4] Schöberl, M.; Schlacher, K.: On an implicit triangular decomposition of nonlinear control systems that are 1-flat - A constructive approach, Automatica, 50, S. 1649–1655, 2014.

[5] Schlacher, K; Schöberl, M; Kolar, B;: A Jet Space Approach to Derive Flat Outputs, 1st IFAC Conference on Modelling, Identification and Control of Nonlinear Systems MICNON, 2015.

JKU

37/37